

ENVIRONMENTAL PROCESSES CONTROLLING THE FATE AND
TRANSPORT OF ARISTOLOCHIC ACID IN AGRICULTURAL SOIL AND
COPPER IN CONTAMINATED LAKE SEDIMENT

By

Chaiyanun Tangtong

A DISSERTATION

Submitted to
Michigan State University
in partial fulfillment of the requirements
for the degree of

Environmental Engineering – Doctor of Philosophy

2014

ABSTRACT

ENVIRONMENTAL PROCESSES CONTROLLING THE FATE AND TRANSPORT OF ARISTOLOCHIC ACID IN AGRICULTURAL SOIL AND COPPER IN CONTAMINATED LAKE SEDIMENT

By

Chaiyanun Tangtong

Fate and transport of toxic chemicals are important processes that describe how chemicals move and transform in the environment. Environmental processes such as adsorption, solubility, complexation, dissolution/precipitation, oxidation/reduction, plant uptake and biodegradation play major roles in controlling the fate and transport of chemicals. Understanding these processes is essential to assess the potential of human health risks, the exposure pathway or even the methods for prevention and remediation of these risks. Environmental problems can be caused by organic or inorganic chemicals and they have different fate and transport behavior in the environment. In this study, the fate and transport of Aristolochic acids (AAs) in soil and copper in sediment were used as examples to show the different behavior of organic and inorganic chemicals that induced problems in environment.

AAs were believed to be causal agents that induced Balkan Endemic Nephropathy (BEN) by food contamination. They are active chemicals in *Aristolochia* species plants which are extensively found in the endemic villages. This study examined the essential environmental partitioning processes that control fate and transport of AAs. The results showed that the octanol-water partitioning coefficient (K_{ow}) of AAs decreased when pH increased, which indicated the different hydrophobicity between neutral and anion forms. This trend was similar to the soil-water partitioning coefficient (K_d). Solubility (S_w) increased when pH increased. These suggested that AAs will be highly mobile in an alkaline environment. The K_{ow} and S_w were

increased when a calcium ion presented in solution. Even if AAs had a high sorption capacity to the soils, they had a high tendency to be desorbed too. The soil adsorption and desorption experiment indicated the cation bridging mechanism may play a major role in soil processes. Root exudates are not the main pathway that release AAs to the soil, but their seed decomposition can release a large amount of AAs, which can be degraded by microorganisms. The plant uptake showed AAs had high accumulation in the roots but less translocation to shoots. All evidence suggested the food contamination hypothesis is possible.

Torch Lake, Houghton County, Michigan, which was impacted by copper mining waste, showed a persistent high level of copper in the top sediment. This copper can never be remediated by natural processes. I hypothesized that copper was released from mining waste by microbial mediate reactions and was sequestered by organic matter and bacteria in the post sediment. To test this hypothesis, the fate and transport of copper were studied with the Phreeqc computer model where the biogeochemical processes (e.g. complexation, precipitation, adsorption, reductive dissolution and biodegradation) were applied to the diffusion process. The results showed that oxidation/reduction conditions highly impact copper fate and transport in sediment. The TEAP process causes the sediment to enter the reducing condition and dissolve the copper waste to pore water. The bacteria in the top sediment adsorbed a large amount of copper but this sorption turned to more stable minerals as time proceeded. Due to the removal of copper by precipitation process, the copper which contributed the solid phases in the top sediment were expected from overlay water. This study showed that this modeling approach is an effective tool to describe the persistent high concentration of copper in Torch Lake sediment.

ACKNOWLEDGEMENTS

First of all, I would like to express my especially thank to my Advisors, Dr. Thomas C. Voice and Dr. David T. Long for their guidance and support over my study in the U.S. They always give me all aspect of learning. Without them, my dissertation could not be completed. I also would like to express special thank for my other committee members, Dr. Phanikumar S. Mantha and Dr. Terence L. Marsh, for their supports and valuable comments and suggestions for my dissertation. I would like to express my special thank to Dr. Alvin J.M. Smucker for his providing the soil samples for this research and Dr. Alison Cupples to gave me valuable advices about microbiology .

Second, I would like to thank to Yan Lang Pan to help me setting up all analytical instrument and Lori who always help me to order the chemicals. Thank for Lisveth for starting up the experiment. Thanks for Lulu, student in my research group, my colleagues Indu, Fernanda, Jean and many others. I could not have fun life at MSU without them. Thank for Han and Tuan from Dr. Phani lab for helping me to install computer program.

I extend my thanks to Thai friends, Thorn, Mink and Michie, Ben, Toh, Oah and many others. I greatly value their friendship. I would to thank the owner of Thai restaurants, Thai princess and Taste of Thai who always give me the delicious food during my study here.

I would like to thank for Royal Thai government for giving me the financial support throughout my study in the U.S. Without their funding, I could not have valuable experience of Ph.D. study at Michigan State University.

I wish to extend my love and thank to my Fiancee' Tik for her support, patience and love and her family here, Ningnong and Roger and Jim and Jeff who alway support me with their true loves. Finally, I would like to express my heart-felt gratitude for my family in Thailand, my Dad, my Mom, my Sister and her daughter, and my Brother. All their loves are the source of my strength. My Ph.D. degree would not be possible without them.

TABLE OF CONTENTS

LIST OF TABLES	xiii
LIST OF FIGURES	xvi
SECTION I Fate and Transport of Aristolochic Acids as Responsible Agent of Balkan Endemic Nephropathy (BEN) and Exposure Pathway	1
Chapter 1 Introduction	1
1.1 The problem concern : Aristolochic acids and Health risks	1
1.2 Aristolochic acids and Balkan endemic nephropathy (BEN)	3
1.3 Environmental characteristic of BEN area study	5
1.4 Aristolochic acids structure and their physical-chemical properties	6
1.5 Hypothesis and objective	7
REFERENCES	9
Chapter 2 Octanol water partitioning coefficient	13
2.1 Introduction : Octanol-water and its environmental significance	13
2.2 Literature reviews	15
2.2.1 K_{ow} of neutral organic compounds	15
2.2.2 K_{ow} of ionized organic compounds and their dependent	16
2.3 Materials and methods	22
2.3.1 K_{ow} by shake flask method	23
2.3.1.1 Buffer aqueous phase	23
2.3.1.2 Preparation of pre-saturation of aqueous and octanol phase	24
2.3.1.3 Analytical method and validation	24
2.3.1.4 Procedure	24
2.3.1.5 pH and ionic strength effect	26
2.3.2 K_{ow} by RP-HPLC method	26
2.4 Result and discussion	28
2.4.1 Ionization of Aristolochic acid	28
2.4.2 Calibration curve and validation	28
2.4.3 Log K_{ow} by shake flask method	30
2.4.4 pH and ionic strength effect	31
2.4.5 Log K_{ow} by HPLC method	34
2.5 Conclusion	36
REFERENCES	37

Chapter 3 Aqueous solubility	42
3.1 Introduction	42
3.2 Literature reviews	43
3.2.1 Solubility of organic acids and pH effect	43
3.2.2 The ionic strength, ions presence and complexation formation effect	46
3.3 Materials and Methods	48
3.3.1 The kinetic test and calcium ion effect	48
3.3.2 The pH effect	49
3.3.3 The type of cation and ionic strength effect	49
3.4 Result and discussion	50
3.4.1 Kinetic study and calcium ion effect	50
3.4.2 The pH effect	53
3.4.3 Cation types and ionic strength effect	54
3.5 Conclusion	56
REFERENCES	57
Chapter 4 Soil-water partitioning coefficient	59
4.1 Introduction	59
4.2 Literature reviews	60
4.2.1 The adsorption components in soil	60
4.2.1.1 Organic matter	60
4.2.1.2 Clays	61
4.2.1.3 Aluminum /Iron oxides	61
4.2.2 Adsorption mechanisms	62
4.2.2.1 Hydrophobic interaction	63
4.2.2.2 H-bonding	63
4.2.2.3 Ion exchange	63
4.2.2.4 Ligand exchange	64
4.2.2.5 Cation bridging	64
4.2.3 Adsorption Isotherm	64
4.2.4 Soil sorption of non-ionized and ionized organic compounds	66
4.2.4.1 Non-ionized organic compounds	66
4.2.4.2 Ionized organic compounds	66
4.2.4.3 Effect of pH	68
4.2.4.4 Effect of ionic strength	68
4.2.4.5 Effect of cations	69
4.2.4.6 Effect of anions	69
4.2.5 Desorption	70
4.2.6 Desorption isotherm	70
4.2.7 Desorption Hysteresis index	72
4.2.8 Factors effect to desorption hysteresis	73
4.2.8.1 Effect of organic matter content	73
4.2.8.2 Initial concentration	74
4.2.8.3 Contacting time	74
4.2.8.4 Effect of pH	74

4.2.8.5 Effect of cations	75
4.2.8.6 Effect of anions	76
4.3 Material and method	76
4.3.1 Soil samples and their properties	76
4.3.2 Methods for determination of CEC and AEC in soils	77
4.3.3 Analytical method validation	78
4.3.3.1 Accuracy and precision	79
4.3.3.2 Linearity	79
4.3.3.3 Limit of detection(LOD) and limit of quantification (LOQ)	79
4.3.4 Adsorption experiment	80
4.3.4.1 Preliminary and kinetic study	80
4.3.4.2 Adsorption Isotherm	82
4.3.4.3 Effect of pH	82
4.3.4.4 Effect of calcium ion	82
4.3.4.5 Effect cations/anions	83
4.3.5 Desorption Experiment	83
4.3.5.1 Desorption kinetic	83
4.3.5.2 Desorption isotherm	84
4.3.5.3 Effect of pH	84
4.3.5.4 Effect of cations /anions	85
4.4 Result and discussion	85
4.4.1 AAs analytical method validation and matrix effect	85
4.4.2 Adsorption experiment	88
4.4.2.1 Adsorption kinetic	88
4.4.2.2 Adsorption Isotherm	90
4.4.2.3 Effect of soil properties	94
4.4.2.4 Effect of pH	95
4.4.2.5 Effect of calcium ion	97
4.4.2.6 Effect of Cations/ Anions	99
4.4.3 Desorption experiment	102
4.4.3.1 Desorption kinetic	102
4.4.3.2 Desorption isotherm	104
4.4.3.3 Effect of initial concentration	107
4.4.3.4 Effect of pH	109
4.4.3.5 Effect of cations/anions	113
4.5 Conclusion	118
REFERENCES	120
Chapter 5 Plant uptake	127
5.1 Introduction	127
5.2 Literature review	128
5.2.1 Root uptake mechanism and pathway	128
5.2.2 Translocation, accumulation and metabolism in plant	130
5.2.3 Plant uptake descriptor	132
5.2.4 Plant uptake of non-ionic compounds	134

5.2.5 Plant uptake of ionized compounds	136
5.3 Materials and methods	139
5.3.1 Calibration curve	140
5.3.2 Analytical method validation	141
5.3.2.1 Accuracy and precision	141
5.3.2.2 Linearity	142
5.3.2.3 Limit of detection(LOD) and limit of quantification (LOQ)	142
5.3.3 Nutrient solution preparation	142
5.3.4 Hydroponic culture experiment	143
5.3.4.1 Extraction method and recovery test	146
5.3.4.2 Degradation of Aristolochic acids in nutrient solution	148
5.3.5 Sand culture experiment	148
5.3.5.1 Sand preparation	148
5.3.5.2 The uptake experiment	149
5.3.5.3 Determination of AAs degradation in sand	150
5.4 Result and discussion	151
5.4.1 Analytical method validation	151
5.4.1.1 The calibration curve in plant matrix solution	151
5.4.1.2 Accuracy, precision and limit of detection	153
5.4.2 Recovery of plant extraction method	154
5.4.3 Hydroponic culture experiment	155
5.4.3.1 The stability of AAs in Knop's nutrient solution	155
5.4.3.2 Kinetic uptake experiment	156
5.4.3.3 AAs accumulation in plant part	158
5.4.4 Sand culture experiment	162
5.4.4.1 The AAs available in treating sand	162
5.4.4.2 AAs accumulation in plant part	163
5.5 Conclusion	165
REFERENCES	166

Chapter 6 Root exudates of *Aristolochia* plants and leaching and decomposition of *Aristolochia Clematitis* seeds

6.1 Introduction	171
6.2 Literature reviews	173
6.2.1 Plant root exudates	173
6.2.2 Root exudates collect method	175
6.2.3 Plant litter leaching and decomposition	176
6.2.4 Cellulose degradation in activated sludge medium	177
6.2.5 Cellulose degradation in anaerobic environment	178
6.3 Material and method	179
6.3.1 Root exudates from hydroponic culture	179
6.3.2 Root exudates from sands culture	181
6.3.3 Leaching from decomposition of <i>Aristolochia Clematitis</i> seeds	182
6.3.3.1 The decomposition in aerobic condition by activated sludge and soil	182

6.3.3.2	The decomposition in anaerobic condition by activated sludge and soil	184
6.4	Results and discussion	185
6.4.1	Root exudates of <i>Aristolochia</i> plant from hydroponic and sand culture	185
6.4.2	Leaching from the decomposition of <i>Aristolochia Clematitis</i> seeds	187
6.4.2.1	The decomposition in aerobic condition by activated sludge and soil	187
6.4.2.2	The decomposition in anaerobic condition by activated sludge and soil	190
6.5	Conclusion	191
	REFERENCES	192
 SECTION II Biogeochemical Modeling of Fate and Transport of Copper from Mining Waste in Torch Lake Sediment		 196
 Chapter 7 Introduction		 196
7.1	The problem of concern and Torch Lake history	196
7.2	Torch Lake study site	197
7.3	The copper state in Torch Lake sediment	198
7.4	State of recovery	201
7.5	The redox state	202
7.6	The evidence of microbial copper sequestration	202
7.7	Torch Lake Sediment composition and mineralogy	205
7.8	Hypothesis and Approach	206
	REFERENCES	208
 Chapter 8 Literature reviews		 211
8.1	Copper speciation, control mechanism and transport in natural water	211
8.1.1	Complexation	211
8.1.2	Precipitation/dissolution	214
8.1.3	Adsorption	216
8.1.3.1	Sorption to metal hydrous oxides	217
8.1.3.2	Sorption to clays	217
8.1.3.3	Sorption to organic matter	218
8.1.3.4	Sorption to microorganisms	219
8.2	Factors control copper mobility in sediment	219
8.2.1	pH	220
8.2.2	Redox state	220
8.3	Microbial mediated reaction	222
8.4	Releasing of heavy metal by reductive dissolution of iron oxide	224
	REFERENCES	226

Chapter 9 Materials and methods	231
9.1 Copper speciation and saturation indices modeling	231
9.1.1 Surface water and top sediment porewater modeling	232
9.1.2 Mine tailing porewater modeling	232
9.2 Adsorption modeling	233
9.2.1 Adsorption to Hydrous Ferric Oxide (HFO) modeling	234
9.2.2 Adsorption to organic matter modeling	235
9.2.3 Adsorption /ion exchange on clay modeling	239
9.2.4 Adsorption to bacteria surface modeling	239
9.2.5 Contribution of all sorbent modeling	241
9.3 Oxidation of dissolve organic compounds by microorganism or TEAP modeling	241
9.4 Reductive dissolution of iron oxides modeling	244
9.5 Diffusion transport modeling	245
9.6 Diffusion transport with reductive dissolution of iron oxides and TEAP modeling	246
9.7 Full combined processes modeling	248
APPENDICES	250
Appendix A.1 Copper speciation in Torch lake surface water modeling	251
Appendix A.2 Copper speciation in top sediment pore water modeling	252
Appendix A.3 Chemical composition in mine tailing pore water modeling	253
Appendix B.1 Adsorption to Hydrous Ferric Oxide (HFO) modeling	254
Appendix B.2 Adsorption to organic matter modeling	256
Appendix B.3 Adsorption / ion exchange on clay modeling	258
Appendix B.4 Adsorption to Bacteria surface modeling	259
Appendix B.5 Contribution of all sorbent modeling	261
Appendix C.1 Oxidation of dissolved organic compounds by microorganism or TEAP modeling	263
Appendix D.1 Reductive dissolution modeling	265
Appendix E.1 Diffusion transport with reductive dissolution and TEAP modeling	268
Appendix F.1 Full combined processes modeling	273
REFERENCES	278
Chapter 10 Result and discussion	280
10.1 Copper speciation and saturation indices modeling	280
10.1.1 Surface water and top sediment porewater modeling	280
10.1.2 Mine tailing porewater modeling	282
10.2 Adsorption Modeling	283
10.2.1 Adsorption to Hydrous Ferric Oxide (HFO) modeling	283
10.2.2 Adsorption to organic matter modeling	284
10.2.3 Adsorption/ion exchange on clay modeling	285
10.2.4 Adsorption to bacteria surface modeling	285
10.2.5 Contribution from various sorbents	286

10.3 Oxidation of dissolve organic compounds by microorganism or TEAP modeling	287
10.4 Reductive dissolution modeling	289
10.5 Diffusion transport with reductive dissolution and TEAP modeling	291
10.6 Full combined processes modeling	294
10.6.1 The dissolved redox species and dissolved copper concentration	295
10.6.2 Copper solid phase concentration	298
REFERENCES	302
Chapter 11 Conclusion	304

LIST OF TABLES

Table 1.1	Aristolochia species, parts and their used (International Agency for Research on Cancer Staff., 2002)	2
Table 1.2	Chemical structure of Aristolochic acid I and II	6
Table 2.1	The molecular structure and literature values of pK _a and log K _{ow} of reference compounds	27
Table 2.2	The log K _{ow} of AA I and II by shake flask method at three different concentrations	30
Table 2.3	The log K _{ow} of reference compounds and their retention time from RP-HPLC system	35
Table 3.1	The pH of buffer solution and mixing ratio between H ₃ PO ₄ 0.01M and K ₂ HPO ₄ 0.01M	49
Table 4.1	Physical, chemical properties and composition of test soil samples	77
Table 4.2	% recovery (accuracy) and % RSD (intra-day and inter-day precision) of AAs analytical method	86
Table 4.3	Linear Ranges, correlation coefficient, quantification and detection limit of Aristolochic Acid I and II	87
Table 4.4	Linear and Freundlich isotherm parameters for sorption of AAI to four soils at natural soil pH	92
Table 4.5	Desorption coefficient (k _{des}) and 1/n _{des} obtained from fitting the model and hysteresis index (HI= $\frac{1/n_{des}}{1/n_{ads}}$) for sorption of AA I and II in all tested soils	107

Table 5.1	The literature values of RCF and TSCF of some non-ionized and ionized chemicals	139
Table 5.2	% recovery (accuracy) and % RSD (intra-day and inter-day precision) of analysis ALs in leave matrix	153
Table 6.1	The organic compounds identified in root exudates (modified from Yoshitomi, 2001)	173
Table 6.2	The AAs analysis in root exudates from three Aristolochia plants over 12 day periods	186
Table 8.1	Stability constant of complex formation of copper (Nriagu, 1979; Stiff, 1971)	213
Table 8.2	Solubility of copper minerals (Elder & Horne, 1978; Nriagu, 1979; Parkhurst & Appelo, 2013)	215
Table 8.3	The biodegradation reaction of sequential terminal electron acceptor	224
Table 8.4	Secondary redox reactions	224
Table 9.1	Modeling input of surface water and top sediment pore water	233
Table 9.2	Acidity constant of HFO and Equilibrium constants (Log K) of copper surface complexation on HFO	234
Table 9.3	The surface characterization parameters of HFO used in the model	235
Table 9.4	Proton dissociation constants and surface complexation constants of copper binding to humic acid in Tipping and Hurley's database, WHAM (Windermere Humic Acid Model of Tipping and Hurley) modeling	236
Table 9.5	Copper ion exchange reaction and its constant	239

Table 9.6	Deprotonation and stability constants of the copper and anionic functional groups on <i>B. Subtilis</i> cell surface	240
Table 9.7	The concentration of each functional groups per unit weight of bacteria <i>B. Subtilis</i>	241
Table 9.8	The biodegradation reaction of sequential terminal electron acceptor	242
Table 9.9	The kinetic rate law of sequential biodegradation reaction	243
Table 9.10	Kinetic Parameter constants of microbial mediation reaction using in the model	243
Table 9.11	Some physical transport properties of Torch Lake sediment in transport modeling	246
Table 9.12	Secondary redox reactions	247
Table 9.13	The kinetic rate law of secondary oxidation reaction	247
Table 9.14	Kinetic parameter constant of secondary oxidation reaction	248
Table 10.1	Oxidation state and speciation of copper in surface water and top sediment porewater	281
Table 10.2	Saturation index of copper minerals in surface water and top sediment porewater	282
Table 10.3	Some properties and copper composition from mine tailing porewater modeling	283

LIST OF FIGURES

Figure 2.1	The extent of ionization as function of pH where AH and A ⁻ is neutral and ionized form of organic acids and B and BH ⁺ is neutral and ionized form of organic bases(Kah & Brown, 2006)	18
Figure 2.2	The apparent log <i>K_{ow}</i> '' as a function of pH (modified from Kah & Brown, 2008)	20
Figure 2.3	Log <i>K_{ow}</i> of organic acids as a function of log ionic strength (Log μ)	22
Figure 2.4	Octanol and aqueous phase separation in shake flask experiment(For the interpretation of the references to color in this and all other figures, the reader is referred to the electronic version of this dissertation)	25
Figure 2.5	Aqueous speciation of Aristolochic acid I and II as function of pH	28
Figure 2.6	The calibration curve of AA I and II in aqueous (a) and octanol (b) solution	29
Figure 2.7	Experimental log <i>K_{ow}</i> '' and the fitted model curve versus pH after equilibrium: AA I (a) and AA II (b)	31
Figure 2.8	Experimental log <i>K_{ow}</i> '' and fitted model at different ionic strength in aqueous phase: AA I (a) and AA II (b)	33
Figure 2.9	Log <i>K_{ow}</i> '' of anion of AA I and II at high pH as a function of logarithm of ionic strength (Log μ)	34
Figure 2.10	The linear correlation between log <i>K_{ow}</i> and log RT of reference compounds and the extrapolation of AA I and II	35
Figure 3.1	Pentachlorophenol (PCP) solubility as a function of pH (modified from Wightman & Fein, 1999)	45

Figure 3.2	Concentration of AA I (a) and AA II (b) dissolved in pure water and CaCl ₂ 0.01M as a function of time	51
Figure 3.3	Concentration AA I and II dissolved in pure water (a) and CaCl ₂ solution (b) as a function of time	52
Figure 3.4	The experimental solubility of AA I (a) and AA II (b) as a function of pH at 7 day of equilibration. Solid line represents the fitted model curve of Eq.3.7	53
Figure 3.5	The solubility of AA I (a), AA II (b) and the pH (c) at the different type of cation and their concentration	55
Figure 4.1	The various types of sorption isotherm of Linear (a), Freundlich (b) and Langmuir (c) (modified from Schwarzenbach et al., 2003)	66
Figure 4.2	The two-compartment desorption isotherm and the splitting linear and exponential compartment model (modified from Barriuso, Baer, & Calvet, 1992)	72
Figure 4.3	AAs equilibrated with soil solution in mechanical shaker	81
Figure 4.4	Separation aqueous phase from soil after centrifuge	81
Figure 4.5	The calibration curve of AA I and II in soil matrix solution	86
Figure 4.6	Matrix effect of analysis AA I (a) and AA II (b) in soil matrix and pure methanol	88
Figure 4.7	Sorption kinetic of AA I (a) and II (b) on four soils	89
Figure 4.8	Sorption isotherm of AA I (a) and AA II (b) in all four soils at native soil pH equilibrium	91

Figure 4.9 Adsorption isotherm of AA I in all four soils at adjusted pH equilibrium	93
Figure 4.10 Soil sorption coefficient (K_d) as a function of % organic carbon (a) and cation exchange capacity (b) of soil	94
Figure 4.11 Soil sorption coefficient as a function of pH for Wooster soils (a) and Hoytville soils (b)	96
Figure 4.12 The sorption coefficient (K_d) and pH (second axis) as a function log CaCl_2 concentration on WT CT soil (a), WT NF soil (b), HY CT soil(c) and HY NF soil (d)	98
Figure 4.13 Adsorption isotherm of AA I (a) and II (b) on Hoytville NF soil in different cations background solution	99
Figure 4.14 Adsorption isotherm of AA I (a) and II (b) on Hoytville NF soil in different anion background solution	101
Figure 4.15 % Desorption of AAI (a) and AA II (b) as function of time for all tested soils	103
Figure 4.16 Sorption and desorption isotherm of AA I and II in WT CT soil (a and b), WT NF soil (c and d), HY CT soil (e and f) and HY NF soil (g and h) (filled symbols-adsorption point open symbols-desorption point	105
Figure 4.17 The hysteresis index of AA I (a) and II (b) as a function of initial concentration for all tested soils	108
Figure 4.18 AAs sorption –desorption isotherm of AA I and II on Hoytville NF soil at adjusted pH 6.0 (a) and (b), original pH 6.56 (c) and (d), adjusted pH8.36 (e) and (f). The pH shown in figure was from an average of pH of adsorption process	110
Figure 4.19 Hysteresis index calculated form sortion- desorption isotherm of all soil as a function with pH of AA I (a) and AA II (b)	112

Figure 4.20	The sorption/desorption isotherm of AA I on Hoytville NF soil in different cation background solution (a) SrCl_2 (b) CaCl_2 (c) MgCl_2 (d) KCl (e) NaCl (filled symbols-adsorption point, open symbols-desorption point)	114
Figure 4.21	The hysteresis index of desorption of AA I and II on HYNF soil at initial concentration 0.2-0.9 $\mu\text{g/ml}$ with different cation background solution	115
Figure 4.22	The sorption/desorption isotherm of AA I on Hoytville NF soil in different anion background solution : KNO_3 (a), K_2SO_4 (b), KCl (c) (filled symbols-adsorption point, open symbols-desorption point)	117
Figure 4.23	The hysteresis index of desorption of AA I and II on HYNF soil at initial concentration 0.2-0.9 $\mu\text{g/ml}$ with different anion background solution	118
Figure 5.1	The diffusion pathway of symplastic and apoplastic (Dettenmaier, 2008)	129
Figure 5.2	The relationship between root concentration factor (RCF) and the octanol – water partition coefficient ($\text{Log } K_{ow}$) of root uptake of o-methylcarbamoyloximes (open circle) and substituted phenylurea (cross mark) by barley plants from nutrient solution (Briggs et al., 1982)	134
Figure 5.3	The relationship between the translocation stream concentration factor and octanol-water partition coefficient of the root uptake of o-methylcarbamoyloximes (open circle) and substituted phenylurea (cross mark) by Barley plants from nutrient solution (Briggs et al., 1982)	135
Figure 5.4	The relationship between stem concentration factor (SCF) and octanol-water partition coefficient ($\text{Log } K_{ow}$) of o-methylcarbamoyloximes in the stem bases (close circle) and central stem(open circle) sections, and substituted phenylureas in the stem bases (closed triangle) and central stem (open triangle) sections taken up by barley plants from nutrient solution (Briggs et al., 1983)	136
Figure 5.5	The root concentration factor of 2,4 dichloro-phenoxyacetic acids(open circle) , and 3,5 dichloro-phenoxyacetic acids (closed circle) uptake by barley as a function of pH of nutrient solution (Briggs et al., 1987)	137

Figure 5.6 The accumulation of weak acids between xylem and phloem by ion trapping effect (Hellstrom, 2004)	138
Figure 5.7 The derivatization of Aristolochic acids to Aristolactam by using zinc powder in acid solution (Chan et al., 2007)	141
Figure 5.8 Cucumber seedlings germinated on wetted towel in box	144
Figure 5.9 AAs uptake by hydroponic culture experimental setup	145
Figure 5.10 Plant parts separation after harvesting	145
Figure 5.11 Plant parts maceration by pestle and mortar	146
Figure 5.12 Plant extracted by sonication in ultrasonic bath	147
Figure 5.13 Supernatant separation from plant tissue after centrifuge	147
Figure 5.14 Plant uptake by sand culture experimental setup	149
Figure 5.15 HPLC-FLD chromatogram of derivative Aristolactum I and II in leaves (a), stem (b) and root (c) matrices solution spiked with AA I and II	151
Figure 5.16 The calibration curve of AL I (a) and AL II (b) in leaf, stem, root matrix and methanol	152
Figure 5.17 The % Recovery from spiked AA I (a) and II (b) standard solution to leaves and stem matrices	154
Figure 5.18 The stability of AAs in Knop's solution as a function of time	156
Figure 5.19 The AA I and II remaining in solution as a function of exposure time	157

Figure 5.20	The AA I and II concentration in shoot as a function of exposure time	157
Figure 5.21	The percentage of AA I (a) and AA II (b) in different parts in cucumber plant parts and residual in media	158
Figure 5.22	AA I (a) and AA II (b) distribution in cucumber plant parts in hydroponic culture	160
Figure 5.23	AAs concentration found in stem and root tissues (a) and stem and leaf concentration factor (b) (SCF and RCF) of cucumber plant uptake AAs from spiked nutrient solution	161
Figure 5.24	AA I and II concentration available in sand as a function of incubation time	162
Figure 5.25	AA I (a) and AA II (b) distribution in cucumber plant parts in sand culture	163
Figure 5.26	AAs concentration found in stem and root tissues (a) and stem and leaf concentration factor (b) (SCF and RCF) of cucumber plants grown in <i>Aristolochia Clematitis</i> seed treating sand	164
Figure 6.1	The experimental setup to collect root exudates in hydroponic culture	180
Figure 6.2	The condensation of collected root exudates by evaporation unit	181
Figure 6.3	The experimental setup to collect root exudates in sand culture	182
Figure 6.4	The prepared bottles for decomposition of <i>A. Clematitis</i> seeds in aerobic condition	183
Figure 6.5	The set of bottles prepared in glove box under N ₂ atmosphere	184
Figure 6.6	AA I (a) and II (b) leaching from the decomposition of <i>A. Clematis</i> seeds in aerobic condition from bottle set A, B, C, D and E as a function of time : A=no microorganism + sterile, B=activated sludge + sterile, C=activated sludge + non sterile, D =soil + sterile, E=soil + non sterile	188

Figure 6.7	The growing of microorganism from activated sludge in bottle A (a) , bottle B (b) and botle C (c) in aerobic decomposition experiments	189
Figure 6.8	The chromatogram of AA I and II leaching from <i>A.Clematitis</i> (bottle set A) analyzed by HPLC-DAD	189
Figure 6.9	AA I (a) and II (b) leaching from the decomposition of <i>A. Clematis</i> seeds in anaerobic condition from bottle set A, B ,C, D and E as a function of time : A=no microorganism + sterile, B=activated sludge + sterile, C=activated sludge + non sterile, D =soil + sterile, E=soil + non sterile	190
Figure 7.1	Map showing location of Torch Lake, Keweenaw Peninsula, Michigan (Fett, 2003)	198
Figure 7.2	Torch Lake sediment core (McDonald & Urban)	200
Figure 7.3	Bulk density (open circles) and solid phase copper concentration (solid circles) profiles of Torch lake sediment at different water depth (a)10 m (b) 13 m and (c) 20 m (modified from C. P. McDonald et al., 2010)	200
Figure 7.4	The location of Gratiot Lake, Torch Lake and Portage Lake (Fett, 2003)	201
Figure 7.5	Normalized concentration of Fe, Mn and Cu in Torch Lake sediment (Fett, 2003)	202
Figure 7.6	Scanning electron microscopy of <i>Ralstonia</i> isolated from Torch lake grown on copper free agar (A) and (C); grown on copper-supplemented agar (B) and (D) (modified from Konstantinidis et al., 2003)	203
Figure 7.7	TEM and SEM of <i>R. pickettii</i> strain 12 J grown in absence copper (TEM: A, C; SEM: E) and presence copper (TEM: B, D; SEM: F) (modified from Yang et al., 2010)	204
Figure 7.8	Model of copper upward diffusion from mine tailing sediment and sequestration by organic matter and bacteria at the surface sediment	206

Figure 8.1	Calculated copper speciation in fresh water when absence (a) and presence (b) of organic chelation NTA (modified from Elder & Horne, 1978)	214
Figure 8.2	The stability diagram for ternary system Cu(II)-H ₂ O-CO ₂ (g) (Nriagu, 1979)	215
Figure 8.3	Sorption of copper by clay minerals as a function of pH (modified from Nriagu, 1979)	218
Figure 8.4	The stability relation between copper compound in system of Cu+H ₂ O+O ₂ + S +CO ₂ (P _{CO2} = 10 ^{-3.5} atm) , total dissolved sulfur species 10 ⁻¹ M at 25°C and 1 atm (Nriagu, 1979)	221
Figure 8.5	The equilibrium aqueous concentration of copper species as a function of pE (Nriagu, 1979)	222
Figure 8.6	Biodegradation with sequential terminal electron acceptors	223
Figure 9.1	The 1-D column for diffusion process modeling between surface water and mine tailing porewater	246
Figure 9.2	The diagram of all processes combined as full model	249
Figure 10.1	The simulation result of adsorption of Cu ⁺ (a) and Cu ²⁺ (b) on strong and weak surface sites of hydrous ferric oxide as a function of pH	284
Figure 10.2	The simulation result of adsorption of Cu ²⁺ on organic matter as a function of pH	284
Figure 10.3	The simulation result of adsorption/ion exchange of Cu ²⁺ on clay	285
Figure 10.4	The simulation result of adsorption of Cu ²⁺ onto bacteria surface	286
Figure 10.5	The simulation result of the distribution of copper adsorption on hydrous ferric oxide (HFO), organic matter, clay, bacteria surface and total sorption of all sites at different dissolved copper concentration	287

Figure 10.6	Concentration of redox species as a function of time result from the sequential biodegradation or TEAP modeling	288
Figure 10.7	Concentration of some redox species, dissolved copper, Tenorite, pE and pH as a function of time in reductive dissolution modeling	290
Figure 10.8	The simulation results of pE, pH, some redox species, dissolved copper and Tenorite concentration profile from diffusion transport with reductive dissolution and TEAP modeling	293
Figure 10.9	The simulation results of dissolved redox species concentration as a function of depth and time in the full combined processes modeling	296
Figure 10.10	The simulation results of copper solid phases concentration as a function of depth and time in the full combined processes modeling	300

SECTION I

Fate and Transport of Aristolochic Acids as Responsible Agent of Balkan Endemic Nephropathy (BEN) and Exposure Pathway

Chapter 1

Introduction

1.1 The problem concern : Aristolochic acids and health risks

Aristolochic acids (AAs) are chemicals that naturally found in plants of *Aristolochia* and *Asarum* species. Many types of aristolochic acids (AAs) and aristolactams (ALs) are found, but among of them, Aristolochic acid I and II are major components (Chan, Lee, Liu, & Cai, 2007; Zhang et al., 2006). Aristolactam I and II (AL I and II) are also found as metabolites of Aristolochic I and II in animals (Krumbiegel, Hallensleben, Mennicke, Rittmann, & Roth, 1987)

In the past, AAs were widely used as traditional herbal medicine as well as botanical-containing dietary supplement. Table 1.1 shows some parts of *Aristolochia* plants which made of the medicines and their used.

Table 1.1 Aristolochia species, parts and their used (International Agency for Research on Cancer Staff., 2002).

Aristolochia species	Part used	Used
<i>Aristolochia fangchi</i>	Root	Oedema, antipyretic and analgesis remedies
<i>Aristolochia manshuriensis</i>	Stem	Anti-inflammatory and diuretic for acute infection of the urinary system and as emmenagogue and galactagogue for amenorrhoea
<i>Aristolochia contorta</i>	Fruit, Herb	Haemorrhoids, cough and asthma, epigastric pain, arthralgia and oedema
<i>Aristolochia debelis</i>	Fruit, Herb and Root	Same as <i>A. contorta</i> and dizziness, headache, abdominal pain, and snake and insect bites

Aristolochic acids containing medicines were used until they were identified as potential carcinogen in rodent in 1980's. The rats treated with Aristolochic acids developed a tumor in forestomach, lung, lymphoid organs and uterus as well as benign and malignant tumor in kidney and urinary tract (Mengs, 1988). High dose of Aristolochid acids treated rats were died from acute renal failure (Mengs, 1987).

The evidence which support Aristolochic acids as nephrotoxic and carcinogenic in human had been reported in early's 1990. At least 100 cases of rapidly developed renal disease in young women who took the drugs which were made from *Aristolochia* species during a slimming regimen were reported in Belgium (Vanherweghem et al., 1993). In 1999, the first 2 cases of specific nephropathy related to ingestion of Chinese herbal medicines had been reported in U.K.

However, by different sources from the cases in Belgium, the patients had taken the eczama herbal preparations. The analysis of these preparations by High Performance Liquid Chromatography and Mass Spectrometry (HPLC-MS) found Aristolochic acid I and II in them (Lord, Tagore, Cook, Gower, & Pusey, 1999). After the original report in Belgium, similar cases were reported worldwide such as United Kingdom, France, Spain, Germany, United States, China, Japan and Taiwan in context of using AAs containing medicines (Debelle, Vanherweghem, & Nortier, 2008). Because of founding renal failure disease which outbreak in patients taking pills containing Chinese herb, this renal disorder was termed as Chinese herb nephropathy (CHN). The AAs were confirmed as a cause of CHN when the doctor detected AA-DNA adducts in the kidney tissue of CHN patients which showing evidence of exposure to AAs (Arlt, Pfohl-Leszkowicz, Cosyns, & Schmeiser, 2001). Moreover, rats which were treated with sliming pill same as CHN patients had developed a renal interstitial fibrosis and showed similar pattern of AA-DNA adduct found in CHN patients. The specific AA-DNA adducts were also found in the kidney tissue samples from urothelial carcinoma patients (Nortier et al., 2000). These evidence supported hypothesis that AAs play a major role in CHN patients. Consequently, the term Chinese herb nephropathy (CHN) had been replaced by Aristolochic acid nephropathy (AAN).

1.2 Aristolochic acids and Balkan endemic nephropathy (BEN)

Balkan endemic nephropathy or BEN is a chronic fatal kidney disease that had first reported around 60 years ago. It was believed as environmentally induced disease which affecting to people living in the rural area of Balkan countries included Bosnia-Herzegovina, Bulgaria, Croatia, Romania and Serbia(Hranjec et al., 2005). Even extensive of researches for etiology of BEN, the causes are still unclear. Over than 20 years, many hypothesis had been set

for the BEN causes such as trace element deficiency, mycotoxin or ochratoxin A which is also nephrotoxic chemical, plant toxin (aristolochic acids) and polycyclic aromatic hydrocarbon (PAHs) from coal deposit which may be leached and contaminated to groundwater (Castegnaro et al., 2006; USGS, 2001; Voice et al., 2006). Among these hypotheses, Aristolochic acids are most possible. The pathological and clinical features of BEN are very similar to those associated with AAN except for AAN is a rapid decline of renal function in 6 month to 2 year where BEN is slower progression and longer accumulation process from 10 -20 years to end-stage renal failure or urothelial cancer (Broe, 2014).

Recently, Grollman *et al.* had identified the AA-derived DNA adduct dA-AL (Aristolactum) and dG-AL in the renal tissue of patients in BEN area, but not found in patients with other chronic renal diseases living in non-BEN area which was the first time proving AAs exposure by BEN patients (Grollman et al., 2007). Moreover, after sequencing the DNA from tumour tissue patients who resided in endemic area for at least 15 year, they found significant mutation pattern which clearly showed the link between urothelial tumour, p53 mutation and AAs exposure (Arlt et al., 2007). So, the most recent researches were more intent to AAs. The long term consumption of dietary contaminated with AAs was hypothesized as cause of BEN (Grollman & Jelakovic, 2007) . Because the *Aristolochic Clematits* plants were found to extensively grow as a weed in wheat field in BEN areas, scientists believed that *Aristolochia clematitis* seeds were mixed with wheat grain during the harvest and the contaminated flour was used to prepare for home-made bread. However, the life cycle of the weed and the grain were too different where *Aristolochia* plant fruits matured in fall but wheat was harvested in the mid summer and the *Aristolochia* plant fruits have a large pulp form which easily remove from the

wheat grain, so the contamination was hard to occur and this hypothesis still has some limitation (Pitt, 2011; Voice et al., 2006).

The long term consumption of dietary contaminated with AAs hypothesis had been investigated from the BEN patients and healthy residents from endemic villages (Hranjec et al., 2005). The majority of subjects reported the extensive growing *Aristolochia Clematitis* in the wheat field more than 30 years ago and the BEN patients had expose significantly more frequently than the controls. These results can imply that the patients from endemic village consume the bread contaminated with *A.Clematitis* seed. However, the changing of lifestyle and farm handling such as applying the herbicide to field had reduced the dietary exposure to aristolochic acids and expect as a cause of decreasing of incidence rate of BEN.

1.3 Environmental characteristic of BEN area study

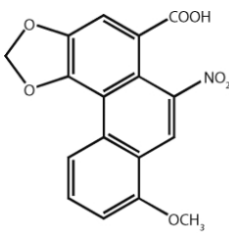
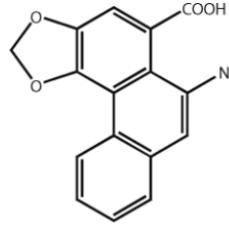
Due to the relation with environmental agents of BEN, the knowing about environmental characteristics between BEN and non-BEN areas is necessary. The environmental differences between endemic and non-endemic village had been studied. These studies showed that there were many sources of nitrate on the soil and high level of nitrate had been found in groundwater. However, there was no statistically significant for concentration of different nitrogen species between BEN and non-BEN village. The water samples that supplied to both village were fail to show high level of organic compounds in BEN areas (Voice et al., 2006). The soil geochemistry between BEN and non-BEN areas had been tested. The results showed that concentration of metals and other elements were usual. However, there were some notes that some elements e.g. Li, Ca, Mg in soil and well water from both villages were higher than world average concentration. K, Ca, Pb, Cd, Mo, Hg and As in soil were greater in endemic villages whereas

Mg, Ba, Mn, Fe, Al, Co and Se were lower in endemic village (Long et al., 2001). The different of soil chemistry between BEN and non-BEN village may response for the occurrence of BEN in Balkan areas.

1.4 Aristolochic acids structure and their physical-chemical properties

Aristolochic acids molecules contain the mixing of hydrophobic and polar structure including nitrophenanthrene, dioxolo and carboxylic acid as shown in Table 1.2 (Pfau, Schmeiser, & Wiessler, 1990). AAs are yellow solid, slightly dissolve in water but completely dissolve in alcohols, acetic acid, acetone, chloroform and diethyl ether (International Agency for Research on Cancer Staff., 2002). AA I and II are different by methoxy group in AA I which cause it less polar than AA II.

Table 1.2 Chemical structure of Aristolochic acid I an II

Compound	Structure	Formula
Aristolochic acid I (8-methoxy-6-nitro-phenanthro (3,4-d)- 1,3-dioxolo-5-carboxylic acid)		$C_{17}H_{11}NO_7$
Aristolochic acid II (6-nitro-phenanthro (3,4-d)- 1,3-dioxolo-5-carboxylic acid)		$C_{16}H_9NO_6$

Aristolochic acids are ionizable organic compounds which can dissociate when dissolved in water. They have two different forms, neutral or ionized forms where the neutral molecules can be deprotonated by losing one proton (H^+) from carboxylic (COOH) group and become as negative charged ions. The extent of ionization will depend on their pK_a and pH of solution. Fu et al., 2011 presented the dissociation constant (pK_a) of AA I and II at 3.3 ± 0.1 and 3.2 ± 0.2 , respectively. No aqueous solubility had been reported.

1.5 Hypotheses and objectives

Because the linkage between consumption of AA-contaminated bread and BEN is not yet confirmed, other exposure pathways should be considered. In this research, a new exposure pathway was investigated. I hypothesize that AAs can be released by *Aristolochia* species plants via root exudates or leaching from the decomposition of dead plant tissues. Once AAs are released to soil, they can move efficiently with water and may be taken up by crop plants, which may be consumed by BEN patients.

To study fate and transport of chemicals in the soil, there are many essential parameters to be determined. The octanol-water partition coefficient shows the hydrophobicity of chemicals and is also related to other environmental partitioning processes. Solubility is a parameter that indicates the ability of chemicals to dissolve in water. Soil sorption and desorption are the main processes in controlling the mobility in soil and availability in other compartments. The root exudates and leaching from decomposition of plant tissues determine the sources of chemicals that are transferred from plants to soils. The uptake of chemicals by crop plants shows the exposure potential to humans and food chain contamination.

In this study, I examined the fate and transport properties of AAs including the octanol-water partition coefficient, solubility, and the soil-water partition coefficient. I also determined AAs' release from *Aristolochia* species plants via root exudation and leaching from their seeds decomposition. The plants' ability to uptake AAs was also determined.

REFERENCES

REFERENCES

- Arlt, V. M., Stiborova, M., vom Brocke, J., Simoes, M. L., Lord, G. M., Nortier, J. L., . . . Schmeiser, H. H. (2007). Aristolochic acid mutagenesis: molecular clues to the aetiology of Balkan endemic nephropathy-associated urothelial cancer. *Carcinogenesis*, *28*(11), 2253-2261. doi: 10.1093/carcin/bgm082
- Broe, M. D. E. (2014). Balkan endemic nephropathy. from <http://www.uptodate.com/contents/balkan-endemic-nephropathy>
- Castegnaro, M., Canadas, D., Vrabcheva, T., Petkova-Bocharova, T., Chernozemsky, I. N., & Pfohl-Leskowicz, A. (2006). Balkan endemic nephropathy: Role of ochratoxins A through biomarkers. *Molecular Nutrition & Food Research*, *50*(6), 519-529. doi: 10.1002/mnfr.200500182
- Chan, W., Lee, K.-C., Liu, N., & Cai, Z. (2007). A sensitivity enhanced high-performance liquid chromatography fluorescence method for the detection of nephrotoxic and carcinogenic aristolochic acid in herbal medicines. *Journal of Chromatography A*, *1164*(1-2). doi: 10.1016/j.chroma.2007.06.055
- Debelle, F. D., Vanherweghem, J. L., & Nortier, J. L. (2008). Aristolochic acid nephropathy: A worldwide problem. *Kidney International*, *74*(2), 158-169. doi: 10.1038/ki.2008.129
- DuarteDavidson, R., & Jones, K. C. (1996). Screening the environmental fate of organic contaminants in sewage sludge applied to agricultural soils .2. The potential for transfers to plants and grazing animals. *Science of the Total Environment*, *185*(1-3), 59-70. doi: 10.1016/0048-9697(96)05042-5
- Dudka, S., & Miller, W. P. (1999). Accumulation of potentially toxic elements in plants and their transfer to human food chain. *Journal of Environmental Science and Health Part B- Pesticides Food Contaminants and Agricultural Wastes*, *34*(4), 681-708. doi: 10.1080/03601239909373221
- Fu, X. F., Liu, Y., Li, W., Bai, Y., Liao, Y. P., & Liu, H. W. (2011). Determination of dissociation constants of aristolochic acid I and II by capillary electrophoresis with carboxymethyl chitosan-coated capillary. *Talanta*, *85*(1), 813-815. doi: 10.1016/j.talanta.2011.03.088
- Gao, Y. Z., & Zhu, L. Z. (2004). Plant uptake, accumulation and translocation of phenanthrene and pyrene in soils. *Chemosphere*, *55*(9), 1169-1178. doi: 10.1016/j.chemosphere.2004.01.037
- Grollman, A. P., & Jelakovic, B. (2007). Role of environmental toxins in endemic (Balkan) nephropathy. *Journal of the American Society of Nephrology*, *18*(11), 2817-2823. doi: 10.1681/asn.2007050537

- Grollman, A. P., Shibutani, S., Moriya, M., Miller, F., Wu, L., Moll, U., . . . Jelakovic, B. (2007). Aristolochic acid and the etiology of endemic (Balkan) nephropathy. *Proceedings of the National Academy of Sciences of the United States of America*, *104*(29), 12129-12134. doi: 10.1073/pnas.0701248104
- Hranjec, T., Kovac, A., Kos, J., Mao, W. Y., Chen, J. J., Grollman, A. P., & Jelakovic, B. (2005). Endemic nephropathy: the case for chronic poisoning by Aristolochia. *Croatian Medical Journal*, *46*(1), 116-125.
- International Agency for Research on Cancer Staff. (2002). *Some Traditional Herbal Medicines, Some Mycotoxins, Naphthalene and Styrene Iarc Monographs* (pp. 590 p.). Retrieved from <http://ezproxy.msu.edu:2047/login?url=http://site.ebrary.com/lib/michstate/Top?id=10252491>
- Krumbiegel, G., Hallensleben, J., Mennicke, W. H., Rittmann, N., & Roth, H. J. (1987). STUDIES ON THE METABOLISM OF ARISTOLOCHIC ACID-I AND ACID-II. *Xenobiotica*, *17*(8), 981-991.
- Long, D. T., Icopini, G., Ganev, V., Petropoulos, E., Havezov, I., Voice, T., . . . Stein, A. (2001). Geochemistry of Bulgarian soils in villages affected and not affected by Balkan Endemic Nephropathy: A pilot study. *International Journal of Occupational Medicine and Environmental Health*, *14*(2), 193-196.
- Lord, G. M., Tagore, R., Cook, T., Gower, P., & Pusey, C. D. (1999). Nephropathy caused by Chinese herbs in the Uh. *Lancet*, *354*(9177), 481-482. doi: 10.1016/s0140-6736(99)03380-2
- Mengs, U. (1987). ACUTE TOXICITY OF ARISTOLOCHIC ACID IN RODENTS. *Archives of Toxicology*, *59*(5), 328-331. doi: 10.1007/bf00295084
- Mengs, U. (1988). TUMOR-INDUCTION IN MICE FOLLOWING EXPOSURE TO ARISTOLOCHIC ACID. *Archives of Toxicology*, *61*(6), 504-505. doi: 10.1007/bf00293699
- Ney, R. E. (1995). *Fate and transport of organic chemicals in the environment : a practical guide* (2nd ed.). Rockville, Md.: Government Institutes.
- Nortier, J. L., Martinez, M. M., Schmeiser, H. H., Arlt, V. M., Bieler, C. A., Petein, M., . . . Vanherweghem, J. L. (2000). Urothelial carcinoma associated with the use of a Chinese herb (Aristolochia fangchi). *New England Journal of Medicine*, *342*(23), 1686-1692. doi: 10.1056/nejm200006083422301
- Pavlovic', N. M., Maksimovic', V., Maksimovic , J. D., Orem, W. H., Tatu, C. A., Lerch, H. E., . . . Paunescu, V. (2012). Possible health impacts of naturally occurring uptake of

- aristolochic acids by maize and cucumber roots: links to the etiology of endemic (Balkan) nephropathy. *Environmental Geochemical Health*.
- Pfau, W., Schmeiser, H. H., & Wiessler, M. (1990). ARISTOLOCHIC ACID BINDS COVALENTLY TO THE EXOCYCLIC AMINO GROUP OF PURINE NUCLEOTIDES IN DNA. *Carcinogenesis*, *11*(2), 313-319. doi: 10.1093/carcin/11.2.313
- Pitt, J. I. (2011). Chinese herbal medicines, aristolochic acid and Balkan endemic nephropathy. *Occupational and Environmental Medicine*, *68*(4), 237-237. doi: 10.1136/oem.2010.061663
- USGS. (2001). Health effect of toxic organic compounds from coal-The case of Balkan Endemic Nephropathy.
- Vanherweghem, J. L., Depierreux, M., Tielemans, C., Abramowicz, D., Dratwa, M., Jadoul, M., . . . Vanhaelen, M. (1993). RAPIDLY PROGRESSIVE INTERSTITIAL RENAL FIBROSIS IN YOUNG-WOMEN - ASSOCIATION WITH SLIMMING REGIMEN INCLUDING CHINESE HERBS. *Lancet*, *341*(8842), 387-391.
- Voice, T. C., Long, D. T., Radovanovic, Z., Atkins, J. L., McElmurry, S. P., Niagolova, N. D., . . . Ganey, V. S. (2006). Critical evaluation of environmental exposure agents suspected in the etiology of Balkan endemic nephropathy. *International Journal of Occupational and Environmental Health*, *12*(4), 369-376.
- Zhang, C. Y., Wang, X., Shang, M. Y., Yu, J., Xu, Y. Q., Li, Z. G., . . . Namba, T. (2006). Simultaneous determination of five aristolochic acids and two aristololactams in *Aristolochia* plants by high-performance liquid chromatography. *Biomedical Chromatography*, *20*(4), 309-318. doi: 10.1002/bmc.565

Chapter 2

Octanol water partitioning coefficient

2.1 Introduction: Octanol-water and its environmental significance

The octanol water partition coefficient (K_{ow} or P) is indicator of hydrophobicity of chemicals. It shows how chemicals favor to partition in water phase or organic liquid phase. K_{ow} widely used in term of prediction of chemical fate and transport in environment compartment because it describes the partitioning between the water and environmental organic medias such as soil, sediment and organic matter (Ney, 1995). Octanol water partition coefficient also relate to other partition coefficients such as soil-water, lipid-water partition coefficient or bioconcentration factor (BCF) which called Linear Free Energy Relationship (LFER). The LFER principle was widely used in environmental field. One is Quantitative Structural Activity Relationships or QSARs which is a regression model relating the physical-chemical properties of chemical to their molecule structure(Yuying, Guanghui, Ying, Zhuang, & Cheng, 2009). The example of application of QSAR is using K_{ow} to predict soil sorption of chemical (Karickhoff, Brown, & Scott, 1979; R. P. Schwarzenbach & Westall, 1981). The high log K_{ow} means the greater potential for chemicals to be sorped in soil, low mobility, low potential to degrade by physical, chemical or biological which lead to persistence in the environment(Ney, 1995). K_{ow} is also used to predict the bioaccumulation potential of terrestrial and aquatic biota which taken the chemicals from contaminated soil or sediment, these can represent in term of bioconcentration factor (BCF). The high log K_{ow} chemicals have high potential for food chain biomagnifications too (Brandt, Becker, & Porta, 2002; Fisk, Norstrom, Cymbalisky, & Muir, 1998). It related to the

toxicity parameters e.g. LD₅₀ where higher K_{ow} means higher toxicity (lower LD₅₀) (Veith, Call, & Brooke, 1983). The K_{ow} also is related to ability of chemicals to be uptake by plant root where lipophilic organic chemicals possess a greater tendency to partition into plant root lipids than hydrophilic chemicals and to distribution in various plant parts (Briggs, Bromilow, Evans, & Williams, 1983; E. M. Dettenmaier, Doucette, & Bugbee, 2009).

Due to AAs are toxic chemicals that causing development of nephropathy and urothelial cancer in human, the physical - chemical properties to predict their fate and transport e.g. octanol-water partition coefficient is very important. However, there are very few literatures reported their log K_{ow}. Most of them are from calculation from various programs that calculated by fragment method. However, for complex structure like AAs, it may have large error due to lack of fragmental value and inaccuracy of database (Han, Qiao, Zhang, Lian, & Ge, 2012). Because of the difficulty in measurement AAs at low concentration and high cost of high quality AAs standard chemicals, the experimental literature values were rarely reported. Moreover, because AAs can ionize when dissolve in water into two different forms, the log K_{ow} of neutral molecules may be different from ionized form for many order of magnitude that make measurement K_{ow} more difficult in term of different method using for each form (R.P. Schwarzenbach, Gschwend, & Imboden, 2003).

The first experimental log K_{ow} of AA I and II were reported by Han et al., 2012 using RP-HPLC method which tried to relate the log K_{ow} of AAs to log K_{ow} of some neutral and ionized compounds. They reported log K_{ow} of AA I and II in neutral form at 4.45 and 3.99 respectively. These numbers indicated that AAs in neutral form are highly hydrophobic(Han et al., 2012). Some programs provided the calculated log K_{ow} online, for example, log Kow of AA I and II from ACD/Labs are 3.41 and 3.50, KOWWIN are 4.19 and 4.11 and ALOGPs are 2.69

and 2.68 (VCCLAB, 2011) . The different between these K_{ow} number means the calculation methods cannot predict them accurately because of highly complex molecule structure and lack of fragmental values.

In this study, the octanol water partition coefficient of Aristolochic acid I and II will be determined by conventional shake flask method and indirectly RP-HPLC method. The shake flask method measured by direct contacting between octanol and water which contained the chemicals. The concentration ratio in both phases will be determine at equilibrium and calculated as K_{ow} , whereas the RP-HPLC method will correlate between retention behavior on C-18 column and the hydrophobicity of reference compounds. This study try to accurately determine the K_{ow} of AAs and their dependence on environment factors which is necessary for prediction the fate and transport when AAs were released to environment.

2.2 Literature reviews

2.2.1 K_{ow} of neutral organic compounds

K_{ow} is a parameter that describes chemical's hydrophobic properties. Octanol is used to represent the lipid-water partition because their polarity is similar to biotic lipid. The K_{ow} is defined by the concentration ratio of compounds distributed in octanol phase to the aqueous phase, when two phases are equilibrium in each other as shown in Eq.2.1. This coefficient indicates the phase that chemicals are favored to partition in.

$$K_{ow} \text{ or } P = \frac{\text{concentration of chemical in octanol phase}}{\text{concentration of chemical in water phase}} \quad (2.1)$$

The concentration in this equation is not solubility of solutes in octanol or water, but it is the concentration in water-saturated octanol and octanol-saturated water. Since K_{ow} of chemicals

have varied in many orders of magnitude, so they always present as base 10 logarithm (Log K_{ow} or Log P). The compounds with high log K_{ow} (more than 3) are determined as hydrophobic whereas the chemical with small log K_{ow} (1 or less) will be determined as hydrophilic. Generally, most hydrophobic compounds are nonpolar and nonionic (Word, 2002).

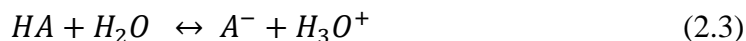
The K_{ow} of nonpolar compounds relates to degree of sorption to organic carbon of natural sorbents which dominated by hydrophobic interaction. Many studies showed the organic carbon-water partition coefficient (K_{oc}) can be related to K_{ow} by Eq. 2.2 where a and b are constant for given compounds (Karickhoff et al., 1979; B. E. Nowosielski & Fein, 1998)

$$\log K_{oc} = a \log K_{ow} + b \quad (2.2)$$

However, this relation may be not fitted for the polar and especially ionizable organic compounds, because variety interactions e.g. ionic exchange reaction rather than hydrophobic interaction had involved to the sorption and the other parameters such as pH and ionic strength become primary order importance (Jafvert, Westall, Grieder, & Schwarzenbach, 1990).

2.2.2 K_{ow} of ionized organic compounds and their dependent

The ionized compounds such as weakly acids will be partially ionized in water which give anion form (A^-) and hydronium ion (H_3O^+) as express in Eq. 2.3. The extent of ionization depend on dissociation constant (K_a) and pH.



From dissociation equation, we can rearrange Eq. 2.3 in term of the ratio of concentration in neutral and anionic form as a function of pK_a and pH as expressed in Eq. 2.4 – 2.7 (Kah & Brown, 2006).

$$K_a = \frac{[A^-][H_3O^+]}{[HA]} \quad (2.4)$$

$$\log K_a = \log \frac{[A^-]}{[HA]} + \log [H_3O^+] \quad (2.5)$$

$$pK_a = \log \frac{[HA]}{[A^-]} + pH \quad (2.6)$$

$$\frac{[HA]}{[A^-]} = 10^{(pK_a - pH)} \quad (2.7)$$

Besides, the proportion species presented in solution can be shown by extent of ionization (α_{ia}) which define as the fraction of neutral species that present in the solution (R.P. Schwarzenbach et al., 2003)

$$\alpha_{ia} = \frac{[HA]}{[HA] + [A^-]} = \frac{1}{1 + \frac{[A^-]}{[HA]}} \quad (2.8)$$

$$= \frac{1}{1 + 10^{(pH - pK_a)}} \quad (2.9)$$

This equation can be plotted between fraction of neutral and ionized form as a function of pH as shown in Figure 2.1. This figure shows that, at $pH \ll pK_a$, the acid form is dominant. However, at $pH \gg pK_a$, the ionized form becomes dominant instead, and at pH equal to pK_a , the fraction of neutral and ionized form will be equal.

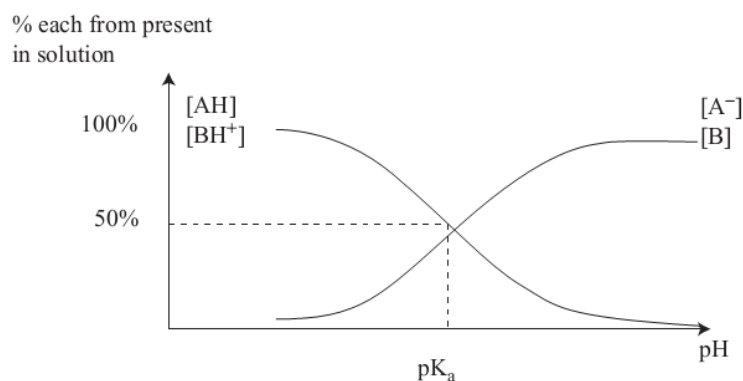


Figure 2.1 The extent of ionization as function of pH where AH and A⁻ is neutral and ionized form of organic acids and B and BH⁺ is neutral and ionized form of organic bases(Kah & Brown, 2006)

Because neutral and ionic species perform different polarities, their hydrophobicity are also different. The ionic species is more soluble in water and would be expected lower K_{ow} . From octanol water partition coefficient definition, we can expand the definition to include the ionic and neutral species in each phase. This partition coefficient is known as “apparent coefficient” (K_{ow}'') which accounts for all contribution species in solution(Westall, Leuenberger, & Schwarzenbach, 1985).

$$K_{ow}'' = \frac{[HA_{oc}] + [A_{oc}^-]}{[HA_w] + [A_w^-]} \quad (2.10)$$

Where $[HA_{oc}]$ and $[HA_w]$ are concentration of neutral species which equilibrium in octanol and aqueous phase respectively and $[A_{oc}^-]$ and $[A_w^-]$ are concentration of ionic species which equilibrium in octanol and aqueous phase.

The K_{ow}'' is rearranged to express in term of pK_a and pH for more practical using as shown in Eq. 2.11 (Word, 2002)

$$K_{ow}'' = \frac{\frac{[HA_{oc}] + [A_{oc}^-]}{[HA_w]} + \frac{[A_w^-]}{[HA_w]}}{1 + \frac{[A_w^-]}{[HA_w]}} \quad (2.11)$$

$$K_{ow}'' = \frac{\frac{[HA_{oc}] + [A_{oc}^-] \frac{[A_w^-]}{[HA_w]}}{[HA_w]} + \frac{[A_w^-]}{[HA_w]}}{1 + \frac{[A_w^-]}{[HA_w]}} \quad (2.12)$$

Introducing, the partition coefficient of neutral species, $K_{ow} = \frac{[HA_{oc}]}{[HA_w]}$, and partition coefficient of ionized species, $K_{ow}^- = \frac{[A_{oc}^-]}{[A_w^-]}$, and from Eq. 2.7, $\frac{[A_w^-]}{[HA_w]} = 10^{(pH-pKa)}$, the K_{ow}'' will become as

$$K_{ow}'' = \frac{K_{ow} + K_{ow}^- 10^{(pH-pKa)}}{1 + 10^{(pH-pKa)}} \quad (2.13)$$

This equation is very useful to predict the apparent K_{ow} of chemicals at given pK_a and pH. It also can predict the octanol-water coefficient of neutral form (K_{ow}) and ionized form (K_{ow}^-) by fitting the experimental data with this equation.

From Eq.2.13 the relationship between $\log K_{ow}''$ and the pH can be represented as sigmoidal curve as shown in Figure 2.2 (solid line). However, some chemicals are very low dissociated in non-aqueous phase, so we can neglect the ionized species in octanol phase and the K_{ow}'' can be express as Eq. 2.14 (Bogdan E. Nowosielski, 1998). This shows as dash line in Figure 2.2 where $\log K_{ow}''$ will be indefinitely decrease when pH increase (Kah & Brown, 2008).

$$K_{ow}'' = \frac{K_{ow}}{1 + 10^{(pH-pKa)}} \quad (2.14)$$

From this figure, the K_{ow} of each form of ionized chemicals may be completely different in many orders of magnitude.

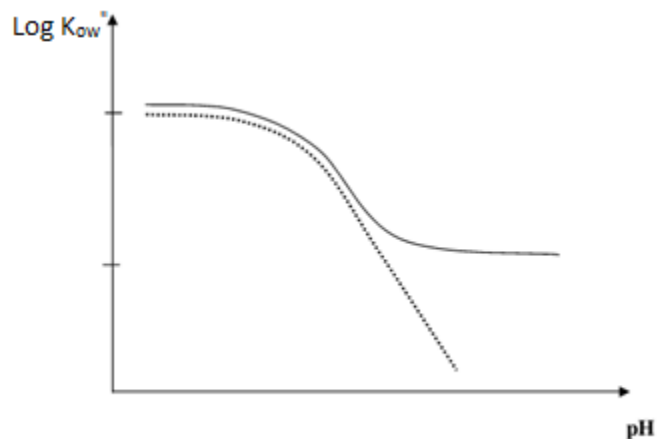


Figure 2.2 The apparent $\log K_{ow}$ as a function of pH (modified from Kah & Brown, 2008)

The type of sigmoidal curve (solid line) had been observed in many ionizable pharmaceutical compounds (Berthod, Carda-Broch, & Garcia-Alvarez-Coque, 1999), trichlorophenol, pentachlorophenol and their derivative (Jafvert et al., 1990; B. E. Nowosielski & Fein, 1998) whereas the continually decreasing of K_{ow} with pH (dash line) was found in dichlorprop (Riise & Salbu, 1992) and pentachlorophenol (Kaiser & Valdmanis, 1982). The difference of $\log K_{ow}$ between neutral and ionic form ($\Delta \log K_{ow}$) of some chemicals has been reported, for example, 2.9 for chlorophenol (B. E. Nowosielski & Fein, 1998) and 2.2 for Dichlorprop (Riise & Salbu, 1992), which mean the neutral species are 100-1,000 times more hydrophobic than the ionized species. To measure K_{ow} of neutral species, the pH at $pK_a - 2$ was recommended. However, to measure the K_{ow}^- of ionic species, the measured pH will depend on the difference of hydrophobicity of neutral and ionic form, which closed to $pK_a + \log \frac{K_{ow}}{K_{ow}^-} + 2$. If $\log K_{ow}^-$ is very small, $\log \frac{K_{ow}}{K_{ow}^-}$ will become large and the pH that determine $\log K_{ow}^-$ will never reach (Kah & Brown, 2008).

The apparent octanol water partition coefficient is also affected by ionic strength and type of counter ions that present in aqueous phase. The ionized organic compounds may form the complex with these counter ions to neutralize their charge and partition in octanol or water as ion-pair which makes the partition coefficient more complicated. The apparent K_{ow}'' calculation that includes ion pairs can be expressed in Eq.2.15 (B. E. Nowosielski & Fein, 1998)

$$K_{ow}'' = \frac{[HA_{oc}] + [A_{oc}^-] + [MA_{oc}]}{[HA_w] + [A_w^-] + [MA_w]} \quad (2.15)$$

Where $[MA_{oc}]$ and $[MA_w]$ is ion-pair between monovalent inorganic cation and ionized organic species in octanol phase and aqueous phase, respectively.

Many studies showed that K_{ow} of some organic acids was a function of ionic strength. They found that, at pH large higher than pK_a where the anion form dominated, the K_{ow} will linearly increase with increasing ionic strength on the log scale as shown in Figure 2.3 (Jafvert et al., 1990; B. E. Nowosielski & Fein, 1998). Moreover, K_{ow} for aqueous solution that contained divalent cations e.g. Ca^{2+} and Mg^{2+} were more than K_{ow} of solution contained monovalent cations e.g. Li^+ , Na^+ , K^+ . This indicated the organic acid anions can form the ion pair with cations in aqueous solution. More concentration of cations will give more chance to form the ion pairs and cross over from aqueous phase to octanol phase. This process will raise the K_{ow} (Jafvert et al., 1990; Lee, Rao, Nkedikizza, & Delfino, 1990; B. E. Nowosielski & Fein, 1998; Word, 2002).

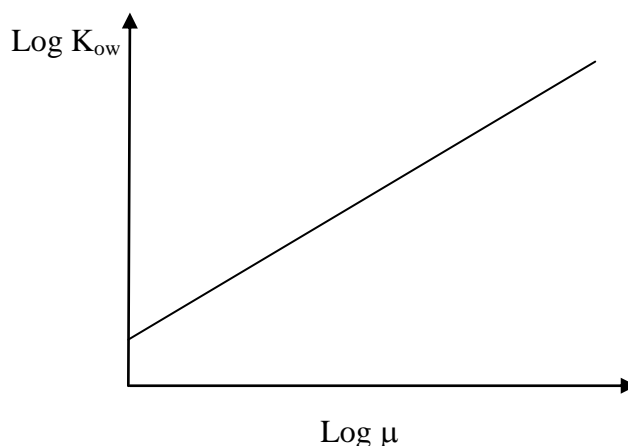


Figure 2.3 Log K_{ow} of organic acids as a function of log ionic strength (Log μ) (modified from B. E. Nowosielski & Fein, 1998)

2.3 Materials and methods

In this study, K_{ow} of Aristolochic acid I & II were measured by direct shake flask method, and indirect RP-HPLC method. Shake flask method is traditional and widely used to determine K_{ow} because it has good repeatability and reliable for the compounds with log K_{ow} between 0 - 4. Although the shake flask method give a reliable result but there are some deficiency especially when dealing with highly hydrophobic compounds. These chemicals will strongly partition into octanol phase and consequently have very low concentration in aqueous phase, so large amount of aqueous phase sample are required for analysis. Moreover, the agitation in shake flask method will produce large amount of droplet of octanol in the aqueous. These droplets may remain after phase separation which induce the overestimation of concentration in aqueous phase, so lower the actual K_{ow} (Brooke, Dobbs, & Williams, 1986). This method is not suitable for highly hydrophobic chemical (log K_{ow} > 4-5) (Debruijn, Busser, Seinen, & Hermens, 1989).

The RP-HPLC method is based on the principle the partitioning of chemical on stationary phase in column and mobile phase in HPLC column which is proportion to their octanol-water partition coefficient. The interaction of solute to hydrophobic stationary phase and hydrophilic mobile phase is similar to the interaction to octanol and aqueous phase. The low K_{ow} chemical will come first whereas the high K_{ow} will come last. This method gives good reproducibility but the accuracy will depend on the correctness of their reported K_{ow} of reference compounds. The set of these compounds have to select from the chemicals which have similar structure to the test chemical (Poole & Poole, 2003). Their K_{ow} also should cover the range of K_{ow} of the test chemical to minimize the error from extrapolation. Although, this method is convenient and cheap, it has limited for determining the K_{ow} of some complex chemicals because of lack of the reliable literature log K_{ow} of reference compounds.

2.3.1 K_{ow} by shake flask method

In general, the standard AAs were contacted with pre-saturated octanol and water in certain volume ratio and shake until reach equilibrium. After phase separation, the solute concentration were directly measured in both phase and K_{ow} can be calculated from concentration ratio between octanol to aqueous phase (Qiao, Xia, & Ma, 2008)

2.3.1.1 Buffer aqueous phase

Due to level of ionization depends on pH, so buffered solution was necessary to control the pH and form of AAs. The aqueous phase were prepared by mixing 10mM H_3PO_4 (pH=2) and 5 mM K_2HPO_4 (pH=9) and adjusted to desired pH by adding a small amount of 1 M HCl or NaOH .

2.3.1.2 Preparation of pre-saturation of aqueous and octanol phase

Before mixing, the two solvents, water and octanol had been pre-saturated with each other to reduce the changing of solvent volume. The octanol-saturated aqueous phase was prepared by adding 100 ml octanol to 100 ml of adjusted pH- buffered water. The mixture was shaken for 1 day in mechanical shaker and left standing for at least 1 day to separate the both phases. The saturated octanol phase and saturated aqueous phase were removed into individual bottles and these solutions were ready to use for shake flask experiment.

2.3.1.3 Analytical method and validation

The reverse-phase HPLC, Pelkin Elmer, equipped with Supelco Discovery C-18 column (25 cm x 4.6 mm, 5 μ m) and diode array detector (DAD) setting wavelength at 255 nm was used to measure AA I and II in octanol and aqueous phase. The mobile phase was pre-mixed solution between methanol and ultrapure water (70:30 of methanol: water) and adjusted the pH to 2.3 by adding aliquot of 85% orthophosphoric acid. The flow rate of mobile phase was constant at 1ml/min. The injection volume was 30 μ l by autosampler. The calibration curve of AA I & II in buffer solution and octanol were prepared separately. To prepare calibration curve, the series concentration of AAs standard solution were prepared separately in water and octanol and analyzed with HPLC-DAD. The linearity range and limit of detection (LOD) of both phases had been investigated. The LOD were determined by three time of signal to noise ratio (S/N).

2.3.1.4 Procedure

Octanol-water partition coefficient was determined by shake flask method following OECD 107(OECD, 1995). In 25 ml glass centrifuge tubes, the 10 ml of octanol-saturated water was overlaid by 5 ml of water- saturated octanol which contain AAs in different concentration

(the volumetric ratio of octanol to water was 1:2). Then, tubes were placed in mechanical shaker at 180 rpm and room temperature for 24 hr to reach equilibrium. To separate the phase, tubes were put in centrifuge machine and rotate at high 5,000 rpm for 15 min and allow to settle for 24 hr. Figure 2.4 shows the phase separation between octanol and aqueous phase. Then the sample in both phase were taken. The 100 μ l octanol sample was taken from the top layer by micropipette. The aqueous phase sample was taken by syringe with removable needle to minimize risk of including traces of octanol. Then, after removal the octanol phase, the pH of aqueous phase was measured by glass electrode pH meter, Orion 550A.



Figure 2.4 Octanol and aqueous phase separation in shake flask experiment (For the interpretation of the references to color in this and all other figures, the reader is referred to the electronic version of this dissertation)

The concentration of AA I and II were measured in both phase samples with RP-HPLC. The aqueous phase sample was directly measured whereas the octanol phase sample will be diluted 10 fold with methanol before measurement. The K_{ow} were calculated from AA I and II concentration ratio between octanol phase and aqueous phase. The mass balance calculation

indicated mass loss by adsorption to cap and tube was less than 10%. The experiment was done at room temperature.

2.3.1.5 pH and ionic strength effect

The experiment was set up similar to the procedure above except the buffered aqueous solution was adjusted pH from 2 to 11 by adding aliquot of 1M HCl or NaOH until it reach desired pH. The AAs stock solution at fixed concentration was added into octanol and then two solutions were mixed together. At equilibrium after taking the sample of both phase, the pH of aqueous phase were measured again as final pH. The obtained $\log K_{ow}$ were plotted with final pH and the non-linear regression according to Eq. 2.13 was fitted to experimental data by using template created in Excel spreadsheet. To determine effect of ionic strength, KCl was used as adjusting salt which was added to the pH adjusted buffer aqueous solution to vary the ionic strength from 0.01 - 1.0 M. The plot between $\log K_{ow}$ and pH in different ionic strength solution were compared.

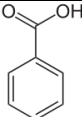
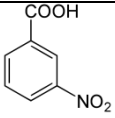
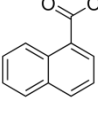
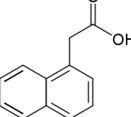
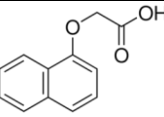
2.3.2 K_{ow} by RP-HPLC method

The K_{ow} were also determined by RP-HPLC method which followed to OECD 117(OECD, 1989). This experiment will be conducted by Pelkin Elmer Reverse phase HPLC model with binary pump and vacuum degasser, autosampler and Supelco Discovery C-18 column (25 cm x 4.6 mm, 5 μ m pore diameter). The six reference compounds were chosen from weakly ionizable monocarboxylic acids which have structure related to AAs and had the reported $\log K_{ow}$. The set of benzoic and naphthalene carboxylic acid and their derivatives were chosen as the reference standard because their structures are quite similar to AAs. Their structure, pK_a and $\log K_{ow}$ were shown in Table 2.1. These values were based on literature values tested by

shake flask method. These reference solutions at 0.1 mg/ml were prepared in methanol and inject to HPLC column. Their retention times (RT) were determined with Diode Array Detector at wavelength 255 nm.

Because these reference chemicals are ionizable, their retention times will be determined under phosphoric acid buffered mobile phase at pH 3 to suppress the ionization. The regression equation will be obtained from plotting between their Log K_{ow} (molecular form) and logarithm of retention time (log RT). The log K_{ow} of Aristolochic acid I and II were calculated from regression equation.

Table 2.1 The molecular structure and literature values of p K_a and log K_{ow} of reference compounds

Chemical	Structure	MW	pKa	Log Kow
benzoic acid		122.12	4.21 ^a	1.87 ^a
3-nitrobenzoic acid		167.12	3.46 ^a	1.83 ^a
1-naphthoic acid (1-naphthalene carboxylic acid)		172.18	3.69 ^b	3.1 ^b
1-naphthaleneacetic acid		186.2	4.24 ^c	2.24 ^d
1-naphthoxyacetic acid (1-Naphthoxyacetic acid)		202.2	3.18 ^e	2.60 ^d

a from Ming, Han, Qi, Sheng, & Lian, 2009; b from Han et al., 2012; c from Dippy, Hughes, & Laxton, 1954; d from Burgos & Pisutpaisal, 2006 ; e from "1-Naphthoxyacetic acid,"

2.4 Result and discussion

2.4.1 Ionization of Aristolochic acid

From the apparent K_{ow} equation (Eq. 2.13) and pK_a of AA I and II of 3.3 and 3.2(X. F. Fu et al., 2011) , we can calculate the speciation of neutral and ionized form correspond to pH as shown in Figure 2.5. It shows that, at $pH < 2$, most of AAs will be in neutral form but they will be most in ionized form at $pH > 6$. In natural environment where the pH is about 6-8, anions will be major form and contribute the behavior in the environment. The neutral and anion form behavior are expected to be different in term of water solubility, soil adsorption and mobility in environment.

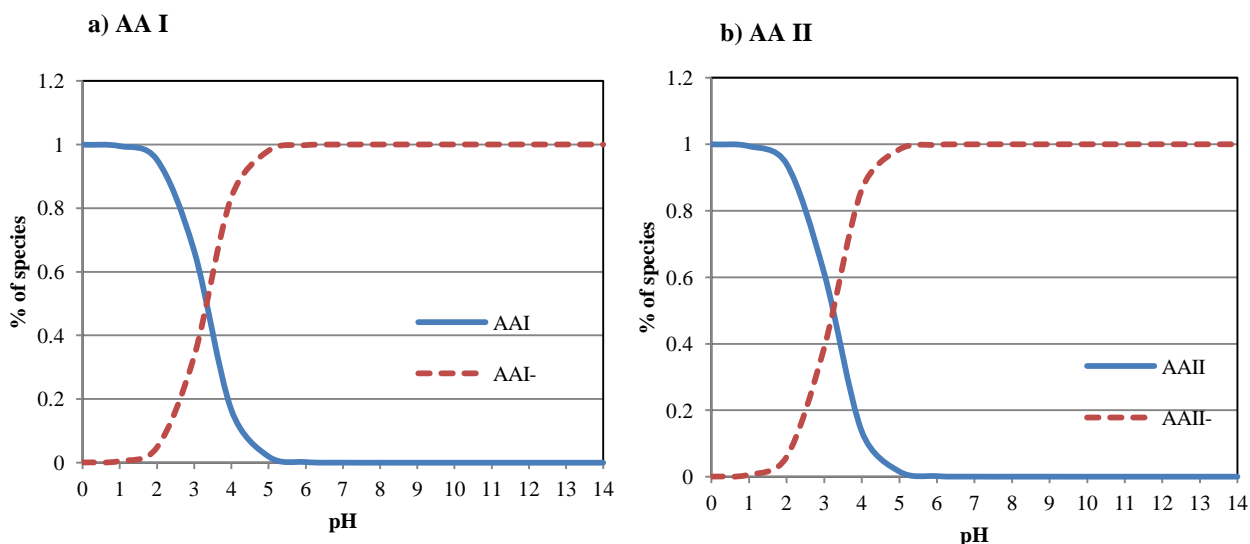


Figure 2.5 Aqueous speciation of Aristolochic acid I and II as function of pH

2.4.2 Calibration curve and validation

From Figure 2.6, the calibration curve of AA I and II were created from both aqueous and octanol phase. The figures showed linear line over concentration range 0.045 – 5.5 μ g/ml of AAs in both aqueous solution and octanol solution with r^2 over 0.999. The limit of detection (LOD)

of AA I and II were 0.01 and 0.014 $\mu\text{g/ml}$ in aqueous solution and 0.008 and 0.009 $\mu\text{g/ml}$ in octanol solution, respectively. This indicated HPLC with DAD detector had a good sensitivity and accuracy in analysis AAs in aqueous and octanol solution.

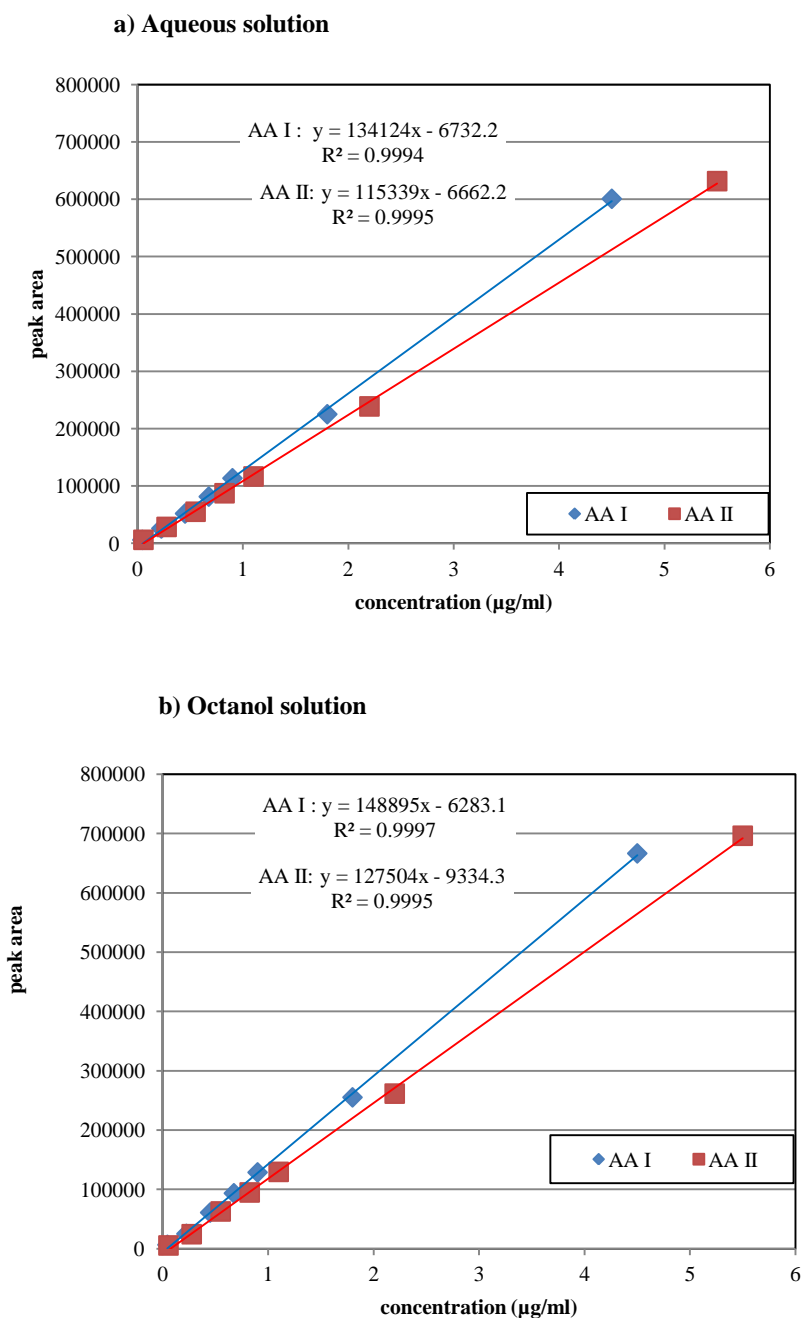


Figure 2.6 The calibration curve of AA I and II in aqueous (a) and octanol (b) solution

2.4.3 Log K_{ow} by shake flask method

The K_{ow} of AAs was determined by shake flask method at different three initial concentrations and native pH of 5-6. The results are shown in Table 2.2. The measured log K_{ow} of AA I and II were quite constant at different initial concentration. The average log K_{ow} of AA I and II were 1.65 and 1.23, respectively which indicate AAs were likely to partition in water. These K_{ow} are lower than K_{ow} of normal PAHs structure compounds such as naphthalene and phenanthrene which expected from weakly acid property of AAs. Log K_{ow} of AA I was more than AA II. This expects to cause by one more alkyl branch on the AA I molecule structure that bring AA I more hydrophobic.

Table 2.2 The log K_{ow} of AA I and II by shake flask method at three different concentrations

AAs Spiked amount (μg)	pH	Log K_{ow}	
		AAI	AAII
80	6.60	1.64	1.24
120	5.66	1.65	1.22
160	5.88	1.66	1.22
Average	6.05	1.65	1.23

2.4.4 pH and ionic strength effect

Figure 2.7 shows the apparent octanol water coefficient ($\log K_{ow}''$) of AA I & II as a function of pH of aqueous solution. At the $\text{pH} < 3$, the $\log K_{ow}''$ was high and independent to pH. However, when the pH increased, the $\log K_{ow}''$ linearly decreased for 4 orders of magnitude until after pH 9, it was independent to pH again. The data were fitted well to the Eq.2.13 with correlation coefficient (r^2) > 0.99. The figures indicated $\log K_{ow}$ of AA I and II were 3.85 and 3.63 for neutral form and -0.55 and -0.85 for anion form, respectively. The $\log K_{ow}$ of neutral form and anion form were 4 log unit or 10,000 times difference. The neutral form of AAs is very hydrophobic and has high affinity to octanol phase whereas the ionized form is highly hydrophilic and has high affinity to water. This indicated that a pH is very important factor that control AAs behavior in environment.

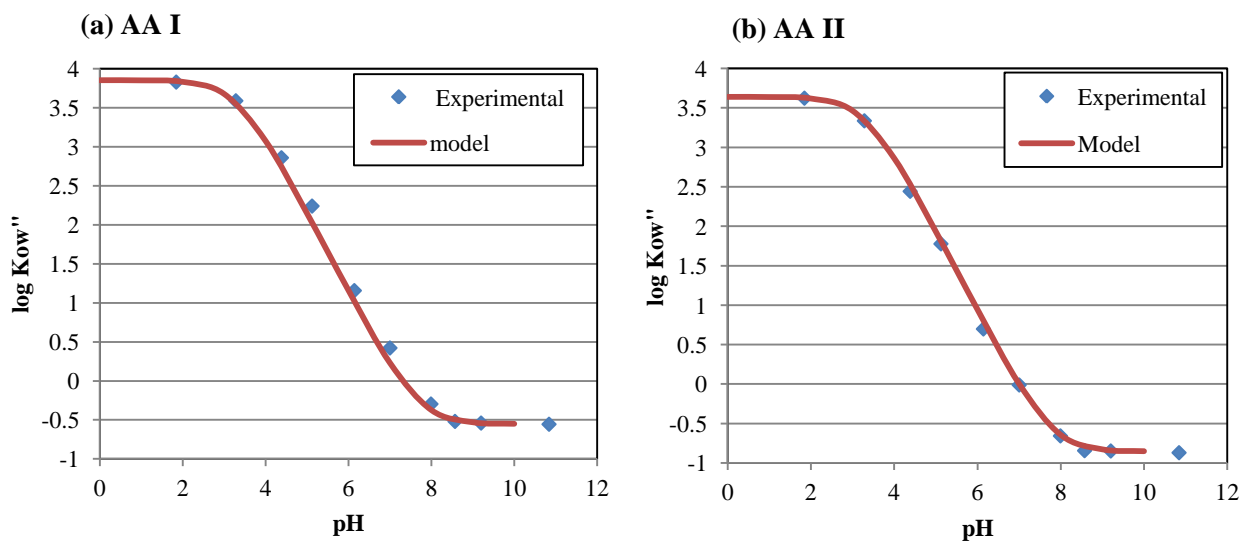


Figure 2.7 Experimental $\log K_{ow}''$ and the fitted model curve versus pH after equilibrium: AA I (a) and AA II (b)

From fitted parameter (K_{ow} and K_{ow}^-) with Eq. 2.13, K_{ow} of AA I and II at various pH can be calculated by Eq. 2.16 and 2.17.

$$AA I : K_{ow}'' = \frac{7,094 + 0.28 \times 10^{(pH-3.3)}}{1 + 10^{(pH-3.3)}} \quad (2.16)$$

$$AA II : K_{ow}'' = \frac{4,339 + 0.14 \times 10^{(pH-3.2)}}{1 + 10^{(pH-3.2)}} \quad (2.17)$$

Figure 2.8 shows effect of ionic strength on $\log K_{ow}''$ over range of pH. It shows that ionic strength had no effect when the pH was low or most molecules were in neutral form. However, ionic strength had obvious effect at the high pH or most molecules were in anion form where the increasing of ionic strength caused increasing of $\log K_{ow}$. This evidence indicated that the complexation between cations (in this case K^+) and AA^- is possible and negative charge of AAs was turned to be neutral and caused AAs transfer to octanol phase. This finding was according to the ion pair transfer mechanism to maintain the electroneutrality of the solution (Word, 2002).

The plotting of $\log K_{ow}$ of anion form (at $pH > 10$) with logarithm of ionic strength in solution shows the linear relationship as shown in Figure 2.9. This finding agreed with previous studies which indicated the K_{ow} of organic anions linearly increased with increasing ionic strength on the log scale (Jafvert et al., 1990; B. E. Nowosielski & Fein, 1998). The results suggest that cations in soil solution can alter mobility of AAs in environment especially in alkaline condition. The regression equations of AA I and II had similar slope 0.6 and the equations can be used to predict $\log K_{ow}$ at other ionic strengths.

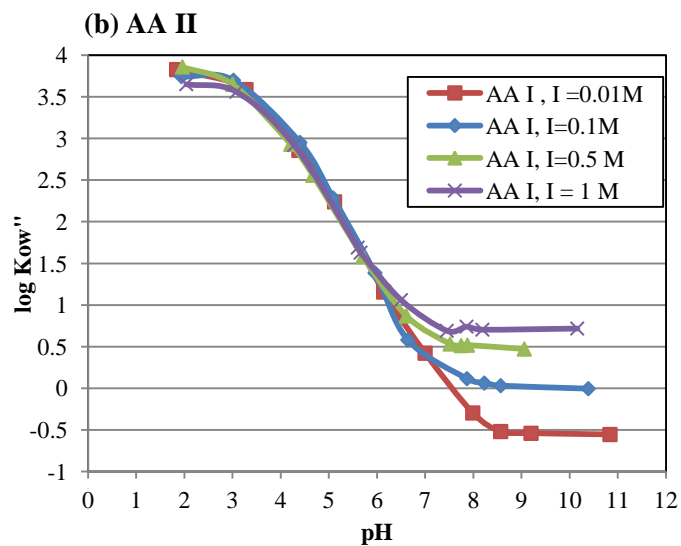
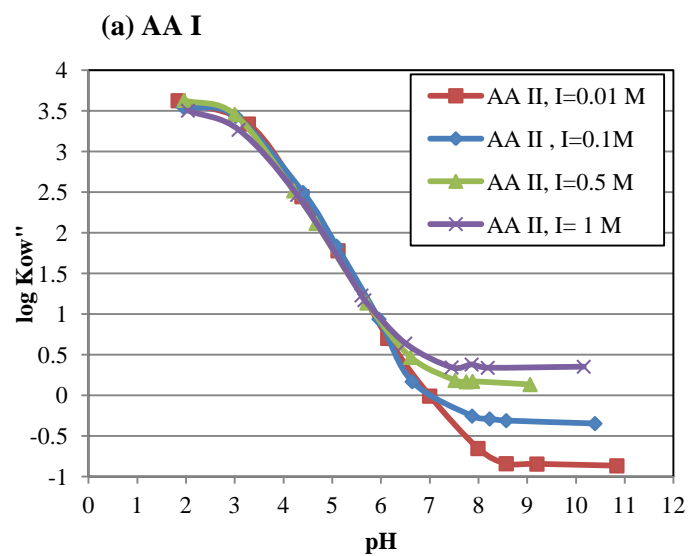


Figure 2.8 Experimental $\log Kow''$ and fitted model at different ionic strength in aqueous phase: AA I (a) and AA II (b)

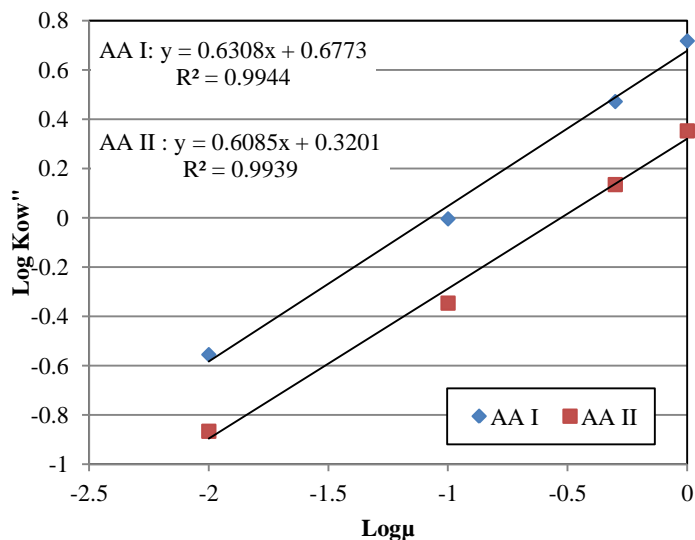


Figure 2.9 Log K_{ow}'' of anion of AA I and II at high pH as a function of logarithm of ionic strength (Log μ)

2.4.5 Log K_{ow} by HPLC method

To measure log K_{ow} by HPLC method, the reference compounds and AA I and II were injected to C-18 column with isocratic mobile phase (methanol: water is 70:30) at the pH 3. The retention time (RT) of their peaks and log K_{ow} are shown in Table 2.3. The RT found to increase with the molecular weight and log K_{ow} of compounds which is general trend for hydrophobic chemicals. Figure 2.10 shows the relationship between logarithm of retention time and log K_{ow} of reference compounds and AA I and II. The RT of AA I and II were over RT from reference compounds because of the larger size of molecules. The reference compounds that had molecular weight more than AA I and II and had reported log K_{ow} by shake flask method from literatures were not found. The linear regression gave equation: $\log K_{ow} = 7.14\log RT - 2.61$. The log K_{ow} of AA I and II calculated from this regression equation were 3.71 and 3.27, respectively. The low correlation coefficient ($r^2 = 0.69$) was expected from the unclear degree of ionization of reference compounds from literatures which resulted in uncertainty of obtained K_{ow} value. This

method quite sensitive to the correctness of K_{ow} of reference compounds (Chamberlain, Evans, & Bromilow, 1996; Paschke, Neitzel, Walther, & Schuurmann, 2004).

Table 2.3 The log K_{ow} of reference compounds and their retention time from RP-HPLC system

Chemical	MW	pK _a	Log K _{ow}	RT
benzoic acid	122.12	4.21	1.87	4.11
3-nitrobenzoic acid	167.12	3.46	1.83	4.33
1-naphthoic acid (1-naphthalene carboxylic acid)	172.18	3.69	3.1	5.4
1-naphthaleneacetic acid	186.2	4.24	2.24	5.18
1-naphthoxyacetic acid (1-naphthyloxyacetic acid)	202.2	3.18	2.60	5.7
AA I	341.27	3.3	-	7.66
AA II	311.25	3.2	-	6.64

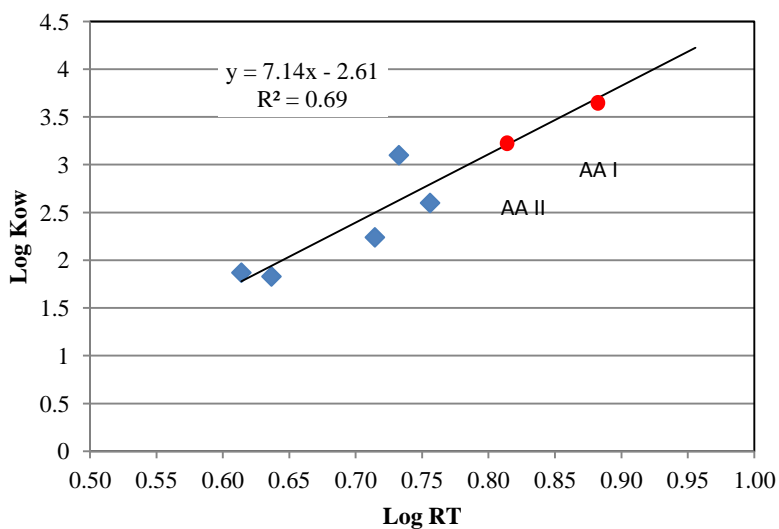


Figure 2.10 The linear correlation between log K_{ow} and log RT of reference compounds and the extrapolation of AA I and II

2.5 Conclusion

This study had measured octanol-water partition coefficient of AA I and II by direct shake flask method and indirect HPLC method. The shake flask method gives reliable K_{ow} if concentrations in both phases are over the detection limit of analytical method. At natural pH, the K_{ow} of AA I and II were 1.65 and 1.23 which indicated AAs were quite hydrophilic. The K_{ow} obtained from HPLC method was questionable because of lacking the accuracy reported K_{ow} of reference compounds. K_{ow} of AAs was strongly effect by the pH where the K_{ow} decreased when pH increased. The AAs in acid solution were very hydrophobic ($\log K_{ow} > 3$) but they were very hydrophilic in basic solution ($\log K_{ow} < 0$). At high pH where most molecules were in anion form, the K_{ow} increased when ionic strength increased. This expected from the complex formation between anion of AAs and counter cation. This study shows that the prediction fate and transport of AAs in environment need to account for the pH and ionic strength of surrounding media.

REFERENCES

REFERENCES

- 1-Naphthoxyacetic acid. Retrieved March 10, 2013, from http://www.chemexper.net/specification_d/chemicals/supplier/cas/1-Naphthoxyacetic%20acid.asp
- Berthod, A., Carda-Broch, S., & Garcia-Alvarez-Coque, M. C. (1999). Hydrophobicity of ionizable compounds. A theoretical study and measurements of diuretic octanol-water partition coefficients by countercurrent chromatography. *Analytical Chemistry*, *71*(4), 879-888. doi: 10.1021/ac9810563
- Brandt, C. A., Becker, J. M., & Porta, A. (2002). Distribution of polycyclic aromatic hydrocarbons in soils and terrestrial biota after a spill of crude oil in Trecate, Italy. *Environmental Toxicology and Chemistry*, *21*(8), 1638-1643. doi: 10.1897/1551-5028(2002)021<1638:dopahi>2.0.co;2
- Briggs, G. G., Bromilow, R. H., Evans, A. A., & Williams, M. (1983). RELATIONSHIPS BETWEEN LIPOPHILICITY AND THE DISTRIBUTION OF NON-IONIZED CHEMICALS IN BARLEY SHOOTS FOLLOWING UPTAKE BY THE ROOTS. *Pesticide Science*, *14*(5), 492-500. doi: 10.1002/ps.2780140506
- Brooke, D. N., Dobbs, A. J., & Williams, N. (1986). OCTANOL - WATER PARTITION COEFFICIENTS(P) - MEASUREMENT, ESTIMATION, AND INTERPRETATION, PARTICULARLY FOR CHEMICALS WITH P-GREATER THAN-10(5). *Ecotoxicology and Environmental Safety*, *11*(3), 251-260. doi: 10.1016/0147-6513(86)90099-0
- Burgos, W. D., & Pisutpaisal, N. (2006). Sorption of naphthoic acids and quinoline compounds to estuarine sediment. *Journal of Contaminant Hydrology*, *84*(3-4), 107-126. doi: 10.1016/j.jconhyd.2005.12.008
- Chamberlain, K., Evans, A. A., & Bromilow, R. H. (1996). 1-octanol/water partition coefficient (K_{ow}) and pK(a) for ionisable pesticides measured by a pH-metric method. *Pesticide Science*, *47*(3), 265-271. doi: 10.1002/(sici)1096-9063(199607)47:3<265::aid-ps416>3.0.co;2-f
- Debruijn, J., Busser, F., Seinen, W., & Hermens, J. (1989). DETERMINATION OF OCTANOL WATER PARTITION-COEFFICIENTS FOR HYDROPHOBIC ORGANIC-CHEMICALS WITH THE SLOW-STIRRING METHOD. *Environmental Toxicology and Chemistry*, *8*(6), 499-512. doi: 10.1897/1552-8618(1989)8[499:dowpcf]2.0.co;2
- Dettenmaier, E. M., Doucette, W. J., & Bugbee, B. (2009). Chemical Hydrophobicity and Uptake by Plant Roots. *Environmental Science & Technology*, *43*(2), 324-329. doi: 10.1021/es801751x

- Dippy, J. F. J., Hughes, S. R. C., & Laxton, J. W. (1954). CHEMICAL CONSTITUTION AND THE DISSOCIATION CONSTANTS OF MONOCARBOXYLIC ACIDS .14. MONOMETHYLCYCLOHEXANECARBOXYLIC ACIDS. *Journal of the Chemical Society(DEC)*, 4102-4106. doi: 10.1039/jr9540004102
- Fisk, A. T., Norstrom, R. J., Cymbalisky, C. D., & Muir, D. C. G. (1998). Dietary accumulation and depuration of hydrophobic organochlorines: Bioaccumulation parameters and their relationship with the octanol/water partition coefficient. *Environmental Toxicology and Chemistry*, 17(5), 951-961. doi: 10.1897/1551-5028(1998)017<0951:daadoh>2.3.co;2
- Fu, X. F., Liu, Y., Li, W., Bai, Y., Liao, Y. P., & Liu, H. W. (2011). Determination of dissociation constants of aristolochic acid I and II by capillary electrophoresis with carboxymethyl chitosan-coated capillary. *Talanta*, 85(1), 813-815. doi: 10.1016/j.talanta.2011.03.088
- Han, S. Y., Qiao, J. Q., Zhang, Y. Y., Lian, H. Z., & Ge, X. (2012). Determination of n-octanol/water partition coefficients of weak ionizable solutes by RP-HPLC with neutral model compounds. *Talanta*, 97, 355-361. doi: 10.1016/j.talanta.2012.04.045
- Jafvert, C. T., Westall, J. C., Grieder, E., & Schwarzenbach, R. P. (1990). DISTRIBUTION OF HYDROPHOBIC IONOGENIC ORGANIC-COMPOUNDS BETWEEN OCTANOL AND WATER - ORGANIC-ACIDS. *Environmental Science & Technology*, 24(12), 1795-1803. doi: 10.1021/es00082a002
- Kah, M., & Brown, C. D. (2006). Adsorption of ionisable pesticides in soils. *Reviews of Environmental Contamination and Toxicology, Vol 188*, 188. doi: 10.1007/978-0-387-32964-2_5
- Kah, M., & Brown, C. D. (2008). LogD: Lipophilicity for ionisable compounds. *Chemosphere*, 72(10), 1401-1408. doi: 10.1016/j.chemosphere.2008.04.074
- Kaiser, K. L. E., & Valdmans, I. (1982). APPARENT OCTANOL WATER PARTITION-COEFFICIENTS OF PENTACHLOROPHENOL AS A FUNCTION OF PH. *Canadian Journal of Chemistry-Revue Canadienne De Chimie*, 60(16), 2104-2106. doi: 10.1139/v82-300
- Karickhoff, S. W., Brown, D. S., & Scott, T. A. (1979). SORPTION OF HYDROPHOBIC POLLUTANTS ON NATURAL SEDIMENTS. *Water Research*, 13(3), 241-248. doi: 10.1016/0043-1354(79)90201-x
- Lee, L. S., Rao, P. S. C., Nkedikizza, P., & Delfino, J. J. (1990). INFLUENCE OF SOLVENT AND SORBENT CHARACTERISTICS ON DISTRIBUTION OF PENTACHLOROPHENOL IN OCTANOL-WATER AND SOIL-WATER SYSTEMS. *Environmental Science & Technology*, 24(5), 654-661. doi: 10.1021/es00075a006

- Ming, X., Han, S. Y., Qi, Z. C., Sheng, D., & Lian, H. Z. (2009). Chromatographic retention prediction and octanol-water partition coefficient determination of monobasic weak acidic compounds in ion-suppression reversed-phase liquid chromatography using acids as ion-suppressors. *Talanta*, 79(3), 752-761. doi: 10.1016/j.talanta.2009.04.069
- Ney, R. E. (1995). *Fate and transport of organic chemicals in the environment : a practical guide* (2nd ed.). Rockville, Md.: Government Institutes.
- Nowosielski, B. E. (1998). *Experimental study of octanol-water partition coefficients for 2,4,6-trichlorophenol and pentachlorophenol: Derivation of an empirical model of chlorophenol partitioning behaviour*. (M.Sc. MQ44235), McGill University (Canada), Canada. Retrieved from <http://ezproxy.msu.edu/login?url=http://search.proquest.com/docview/304504053?accountid=12598> ProQuest Dissertations & Theses (PQDT); ProQuest Dissertations & Theses A&I database.
- Nowosielski, B. E., & Fein, J. B. (1998). Experimental study of octanol-water partition coefficients for 2,4,6-trichlorophenol and pentachlorophenol: Derivation of an empirical model of chlorophenol partitioning behaviour. *Applied Geochemistry*, 13(7), 893-904. doi: 10.1016/s0883-2927(98)00015-8
- OECD. (1989). OECD Guideline for the testing of chemicals *Partition Coefficient (n-octanol/water), High Performance Liquid Chromatography (HPLC) Method*.
- OECD. (1995). OECD Guideline for the testing of chemicals *Partition Coefficient (n-octanol/water): Shake Flask Method*.
- Paschke, A., Neitzel, P. L., Walther, W., & Schuurmann, G. (2004). Octanol/water partition coefficient of selected herbicides: Determination using shake-flask method and reversed-phase high-performance liquid chromatography. *Journal of Chemical and Engineering Data*, 49(6), 1639-1642. doi: 10.1021/je049947x
- Poole, S. K., & Poole, C. F. (2003). Separation methods for estimating octanol-water partition coefficients. *Journal of Chromatography B-Analytical Technologies in the Biomedical and Life Sciences*, 797(1-2), 3-19. doi: 10.1016/j.jchromb.2003.08.032
- Qiao, Y., Xia, S., & Ma, P. (2008). Octanol/water partition coefficient of substituted benzene derivatives containing halogens and carboxyls: Determination using the shake-flask method and estimation using the fragment method. *Journal of Chemical and Engineering Data*, 53(1), 280-282. doi: 10.1021/je700381u
- Riise, G., & Salbu, B. (1992). MOBILITY OF DICHLORPROP IN THE SOIL-WATER SYSTEM AS A FUNCTION OF DIFFERENT ENVIRONMENTAL-FACTORS .1. A BATCH EXPERIMENT. *Science of the Total Environment*, 123, 399-409. doi: 10.1016/0048-9697(92)90163-m

- Schwarzenbach, R. P., Gschwend, P. M., & Imboden, D. M. (2003). *Environmental Organic Chemistry* (2nd Ed.). New Jersey: John Wiley & Sons, Inc.
- Schwarzenbach, R. P., & Westall, J. (1981). TRANSPORT OF NON-POLAR ORGANIC-COMPOUNDS FROM SURFACE-WATER TO GROUNDWATER - LABORATORY SORPTION STUDIES. *Environmental Science & Technology*, 15(11), 1360-1367. doi: 10.1021/es00093a009
- VCCLAB. (2011). Virtual Computational Chemistry Laboratory. 2012, from <http://www.vcclab.org/lab/alogps/>
- Veith, G. D., Call, D. J., & Brooke, L. T. (1983). STRUCTURE TOXICITY RELATIONSHIPS FOR THE FATHEAD MINNOW, PIMEPHALES-PROMELAS - NARCOTIC INDUSTRIAL-CHEMICALS. *Canadian Journal of Fisheries and Aquatic Sciences*, 40(6), 743-748.
- Westall, J. C., Leuenberger, C., & Schwarzenbach, R. P. (1985). INFLUENCE OF PH AND IONIC-STRENGTH ON THE AQUEOUS NONAQUEOUS DISTRIBUTION OF CHLORINATED PHENOLS. *Environmental Science & Technology*, 19(2), 193-198. doi: 10.1021/es00132a014
- Word, R. C. (2002). *Partition of ionized and neutral halogenated phenols between octanol and water, lipid membranes and water, and sarcoplasmic reticulum and water*. (Doctor of Philosophy), Portland State University.
- Yuying, D., Guanghui, D., Ying, C., Zhuang, W., & Cheng, S. (2009). Determination and estimation of partitioning properties for substituted phosphates and thiophosphates. *Environmental Monitoring and Assessment*, 152(1-4), 443-450. doi: 10.1007/s10661-008-0328-0

Chapter 3

Aqueous solubility

3.1 Introduction

Aqueous solubility is an important parameter that controls many fate and transport processes such as soil adsorption, complexation, bioaccumulation and plant uptake. It determines amount of chemicals that can be available in environment (P.G. Wightman, 1997). It predicts how much of chemicals can be leach into groundwater or runoff with surface water. It is also related to the aqueous phase partitioning properties such as octanol-water partition coefficient (K_{ow}) or soil-water partition coefficient (K_d) (Arcand, Hawari, & Guiot, 1995). Due to its importance to environmental processes, the knowledge about the solubility of organic pollutants is necessary (M. T. C. Figueroa, 1989)(M. T. C. Figueroa, 1989).

The definition of aqueous solubility is amount of chemicals (solids, liquids and gases) that equilibrated as pure phase in the water. It is the saturation concentration where chemicals can be dissolved in pure water at given temperature. For non-polar hydrophobic compounds, solubility mainly effect by temperature and dissolved inorganic salt. The increasing of temperature will increase the solubility of solid due to less energy required to melt the solid at high temperature. In general, the presence of inorganic ions such as Na, K, Mg, Ca, Cl, HCO_3 , SO_4 will decrease solubility by increasing activity coefficient of compounds which referred as “salting out” effect. The presence of highly water soluble organic compounds e.g. methanol ethanol can increase the solubility of organic solid by “cosolvent” phenomenon (R.P. Schwarzenbach et al., 2003).

Unlike the non-polar hydrophobic chemicals, the solubility of ionized organic chemicals was largely affected by pH because of different forms of solute molecules, other than temperature. The ionic strength and the presence of other ions also had been reported to alter the solubility by affecting their activity coefficient (M. T. C. Figueroa, 1989). The ion-pair formation between organic and inorganic were reported which raise the solubility of ionized organic compounds. Moreover, the complexation may alter the sorption properties of both metal and organic acids by changing their electrostatic charge which affect the mobility of these chemicals in environment (Daughney & Fein, 1997).

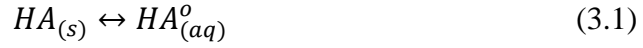
Due to the solubility of AAs in aqueous phase can govern many processes, so the knowledge about aqueous solubility behavior of AAs is essential. Since environmental factors such as pH, ion presence, ionic strength affected the solubility, so these dependence parameters were also included in this study.

3.2 Literature reviews

3.2.1 Solubility of organic acids and pH effect

Organic acids when dissolved in water can be dissociated as ionized molecules and can exist as 2 forms, neutral and ionized. The aqueous solubility among these 2 forms was reported to be largely different. Generally, the neutral molecules are relative hydrophobic and not likely to dissolve in water and their solubility are independent to pH. In the other hand, the charged molecules are very polar and interact with water very well and then high solubility (Arcand et al., 1995; P. G. Wightman & Fein, 1999).

To develop the model to estimate solubility of organic acid, we assume the organic acid solid phase is dissolved in water until equilibrium as Eq.3.1. This dissolved organic acids (HA) can be dissociated when $\text{pH} > \text{pK}_a$ as anion species and proton as Eq. 3.2.



The total solubility of organic acids is the summation of molality of unionized and ionized species which express as Eq. 3.3 (P.G. Wightman, 1997).

$$[HA_{total}] = [HA^o] + [A^-] \quad (3.3)$$

From dissociation constant (K_a) equation of the acid which is expressed in Eq 3.4, it can be rearrange to present in term of molarity of anion in Eq. 3.5 by assuming activity coefficient of neutral species equal to 1.

$$K_a = \frac{\gamma_{A^-}[A^-]\gamma_{H^+}[H^+]}{[HA^o]} \quad (3.4)$$

$$[A^-] = \frac{K_a[HA_{(aq)}^o]}{\gamma_{A^-}\gamma_{H^+}[H^+]} \quad (3.5)$$

From $\gamma_{H^+}[H^+] = 10^{-\text{pH}}$ and $K_a = 10^{-\text{pK}_a}$, and assuming $\gamma_{A^-} = 1$ in dilute solution, the molarity of anion can be written as Eq.3.6

$$[A^-] = [HA_{(aq)}^o](10^{\text{pH}-\text{pK}_a}) \quad (3.6)$$

Put this term in Eq. 3.3, and finally the total solubility will be expressed as Eq. 3.7.

$$[HA_{total}] = [HA_{(aq)}^o](1 + 10^{\text{pH}-\text{pK}_a}) \quad (3.7)$$

This equation is very useful to estimate the solubility of organic acids at any pH when $[HA^0_{(aq)}]$ and pK_a are known (Arcand et al., 1995; P. G. Wightman & Fein, 1999). For example, Wightman & Fein, 1999 showed this model were fitted well with pentachlorophenol (PCP) solubility data as shown in Figure 3.1.

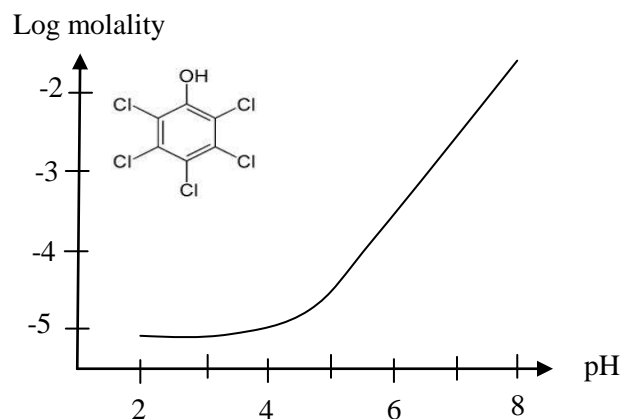


Figure 3.1 Pentachlorophenol (PCP) solubility as a function of pH (modified from Wightman & Fein, 1999)

This figure shows that the solubility increase when the pH increase. At $pH < 4$, the solubility is constant which indicates the solubility of undissociated form is not effect by pH. At $pH > 5$, the log solubility increase with pH and close to linear relationship.

However, this equation is best applied in pure water or dilute electrolyte solution, it could not be generalized to concentrated electrolyte solution. Wightman, 1999 showed the solubility of PCP was enhanced and deviated out from the linear line at high pH and high concentration of salts. This non-linear increasing was explained by metal-PCP complex formation.

3.2.2 The ionic strength, ions presence and complexation formation effect

In non-dilute electrolyte solution, the activity coefficient of ionized compounds (γ_{A^-}) in Eq.3.5 is not equal to 1 and the solubility will be effected by ionic strength by changing their activity coefficient.

From Debye-Huckle equation, the activity coefficient (γ) were related to ionic strength as shown in Eq.3.8 (M. T. C. Figueroa, 1989).

$$-\log \gamma_i = \frac{0.507I^{1/2}}{1+1.5I^{1/2}} \quad (3.8)$$

Hence, from combining between Eq. (5) and (7) , the solubility can be related to ionic strength as shown Eq. 3.9. This equation shows the solubility will increase with increasing ionic strength.

$$[HA_{total}] = [HA_{(aq)}^o] \left(1 + 10^{pH - pKa + \frac{0.507I^{1/2}}{1+1.5I^{1/2}}}\right) \quad (3.9)$$

The presence of different ions also has influence to solubility of organic acids. Some studies show the organic acids have high tendency to form the complex with metal that dissolved in the solution (Daughney & Fein, 1997; P. G. Wightman & Fein, 1999). The metal – organic acid complexes were known to exist in aqueous solution that contains the anion and metal in high concentration. These complexes can enhance the solubility of organic acids. The potentiometric studies which measure activities of free metal ions e.g. Cd^{2+} , Cu^{2+} in solution that contain organic acids showed the activity of free metals decreased when the concentration of organic acids increased which was expected from complexation between metals and organic anion (Daughney & Fein, 1997).

Wightman, 1997 found that the solubility of PCP at high salt and high pH condition were largely increased which cannot be described by only ionic strength effect but also with the presence of metal-PCP complex. To incorporate the complexation to the model, Daughney & Fein, 1997 and Wightman & Fein, 1999 introduce the 1:1 complexation model between monovalent metals (M^+) with anion of organic acids (A^-) where equilibrium reaction at fixed temperature and pressure was shown in Eq. 3.10



Where the stability constant (K) express as:

$$K = \frac{[MA_{(aq)}^o]}{\gamma_{M^+}[M^+]\gamma_{A^-}[A^-]} \quad (3.11)$$

$$[MA_{(aq)}^o] = K\gamma_{M^+}[M^+]\gamma_{A^-}[A^-] \quad (3.12)$$

The metal-organic complex activity was accounted in mass balance equation which shows in Eq.3.13. The model that included metal-organic complex found to fit with experimental data very well.

$$[HA_{total}] = [HA^o] + [A^-] + [MA^o] \quad (3.13)$$

The degree of increasing solubility by the complexation found to depend on the strength of stability constant between organic acids and metal cations. The strength of stability constant determine by the polarizing effect of cations which increase with increasing the charge (Z) and decreasing of radius (r) of cations or combine as ratio Z/r. So, the stability constants of monovalent cations are expect to be less than divalent or trivalent cations (Orlov & Belkina, 2011). Mantoura et al. 1978 had determined the stability constant of the complexes of humic

material and metals. They found that the order of stability constant follow to the Irving-William series e.g. $Mg^{2+} < Ca^{2+} < Cd^{2+} \sim Mn^{2+} < Co^{2+} < Zn^{2+} \sim Ni^{2+} < Cu^{2+} < Hg^{2+}$. With high stability constant of Cu^{2+} and Hg^{2+} , more than 90% of Cu and Hg were found as a complex with humic material, whereas less than 10% of other ions can formed the complex. However, in seawater, more than 99% of humic acids were form the complex with Ca^{2+} and Mg^{2+} due to their high concentration.

3.3 Materials and Methods

To determine the aqueous solubility of AAs, the conventional batch equilibration method was selected to prepare saturated solution of AAs following OECD 105 (OECD, 1995).

Generally, the excess amounts of AAs were added to solution and gently shaking until reach equilibrium. After equilibrium, the undissolved AAs were separated from the solution and the supernatant were analyzed for saturation concentration.

3.3.1 The kinetic test and calcium ion effect

The standard AAs 0.5 mg (excess amount) was dissolved in 10 ml of pure water and 0.01 M $CaCl_2$ solution. The solution was put in glass centrifuge tube, place in the orbital shaker at 180 rpm at room temperature (20-25 °c) and keep out from the light. The aliquot samples were taken at 24 hr after contacting where tubes were centrifuged at 7,500 rpm for 20 min to separate undissolved solid AAs. After take the samples, tubes were shaken again and the samples were taken at day 3, 5, 7, 9 and 11. At final sample (day 11), the pH of supernatant was measured by pH meter, ORION electrode. The samples were analysis in same manner of octanol-water coefficient experiment.

3.3.2 The pH effect

Solubility of AAs were measured at different pH by dissolving 0.5 mg AAs in 10 ml buffered solution prepared by mixing of H_3PO_4 0.01M and K_2HPO_4 0.01M at different ratio. The pH and mixing ratio were shown in Table 3.1. After placing in shaking machine, the samples were taken at day 7 (was reach equilibrium from kinetic study). The shaking condition, taking sample and analysis procedure were similar to kinetic experiment and final pH of supernatant was measured after taking sample.

Table 3.1 The pH of buffer solution and mixing ratio between H_3PO_4 0.01M and K_2HPO_4 0.01M

H_3PO_4 0.01M	K_2HPO_4 0.01M	pH
20 ml	5 ml	2.61
15 ml	10ml	3.26
14 ml	11 ml	4.32
12.5 ml	12.5 ml	5.61
10 ml	15 ml	6.52
5 ml	20 ml	7.21
2 ml	23 ml	7.91
0 ml	25ml	9.20

3.3.3 The type of cation and ionic strength effect

The influence of cation type to solubility was tested by dissolving AAs 0.5 mg in 10 ml. of NaCl , KCl , CaCl_2 , MgCl_2 , SrCl_2 solution which already buffered with H_3PO_4 and K_2HPO_4 at pH 5.61 (1:1 ratio). For each type of cations, salts were varied at 5 different concentrations 0.005, 0.01, 0.05, 0.1, 0.5 M to see the effect of ionic strength. All samples were equilibrated on mechanical shaker for 7 days at 180 rpm at room temperature and keep out of the light before taking the sample.

3.4 Result and discussion

3.4.1 Kinetic study and calcium ion effect

The kinetic of dissolution of AAs were tested by using pure water and 0.01M CaCl₂ solution as a solvent and equilibrated for 11 days. Figure 3.2 shows the dissolved AAs concentration as a function of time. AAs dissolution in pure water was quite slow process where the concentration gradually increased when time proceeded. The dissolution of AAs in CaCl₂ solution was faster and larger than dissolution in pure water. This dissolution enhancement suggested the complex formation between AAs and Ca²⁺ ion according to the metal-organic acids complexation concept in literature (P. G. Wightman & Fein, 1999). Figure 3.3 compares the solubility of AA I and II in both pure water and CaCl₂ solution which indicated AA II can get more dissolution than AA I. This expected as a result from higher polarity and low hydrophobicity of AA II.

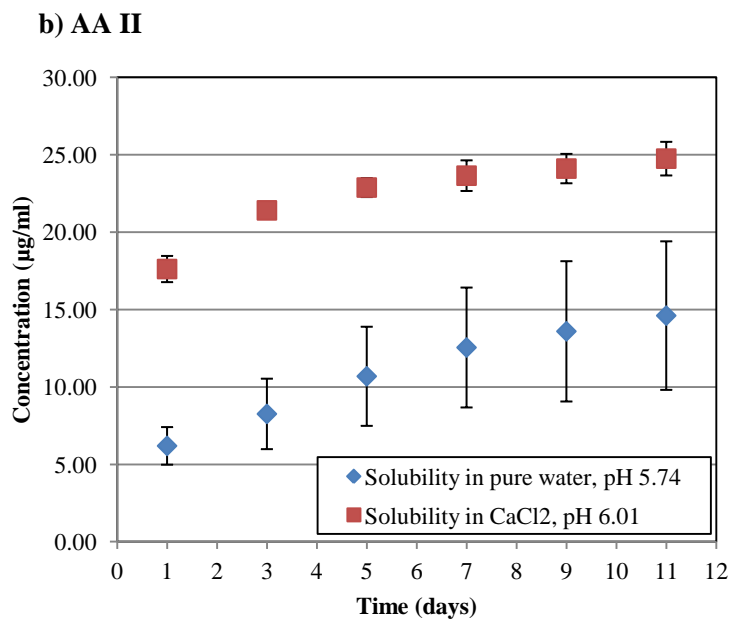
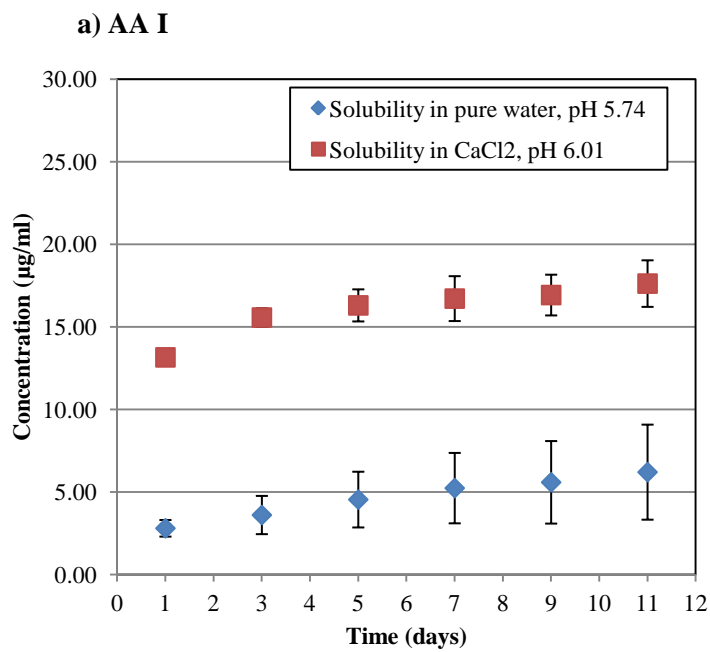


Figure 3.2 Concentration of AA I (a) and AA II (b) dissolved in pure water and CaCl₂ 0.01M as a function of time

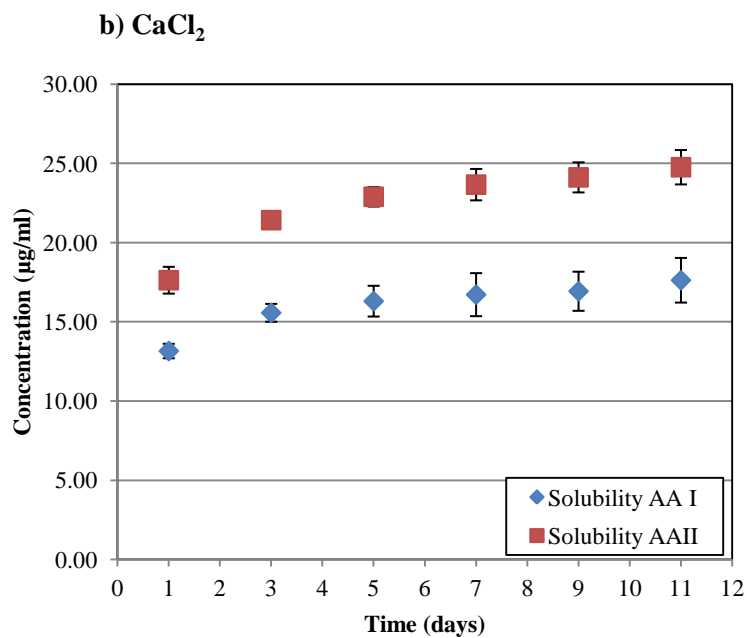
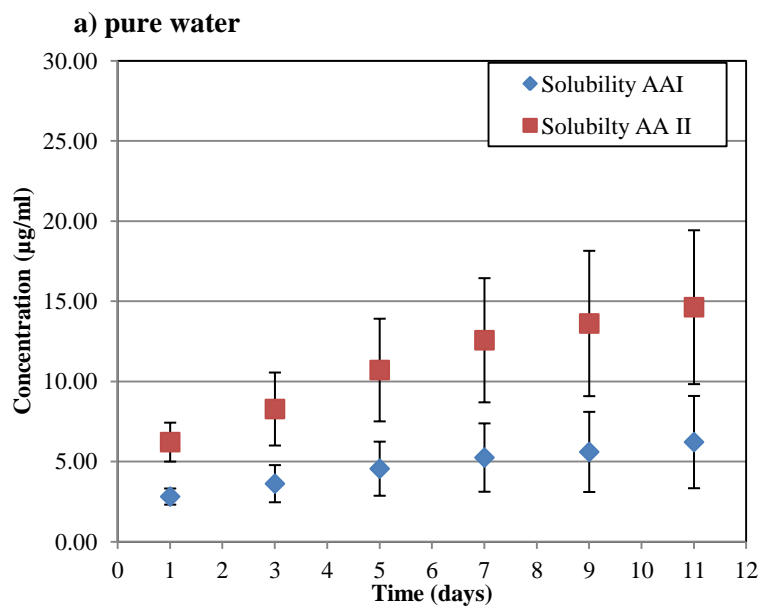


Figure 3.3 Concentration AA I and II dissolved in pure water (a) and CaCl₂ solution (b) as a function of time

3.4.2 The pH effect

Figure 3.4 shows the solubility of AA I and II as a function of pH and the fitted curve model with Eq.3.7. From this figure, the solubility of AA I and II were highly depended on the pH where the solubility increased when pH increased. However, due to the limit of pH of buffer solution, the solubility at extremely low pH and high pH were not determined. The AAs in anion form at high pH had higher solubility than neutral form at low pH 1-2 orders of magnitude which indicated anion of AAs can interact with water very well. The AAs solubility was good agreement with the model for entire pH range. The solubility of neutral form of AA I and II which obtained by fitting the model according to Eq. 3.7 were 0.46 and 0.49 $\mu\text{g/ml}$, respectively.

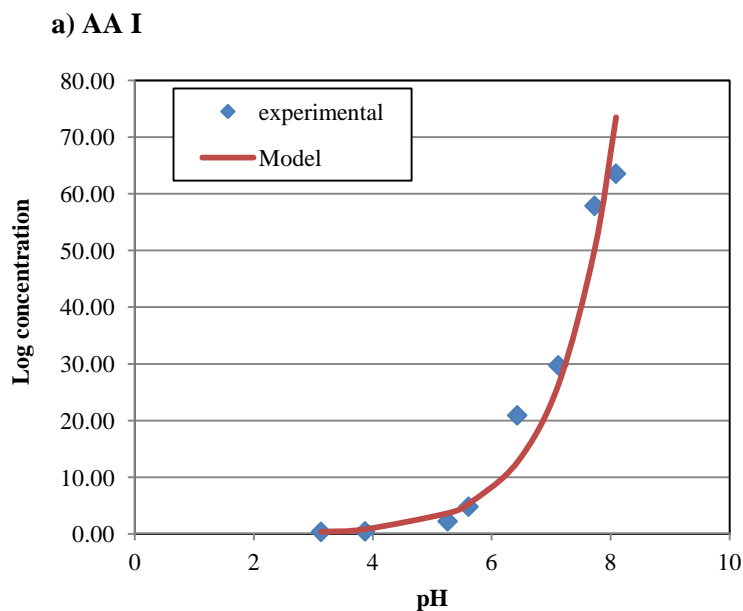
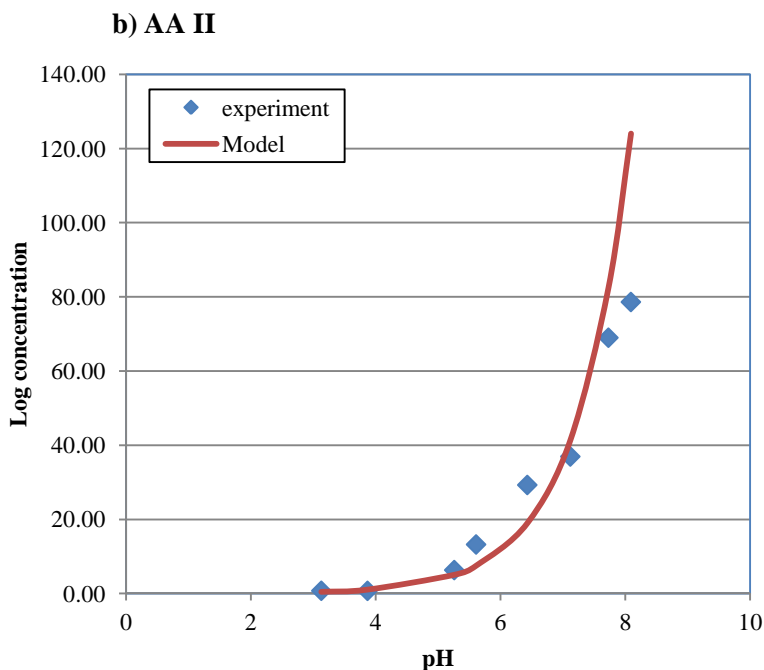


Figure 3.4 The experimental solubility of AA I (a) and AA II (b) as a function of pH at 7 day of equilibration. Solid line represents the fitted model curve of Eq.3.7

Figure 3.4 (cont'd)



3.4.3 Cation types and ionic strength effect

The effect of cation types and ionic strength on solubility of AA I and AA II are shown in Figure 3.5 (a) and (b) whereas the pH of each electrolyte solution is shown in Figure 3.5 (c). The figures show that the solubility of AA I and II were not clearly impacted by cation types and ionic strength. Instead, the difference in solubility was effect from the different pH of each electrolyte solution. Because the buffer solution was not strong enough to control the pH of each cation solution, so the effect of cation types and ionic strength to solubility may not be determined from this experiment.

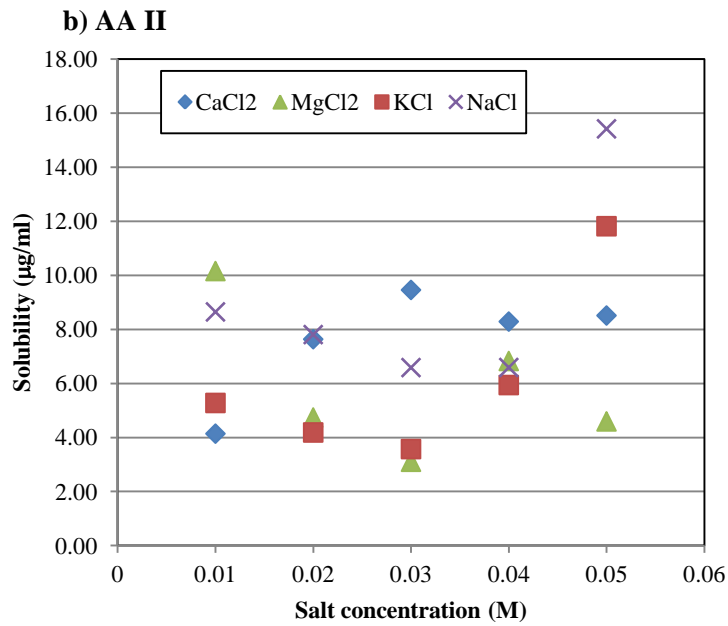
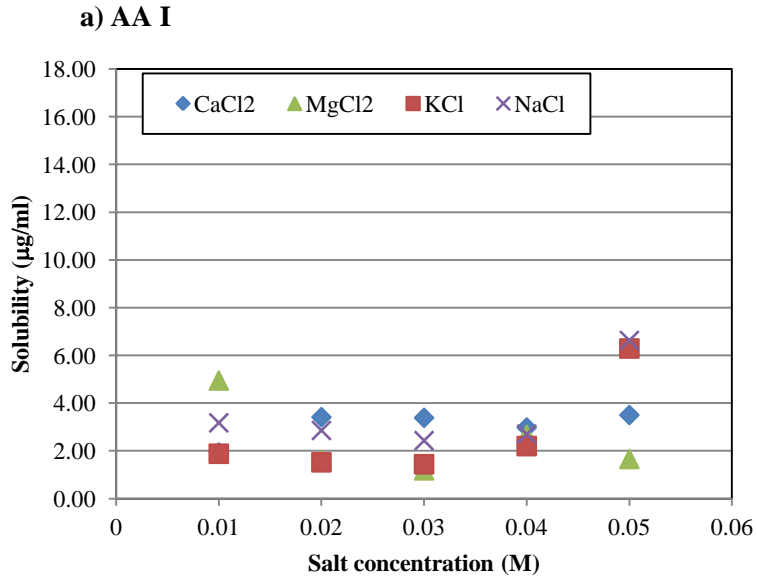
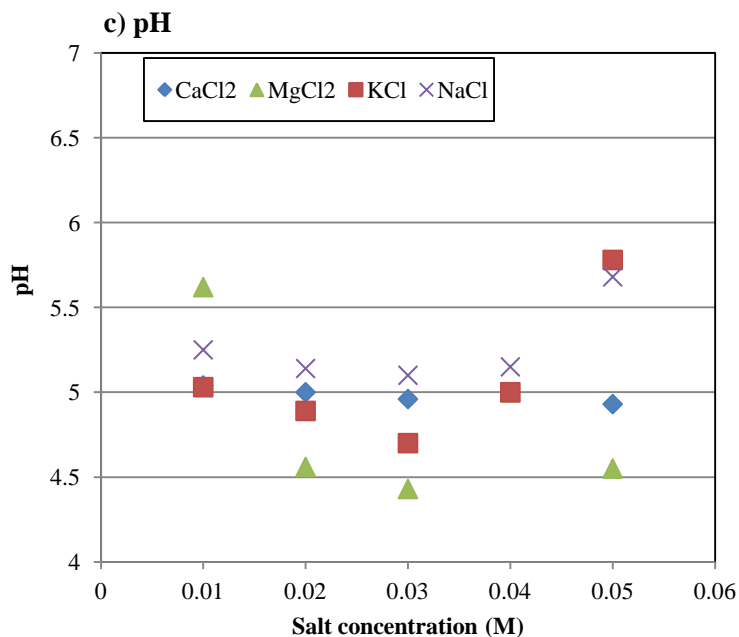


Figure 3.5 The solubility of AA I (a), AA II (b) and the pH (c) at the different type of cation and their concentration.

Figure 3.5 (cont'd)



3.5 Conclusion

The solubility of AAs was determined in this study. The kinetic study showed that, in pure water, AAs had low solubility and dissolution process was quite slow. However, the AAs could get more dissolved when calcium ion had presented in water. This suggested the complexation between calcium ion and anion of AAs is possible. The solubility found to be a function of the pH where the solubility was very low at low pH or when AAs were in neutral form but it linearly increased when pH increased with no found limit value. The experimental data agree well with the solubility model of organic acids. This study did not show the clearly effect of cation types and ionic strength to solubility because the used buffer solution was not strong enough to control pH of each cation and ionic strength experiment.

REFERENCES

REFERENCES

- Arcand, Y., Hawari, J., & Guiot, S. R. (1995). SOLUBILITY OF PENTACHLOROPHENOL IN AQUEOUS-SOLUTIONS - THE PH EFFECT. *Water Research*, 29(1), 131-136. doi: 10.1016/0043-1354(94)e0104-e
- Daughney, C. J., & Fein, J. B. (1997). Aqueous complexation of cadmium, lead, and copper by 2,4,6-trichlorophenolate and pentachlorophenolate. *Geochimica Et Cosmochimica Acta*, 61(4), 719-729. doi: 10.1016/s0016-7037(96)00378-x
- Figueroa, M. T. C. (1989). *Solubility of quinolone in aqueous systems: effect of pH and ionic strength*. University of Arizona.
- Orlov, Y. F., & Belkina, E. I. (2011). Correlations between the stability constants of metal hydroxo complexes and the solubility products of crystalline hydroxides. Series of the polarizing effect of metal cations. *Russian Journal of Inorganic Chemistry*, 56(6), 975-980. doi: 10.1134/s0036023611060192
- Schwarzenbach, R. P., Gschwend, P. M., & Imboden, D. M. (2003). *Environmental Organic Chemistry* (2nd Ed.). New Jersey: John Wiley & Sons, Inc.
- Wightman, P. G. (1997). *Experimental study of 2,4,6-trichlorophenol and pentachlorophenol solubilities in aqueous solution :derivation of speciation-based chlorophenol solubility model.*, McGill University, Montreal, Canada.
- Wightman, P. G., & Fein, J. B. (1999). Experimental study of 2,4,6-trichlorophenol and pentachlorophenol solubilities in aqueous solutions: derivation of a speciation-based chlorophenol solubility model. *Applied Geochemistry*, 14(3), 319-331. doi: 10.1016/s0883-2927(98)00054-7

Chapter 4

Soil-water partitioning coefficient

4.1 Introduction

Sorption property is a very important characteristic of chemicals when predict fate and transport in soil. Sorption and desorption of chemicals determine their availability in environment compartments. Soil sorption also important in term of buffer action that pollutions will transport from sources to human food e.g. animals or plants (Dudka & Miller, 1999). High adsorbed chemicals will not be available for other environmental compartments. They cannot be accessed by light or microorganisms, subsequently, hardly to degrade and lead to persistent in environment. The chemical uptake by plant is also lower. In other hand, low adsorbed chemical will be leached to groundwater, or run off to surface water (R.P. Schwarzenbach et al., 2003).

AAs were believed as BEN induced agents that were exposed by residents in the village. The consumption of food crop contaminated with AAs was hypothesized as exposure pathways. Soil became major environment media that controlled this pathway by governing the fate and transport from sources to the crop plants. Understanding the fate and transport in soil are necessary to assess this hypothesis.

Ionizable organic compounds included weak organic acids or bases are important in environment problems because they can be ionized in environment condition and their sorption process are quite complex. Non-ionized and ionized compounds have different sorption manner in the soil. Non-ionized compounds partition into the soil by hydrophobic interaction whereas

ionized compounds can be adsorbed by combination of various mechanisms such as electrostatic interaction, ion exchange, H-bonding, cation bridging and also hydrophobic partition as well. The soil sorption coefficient of both forms may vary many orders of magnitude (Kah & Brown, 2006).

The objective of this study is to address the sorption properties of AAs in the soil. The sorption isotherm and soil sorption coefficient (K_d) were determined. Then, the factors that differentiate sorption properties such as component of soil, pH, ionic strength and the presence of other ions also were investigated. The desorption efficiency of AAs were determined by desorption isotherm and hysteresis index. The effect of soil type, pH and the presence of other ions to desorption hysteresis were also investigated.

4.2 Literature reviews

4.2.1 The adsorption components in soil

Organic chemicals can be adsorbed by various components in soil including organic matter, clay and minerals. The contribution from each component will depend on type of organic chemicals and environment factors such as pH and other ion presences.

4.2.1.1 Organic matter

The organic materials in soil are mixtures of organic macromolecules such as protein, lipid, cellulose and lignin. These complex organic substances are divided into humic substance if they are soluble in water and humin if they are not (R.P. Schwarzenbach et al., 2003). Humic substances can further divide into fulvic acids if they are soluble in acid and basic solution and humic acids if they are only dissolved in basic solution. The organic matter structure contains two parts, hydrophobic and hydrophilic parts. The hydrophobic parts contain the aliphatic and aromatic hydrocarbon that mainly attach to organic chemicals via hydrophobic interaction and

van der Waal force. The polar parts contain functional groups such as carboxyl, hydroxyl, phenolic, carbonyl and amino groups. These polar groups can be charged in natural soil pH, so they are able to interact with charged molecules via ion exchange. Also, they can attach to the polar chemicals by H-bonding (Calvet, 1989; R.P. Schwarzenbach et al., 2003). Many studies showed the adsorption of ionized compounds had positive correlation with organic carbon content of soils. However, some reported negative relationship, instead they indicated Fe/Al oxide surfaces play a significant role in adsorption of organic acids (Dubus, Barriuso, & Calvet, 2001). These evidence show the significance of ion exchange mechanism to weak organic acids adsorption.

4.2.1.2 Clays

Clay fraction in the soil consists of crystalline and amorphous minerals. Amorphous clays can adsorb some hydrophobic compounds whereas crystalline clays such as quartz have very little sorption capacity. Clays can adsorb both neutral and ionized molecules. The neutral molecules are adsorbed by H-bonding or van der Waal force whereas charged molecules are adsorbed by electrostatic ion exchange (Fruhstorfer, Schneider, Weil, & Niessner, 1993). Clays mostly own negative charge in natural condition and mainly attract to cations (Calvet, 1989). Sorption of clays found to proportional to the surface area, e.g. montmorillonite has surface area and sorption capacity more than illite and kaonillite (Herwig, Klumpp, Narres, & Schwuger, 2001). Even, not many cases showed the sorption was correlated with clay, clays were found to play significant role in low organic matter soil (Barriuso, Laird, Koskinen, & Dowdy, 1994).

4.2.1.3 Aluminum /Iron oxides

The Al/Fe oxides are common minerals that found in soil and sediment. These oxides come from weathering processes which typically found in tropical soil. They are important

adsorbents due to high surface activity. They can contain different charge from negative to neutral and to positive varying by the pH as expressed by Eq. 4.1



Where M is Fe or Al. At low pH, the OH are protonated and the oxides become positive whereas at high pH, the OH are deprotonated and owe the negative charges (Langmuir, 1997). The positive charged surfaces play significant role in sorption of weak organic acid anions such as clofenset, salicylic acid, 2,4 D, imazaquin (Dubus et al., 2001; Regitano, Alleoni, Vidal-Torrado, Casagrande, & Tornisielo, 2000). The binding mechanisms can be electrostatic interaction (cation/anion exchange) or ligand exchange where the OH groups in oxide surface are substituted with organic anions and forming as surface complexes (Kummert & Stumm, 1980; Regitano et al., 2000)

4.2.2 Adsorption mechanisms

Understanding the sorption mechanism is important because it tell us what factors that important to control the adsorption of chemical to soil. The sorption mechanism will depend on soil properties e.g. content of organic matter and clay, soil pH, soil surface area and ion exchange capacity and the chemical properties e.g. polarity, charged, hydrophobicity and chemical functional groups. The adsorption mechanisms include hydrophobic partitioning in organic matter which is main mechanism for non-polar chemical. For polar or ionic chemicals, they can be adsorbed on both organic matter and mineral surfaces (e.g. clay or metal oxide) via several mechanisms such as H-bonding, ionic exchange, charge transfer, ligand exchange and water bridging. However, it is difficult to identify the exact mechanism because of the variety of soil components (Kah & Brown, 2006).

4.2.2.1 Hydrophobic interaction

Hydrophobic interaction is a mechanism occurred in hydrophobic active site of humic substance in organic matter where the chemicals were expelled from water and partition into hydrophobic site such as lipid portion of humic substance (Senesi, 1992). This process is thermodynamically favor because it increases the entropy (Vonoepen, Kordel, & Klein, 1991). For ionized compounds, hydrophobic mechanism is still the main sorption mechanism of the neutral form (Lee et al., 1990; R.P. Schwarzenbach et al., 2003). The hydrophobic sorption mechanism is usually considered as pH-independent.

4.2.2.2 H-bonding

H-bonding is physical attractive force between polar molecules. It occurs by forming the bond between chemicals that contained electronegative atoms (F, O, N) and hydrogen atom in hydroxyl(OH), carboxyl(COOH) and amide (NH) functional groups in humic substances (Kah & Brown, 2006).

4.2.2.3 Ion exchange

Ion exchange is non-specific electrostatic attraction between ionized chemical and charged sorption sites in the soil. It divides as anion and cation exchange. The anion exchange is the attraction between positive charge of surface and anion molecules. It is not likely to occur in soil at natural condition because large amount of clay and organic matter have negative charge. However, it may be significant in soil which has large amount of Al/ Fe oxides (Kah & Brown, 2006). On the other hand, cationic exchange which is the interaction between cation molecules and negative charged sorption sites is significant mechanism in mostly soil because clay and organic matter contain negative charge at this condition.

4.2.2.4 Ligand exchange

Ligand exchange is sorption mechanism where organic chemicals had replaced the water or other weak ligands associated to soil organic matter or Fe/Al hydrous oxide in soil and form ion-pair surface complex (Evanko & Dzombak, 1998; Kummert & Stumm, 1980). This mechanism is dominant for several organic acids contained function group such as carboxyl (COOH) or hydroxyl (OH).

4.2.2.5 Cation bridging

Cation bridging is surface complexation between cation exchange sites on clay or organic matter in the soil and anionic molecules or polar groups of organic compounds. The inorganic cations e.g. Ca^{2+} in soil solution will enhance the adsorption by bridging the organic anions and negative charged sites close together and form stronger complex (Caceres, Fuentes, Escudey, Fuentes, & Baez, 2010; Clausen & Fabricius, 2001; R. A. Figueroa, Leonard, & Mackay, 2004; Jafvert, 1990)

4.2.3 Adsorption Isotherm

The partition of chemical between solid and aqueous phase in soil is represented by soil sorption coefficient (K_d) which defines as ratio of equilibrium concentration of compounds in solid phase (C_s) to aqueous phase (C_e) as shown in Eq. 4.2.

$$K_d = \frac{C_s}{C_e} \quad C_s = K_d C_e \quad (4.2)$$

Because variation of K_d depends on organic carbon content (f_{oc}), the normalization coefficient to organic carbon (K_{oc}) is calculated by Eq.4.3.

$$K_{oc} = \frac{K_d}{f_{oc}} \quad (4.3)$$

From the equilibrium of multiple concentration at constant temperature, the adsorption isotherm can be created which shows the relation between sorbed concentration (C_s) and concentration left in solution (C_e) (R.P. Schwarzenbach et al., 2003). The shape of isotherms may vary depend on the sorption property of sorbent and sorbate. The easiest form is linear isotherm (Figure 4.1a) where the affinity of chemicals to sorbent are equal over the observed concentration range and the sorption sites are far to saturation, so no competition between sorbate molecules. The linear isotherm can be described by Eq. 4.2.

The second common form is Freundlich isotherm as shown in Figure 4.1b where the sorption is harder at high aqueous phase concentration. This isotherm expresses as Eq. 4.4.

$$C_s = K_f C_e^{1/n} \quad (4.4)$$

Where K_f is Freundlich constant and $1/n$ is Freundlich exponent or linear parameter. If $1/n$ equal to 1, K_f will equivalent to K_d .

The third isotherm shows the extreme case where all sites are saturated and no more adsorption can occur (Figure 4.1 c). This is called “Langmuir isotherms” and expressed by Eq.4.5.

$$C_s = \frac{C_{s,max} K_L C_e}{1 + K_L C_e} \quad (4.5)$$

Where $C_{s,max}$ is maximum sorbed concentration on solid phase, K_L is Langmuir constant. This isotherm is found in the adsorption of organic chemicals to clay or minerals which have limited sites (Tolls, 2001).

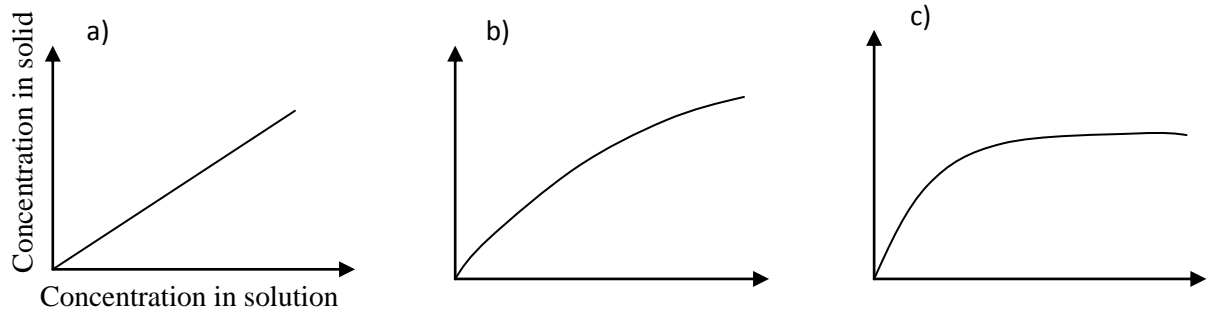


Figure 4.1 The various types of sorption isotherm of Linear(a), Freundlich (b) and Langmuir (c) (modified from Schwarzenbach et al., 2003)

4.2.4 Soil sorption of non-ionized and ionized organic compounds

Both non-ionized and ionized compounds can be adsorbed by several mechanisms which depend on structure and functional groups of chemicals and components in soil.

4.2.4.1 Non-ionized organic compounds

Most of non-ionized organic compounds tend to escape the water and associate to organic matter via hydrophobic partitioning which is similar to partition to organic liquid e.g. octanol. The compounds will be uniformly distributed on organic phase where no specific bonds occur and mostly can be described by linear sorption isotherm (John Paul DiVincenzo, 1996; Karickhoff et al., 1979; Means, Wood, Hassett, & Banwart, 1980). These compounds will not associate with mineral surfaces e.g. clays and metal oxides due to repulsive force from polar or charged surface and there are no influence from pH variation to sorption of non-ionized chemicals.

4.2.4.2 Ionized organic compounds

Unlike sorption of non-ionized compound, the sorption of ionized compounds is more complex because they can adsorb to both organic matter and mineral surface in the soil. The

mechanism will involve the electrostatic interaction as well as specific interactions such as ligand exchange and H-bonding between ionized molecules and charged mineral surface sites. pH and ionic strength are important factors that influence to sorption of ionized compounds because they control surface charge of sites and ionized state of compounds (Burgos & Pisutpaisal, 2006).

Likewise to the octanol-water partitioning coefficient, the apparent soil sorption coefficient (K_d'') which shows contribution from non-ionized and ionized molecules can be described by Eq. 4.6 (Franco, Fu, & Trapp, 2009).

$$K_d'' = \alpha K_d + (1 - \alpha) K_d^- \quad (4.6)$$

Where K_d and K_d^- are sorption coefficient of non-ionized species and ionized species, respectively.

This apparent sorption coefficient also can be written in term of concentration ratio of compounds that partition in soil and water as Eq. 4.7 (Jafvert, 1990; Lee et al., 1990).

$$K_d'' = \frac{[HA_{soil}] + [A_{soil}^-]}{[HA_w] + [A_w^-]} \quad (4.7)$$

Where $[HA_{soil}]$ and $[HA_w]$ are concentration of neutral species which partition in soil and in aqueous phase, respectively and $[A_{soil}^-]$ and $[A_w^-]$ are concentration of ionized species which partition in soil and aqueous phase.

By assume $K_d = \frac{[HA_{soil}]}{[HA_w]}$ and $K_d^- = \frac{[A_{soil}^-]}{[A_w^-]}$, the K_d'' can express in term of pK_a and pH as shown in Eq. 4.8 (Franco et al., 2009).

$$K_d'' = \frac{K_d + K_d^- 10^{(pH-pKa)}}{1 + 10^{(pH-pKa)}} \quad (4.8)$$

This model had been observed in influence of soil pH to K_d for several organic acids and bases (Hyun & Lee, 2004; Sassman & Lee, 2007; ter Laak, Gebbink, & Tolls, 2006)

4.2.4.3 Effect of pH

pH has largely influence to adsorption of ionized compounds but not effect to non-ionized compounds. pH has effect to the extent of ionization of compounds, also it alter the charge of organic matter and metal oxides surface. The sorption coefficient of neutral form may be larger than ionized form for several orders of magnitude. For weakly acid compounds, the K_d was found to strongly increase when pH decrease. This evidence could be explain by at low pH, the hydrophobicity of neutral molecules were larger than ionized molecules as a result in more partitioning in organic matter. Also, the ionized molecules were repulsed by negative charged surface. Moreover, at high pH, the high concentration of OH^- may compete for the positive charge sites in the soil (Kah & Brown, 2006).

4.2.4.4 Effect of ionic strength

Likewise the pH, the ionic strength has the effect to the adsorption of ionized molecules but not effect to the uncharged molecules (Clausen & Fabricius, 2001). It found that the increasing of ionic strength increased the adsorption of weakly acid compounds. This may explain by the added cations from salts will replace H^+ of the sorption surface and release to solution which reduce the pH of solution and cause more molecules in neutral form (Kah & Brown, 2006). Also, cations may form the complex with anion functional groups on humic acid which can reduce repulsion force from the negatively charged surfaces, so increase the adsorption (Westall, Chen, Zhang, & Brownawell, 1999).

4.2.4.5 Effect of cations

The studies of effect of electrolyte background solution to sorption of organic compound showed that cations presence had significant influence to the adsorption. The adsorption of organic acids found to increase with increasing the order of replaceability of cations ($\text{Li}^+ < \text{Na}^+ < \text{K}^+ < \text{Mg}^{2+} < \text{Ca}^{2+} < \text{Sr}^{2+}$) which correspond to atomic radius, valence charge and electronegativity of cations (Carroll, 1959). The enhancement of adsorption when present cation in high pH solution can be explained by the strong replacibility cations such as Ca^{2+} had replaced the other cations in cation exchange sites in the soil and form the bridging bond of calcium to organic acid anions. This effect was not significant for soil with low cation exchange capacity (R. A. Figueroa et al., 2004).

4.2.4.6 Effect of anions

The presence of inorganic anions found to impact the adsorption of organic anions by competing to positive charge sites on the soil which mostly were Fe/Al oxides. The extent of competition will depend on their selectivity to the sites. The selectivity increases in the order of phosphate>silicate>sulfate>> nitrate > chloride (Hyun, Lee, & Rao, 2003). The studies showed that phosphate and sulfate had inhibited the adsorption of organic anion due to the competition to anion exchange sites. This effect will be much greater for soils that have high content of Fe/Al oxides. There were some studies showed that phosphate can form specific adsorption via ligand exchange with clay minerals or Fe/Al oxides in soil (Hyun et al., 2003; Regitano, Bischoff, Lee, Reichert, & Turco, 1997). These indicate that the high volume of organic chemicals could be release back in to the solution if there are applying phosphate to the soil.

4.2.5 Desorption

Desorption is the important process that control the fate and transport of chemicals in environment. It determines the amount of adsorbed chemical released back into water which increase risk to environment such as contaminating in surface or ground water. The sorbed chemicals will not be available for degradation by microorganism or uptake by plant before the desorption (Ren, Wang, & Zhou, 2011). The desorption determines whether the sorption process reversible or irreversible. If total desorption is more than 75% of amount adsorbed, the adsorption is considered as reversible.

The sorption and desorption isotherm of most organic chemicals, are significantly deviated. Mostly, the desorption is delayed or hindered when compare to adsorption process. Desorption may be described by 2 steps, the fast release step and slow diffuse out step. The fast desorption step represents the molecule adsorbed on non-porous mineral surface sites whereas the slow desorption step represents the molecules adsorbed in micropores in organic matter matrices which are more difficult to release (Ren et al., 2011; G. S. Yuan & Xing, 2001)

4.2.6 Desorption isotherm

The desorption isotherm can be determined from several desorption cycles of same sample. The plotting between remaining concentration of chemicals in solid and concentration released in liquid phase at equilibrium of each cycle will be desorption isotherm. Mostly, the desorption isotherm can be described by Freundlich model as expressed in Eq 4.9. (Chefetz, Bilkis, & Polubesova, 2004; Piwowarczyk & Holden, 2012) :

$$C_s^{des} = k_{des} C_e^{des 1/n_{des}} \quad (4.9)$$

Where k_{des} is desorption coefficient, C_e^{des} and C_s^{des} are concentration of chemicals in liquid and solid phase respectively and $1/n_{des}$ is desorption Freundlich exponent which indicates the non-linearity of isotherm. Values of k_{des} and $1/n_{des}$ can be obtained from fitting the model to experimental data.

Some studies introduced two-compartment desorption isotherm to represents two different desorption rates, “fast and slow”, which can be described by Eq. 4.10. This model cooperates the linear term and inverse exponential term which correspond to two different sorption sites. The linear compartment represents the weak adsorption and the easily releasing of sorbate to solution whereas the exponential compartment represents the strong retentive force which requires longer time to desorb. This model can describe the desorption isotherm better than Freundlich model especially for extreme point of isotherm (Barriuso, Baer, & Calvet, 1992).

$$C_s = K_{f1}C_e + C_{sn}(1 - e^{-K_{f2}C_e}) \quad (4.10)$$

Where C_e and C_s are equilibrium concentration of chemical in solution and adsorbed in the solid phase, respectively. C_s is concentration of chemical adsorbed in exponential compartment. K_{f1} and K_{f2} are linear and exponential parameters. The example of two-compartment desorption isotherm and the split up of linear and exponential component are shown in Figure 4.2.

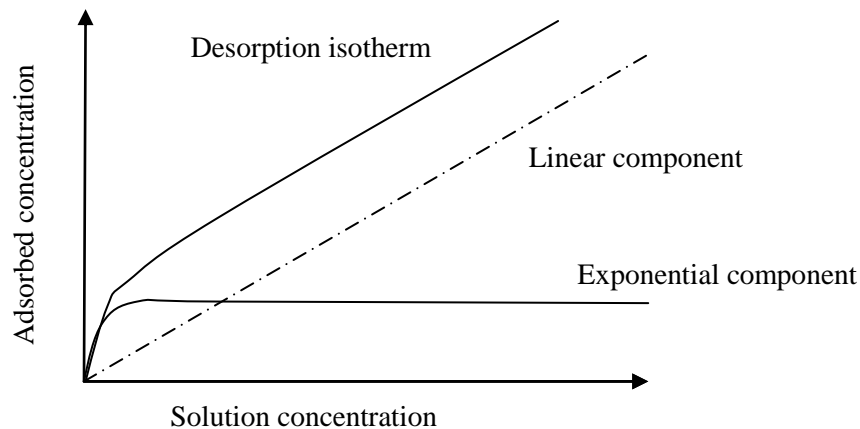


Figure 4.2 The two-compartment desorption isotherm and the splitting linear and exponential compartment model (modified from Barriuso, Baer, & Calvet, 1992.)

4.2.7 Hysteresis index

The desorption deviation is frequently described by hysteresis index (HI). The hysteresis implied the rules that the adsorbed chemical has different limit degree of reversibility which depend on physico-chemical properties of soils and chemicals. Hysteresis coefficient can be calculated from the ratio of Freundlich exponent of desorption isotherm ($1/n_{des}$) to the adsorption isotherm ($1/n_{ads}$) as shown in Eq. 4.11. (Chefetz et al., 2004; Cox, Koskinen, & Yen, 1997; Piwowarczyk & Holden, 2012) :

$$HI = \frac{1/n_{des}}{1/n_{ads}} \times 100 \quad (4.11)$$

If the Freundlich coefficient of desorption and sorption are equal, HI is 100 and the hysteresis will not be observed. The lower HI value indicates more desorption hysteresis or more difficulty of the sorbed molecules to desorb from the soil matrices. The hysteresis occurs by many reasons which may include the effect of experimental procedure such as loss of solute by

volatilization, sorption to tube or biodegradation or strongly binding to the sorbent (G. S. Yuan & Xing, 2001). The degree of hysteresis is depended on physico-chemical properties of chemicals, soil and environmental condition.

4.2.8 Factors effect to desorption hysteresis

4.2.8.1 Effect of organic matter content

The desorption hysteresis can be impacted by organic matter content in soil. Some studies showed the hysteresis increase with increase organic matter. The resistance to desorption of hydrophobic compounds is believed from the strongly bound of chemicals to soil organic matter (G. M. Fu, Kan, & Tomson, 1994; Jenks, Roeth, Martin, & McCallister, 1998). This hysteresis from organic carbon is also controlled by type and location of organic matter. The aged and more condensed of soil organic matter shows more apparent sorption – desorption hysteresis (Liang, Dang, Liu, & Huang, 2005). The organic matter of aged soil will have reduced and condensed structure like glassy state while the young organic matter are mainly contained oxygen functional group and easily hydrated in aqueous solution like the rubbery state where the sorbed molecules can freely diffuse in and out. The rubbery phase is responsible for linear and simultaneously sorption/desorption of solute whereas the glassy phase is responsible for non-linear and slow sorption by “hole filling” and slow desorption which leading to hysteresis (Chefetz et al., 2004; Lesan & Bhandari, 2003)

However, some studies showed the result in opposite direction where small organic matter soils had more desorption hysteresis than high organic matter soils. Even, the larger fraction of molecules adsorbed in high organic matter soil, they were able to desorb rapidly than low organic matter soil. This can be explained that organic matter provides preferential and

easily accessible sorption sites, so it retard the chemical to adsorb on mineral surface sites which may form stronger adsorption (Lesan & Bhandari, 2003).

4.2.8.2 Initial concentration

The initial concentration of sorbate is also affected to hysteresis. High concentration of sorbate found to increase desorption hysteresis because high concentration gradient will drive molecules into deeper sites in organic matter matrices or microporous region. The strong bond such as H-bond may be formed, resulting in decrease fraction of sorbate to be desorbed, and then the hysteresis increases (Chefetz et al., 2004; Ren et al., 2011).

4.2.8.3 Contacting time

The hysteresis also depends on contacting time where slowing desorption was observed when increasing the sorption time. This is because the compounds can diffuse into deeper sites and form the stronger bound to sorption sites which increases hysteresis effect. The sorption is considered to reversible for small contact time. Some studies showed that, the chemicals desorbed from slow sorption in aged soil were 2 or 3 orders of magnitude less than freshly spiked soil. Moreover, the hysteresis also was found to relate with Freundlich coefficient(K_f) which means the hysteresis will increase when greater amount of sorbate had been adsorbed. (J. P. Gao, Maguhn, Spitzauer, & Kettrup, 1998; Lesan & Bhandari, 2003).

4.2.8.4 Effect of pH

Desorption of ionized organic compounds is strongly effect by pH. At low pH where the sorbate in molecular form, the desorption and adsorption isotherm are similar or no hysteresis occur. However, when pH increased, most of organic acids are in anion form and charged

surface sites become more negative, so the cation bridging may be occurred. As a result, the desorption isotherm at high pH found to be more deviate from adsorption isotherm. These patterns also can be observed by hysteresis coefficient which reduce when pH increase. The more difficulty of the desorption of ionized form is due to the formation of more stronger binding energy of ion exchange or cation-bridging than weaker hydrophobic interaction (Caceres et al., 2010; Ren et al., 2011).

4.2.8.5 Effect of cations

Desorption of ionized organic compounds also impacted by presence of cations in the soil solution. For example, Chen, Wang, & Pei, 2014 showed that Ag^+ , Zn^{2+} , Al^{3+} had promoted the desorption of Trichlorophenol (TCP) from ash. They implied that these metals replaced the previous adsorbed TCP and the hysteresis decreased when increased valence of cation where TCP was easiest to desorp in Al^{3+} solution. Weber, 1982 showed that adsorbed pesticides on organic matters/clays were desorbed in paraquat (2^+) solution much better than only water. The probably desorption mechanism was cation exchange where paraquat (2^+) replaced the adsorbed pesticides. The desorption reaction enhanced by cation exchange reaction was introduced by Wu et al.,2013 and Weber, 1982 which expressed in Eq. 4.12 where M is exchangeable cations and C is ionizable organic compounds. They found that desorption increased with increasing charge of exchange cations e.g. $\text{Al}^{3+} > \text{Ca}^{2+} > \text{Na}^+$.



However, the presence of cations can also inhibit the desorption if they can form strongly bond between soil and organic compounds. Moreale & Vanbladel, 1979 showed that the desorption hysteresis of amines adsorbed on saturated cations clays increased with increasing polarizing power of cations e.g. $\text{Fe}^{3+} > \text{Mg}^{2+} > \text{Ca}^{2+} > \text{K}^+ > \text{Na}^+$. This was explained by the increasing stability of amines - cations surface complex on clay. The sorption in Fe solution was almost irreversible due to the very strong Fe-amines complex.

4.2.8.6 Effect of anions

Hyun et al., 2003 studied the effect of presence of anions to desorption hysteresis of organic compounds that adsorb to soil by anion exchange mechanism. They found that there were no or little hysteresis occur when desorption organic chemicals in Cl^- or PO_4^{3-} solution which indicated the Cl^- or PO_4^{3-} can replace organic chemicals very well. The desorption increase with the effectiveness of replacibility of anions e.g. the PO_4^{3-} can displace organic anions better than Cl^- .

4.3 Material and method

To study the adsorption – desorption process of AAs in the soil, the batch equilibrium method (OECD 106) was followed for experimental set up as describe below(OECD, 2000).

4.3.1 Soil samples and their properties

Four types of soils, Wooster CT, Wooster NF, Hoytville CT and Hoytville NF, provided by Department of plant, soil and microbial sciences, Michigan State University had been used in this study. The soil samples were collected from long-term tillage treatment research site at the Ohio Agricultural Research and Development center at depth 0- 5 cm (E. J. Park & Smucker,

2005). The CT and NF mean samples taken from conventional tilled (CT) site and site adjoining to native forest (NF), respectively. The Wooster is fine, loamy, mesic Typic Fragiudalf soil and Hoytville is fine, illitic, mesic Mollic Epiaqualf soil. Some physical and chemical properties of these soils are shown in Table 4.1. Soils were gently ground by mortar and pestle, 2 mm sieved and stored in dry and room temperature prior use.

Table 4.1 Physical, chemical properties and composition of test soil samples

Soil	pH ^a	%OC	Composition			Soil texture	Bulk density (g/cm ³)	CEC ^b (cmol/kg)	AEC ^b (cmol/kg)
			% clay	%silt	%sand				
Wooster CT	5.78	0.9	14.8	64.8	20.4	Silt loam	1.74	7.10	-0.36
Wooster NF	3.91	2.8	11.7	64.3	24.0	Silt loam	1.38	4.00	-0.26
Hoytville CT	5.88	2.3	35.9	45.9	18.2	Silty clay loam	1.84	10.95	-0.62
Hoytville NF	5.98	7.6	36.7	47.0	16.3	Silty clay loam	1.60	12.48	-0.94

a Soil pH was determined in CaCl₂ 0.01 M at soil: solution ratio= 1:5 (Al-Busaïdi, Cookson, & Yamamoto, 2005)

b CEC and AEC measure at native soil pH range 5-7 by method described below

4.3.2 Methods for determination of CEC and AEC in soils

The cation ion exchange capacity and anion exchange capacity were determined by point at zero net charge determination at natural soil pH (Zelazny, He, & Vanwormhoudt, 1996). The 1 g of soil samples were added to 25 ml glass centrifuge tube and measure weight of tube plus soil sample. Soils were saturated with 20 ml of 1 M KCl and shake for 1 hr with mechanical shaker at 150 rpm. Then, centrifuge the soil solution at 7,500 rpm for 30 min and discard the supernatant. Wash these soils with 20 ml 0.01M KCl for ½ hr and centrifuge to remove the

supernatant, repeat this washing steps for 3 times. The final supernatants were collected to determine pH, K^+ and Cl^- in retain solution (C_1). Weigh the tube to calculate the retain volume of final wash solution in the soil (V_1). The soil pellet were saturated with 10ml 0.5 M $NaNO_3$ solution where the Na^+ and NO_3^- will replace K^+ and Cl^- in the soil, respectively. Shake the tube for 1 hr, centrifuge at 7,500 rpm for 30 min and collect the replacing solution in volumetric flask. This step was repeated for 3 times and supernatant were bring together and measured the volume (C_2). Analyze K^+ and Cl^- of this displacing solution by Atomic Absorption Spectrophotometer (AAS) or Ion Chromatography(C_2). The CEC and AEC in centimole per kg were calculated according to the equation 4.13 and 4.14:

$$CEC \left(\frac{cmol}{kg} \right) = \frac{0.1(C_2V_2 - C_1V_1)}{39W} \quad (4.13)$$

$$AEC \left(\frac{cmol}{kg} \right) = \frac{0.1(C_2V_2 - C_1V_1)}{35.5W} \quad (4.14)$$

4.3.3 Analytical method validation

The blank soil matrix solution was obtained by equilibrate most adsorbability soil (Hoytville NF) 0.2 g in 20 ml 0.01 M $CaCl_2$ for overnight and then centrifuge at 7,500 rpm to obtain the supernatant. The certain amount of standard mixture of Aristolochic Acid I and II were added to blank matrix solution within concentration range 0.05 – 1 $\mu g/ml$ for set up calibration solutions and were analyzed by HPLC- DAD. The accuracy, precision, reproducibility, detection limit and recovery had been investigated.

4.3.3.1 Accuracy and precision

The accuracy of the measurement method was determined by spiking standard solution of AAI and AAI in soil blank matrix (0.045 , 0.45 and 0.9 $\mu\text{g/ml}$ for AAI and 0.055 , 0.55 and 1.1 $\mu\text{g/ml}$ for AAI) and analyzed for 6 times (n=6). % recovery was calculated from Eq. 4.15 and reported as accuracy at each concentration.

$$\%recovery = \frac{\text{concentration from spiked solution} - \text{concentration of blank solution}}{\text{concentration of standard solution}} \times 100 \quad (4.15)$$

The precision of AAI and AAI were tested from three standard solutions (0.045 , 0.45 and 0.9 $\mu\text{g/ml}$ for AAI and 0.055 , 0.55 and 1.1 $\mu\text{g/ml}$ of AAI) for 6 time in one day (intraday, n=6) and twice a day over 3 consecutive days (interday, n=6). % relative standard deviation (%RSD) of peak area of each concentration were calculated and reported as precision at each concentration (Kuo et al., 2010; J. B. Yuan et al., 2008).

4.3.3.2 Linearity

Linearity of the method was tested by six concentration of standard solution of AAI and AAI ranging from 0.045 -0.9 and 0.055-1.1 $\mu\text{g/ml}$, respectively. Each concentration was analyzed for three times. The average peak areas were plot with concentration. The linear regression equation and correlation coefficient (r^2) was obtained from graph.

4.3.3.3 Limit of detection(LOD) and limit of quantification (LOQ)

The limit of detection (LOD) and quatification (LOQ) of AAI and AAI were tested by analyzing minimum concentration (0.045 and 0.055 ug/ml of AA I and II respectively) for 7 times and calculated for standard deviation (SD). The LOD was equal to three times of SD (signal to noise ratio = 3) and LOQ was equal to ten times of SD (signal to noise ratio =10).

4.3.4 Adsorption experiment

4.3.4.1 Preliminary and kinetic study

First, the adsorption kinetic of all soils was determined. The 0.1 g of each soil was added to 7 centrifuge tubes with Teflon-liner screw cap. Soil solutions were pre-equilibrated with 9 ml of 0.01 M CaCl_2 solution for overnight (12hr) and then 1 ml of stock AAs solution was spiked to make final volume to 10 ml. The mixtures were shaken with mechanical shaker at 150 rpm as shown in Figure 4.3. Time of mixing of each tube was 0.5, 1, 2, 5, 24, 48, 72 hr. After that, soil solutions were centrifuged at 7,500 rpm for 30 min to separate the aqueous phase from soil, as shown in Figure 4.4. The AAs in aqueous phase were determined by RP-HPLC. The percentage of adsorption and concentration in aqueous phase were calculated and plotted versus time. Two control samples (spiked AAs but no soil) had been included to check stability and adsorption of AAs on the tube and cap. One blank sample of each soil (no spiked AAs but had soil) was prepared to serve as background and to detect other interference compounds. The control and blank samples also were taken at same time interval. From control sample analysis, it showed AA I and II were not adsorbed on centrifuge tube and cap, the recovery of AA I and II in four soils are over 90%. The blank samples showed no AA I and II contained in all original soils.



Figure 4.3 AAs equilibrated with soil solution in mechanical shaker



Figure 4.4 Separation aqueous phase from soil after centrifuge

4.3.4.2 Adsorption Isotherm

The soil sorption isotherm of four soils was determined. The method is generally similar to the kinetic study. Different volume of AAs stock solution was added to make seven different initial concentrations ranging from 0.05 -2 $\mu\text{g/ml}$ whereas amount of soil was keep constant (soil 0.1 g in solution 10 ml). Soil solutions were equilibrated for 24 hr. The experiments were done at room temperature. pH of adsorption were measured in aqueous phase after take the samples. The AAs concentration in aqueous phase (C_e) was measured by HPLC while the amount of AAs adsorbed to soil (C_s) was calculate from mass balance.

4.3.4.3 Effect of pH

To investigate the difference adsorption of neutral and anion molecules, pH of soil solutions were varied. The batch experiments were used same as before but during soil pre-equilibrating period (first 12 hr), the pH of soil solutions was adjusted in the range of 2 - 11 by adding small amount of 0.1 M HCl or 0.1 M NaOH until the change of target pH was low as possible. After that AAs stock solution was spiked to soil solution. Equilibrate for 24 hr and centrifuge to obtain supernatant. After taken the aqueous samples, the pH of remaining soil solutions were measured as equilibrium pH.

4.3.4.4 Effect of calcium ion

To investigate the effect of calcium ion, the CaCl_2 at different concentration (0.0005-0.1 M) were used as background electrolyte. No pH adjustment was applied to avoid changing of ionic strength. The sorption was test at one initial concentration (0.4 $\mu\text{g/ml}$ of AA I and 0.5 $\mu\text{g/ml}$ of AA II) for all four soils. The concentration in aqueous phase (C_e) and concentration

adsorbed in soil (C_s) were determined and calculated for the soil sorption coefficient (K_d) as in Eq. 4.2. These K_d were plotted versus \log CaCl_2 concentration for each soils.

4.3.4.5 Effect of cations/anions

To test the contribution from cation /anion exchange capacity, monovalent cation salt (KCl , NaCl) and divalent cation salt (MgCl_2 , CaCl_2 , SrCl_2) were use as background solution to test cation effect whereas KCl , KSO_4 and KNO_3 were used as background solution to test anion effect. The Hoytville NF which is highest organic matter and clay content soil was used. The concentration of each background solutions was adjusted to have same ionic strength. The sorption isotherms of each cation/anion type were compared. The measured final equilibrium pH showed that each salt solution gave similar pH, so the obtained isotherms were not effect by the different pH.

4.3.5 Desorption Experiment

4.3.5.1 Desorption kinetic

The desorption experiment was done by decant and refill technique immediately after sorption equilibrium. The desorption kinetic study was conducted to determine the contact time to reach desorption equilibrium of each soil. First, sets of soil samples were prepared same as adsorption experiment. After mixing for 24 hr, soil solutions were centrifuged at 7,500 rpm for 30 min and 5 ml of supernatant were removed. The removed aqueous phase were replaced by fresh CaCl_2 0.01 M in same volume. This soil solutions were shaken again and the aliquot of samples were taken after desorption at interval of time 0.5, 1, 2, 5, 24, 48, 72 hr. Concentration of AAs desorbed in aqueous phase was measured and % desorption was plotted versus time to determine time to reach desorption equilibrium.

4.3.5.2 Desorption isotherm

Desorption isotherm were determined by sequential decant and refill technique. The desorption kinetic study showed that 24 hr shaking period for each step was enough to reach desorption equilibrium. First, the sets of soils solution were prepared same as adsorption isotherm experiment. After equilibrium of adsorption step, the three different initial concentration of AAs were chosen to study desorption isotherm. After centrifuge, 5 ml of supernatant were removed and replacing with 5 ml of fresh 0.01 M CaCl_2 solution and shaking for another 24 hr. This step was repeated for three times in a roll. The desorbed AAs in aqueous phase (C_e) and concentration remaining in soil (C_s) of each cycle were determined. The desorption isotherms were plotted between the obtained C_e and C_s of each desorption cycle. These isotherms were fitted with Freundlich model. The adsorption –desorption hysteresis were quantified by hysteresis index (HI) calculated from Eq. 4.10.

4.3.5.3 Effect of pH

The adsorption- desorption were tested at 3 different pH, one of original soil pH and other two adjusted pH. The pH of soil solution were adjusted by spiking very small amount of 1M HCl or NaOH to solution in pre-equilibration in adsorption step. The desorption steps were conducted as three times in a roll same as mention before but no pH adjustment was applied in desorption step. The pH of aqueous phase after taking the sample of each cycle was measured as pH of desorption. The desorption isotherms of each pH were constructed. The hysteresis indexes were calculated and plotted with the pH of adsorption.

4.3.5.4 Effect of cations/anions

After the cation/anion effect adsorption experiment, the soil solutions were continued to study desorption step where KCl, NaCl, MgCl₂, CaCl₂, SrCl₂ (for cation experiment) and KCl, KSO₄ and KNO₃ (for anion experiment) were used as fresh replacement solution. The desorption isotherm of each cation/anion were created. The experiment show that the pH of desorption of each cation/anion solution did not deviate much from pH of adsorption, so the desorption isotherms should not be effect by pH. The hysteresis index were calculated and plotted with cation or anion types.

4.4 Result and discussion

4.4.1 AAs analytical method validation and matrix effect

The calibration curve of six concentrations of AA I and II ranging from 0.045 -0.9 and 0.055-1.1 µg/ml, were prepared in soil matrix solution and were analyzed by HPLC-DAD. The area of each peak and their concentrations are plotted and showed in Figure 4.5. The linear regression equation of AA I is $y=113,345x-5,306.5$ and AA II is $y = 115,184x - 6,386.6$. Both of them show good linearity correlation ($r^2>0.99$).

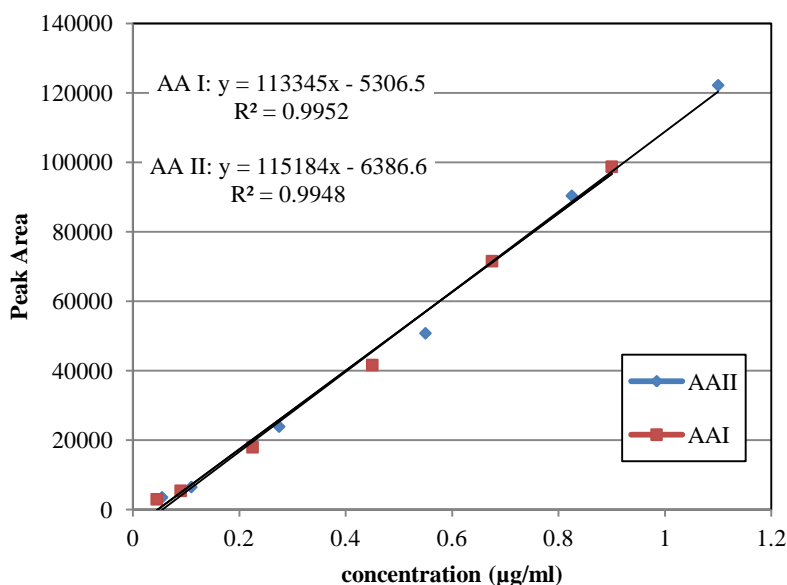


Figure 4.5 The calibration curve of AA I and II in soil matrix solution

The accuracy and precision of this method were reported as % recovery and % relative standard deviation (%RSD) as shown in Table 4.2. The result showed that the precision of intraday and interday are similar. However, the analysis at low concentration gave less accuracy and precision than analysis at high concentration because of closing to the detection limit.

Table 4.2 % recovery (accuracy) and % RSD (intra-day and inter-day precision) of AAs analytical method

Chemical	Concentration (µg/ml)	%recovery (mean, n=6)	%RSD (intra-day, n=6) ^a	%RSD (inter-day, n=6) ^b
AA I	0.045	147.59	22.95	23.89
	0.45	88.97	4.39	8.24
	0.9	99.28	3.88	3.25
AA II	0.055	169.21	28.82	22.50
	0.55	88.36	6.48	6.08
	1.1	98.06	3.04	3.79

^a The samples were analyzed 6 times in 1 day

^b The samples were analyzed 6 times over 3 three consecutive days

The linearity range and correlation coefficient are presented in Table 4.3. The result showed that the linear range of analysis with HPLC-DAD can extend over two orders of magnitude of concentration. Limit of detection and quantification were defined as the minimum concentration which gave signal to noise ratio (S/N) equal three and ten, respectively. The values were also shown in Table 4.3. The obtained LOD of AA I and II from this study were 0.013 and 0.010 µg/ml, respectively. These detection limits of analysis were according to literature at 0.0109 µg/ml for AA I and 0.0148 µg/ml for AA II (Zhang et al., 2006).

To determine soil matrix effect, the standard solution which prepared in methanol was analyzed same as standard solution prepared in soil matrix solution. The calibration curve of both standards were compared together. Figure 4.6 show that both calibration curve of soil matrix and pure methanol were close together which indicated no interference from soil matrix to analysis by HPLC-DAD.

Table 4.3 Linear ranges, correlation coefficient, quantification and detection limit of Aristolochic Acid I and II

Chemical	Linear range (µg/ml)	r²	LOD (µg/ml)	LOQ (µg/ml)
Aristolochic Acid I	0.045-0.9	0.9952	0.013	0.042
Aristolochic Acid II	0.055-1.1	0.9948	0.010	0.034

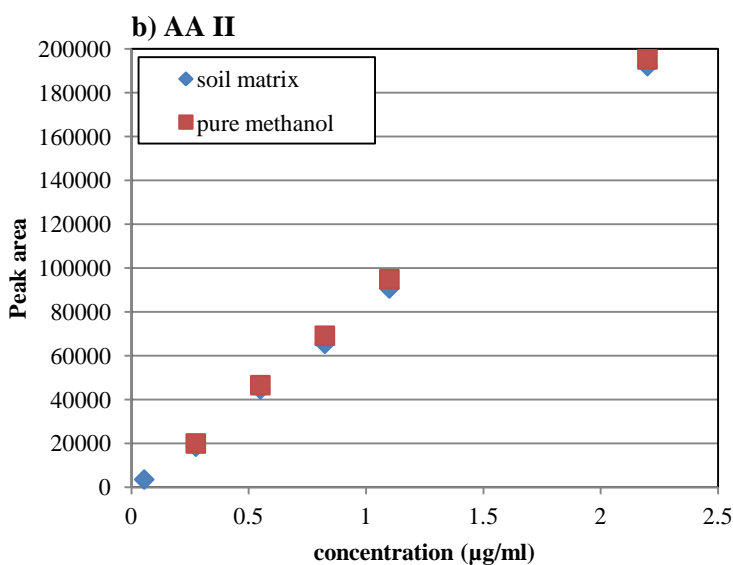
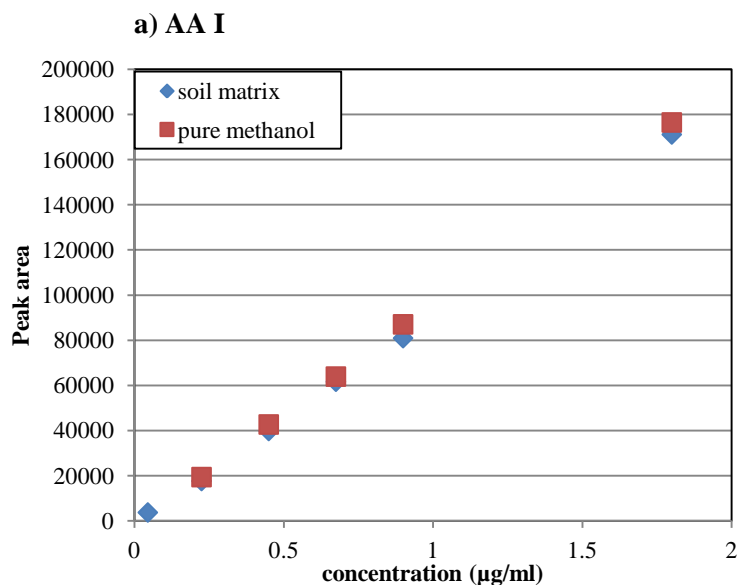


Figure 4.6 Matrix effect of analysis AA I (a) and AA II (b) in soil matrix and pure methanol

4.4.2 Adsorption experiment

4.4.2.1 Adsorption kinetic

The preliminary kinetic studies showed the sorption of AAs to all soils were rapid process where more than 90% of sorption capacity was reached for less than 24 hr of mixing as shown in Figure 4.7. This is according to a simple two-site sorption model , where the sorption

take place rapidly on surface of sorbent called “ apparent equilibrium” and the slow process when molecules diffuse into micropore of organic matter (J. P. DiVincenzo & Sparks, 2001; Piwowarczyk & Holden, 2012). However, the slow sorption process was not included in this study.

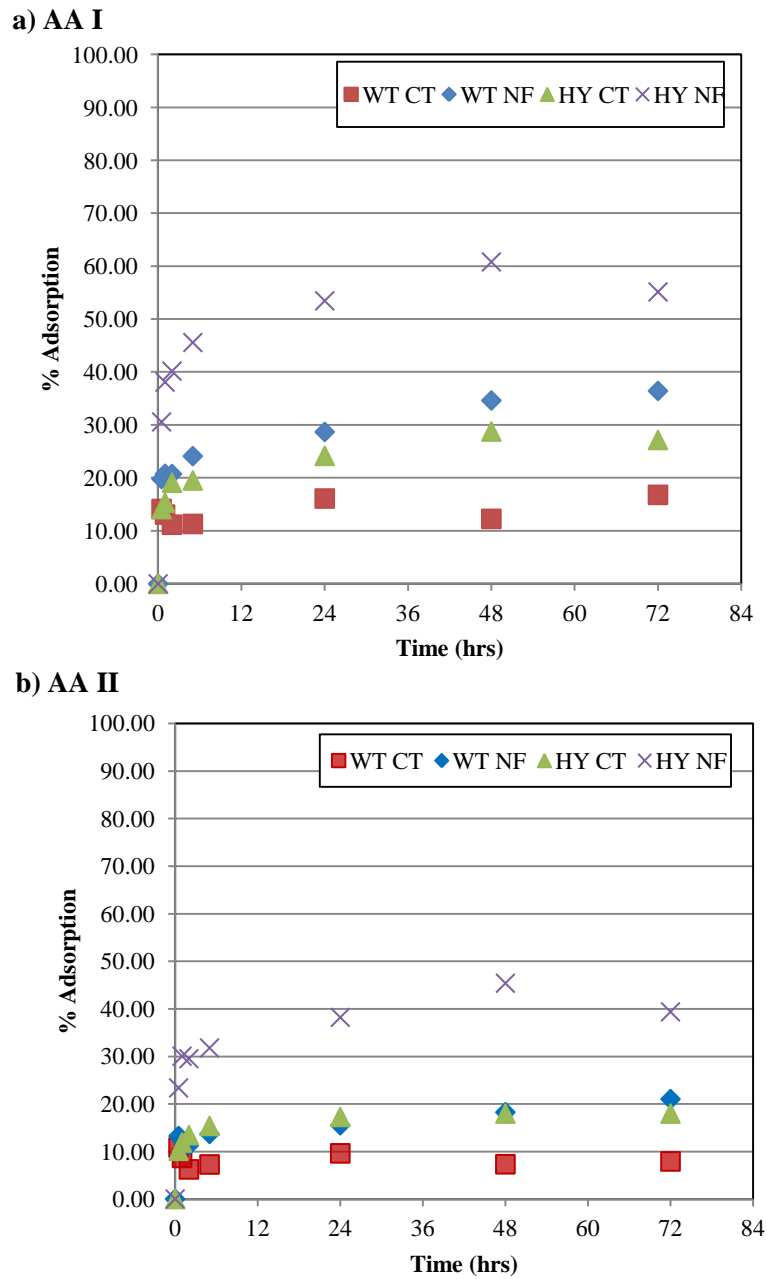


Figure 4.7 Sorption kinetic of AA I (a) and II (b) on four soils

4.4.2.2 Adsorption Isotherm

The concentration of AAs remained in aqueous phase (C_e) and AAs sorbed in soil (C_s) were plotted as adsorption isotherm shown in Figure 4.8. The isotherms were fitted well with linear and freundlich isotherm with $r^2 > 0.9$ as shown in Table 4.4 and the K_d , K_f and $1/n$ were obtained by fitting the data to the model. The linear isotherm indicated that sorption concentration of AAs were lower the sorption capacity of the soils. The different K_d indicated different sorption capacity of each soils and may relate to soil composition (R.P. Schwarzenbach et al., 2003; W. C. Yang, Mang, Zhang, Zhu, & Chen, 2009).

Even AAs were in anion form at this native pH, the $\log K_{oc}$ calculated from Eq.4.3 were high in the range of 3.3-3.5. This number contradicted with $\log K_{ow}$ of AAs at natural pH which was very low. This indicates that other sorption mechanisms may involve other than simple hydrophobic interaction. From the point of view of AAs structure, we can assume that the phenanthrene group is responsible for hydrophobic interaction with organic matter whereas the carboxylic acid and nitro group are attribute to other specific interaction such as the H-bonding or ion exchange (Senesi, 1992; Westall et al., 1999). Moreover, the Ca^{2+} presenting in solution may enhance the adsorption by adsorb to negative charged sites in soil and make them less negative, thereby reduce electrostatic repulsion or even forming the complex with AAs by cation bridging mechanism which are general patterns for organic acids (Jafvert et al., 1990).

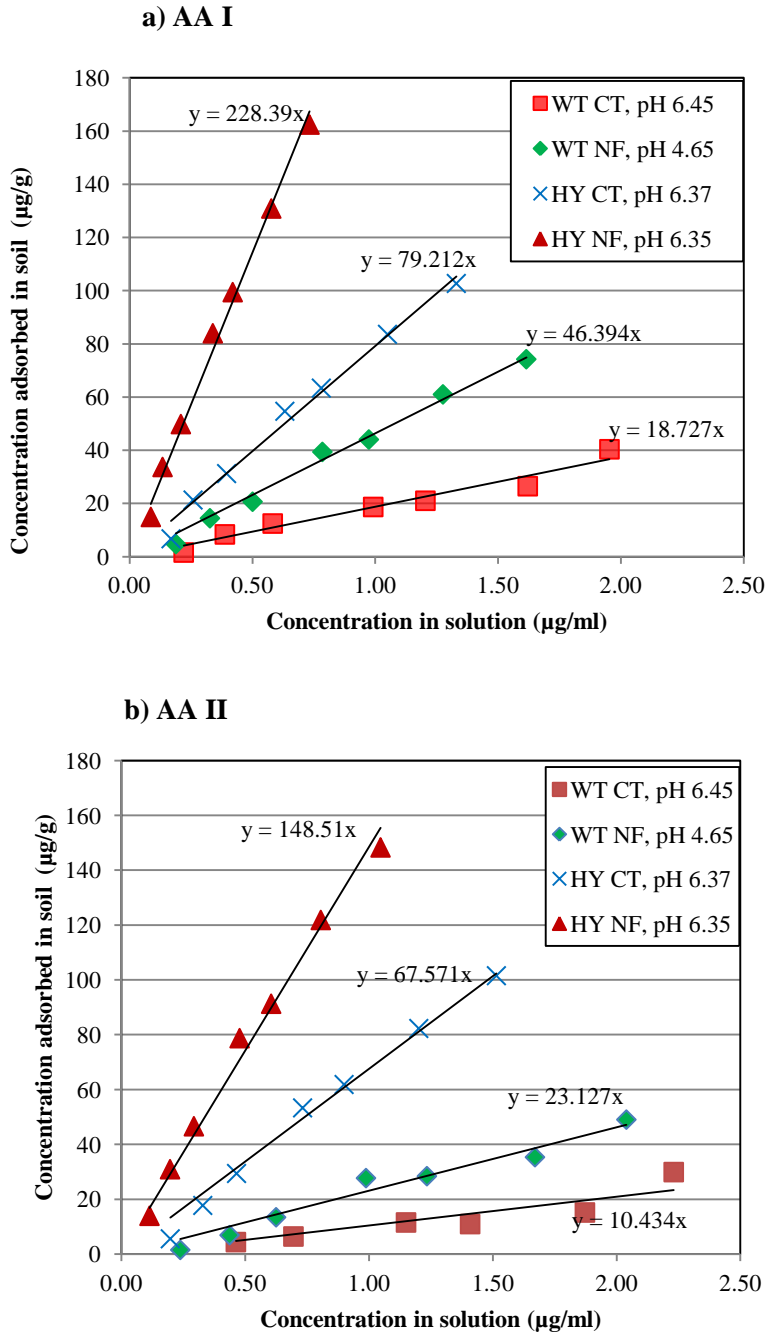


Figure 4.8 Sorption isotherm of AA I (a) and AA II (b) in all four soils at native soil pH equilibrium

Table 4.4 Linear and Freundlich isotherm parameters for sorption of AAI to four soils at natural soil pH

Soil	pH	Linear isotherm			Freundlich isotherm		
		K_d (ml/g)	r^2	Log K_{oc}	$K_f(\mu\text{g}^{1-1/n} \text{g}^{-1})(\text{ml}^{1/n})$	1/n	r^2
Wooster CT	6.45	18.73	0.93	3.32	18.23	1.07	0.96
Wooster NF	4.65	46.39	0.99	3.22	46.01	1.04	0.99
Hoytville CT	6.37	79.21	0.99	3.54	79.19	0.98	0.99
Hoytville NF	6.35	228.39	0.99	3.48	220.07	0.94	0.99

However, to compare the sorption of organic acid where pH is dominant factor, the similar adjusted pH would be more accurate. The adjusted pH sorption isotherms were shown in Figure 4.9. It was observed that, after adjusted the pH, the sorption of WT NF was lower than WT CT even it had higher organic carbon content. Instead, it was positively correlated to the clay content. This indicated that, for low organic carbon content soil e.g. Wooster soil, the AAs has higher affinity to clay rather than organic matter in soil.

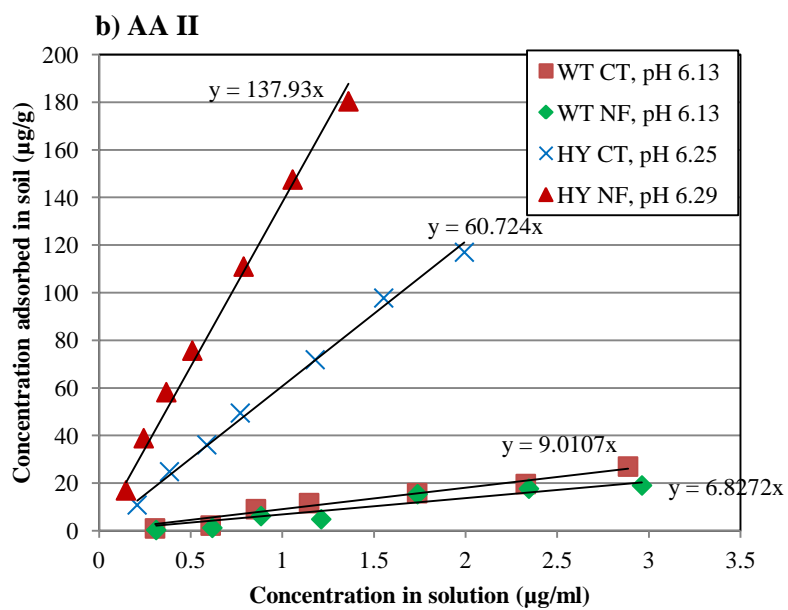
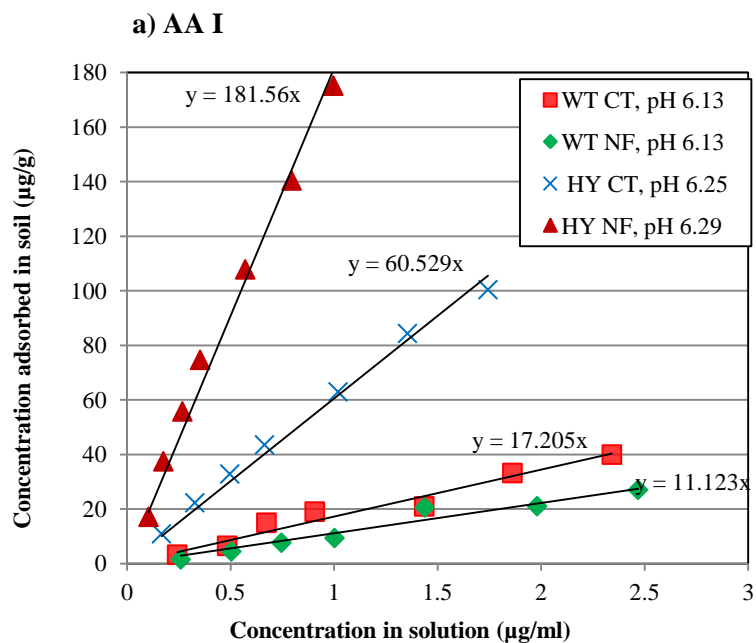


Figure 4.9 Adsorption isotherm of AA I (a) and AA II (b) in all four soils at adjusted pH equilibrium

4.4.2.3 Effect of soil properties

To determine the effect soil properties, the obtained soil partition coefficient (K_d) of each soil were plotted as a function of %organic carbaon content and cation exchange capacity (CEC) as shown in Figure 4.10 (a) and (b). The results show that K_d had low correlation with % organic carbon but instead, it had better correlation with cation exchange capacity (CEC). These finding indicate that AAs sorption mechanism is not only simple hydrophobic partitioning but rather related to cation exchange mechanism.

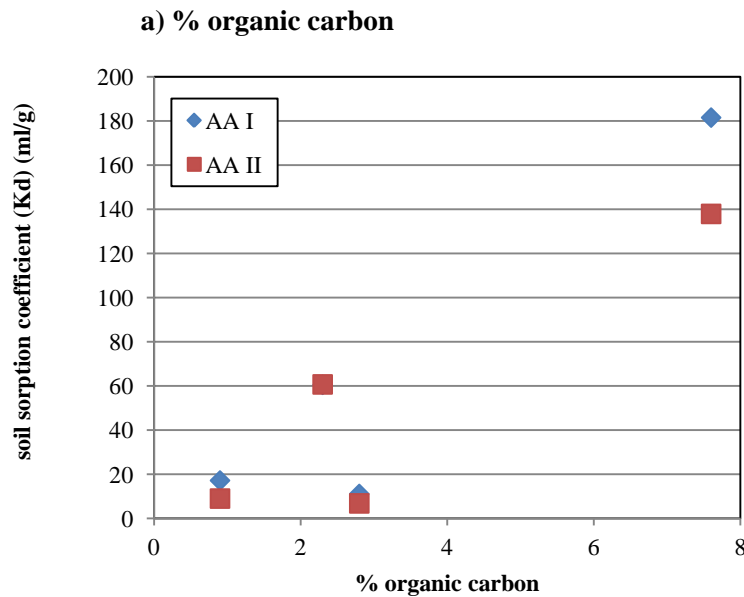
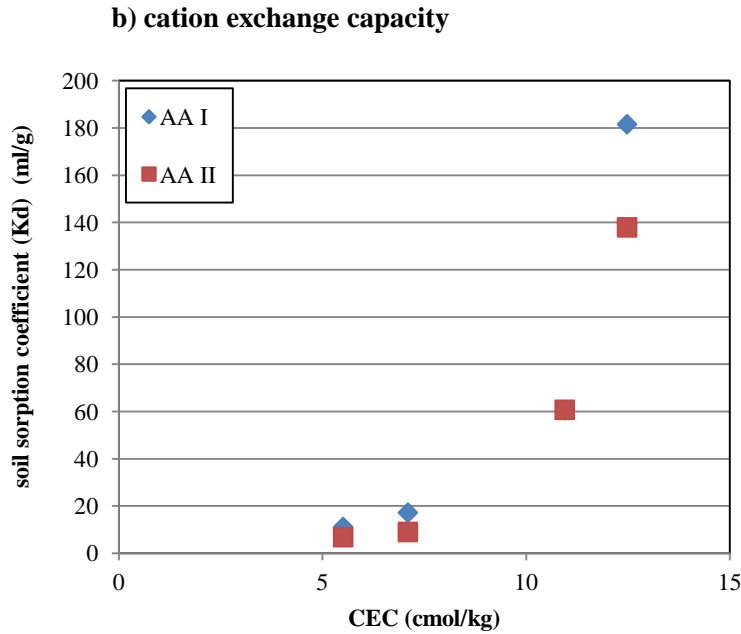


Figure 4.10 Soil sorption coefficient (K_d) as a function of % organic carbon (a) and cation exchange capacity (b) of soil

Figure 4.10 (cont'd)



4.4.2.4 Effect of pH

The sorption coefficient (K_d) of all soil were plotted with pH as shown in Figure 4.11. The figures show that AAs adsorption was strongly depended on the pH of soil solution. The shape of K_d with pH were sigmoidal curve for all soils where the K_d found to decrease 20-100 times when the pH increased from 2 to 6 but the effect may differ between soil. These data were fitted well with apparent sorption coefficient (K_d'') equation considering the contribution from neutral and anion forms of AAs (Eq.4.8). The ionized molecules at high pH were much less adsorbed than neutral molecules at low pH. This may be explained that the neutral molecules were partition in organic matter in soil very well. However, anion molecules which had largely less hydrophobicity were less partition to organic matter. Also, at high pH, the surface of soils had negative charge which will repulse with anion of AAs (Hyun et al., 2003). These evidence may imply that AAs adsorb to the soil by hydrophobic partitioning at low pH but by ion exchange at high pH.

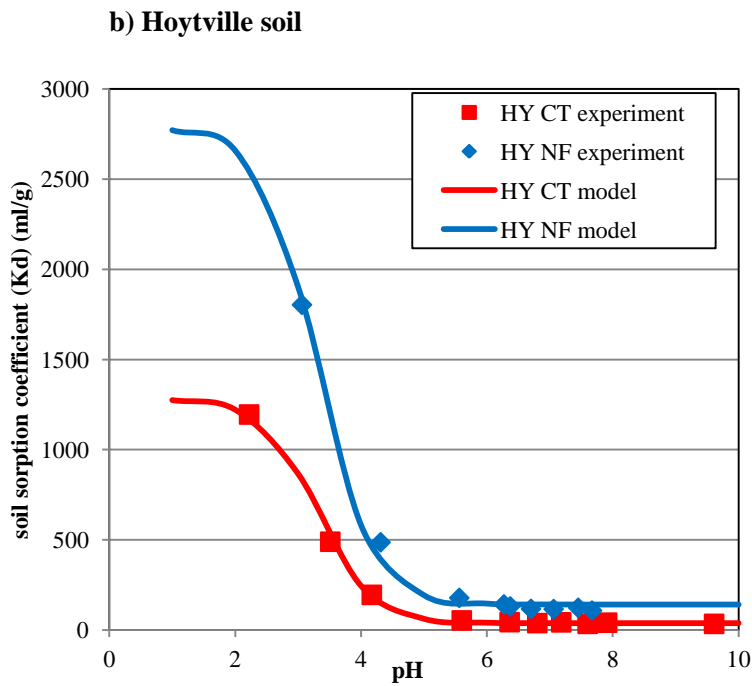
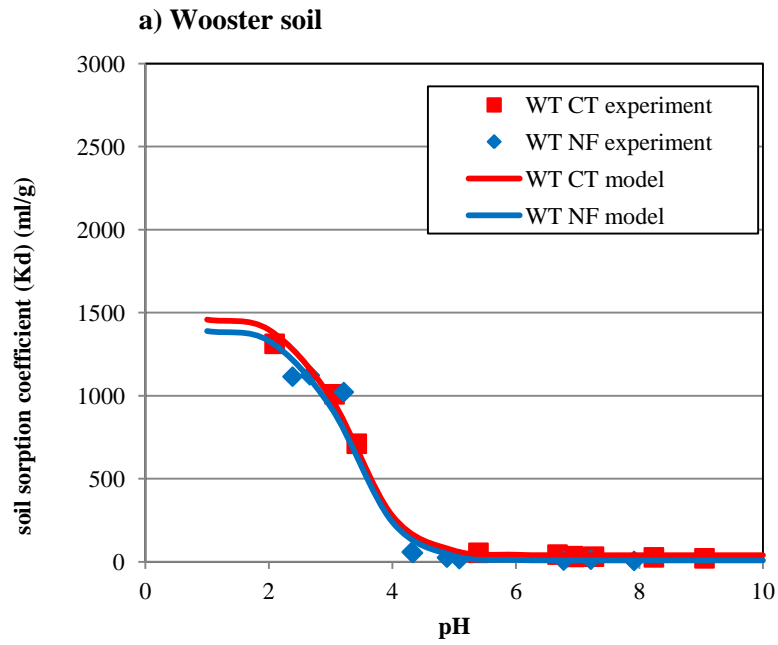


Figure 4.11 Soil sorption coefficient as a function of pH for Wooster soils (a) and Hoytville soils (b)

4.4.2.5 Effect of calcium ion

The influence of ions presented in solution on adsorption was examined. The single point adsorption at fixed initial concentration was determined in CaCl_2 background solution from 0.0005 – 0.1 M. The soil sorption coefficient (K_d) were calculated and plotted with $\log \text{CaCl}_2$ concentration for all soil as shown in Figure 4.12 (a)-(d). The figures show that Ca^{2+} enhanced the adsorption of AAs in only Hoytville NF soil which is highest CEC soil but there were no effect observed on other lower CEC soils. This indicated that cation exchange was important mechanism. The Ca^{2+} enhanced adsorption can be explained by two possible mechanisms; first, Ca^{2+} which is highly exchange capacity cation were adsorbed at negative charged sites, so the electrostatic repulsion was reduced or the surface complexation between anion AAs and Ca^{2+} via cation bridging mechanism was possible (Jafvert, 1990). Second, the complex formation between anion AAs and Ca^{2+} in solution may turned the molecules to positive charge and they favored to be adsorbed on the cation exchange sites (Westall et al., 1999).

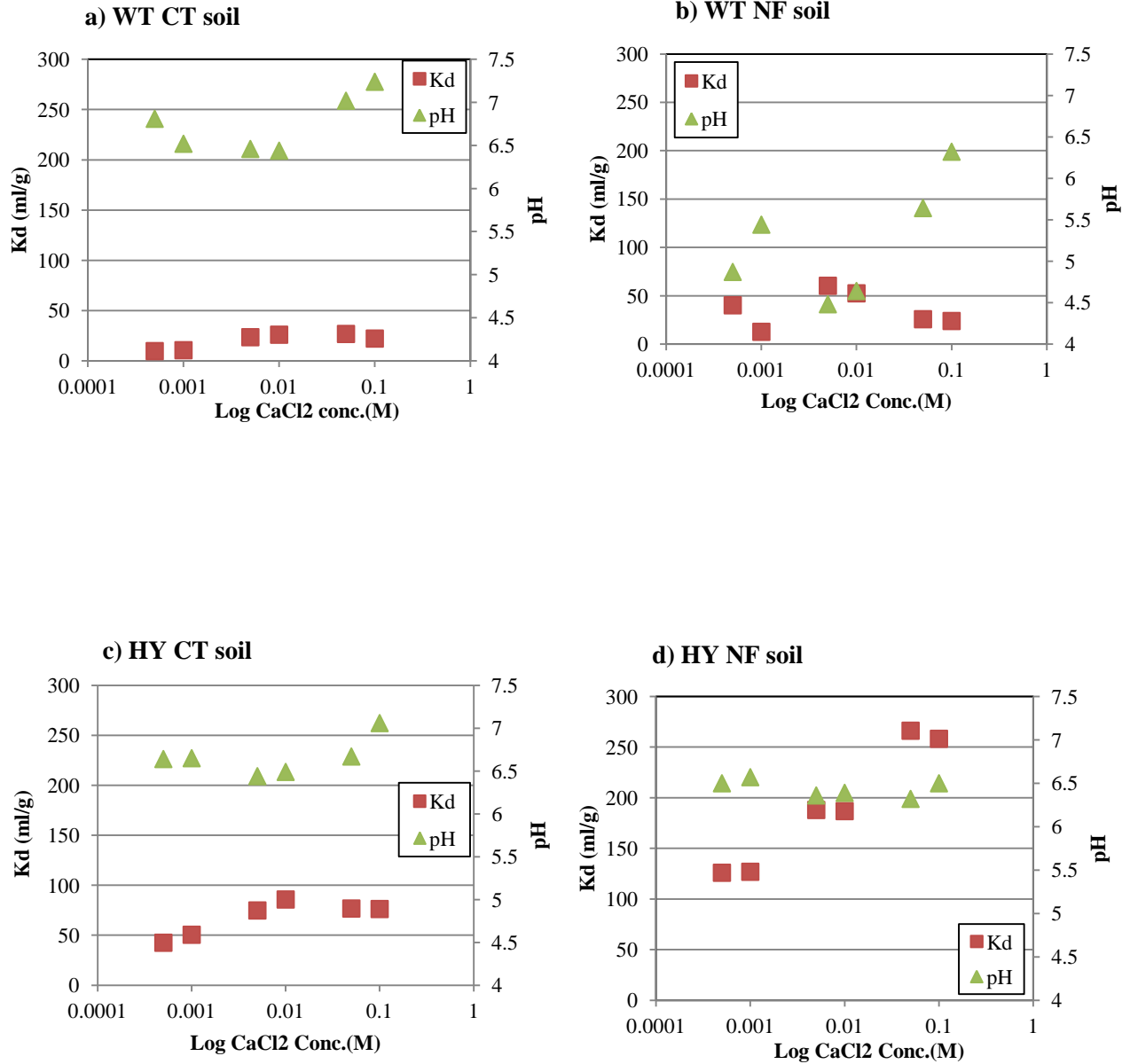


Figure 4.12 The sorption coefficient (K_d) and pH (second axis) as a function log CaCl_2 concentration on WT CT soil (a), WT NF soil (b), HY CT soil(c) and HY NF soil (d)

4.4.2.6 Effect of Cations/ Anions

To test the effect of cation types on the adsorption of AAs, the salt solution of CaCl_2 , MgCl_2 , SrCl_2 , KCl , NaCl and also deionized water were used as background solution and sorption isotherm of each salt were determined as shown in Figure 4.13. The results show that the presence of divalent cation will enhance the adsorption more than monovalent cation e.g. $\text{SrCl}_2 \cong \text{CaCl}_2 \cong \text{MgCl}_2 > \text{KCl} \cong \text{NaCl} > \text{DI}$. This order accords to the power of replaceability of cations where the higher valent cation will have more replacing power e.g. $\text{Sr}^{2+} > \text{Ca}^{2+} > \text{Mg}^{2+} > \text{K}^+ > \text{Na}^+ > \text{Li}^+$ (Carroll, 1959; R. A. Figueroa et al., 2004). This sorption enhancement by power of replacibility of cation suggested the cation –bridging mechanism because divalent cations can form stronger bond to cation exchange site than monovalent cations (Hyun & Lee, 2005).

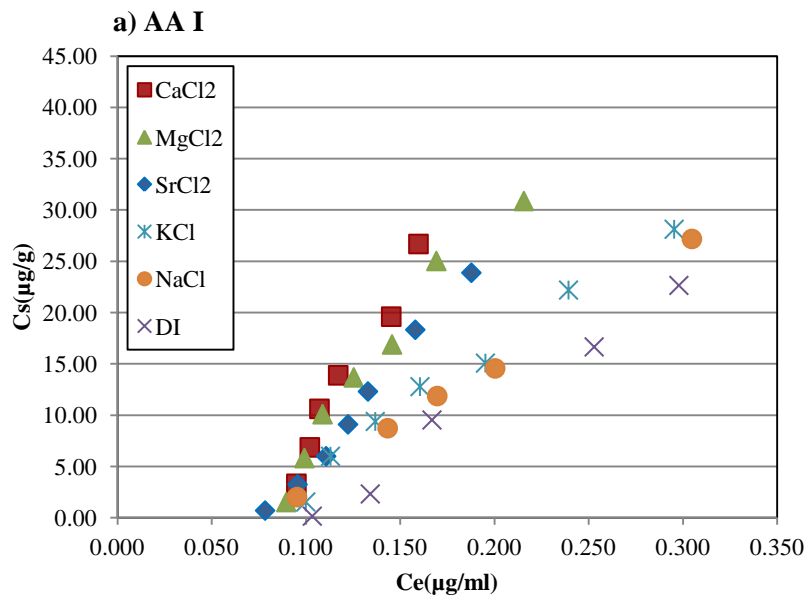
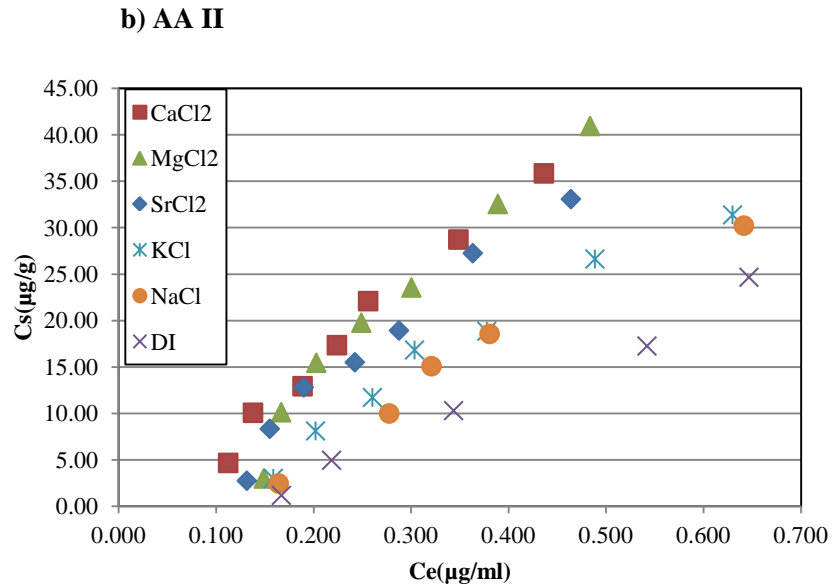


Figure 4.13 Adsorption isotherm of AA I (a) and II (b) on Hotyville NF soil in different cations background solution

Figure 4.13 (cont'd)



The effect of anions on the adsorption of AAs was also tested and the results showed in Figure 4.14. This figure shows that the adsorption of AAs in KCl as background solution were similar to KNO_3 and K_2SO_4 . The non-difference in AAs sorption from different anion type even Cl^- , SO_4^{2-} , NO_3^- , have different affinity to anion exchange capacity sites. This indicated that adsorption of AAs were not affected by anions exchange mechanisms. Also, because of the tested soil at high pH has low AEC, so the contribution from anion exchange was limited.

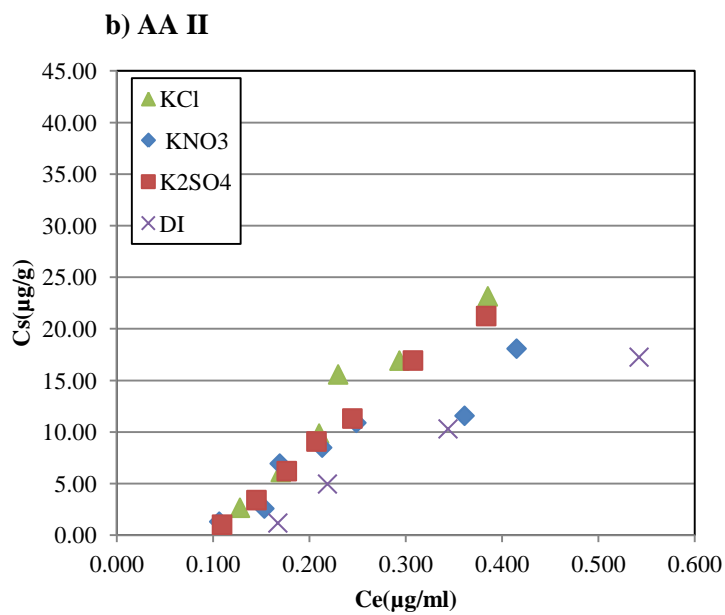
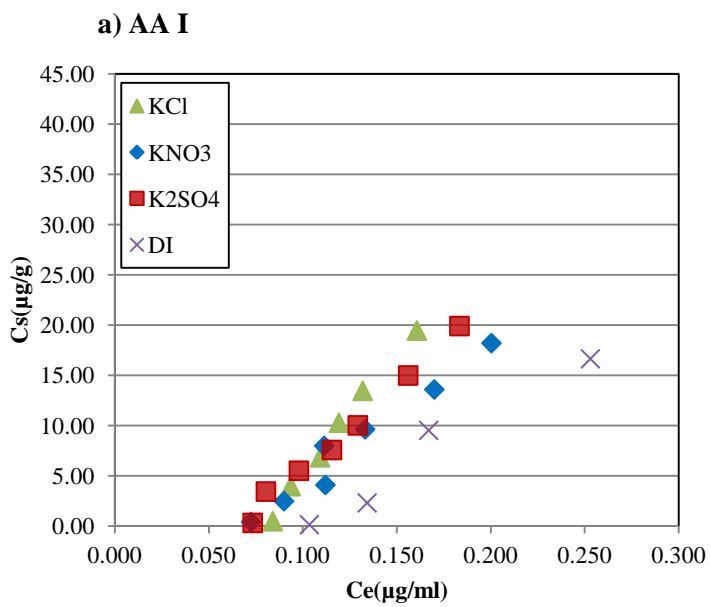


Figure 4.14 Adsorption isotherm of AA I (a) and II (b) on Hotyville NF soil in different anion background solution.

4.4.3 Desorption experiment

4.4.3.1 Desorption kinetic

Figure 4.15 show % desorption of AA I and II from all soils as function of time. The figures show that the desorption of AAs were quite rapid where nearly 90% of desorbed amount released in first 2 hr. The desorption equilibrium can be reach about 24 hr for Wooster CT and NF soils. However, the desorption for Hoytville CT and NF were slower and were reach to equilibrium about 48 hr. The rapid desorption can be explained that mostly sorbed AAs were attached on the surface sites and not diffused to stronger adsorption sites in the organic matter matrices. The results show that the adsorbed AAs on Wooster soil can be desorb more than Hoytville soil which may due to the higher clay and organic matter content of Hoytville soil. This supports the idea that soils which give less adsorb will have greater tendency to desorb (Piwowarczyk & Holden, 2012).

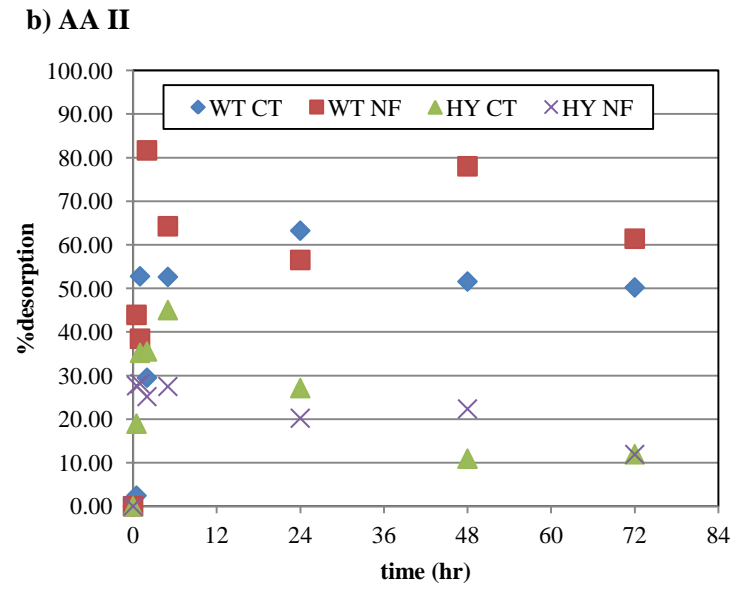
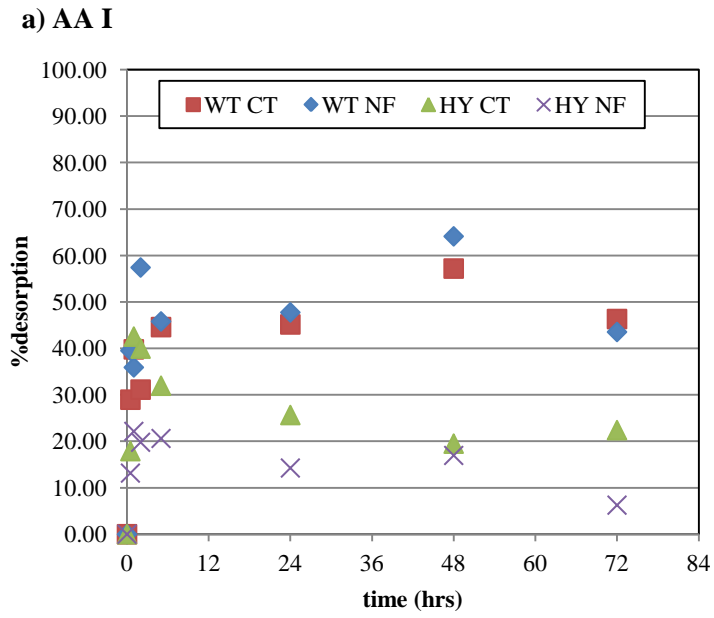
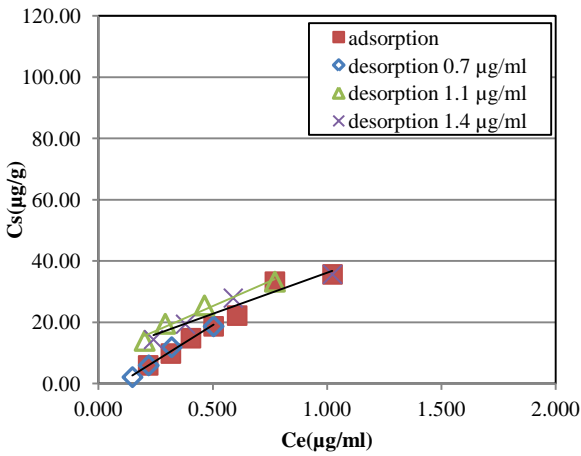


Figure 4.15 % Desorption of AA I (a) and AA II (b) as function of time for all tested soils

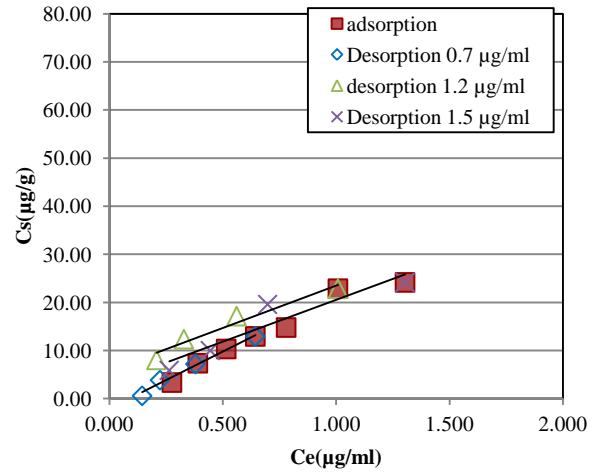
4.4.3.2 Desorption isotherm

To determine the desorption isotherm, the supernatant was removed and replaced by fresh CaCl_2 background solution. This technique will reduce AAs in solution and the adsorbed AAs will be released to reach the equilibrium again. The concentration remaining in solution and sorbed in soil were plotted as desorption isotherm as shown in Figure 4.16. It shows that most of the desorption isotherms were fitted well with the Freundlich equation ($r^2 > 0.9$) as shown in Table 4.5. The figures show that the sorption and desorption isotherm of all tested soils were not much deviated. The hysteresis index (HI) which is calculated from the ratio of the exponent of the desorption isotherm to the sorption isotherm ($n_{\text{des}}/n_{\text{ads}}$) according to Eq. 4.11 were shown in Table 4.5. The HI values of all soils were nearly 100 at low initial concentration, which indicated that the sorption of AAs to soils is largely reversible. However, at higher concentrations, the HI was found to decrease where the hysteresis increased. The easy desorption of AAs may be caused by the short contact time where AAs cannot get deep inside into organic matter matrices (Lesan & Bhandari, 2003).

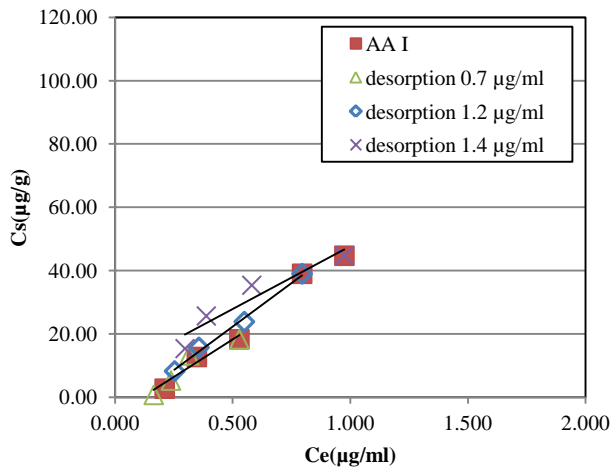
a) WT CT, AA I, original pH 6.39



b) WT CT AA II, original pH 6.39



c) WT NF AA I, original pH 4.57



d) WT NF AA II, original pH 4.57

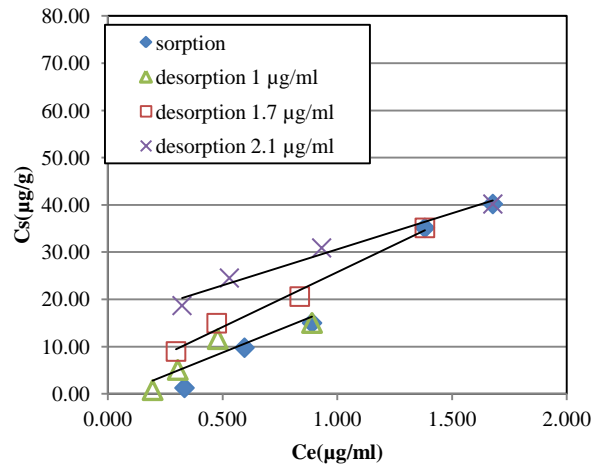
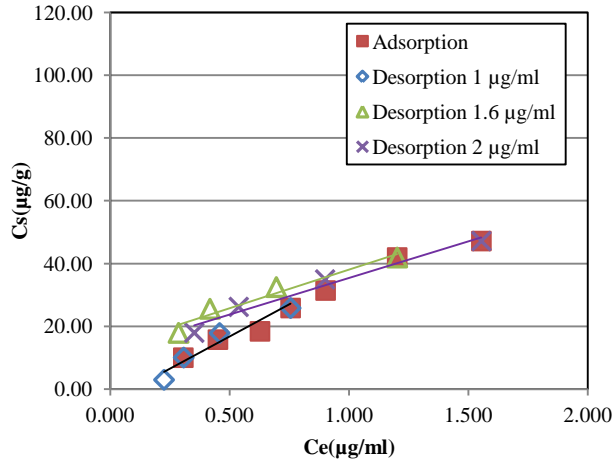


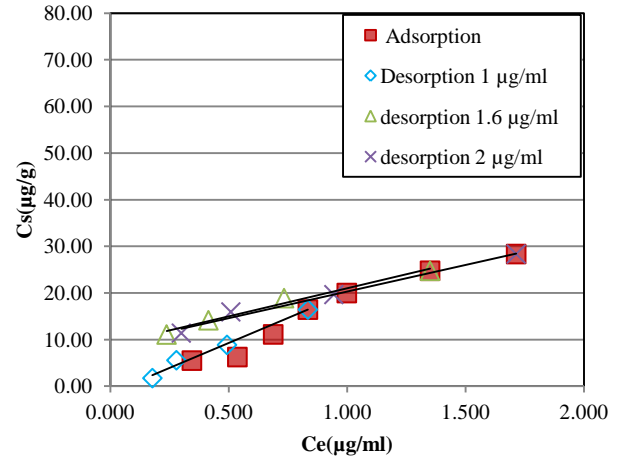
Figure 4.16 Sorption and desorption isotherm of AA I and II in WT CT soil (a and b), WT NF soil (c and d), HY CT soil (e and f) and HY NF soil (g and h) (filled symbols-adsorption point, open symbols-desorption point)

Figure 4.16 (cont'd)

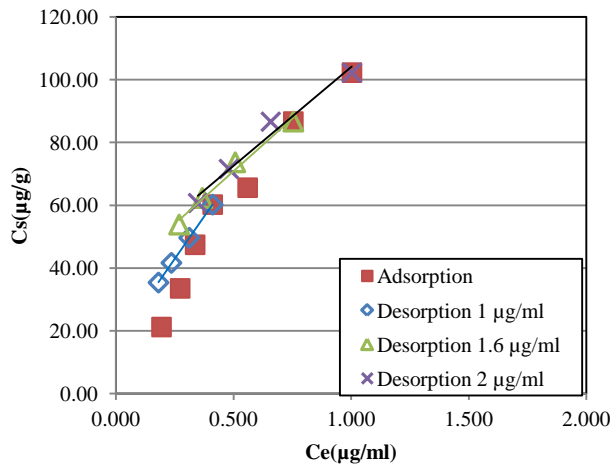
e) HY CT, AA I, original pH 6.66



f) HY CT, AA II, original pH 6.66



g) HY NF, AA I, original pH 6.56



h) HY NF, AA II, original pH 6.56

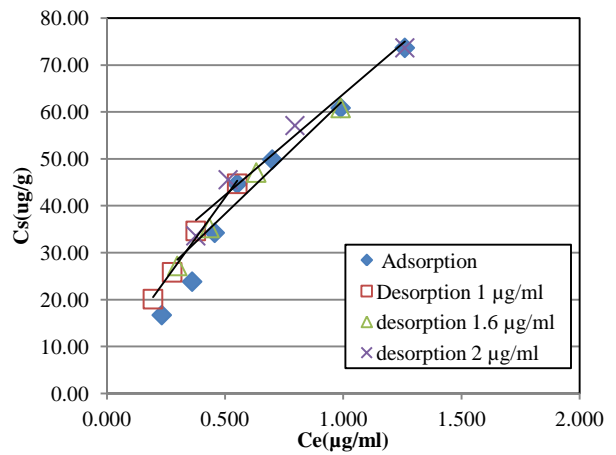


Table 4.5 Desorption coefficient (k_{des}) and $1/n_{des}$ obtained from fitting the model and hysteresis index ($HI = \frac{1/n_{des}}{1/n_{ads}}$) for sorption of AA I and II in all tested soils

Soil	AA I					AA II				
	Initial concentration	K_{des}	$1/n_{des}$	r^2	HI	Initial concentration	K_{des}	$1/n_{des}$	r^2	HI
WT CT	0.7 µg/ml	49.41	1.37	0.97	133	0.7 µg/ml	23.26	1.29	0.97	126
	1.1 µg/ml	39.36	0.6	0.99	58	1.2 µg/ml	22.89	0.53	0.99	52
	1.4 µg/ml	35.84	0.61	0.98	58	1.5 µg/ml	20.81	0.75	0.90	73
WT NF	0.7 µg/ml	52.19	1.55	0.85	111	1 µg/ml	16.99	0.78	0.94	52
	1.2 µg/ml	55.06	1.46	0.97	105	1.7 µg/ml	26.03	0.87	0.98	58
	1.4 µg/ml	47.10	0.72	0.92	52	2.1 µg/ml	31.88	0.45	0.99	30
HY CT	1 µg/ml	37.34	1.17	0.92	125	1 µg/ml	20.28	1.16	0.98	116
	1.6 µg/ml	38.54	0.53	0.98	57	1.6 µg/ml	21.55	0.46	0.99	46
	2 µg/ml	33.25	0.84	0.94	91	2 µg/ml	21.24	0.51	0.98	50
HY NF	1 µg/ml	106.93	0.65	0.99	82	1 µg/ml	71.35	0.77	0.99	98
	1.6 µg/ml	99.21	0.46	0.99	58	1.6 µg/ml	61.67	0.64	0.99	81
	2 µg/ml	102.72	0.58	0.92	74	2 µg/ml	64.67	0.60	0.99	76

4.4.3.3 Effect of initial concentration

The effect of different initial concentration to desorption hysteresis of each soil are shown in Figure 4.17. The figures show that hysteresis index (HI) had been decrease when concentration increased which indicated the desorption was more difficult at higher concentration. This can be explained that, at low concentration, AAs had low concentration gradient where the few molecules could penetrate to organic matter matrix. However, at high concentration, the AAs had more driving force to go deeper sites in the soil, and they can form

the stronger bond such as H-bonding with organic matter which caused them less to desorb (Chefetz et al., 2004).

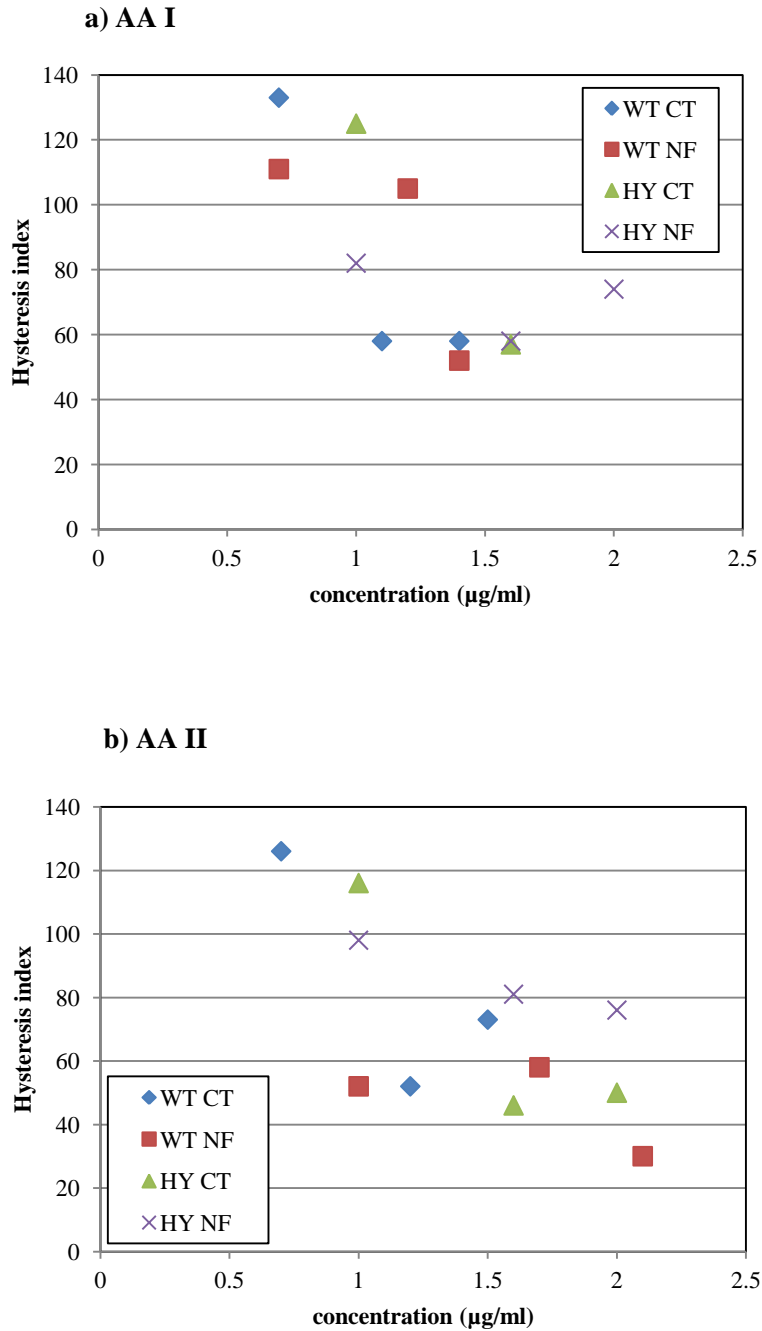


Figure 4.17 The hysteresis index of AA I (a) and II (b) as a function of initial concentration for all tested soils

4.4.3.4 Effect of pH

To investigate the effect of pH on desorption process, the desorption at different pH were tested with all soils. Because similar trend was found, the only isotherms of Hoytville soil are presented here. From Figure 4.18, the sorption and desorption isotherm at low pH are quite similar. However, when the pH increase, the desorption increasingly deviated from adsorption isotherm.

Figure 4.19 plots the calculated hysteresis index (HI) of desorption isotherm of all soil at different pH. The figures show the HI values were gradually decreased when the pH increased. These evidence showed the different desorption mechanism between neutral and anion form of AAs. The desorption was readily when AAs were in neutral form but the desorption will be harder when AAs were in anion form at high pH. The anion molecules can form specific interaction e.g. cation bridging mechanism to soil which was quite strong and therefore resist to desorption (Caceres et al., 2010; Ren et al., 2011).

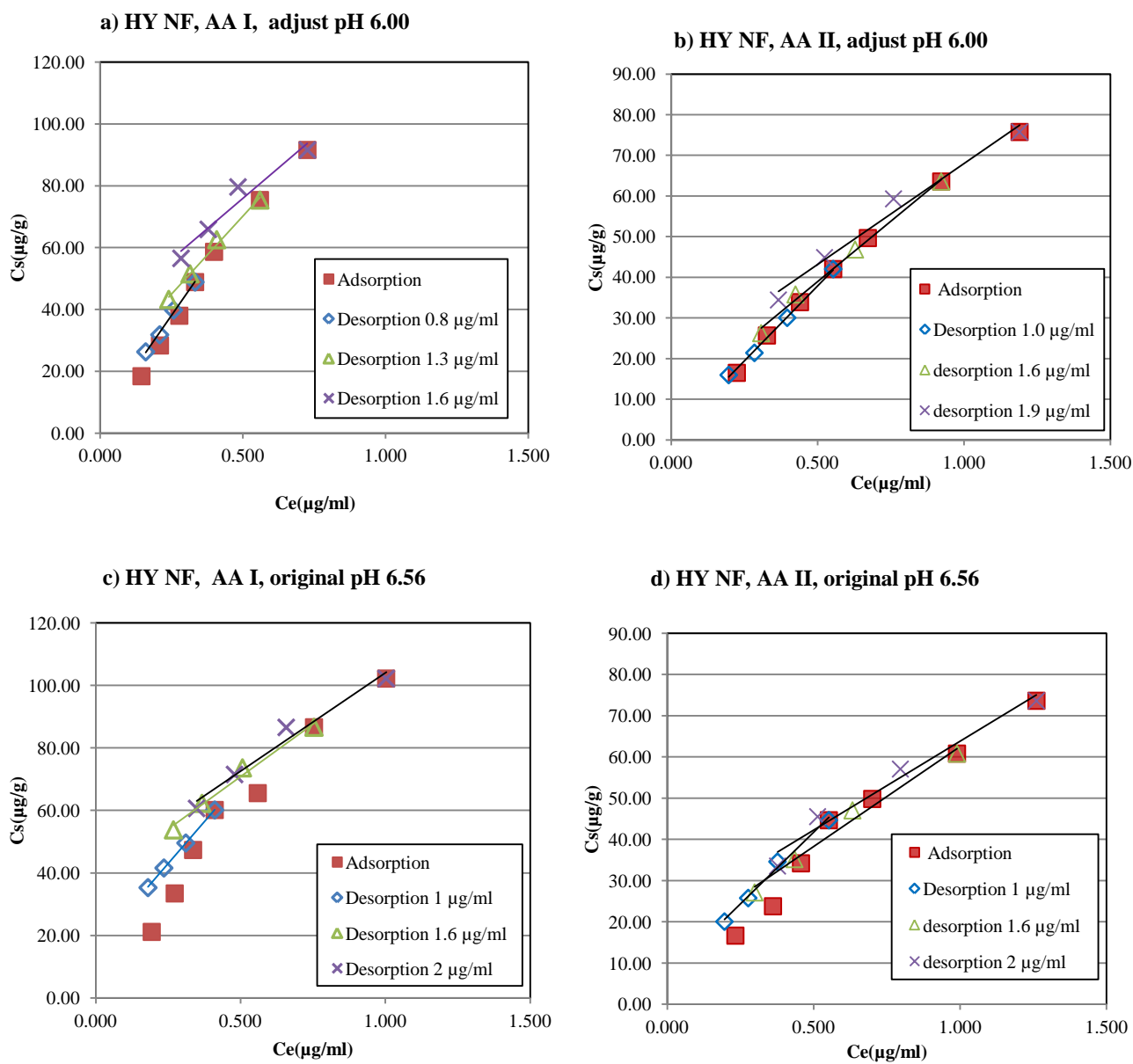
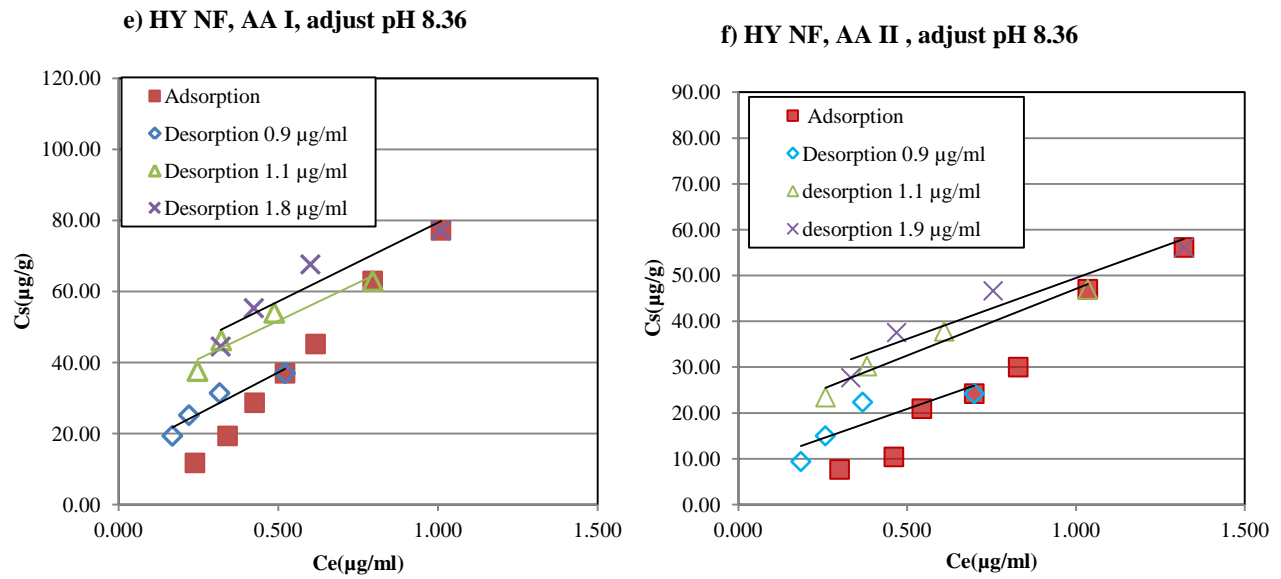


Figure 4.18 AAs sorption –desorption isotherm of AA I and II on Hoytville NF soil at adjusted pH 6.0 (a) and (b), original pH 6.56 (c) and (d), adjusted pH8.36 (e) and (f). The pH shown in figure was from an average of pH of adsorption process.

Figure 4.18 (cont'd)



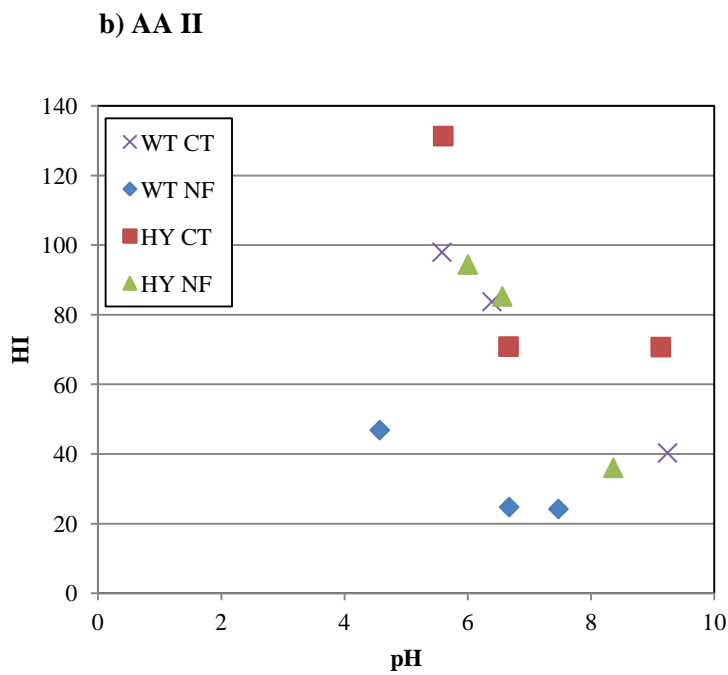
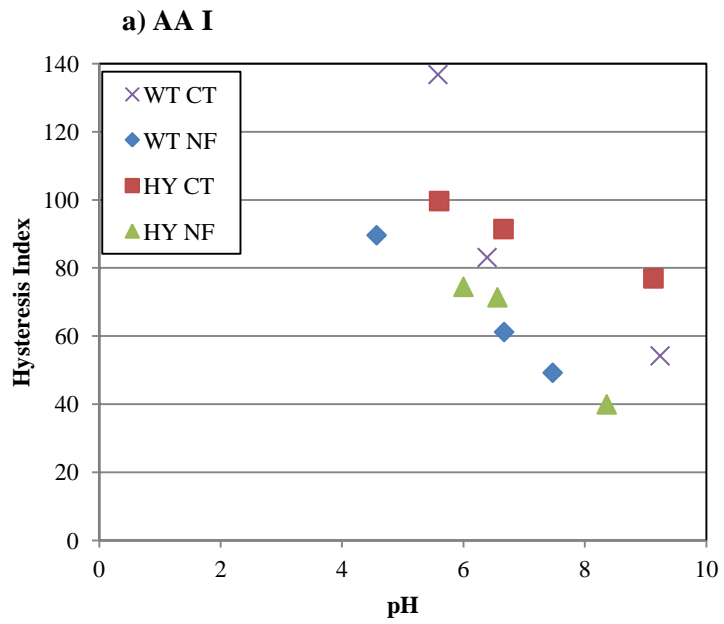


Figure 4.19 Hysteresis index calculated from sorption-desorption isotherm of all soil as a function with pH of AA I (a) and AA II (b)

4.4.3.5 Effect of cations/anions

The effect of cation type to desorption process was tested on Hoytville NF soil. The desorption isotherm of AA I with different cation background solution had been created as shown in Figure 4.20. The hysteresis indexes were calculated and plotted with cations types which showed in Figure 4.21. Divalent cation (Mg^{2+} , Ca^{2+} and Sr^{2+}) found to have more hysteresis than monovalent cations (Na^+ and K^+). This indicated the adsorption was largely reversible when AAs dissolved in deionized water or monovalent cations solution, whereas the irreversibility or hysteresis increased when AAs dissolved in divalent cations solution. The reversibility of sorption in monovalent cation solution suggests non-specific cation exchange sorption reaction were dominant whereas higher hysteresis in divalent cation solution indicated stronger specific binding mechanisms e.g. cation bridging were dominant. The hysteresis increase in order of $Na < K < Mg < Ca \approx Sr$ which according the replacibility of cations e.g. $Li^+ < Na^+ < K^+ < Mg^{2+} < Ca^{2+} < Sr^{2+}$ (Carroll, 1959). The more valent cations can create the stronger bond, so it should be more difficult of AAs to be desorbed. The high sorption and low desorption on divalent cations supports the idea of cation bridging as mainly mechanism.

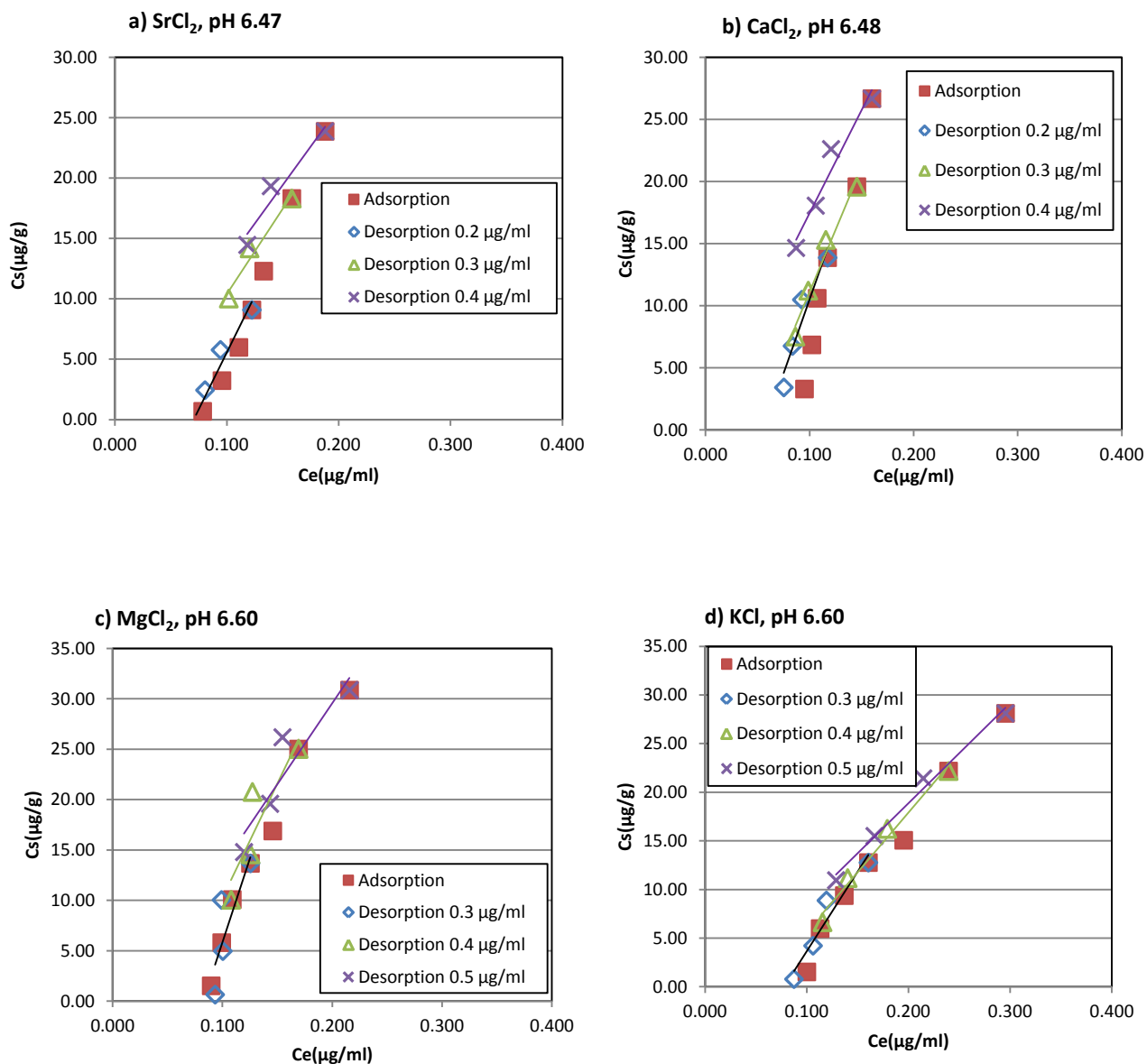


Figure 4.20 The sorption/desorption isotherm of AA I on Hoytville NF soil in different cation background solution (a) SrCl₂ (b) CaCl₂ (c) MgCl₂ (d) KCl (e) NaCl (filled symbols-adsorption point, open symbols-desorption point)

Figure 4.20 (cont'd)

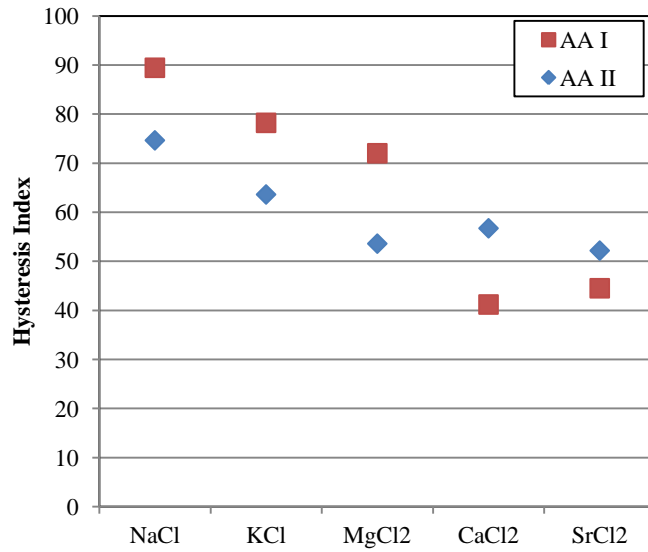
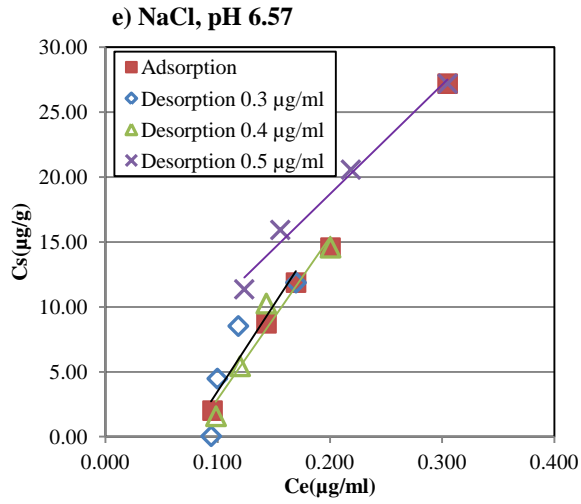


Figure 4.21 The hysteresis index of desorption of AA I and II on HYNF soil at initial concentration 0.2-0.9 µg/ml with different cation background solution

The effect of anions type to desorption was shown in Figure 4.22 where the desorption of AA I from Hoytville soil in different anion background solution was presented. The figures show that the desorption isotherm of AA I were not deviated from adsorption isotherm or no desorption hysteresis had been observed in NO_3^- , SO_4^{2-} and Cl^- solution. However, even the AAs sorption is not significantly related to anion exchange mechanism (from previous studies), the plot between HI and anion types (Figure 4.23) showed the HI of NO_3^- were much higher than SO_4^{2-} and Cl^- . This means higher amount of AA I can be desorbed in NO_3^- solution more than in SO_4^{2-} and Cl^- solution or NO_3^- was more compete to AAs sorption sites than SO_4^{2-} and Cl^- . This evidence is according to the result from Moharami & Jalali, 2013 where they indicated that NO_3^- had high attractive force to cations sorption sites of the soil.

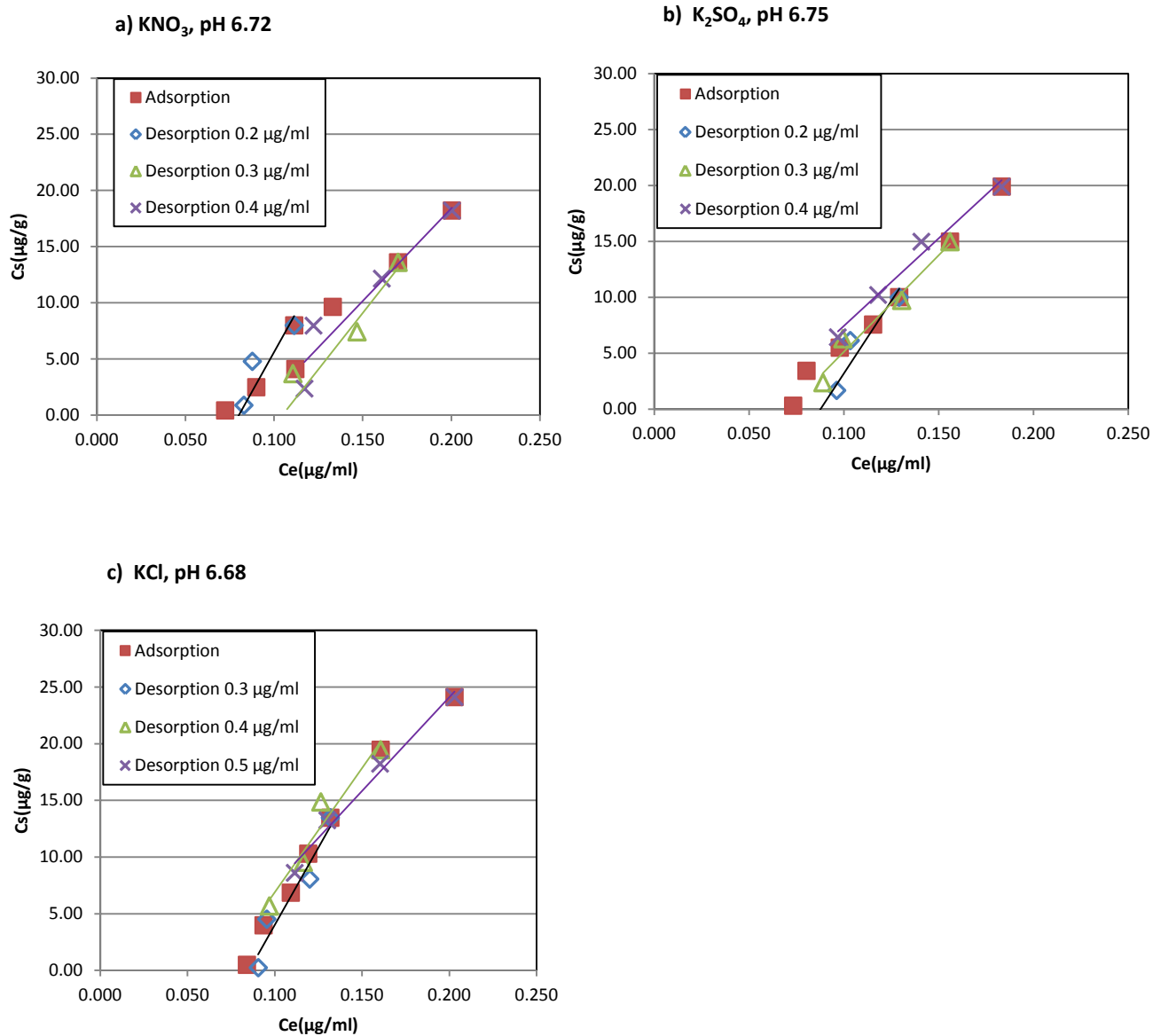


Figure 4.22 The sorption/desorption isotherm of AA I on Hoytville NF soil in different anion background solution: KNO₃ (a), K₂SO₄ (b), KCl (c) (filled symbols-adsorption point, open symbols-desorption point)

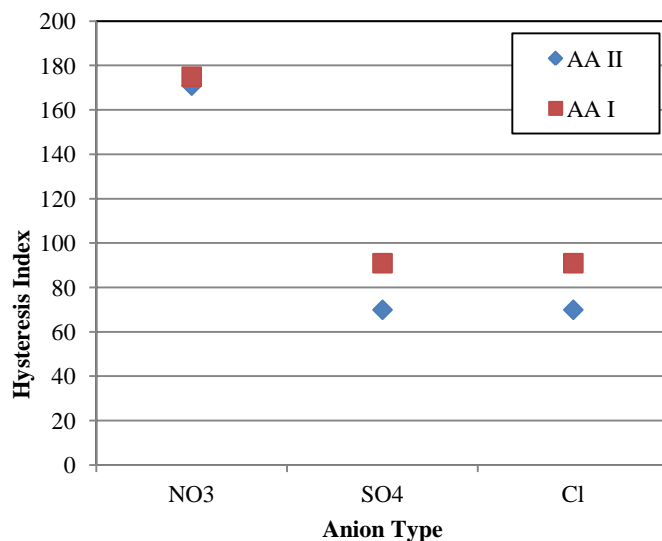


Figure 4.23 The hysteresis index of desorption of AA I and II on HYNF soil at initial concentration 0.2-0.9 $\mu\text{g/ml}$ with different anion background solution

4.5 Conclusion

From adsorption studies suggest that the organic matter is important soil content that response to sorption of AAs. However, in low organic matter soil, clays are important content that response the adsorption too. The low organic matter and clay content soil will have less sorption and the AAs will be more mobile. The neutral and ionized forms of AAs have different sorption mechanism. The neutral form in low pH solution can create a hydrophobic adsorption which was much higher than adsorption of anion form at high pH by ionic exchange. The increasing of adsorption with calcium ion and replacibility of cation indicated the adsorption via cation bridging mechanism.

The desorption studies suggest that AAs can be easily desorbed from soil but the hysteresis will be increased when concentration of AAs in solution increases. The desorption was clearly affected by the pH of solution where the anion molecules at high pH showed more

resistance to desorb than neutral molecules at low pH. This result expects from the strong specific interaction e.g. cation bridging mechanism between anion AAs and cation on the soil. The increasing hysteresis with the order of replacing power of cations also supports this idea.

REFERENCES

REFERENCES

- Al-Busaidi, A., Cookson, P., & Yamamoto, T. (2005). Methods of pH determination in calcareous soils: use of electrolytes and suspension effect. *Australian Journal of Soil Research*, 43(4), 541-545. doi: 10.1071/sr04102
- Barriuso, E., Baer, U., & Calvet, R. (1992). ORGANIC-CHEMICALS IN THE ENVIRONMENT - DISSOLVED ORGANIC-MATTER AND ADSORPTION-DESORPTION OF DIMEFURON, ATRAZINE, AND CARBETAMIDE BY SOILS. *Journal of Environmental Quality*, 21(3), 359-367.
- Barriuso, E., Laird, D. A., Koskinen, W. C., & Dowdy, R. H. (1994). ATRAZINE DESORPTION FROM SMECTITES. *Soil Science Society of America Journal*, 58(6), 1632-1638.
- Burgos, W. D., & Pisutpaisal, N. (2006). Sorption of naphthoic acids and quinoline compounds to estuarine sediment. *Journal of Contaminant Hydrology*, 84(3-4), 107-126. doi: 10.1016/j.jconhyd.2005.12.008
- Caceres, L., Fuentes, R., Escudey, M., Fuentes, E., & Baez, M. E. (2010). Metsulfuron-methyl Sorption/Desorption Behavior on Volcanic Ash-Derived Soils. Effect of Phosphate and pH. *Journal of Agricultural and Food Chemistry*, 58(11), 6864-6869. doi: 10.1021/jf904191z
- Calvet, R. (1989). ADSORPTION OF ORGANIC-CHEMICALS IN SOILS. *Environmental Health Perspectives*, 83, 145-177. doi: 10.2307/3430653
- Carroll, D. (1959). ION EXCHANGE IN CLAYS AND OTHER MINERALS. *Geological Society of America Bulletin*, 70(6), 749-779. doi: 10.1130/0016-7606(1959)70[749:ieicao]2.0.co;2
- Chefetz, B., Bilkis, Y. I., & Polubesova, T. (2004). Sorption-desorption behavior of triazine and phenylurea herbicides in Kishon river sediments. *Water Research*, 38(20), 4383-4394. doi: 10.1016/j.watres.2004.08.023
- Clausen, L., & Fabricius, I. (2001). Atrazine, isoproturon, mecoprop, 2,4-D, and bentazone adsorption onto iron oxides. *Journal of Environmental Quality*, 30(3), 858-869.
- Cox, L., Koskinen, W. C., & Yen, P. Y. (1997). Sorption-desorption of imidacloprid and its metabolites in soils. *Journal of Agricultural and Food Chemistry*, 45(4), 1468-1472. doi: 10.1021/jf960514a
- DiVincenzo, J. P. (1996). *Slow sorption kinetics of pentachlorophenal on soil*. (Ph.D.), University of Delaware.

- DiVincenzo, J. P., & Sparks, D. L. (2001). Sorption of the neutral and charged forms of pentachlorophenol on soil: Evidence for different mechanisms. *Archives of Environmental Contamination and Toxicology*, 40(4), 445-450.
- Dubus, I. G., Barriuso, E., & Calvet, R. (2001). Sorption of weak organic acids in soils: clofencet, 2,4-D and salicylic acid. *Chemosphere*, 45(6-7), 767-774. doi: 10.1016/s0045-6535(01)00108-4
- Dudka, S., & Miller, W. P. (1999). Accumulation of potentially toxic elements in plants and their transfer to human food chain. *Journal of Environmental Science and Health Part B-Pesticides Food Contaminants and Agricultural Wastes*, 34(4), 681-708. doi: 10.1080/03601239909373221
- Evanko, C. R., & Dzombak, D. A. (1998). Influence of structural features on sorption of NOM-analogue organic acids to goethite. *Environmental Science & Technology*, 32(19), 2846-2855. doi: 10.1021/es980256t
- Figueroa, R. A., Leonard, A., & Mackay, A. A. (2004). Modeling tetracycline antibiotic sorption to clays. *Environmental Science & Technology*, 38(2), 476-483. doi: 10.1021/es0342087
- Franco, A., Fu, W. J., & Trapp, S. (2009). INFLUENCE OF SOIL pH ON THE SORPTION OF IONIZABLE CHEMICALS: MODELING ADVANCES. *Environmental Toxicology and Chemistry*, 28(3), 458-464. doi: 10.1897/08-178.1
- Fruhstorfer, P., Schneider, R. J., Weil, L., & Niessner, R. (1993). FACTORS INFLUENCING THE ADSORPTION OF ATRAZINE ON MONTMORILLONITIC AND KAOLINITIC CLAYS. *Science of the Total Environment*, 138(1-3), 317-328. doi: 10.1016/0048-9697(93)90425-6
- Fu, G. M., Kan, A. T., & Tomson, M. (1994). ADSORPTION AND DESORPTION HYSTERESIS OF PAHS IN SURFACE SEDIMENT. *Environmental Toxicology and Chemistry*, 13(10), 1559-1567. doi: 10.1897/1552-8618(1994)13[1559:aadhop]2.0.co;2
- Gao, J. P., Maguhn, J., Spitzauer, P., & Kettrup, A. (1998). Sorption of pesticides in the sediment of the Teufelsweiher pond (Southern Germany). II: Competitive adsorption, desorption of aged residues and effect of dissolved organic carbon. *Water Research*, 32(7), 2089-2094. doi: 10.1016/s0043-1354(98)00140-7
- Herwig, U., Klumpp, E., Narres, H. D., & Schwuger, M. J. (2001). Physicochemical interactions between atrazine and clay minerals. *Applied Clay Science*, 18(5-6), 211-222. doi: 10.1016/s0169-1317(01)00024-2
- Hyun, S., & Lee, L. S. (2004). Factors controlling sorption of prosulfuron by variable-charge soils and model sorbents. *Journal of Environmental Quality*, 33(4), 1354-1361.

- Hyun, S., & Lee, L. S. (2005). Quantifying the contribution of different sorption mechanisms for 2,4-dichlorophenoxyacetic acid sorption by several variable-charge soils. *Environmental Science & Technology*, 39(8), 2522-2528. doi: 10.1021/es04820p
- Hyun, S., Lee, L. S., & Rao, P. S. C. (2003). Significance of anion exchange in pentachlorophenol sorption by variable-charge soils. *Journal of Environmental Quality*, 32(3), 966-976.
- Jackson, C. B. (2000). *Sorption and desorption of Metribuzin with soil and sewage biosolids organic matter: interpretations base on mechanistic and kinetic models*. Colorado State University.
- Jafvert, C. T. (1990). SORPTION OF ORGANIC-ACID COMPOUNDS TO SEDIMENTS - INITIAL MODEL DEVELOPMENT. *Environmental Toxicology and Chemistry*, 9(10), 1259-1268. doi: 10.1897/1552-8618(1990)9[1259:sooact]2.0.co;2
- Jafvert, C. T., Westall, J. C., Grieder, E., & Schwarzenbach, R. P. (1990). DISTRIBUTION OF HYDROPHOBIC IONOGENIC ORGANIC-COMPOUNDS BETWEEN OCTANOL AND WATER - ORGANIC-ACIDS. *Environmental Science & Technology*, 24(12), 1795-1803. doi: 10.1021/es00082a002
- Jenks, B. M., Roeth, F. W., Martin, A. R., & McCallister, D. L. (1998). Influence of surface and subsurface soil properties on atrazine sorption and degradation. *Weed Science*, 46(1), 132-138.
- Kah, M., & Brown, C. D. (2006). Adsorption of ionisable pesticides in soils. *Reviews of Environmental Contamination and Toxicology*, Vol 188, 188. doi: 10.1007/978-0-387-32964-2_5
- Karickhoff, S. W., Brown, D. S., & Scott, T. A. (1979). SORPTION OF HYDROPHOBIC POLLUTANTS ON NATURAL SEDIMENTS. *Water Research*, 13(3), 241-248. doi: 10.1016/0043-1354(79)90201-x
- Kummert, R., & Stumm, W. (1980). THE SURFACE COMPLEXATION OF ORGANIC-ACIDS ON HYDROUS GAMMA-AL₂O₃. *Journal of Colloid and Interface Science*, 75(2), 373-385. doi: 10.1016/0021-9797(80)90462-2
- Kuo, C. H., Lee, C. W., Lin, S. C., Tsai, I. L., Lee, S. S., Tseng, Y. J., . . . Wei-Chu, L. (2010). Rapid determination of aristolochic acids I and II in herbal products and biological samples by ultra-high-pressure liquid chromatography-tandem mass spectrometry. *Talanta*, 80(5), 1672-1680. doi: 10.1016/j.talanta.2009.10.003
- Langmuir, D. (1997). *Aqueous Environmental Geochemistry*. New Jersey: Prentice-Hall, Inc.

- Lee, L. S., Rao, P. S. C., Nkedikizza, P., & Delfino, J. J. (1990). INFLUENCE OF SOLVENT AND SORBENT CHARACTERISTICS ON DISTRIBUTION OF PENTACHLOROPHENOL IN OCTANOL-WATER AND SOIL-WATER SYSTEMS. *Environmental Science & Technology*, 24(5), 654-661. doi: 10.1021/es00075a006
- Lesan, H. M., & Bhandari, A. (2003). Atrazine sorption on surface soils: time-dependent phase distribution and apparent desorption hysteresis. *Water Research*, 37(7), 1644-1654. doi: 10.1016/s0043-1354(02)00497-9
- Liang, C. S., Dang, Z., Liu, C. Q., & Huang, W. L. (2005). Effects of soil organic matters on adsorption-desorption equilibria of phenanthrene. *Chemical Journal of Chinese Universities-Chinese*, 26(4), 671-676.
- Means, J. C., Wood, S. G., Hassett, J. J., & Banwart, W. L. (1980). SORPTION OF POLYNUCLEAR AROMATIC-HYDROCARBONS BY SEDIMENTS AND SOILS. *Environmental Science & Technology*, 14(12), 1524-1528. doi: 10.1021/es60172a005
- Moharami, S., & Jalali, M. (2013). Effects of cations and anions on iron and manganese sorption and desorption capacity in calcareous soils from Iran. *Environmental Earth Sciences*, 68(3), 847-858. doi: 10.1007/s12665-012-1787-8
- OECD. (2000). OECD Guideline for the testing of chemicals *Adsorption - Desorption Using a Batch Equilibrium Method*.
- Park, E. J., & Smucker, A. J. M. (2005). Erosive strengths of concentric regions within soil macroaggregates. *Soil Science Society of America Journal*, 69(6), 1912-1921. doi: 10.2136/sssaj2004.0400
- Piwowarczyk, A. A., & Holden, N. M. (2012). Adsorption and Desorption Isotherms of the Nonpolar Fungicide Chlorothalonil in a Range of Temperate Maritime Agricultural Soils. *Water Air and Soil Pollution*, 223(7), 3975-3985. doi: 10.1007/s11270-012-1165-x
- Regitano, J. B., Alleoni, L. R. F., Vidal-Torrado, P., Casagrande, J. C., & Tornisiello, V. L. (2000). Imazaquin sorption in highly weathered tropical soils. *Journal of Environmental Quality*, 29(3), 894-900.
- Regitano, J. B., Bischoff, M., Lee, L. S., Reichert, J. M., & Turco, R. F. (1997). Retention of imazaquin in soil. *Environmental Toxicology and Chemistry*, 16(3), 397-404. doi: 10.1897/1551-5028(1997)016<0397:roiis>2.3.co;2
- Ren, W. J., Wang, M. E., & Zhou, Q. X. (2011). Effect of soil pH and organic matter on desorption hysteresis of chlorimuron-ethyl in two typical Chinese soils. *Journal of Soils and Sediments*, 11(4), 552-561. doi: 10.1007/s11368-011-0337-4

- Sassman, S. A., & Lee, L. S. (2007). Sorption and degradation in soils of veterinary ionophore antibiotics: monensin and lasalocid. *Environmental Toxicology and Chemistry*, 26(8), 1614-1621. doi: 10.1897/07-073r.1
- Schwarzenbach, R. P., Gschwend, P. M., & Imboden, D. M. (2003). *Environmental Organic Chemistry* (2nd Ed.). New Jersey: John Wiley & Sons, Inc.
- Senesi, N. (1992). BINDING MECHANISMS OF PESTICIDES TO SOIL HUMIC SUBSTANCES. *Science of the Total Environment*, 123, 63-76. doi: 10.1016/0048-9697(92)90133-d
- ter Laak, T. L., Gebbink, W. A., & Tolls, J. (2006). The effect of pH and ionic strength on the sorption of sulfachloropyridazine, tylosin, and oxytetracycline to soil. *Environmental Toxicology and Chemistry*, 25(4), 904-911. doi: 10.1897/05-232r.1
- Tolls, J. (2001). Sorption of veterinary pharmaceuticals in soils: A review. *Environmental Science & Technology*, 35(17), 3397-3406. doi: 10.1021/es0003021
- Vonoepen, B., Kordel, W., & Klein, W. (1991). SORPTION OF NONPOLAR AND POLAR COMPOUNDS TO SOILS - PROCESSES, MEASUREMENTS AND EXPERIENCE WITH THE APPLICABILITY OF THE MODIFIED OECD-GUIDELINE-106. *Chemosphere*, 22(3-4), 285-304. doi: 10.1016/0045-6535(91)90318-8
- Westall, J. C., Chen, H., Zhang, W. J., & Brownawell, B. J. (1999). Sorption of linear alkylbenzenesulfonates on sediment materials. *Environmental Science & Technology*, 33(18), 3110-3118. doi: 10.1021/es9804316
- Yang, W. C., Mang, J., Zhang, C. D., Zhu, L. Y., & Chen, W. (2009). Sorption and Resistant Desorption of Atrazine in Typical Chinese Soils. *Journal of Environmental Quality*, 38(1), 171-179. doi: 10.2134/jeq2007.0674
- Yuan, G. S., & Xing, B. S. (2001). Effects of metal cations on sorption and desorption of organic compounds in humic acids. *Soil Science*, 166(2), 107-115. doi: 10.1097/00010694-200102000-00004
- Yuan, J. B., Liu, Q., Zhu, W. F., Ding, L., Tang, F., & Yao, S. Z. (2008). Simultaneous analysis of six aristolochic acids and five aristolactams in herbal plants and their preparations by high-performance liquid chromatography-diode array detection-fluorescence detection. *Journal of Chromatography A*, 1182(1), 85-92. doi: 10.1016/j.chroma.2007.12.076
- Zelazny, L. W., He, L., & Vanwormhoudt, A. (1996). *Charge analysis of soils and anion exchange* (D. L. e. a. Sparks Ed.). Madison, WI: SSSA.

Zhang, C. Y., Wang, X., Shang, M. Y., Yu, J., Xu, Y. Q., Li, Z. G., . . . Namba, T. (2006). Simultaneous determination of five aristolochic acids and two aristololactams in *Aristolochia* plants by high-performance liquid chromatography. *Biomedical Chromatography*, 20(4), 309-318. doi: 10.1002/bmc.565

Chapter 5

Plant uptake

5.1 Introduction

Uptake of organic chemicals by plants grown in contaminated area is an important process to assess the human health risk by food contamination. Plants can take many of organic chemicals such as chlorinated solvents, pesticides, PAHs, PCBs and pharmaceuticals from soil that contained these chemicals or was irrigated with contaminated wastewater (Aslund, Rutter, Reimer, & Zeeb, 2008; Kipopoulou, Manoli, & Samara, 1999; Shenker, Harush, Ben-Ari, & Chefetz, 2011). These chemicals will be taken up directly from root and translocated to aboveground tissue e.g. stems, leaves and fruits. Some edible vegetables and fruits have been detected these chemicals over the safe exposure limit. For example, the dieldrin and endrin which are extremely persistent pesticides had been detected in cucumber fruits that grown in contaminated sites exceeding the concentration set by the food sanitation law (Hashimoto, 2005). Therefore, the plant uptake process is important for accumulation of organic chemicals in environment by increasing concentration of the chemicals in food chain.

The pollutant chemicals can be transferred to plant tissues in various extent which depend on concentration in the media, physicochemical properties of contaminants (hydrophobicity, water solubility), plant species, exposure time, soil properties (pH, organic matter content, cation exchange capacity) and the interaction between contaminants and plant composition (Chiou, Sheng, & Manes, 2001; Su, Zhu, & Liang, 2009). The pollutant organic chemicals can be taken by plant roots in proportion to amount of water transpired via root tips and root hairs.

Chemicals enter into the plants by two different processes, first is passive process which is diffusion across membrane by concentration gradient and second is active process where chemicals incorporate to nutrient uptake and energy consuming processes (Su, Zhu, & Du, 2005; Trapp, 2004). After chemicals get into the root, they will transport via 2 vessel system, xylem and phloem where chemical can move from root to shoot or shoot to root follow concentration gradient (Hellstrom, 2004; Su, Liu, & Liang, 2010). The study of distribution of chemicals into the plants mostly will be described by root concentration factor (RCF) and transpiration stream concentration factor (TSCF) which is define as concentration accumulated in root tissue or concentration in transpiration stream divide by concentration in external media concentration, respectively (Briggs et al., 1983; Su et al., 2010). The obtained values of RCF and TSCF are useful to predict the contamination in the crops. They evaluate the capacity of chemical that can adsorb on the plant root and transpiration across the root membrane to xylem and translocation to other parts e.g. stems and leaves.

To evaluate the AAs potential exposure pathway via food crop contamination, the determination the plant uptake and accumulation capacity is important. This study will provide the basic plant-AAs uptake data. It will address the potential of AAs enter to plant through the root and translocate and accumulate in the shoots in hydroponic and sand culture system.

5.2 Literature reviews

5.2.1 Root uptake mechanism and pathway

Organic chemicals can move from external solution into the plant by transpiration process with water. The chemical transfer process can divide into passive and active mechanism. For the passive process, organic chemicals will diffuse from root pass through bundle of root

cells until reach the xylem column driving by concentration gradient. Typically, there are two pathways for transportation organic chemicals in root cells, the symplastic and apoplastic. In symplastic, the water and chemicals will move across the plasma membrane to each root cell and endodermis until they get into the xylem whereas, for apoplastic, the water and chemicals will move between the root cell membrane until reaching the xylem as shown in Figure 5.1 The transport of compounds may be combination between these two pathways (E. Dettenmaier, 2008; Steudle & Peterson, 1998). Most organic compounds move by passive process and the uptake rate is controlled by diffusion across these lipid membrane and concentration gradient as transport driving energy.

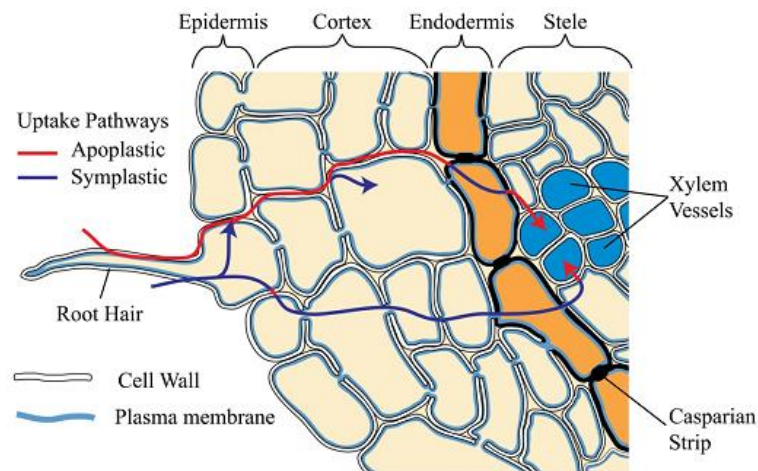


Figure 5.1 The diffusion pathway of symplastic and apoplastic (Dettenmaier, 2008)

Unlike the neutral organic compounds, ionized compounds are not likely to passively transport across lipid membrane by concentration driving because of high activation energy required. However, they cross the membrane rather by synergistic with specific protein spanning in the membrane in ADP-ATP proton pumping process. The hydrogen ions are pumping in and out across the membrane during cell respiration which produces concentration and electrical potential gradient. This charge gradient will drive cationic or anionic species to cross the membrane to obtain the electrical potential balance. This is called “active process” (E. Dettenmaier, 2008). Except the hormone-like chemicals e.g. 2,4-dichlorophenoxyacetic acid, there are no anthropogenic chemicals taken up by active process.

5.2.2 Translocation, accumulation and metabolism in plant

Once the compounds pass through the root cell, they diffuse from cell to cell into the xylem where the compounds can move to other parts of the plant by xylem flow (E. Dettenmaier, 2008). In xylem, the water and soluble mineral nutrients will be transported from the root to aerial parts e.g. stems and leaves to replace the water lost in transpiration and photosynthesis processes. The water and solute move in xylem by mass flow or pressure potential induced by transpiration process rather than cell diffusion.

In Phloem, water and food e.g. sugar and amino acids produced by photosynthesis will be moved to storage organs e.g. roots, seeds, fruit, tubers and bulbs. The organic substances will be transported by diffusion gradient and phloem sap moved by positive hydrostatic pressure. The phloem is located on the outer side of vascular bundle whereas the xylem is located inside the bundle (Diffen; Hellstrom, 2004).

The organic chemicals that were taken up by root will translocate throughout the plant tissues via xylem and phloem vessel. The accumulation may be presented in photosynthesis areas or sites with great transpiration, e.g. mature leaf. Most nonionized compound can partition to the stem xylem tissue which is dominant factor that impede the long distance movement of compounds. The transport of organic compounds in stem is similar to reverse phase column chromatography. They may adsorb to the vessel wall or partitioning to lipophilic component in xylem tissues which also related to the hydrophobicity (K_{ow}) of chemicals (McCrary, McFarlane, & Lindstrom, 1987). The more hydrophobic chemicals are likely to retain by the stem base. In xylem, the compounds can also diffuse to adjacent tissue e.g. phloem but degree of exchange depend on characteristic tissue to the chemicals (Trapp & McFarlane, 1995). Many studies show that some plants are also effective in translocation and accumulation organic and inorganic compounds in the leaf (Cui et al., 2014; Lin, Zhu, He, & Tu, 2006) and in fruit (Hulster, Muller, & Marschner, 1994) as well, even if they were much less than root and stem. The accumulation in leaf will be higher if plant has high transpiration rate (Polder, Hulzebos, & Jager, 1995).

Although plant can uptake and accumulate the organic pollutants, live cells plants can metabolic degradation the chemicals that foreign to them e.g. pesticides. Plant can metabolize even persistent chemicals such as the insecticide, DDT or fungicide, hexachlorobenzene (Sandermann, Scheel, & Vandertrenck, 1984). Plant metabolism are similar to liver processes ,by transform the xenobiotic compounds to non-toxic chemical and then form conjugate with glucose or amino acid or even cell wall in the plant. The different between plant and liver metabolism is the conjugates will be excreted in animals but they will be stored or compartmentalized in the plant cells (Hellstrom, 2004; Trapp & McFarlane, 1995). For example, atrazine was metabolited

in corn seedling to OH-derivative of atrazine. This transformation was readily after parent compounds enter the plant (Raveton, Ravanel, Serre, Nurit, & Tissut, 1997). Palazzo, 1986 reported the founding TNT metabolites in terrestrial plants expose to TNT in hydroponic solution. Although metabolic fate of organic compounds in plant had been intensively studied, it is still difficult to predict and largely differ among plant species.

5.2.3 Plant uptake descriptor

The potential uptake of chemical by plant can quantitatively described by bioconcentration factor (BCF) and transpiration stream concentration factor (TSCF). The bioconcentration factor, similar using in fish, use to determine the ability of chemicals accumulated in plant tissue and simply define by ratio of concentration in plant tissue to concentration in the media that plant growing in e.g. nutrient concentration or soil concentration (Briggs, Bromilow, & Evans, 1982; Y. Z. Gao & Zhu, 2004; Oconnor, Kiehl, Eiceman, & Ryan, 1990; Trapp, 2000). The root concentration factor is used to describe the accumulation of chemical in root as Eq. 5.1:

$$\text{Root concentration factor} = \frac{\text{concentration in roots}(\mu\text{g/g})}{\text{concentration in external solution}(\mu\text{g/ml})} \quad (5.1)$$

Likewise the root concentration factor (RCF), Brigg et al. also defined stem concentration factor (SCF) to describe ability of compounds accumulate in stem which is the ratio of concentration in stem to external solution as defined in Eq. 5.2

$$\text{Stem concentration factor} = \frac{\text{concentration in stems}(\mu\text{g/g})}{\text{concentration in external solution}(\mu\text{g/ml})} \quad (5.2)$$

However, some substances can accumulated in leaf with high concentration more than stem if transpiration rate at leaf is high. So, the stem concentration factor may not a good ratio to

represent the concentration in plant. Many studies use the whole aboveground plant tissue e.g. stem and leaves to show ability of translocation from root to shoot. The shoot concentration factor defined as ratio of concentration of chemicals in whole shoot to concentration in the medium as shown in Eq. 5.3 (Y. Z. Gao & Zhu, 2004; Polder et al., 1995)

$$\text{Shoot concentration factor} = \frac{\text{concentration in shoot } (\mu\text{g/g})}{\text{concentration in external solution } (\mu\text{g/ml})} \quad (5.3)$$

The ability of compounds to be passively transport from root to shoot with the transpiration stream can be expressed by transpiration stream concentration factor (TSCF) and defined by the ratio of concentration in xylem to the external solution and expressed as Eq.5.4 (Briggs et al., 1982). However, because the concentration of xylem is difficult to measure directly, it is usually determined from mass of chemical accumulated in the shoot compare to known amount of water transpired (e.g. over 24-48 hr) as shown in Eq. 5.5 (Briggs et al., 1982; Trapp, 2000). This approach assumes that the degradation of chemicals in transpiration stream is neglect and transport back to root by phloem is insignificant.

$$TSCF = \frac{\text{concentration in xylem}}{\text{concentration in external solution}} \quad (5.4)$$

$$TSCF = \frac{\text{Concentration in the shoots } (\mu\text{g}) / \text{wt of water transpired}(g)}{\text{Concentration in external solution } (\frac{\mu\text{g}}{\text{ml}})} \quad (5.5)$$

The TSCF of water is 1, the nutrients that actively taken by plant e.g. nitrogen, potassium and phosphorus have TSCF value greater than 1. The TSCF of most organic pollutants are less than 1 indicated that they are passively move from root to shoot with transpiration water (Orita, 2012).

5.2.4 Plant uptake of non-ionic compounds

Uptake and translocation of non-ionized chemicals are largely determined by hydrophobicity of chemicals which can describe by octanol water partition coefficient (K_{ow}). The RCF increases with increasing the hydrophobicity of chemicals as shown in Figure 5.2. Briggs et al., 1982 had setup the equation that showed the relation between RCF and $\log K_{ow}$ as shown in Eq. 5.6.

$$\log(RCF - 0.82) = 0.77\log K_{ow} - 1.52 \quad (5.6)$$

From the increasing uptake of more hydrophobic compounds and the positive relation between RCF and root lipid content suggest the partitioning of hydrophobic compounds in lipophilic root solid is main mechanism (Briggs et al., 1982; Briggs et al., 1983; Y. Z. Gao & Zhu, 2004). This behavior is supported by the similar sorption coefficient of compounds to macerated root to the coefficient from plant uptake experiment which indicates the partition process is most account for observed RCF of compounds (Briggs et al., 1982; de Carvalho, Bromilow, & Greenwood, 2007b)

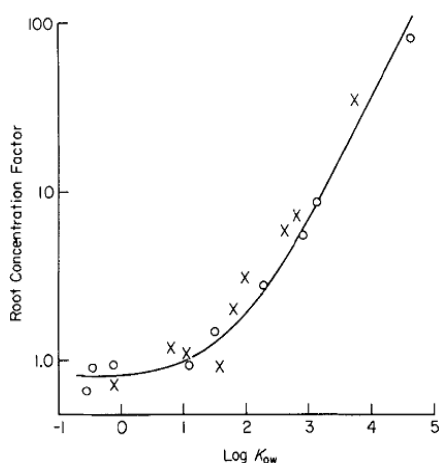


Figure 5.2 The relationship between root concentration factor (RCF) and the octanol – water partition coefficient ($\log K_{ow}$) of root uptake of o-methylcarbamoyloximes (open circle) and substituted phenylurea (cross mark) by barley plants from nutrient solution (Briggs et al., 1982)

The translocation of non-ionized compounds is unlike to the root uptake. It fitted to bell-shape curve with most effective translocation at intermediate of hydrophobicity ($\log K_{ow} \sim 2$). The highly hydrophobic ($\log K_{ow} > 4.5$) or highly polar ($\log K_{ow} < 1$) compounds have small translocation capacity as shown in Figure 5.3 (Briggs et al., 1982; de Carvalho, Bromilow, & Greenwood, 2007a). The reason of this most efficient $\log K_{ow}$ is unclear. The polar compounds have difficulties in diffusion cross the lipid-like membrane of endodermis and the highly hydrophobic compound can cross the endodermis much less than water may be the explanation (Trapp & McFarlane, 1995). This evidence had been mention in that most hydrophobic chemical found to uptake by root but no translocation to the shoot (Hellstrom, 2004). This indicated that there are selective rejections for highly polar and hydrophobic chemical occuring at membrane barrier in the root. Briggs et al., 1982 had shown the Gaussian curve that fitted to TSCF data and $\log K_{ow}$ of nonionized compounds as shown in Eq.5.7.

$$TSCF = 0.784 \exp -[(\log K_{ow} - 1.78)^2 / 2.44] \quad (5.7)$$

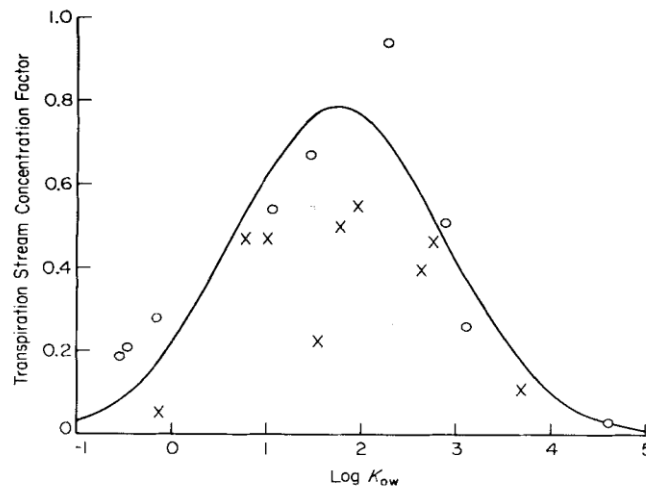


Figure 5.3 The relationship between the translocation stream concentration factor and octanol-water partition coefficient of the root uptake of 0-methylcarbamoyloximes (open circle) and substituted phenylurea (cross mark) by Barley plants from nutrient solution (Briggs et al., 1982)

For accumulation in stem, the stem concentration factor (SCF) or amount of chemicals that partition to stem found increase with increasing hydrophobicity. The mainly mechanism is partition to solid phase of stem. However, the maximum calculated SCF showed at $\log K_{ow}$ about 4.5, then the SCF will decrease with the same reason of decreasing of TSCF as shown in Figure 5.4 (Briggs et al., 1983).

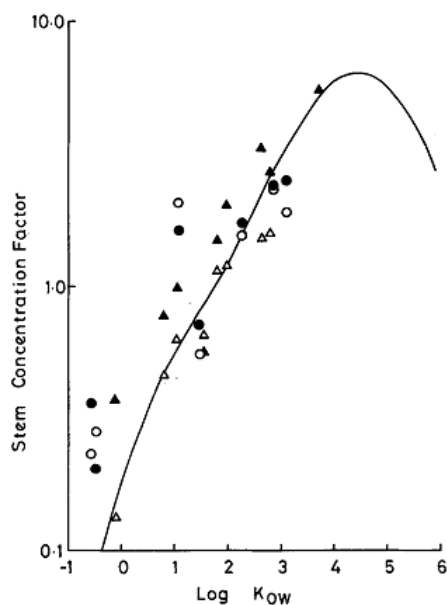


Figure 5.4 The relationship between stem concentration factor (SCF) and octanol-water partition coefficient ($\log K_{ow}$) of o-methylcarbamoyloximes in the stem bases (close circle) and central stem (open circle) sections, and substituted phenylureas in the stem bases (closed triangle) and central stem (open triangle) sections taken up by barley plants from nutrient solution (Briggs et al., 1983)

5.2.5 Plant uptake of ionized compounds

The transport of ionizable compounds across the membrane is more complex because pH in the plant compartments is different. The molecules can change their form when partition in different compartment as a result in different membrane permeation property (Briggs, Rigitano, & Bromilow, 1987). The diffusion across the membrane in cell protoplast of neutral molecules is quite rapid whereas it is much slower for the ionized molecules, so chemicals tend to

accumulate in high-pH plants compartment e.g. cytoplasm. This process is called “ion trapping” (Trapp & McFarlane, 1995). Because the permeability of membrane to anion is very low, so the transport of anion across the endodermis is not efficient (Trapp & McFarlane, 1995). Orita, 2012 indicated the ionized organic compounds are not taken up well as the non-ionized compounds because they are cross membrane by proton pumping process which required high activation energy from ATP-ADP reaction. The uptake of weak organic acids is found to increase when the pH of nutrient solution decrease where the compounds are in neutral form. This was confirmed from the increasing of RCF of 2,4 D from 0.92 at pH 7 to 33.3 at pH 4 as shown in Figure 5.5 (Briggs et al., 1987; Inoue, Chamberlain, & Bromilow, 1998).

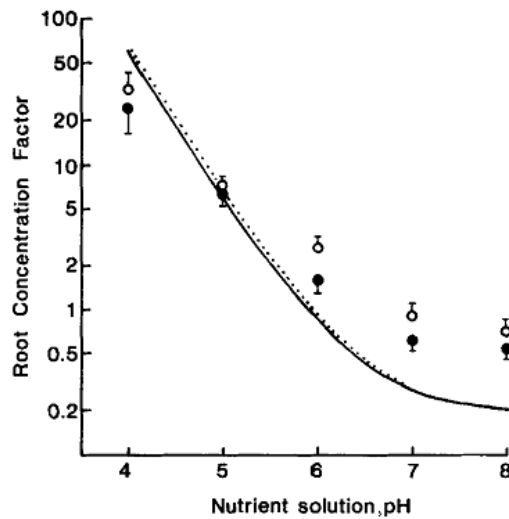


Figure 5.5 The root concentration factor of 2,4 dichloro-phenoxyacetic acids(open circle) , and 3,5 dichloro-phenoxyacetic acids (closed circle) uptake by barley as a function of pH of nutrient solution (Briggs et al., 1987)

Weak acids are major compounds that mobile and accumulate in phloem by ion trapping. This process can be explained that the neutral molecules can freely cross the lipophilic membrane from xylem to phloem. However, the pH in phloem (~ 8) are more basic than xylem (~ 5.5), so compounds will be ionized in phloem and these ionized molecules cannot cross the membrane back to xylem , so they are in trapped and accumulated in phloem as shown in Figure 5.6. This process reduce the long distance transport in the plant and accumulation in the leave of weak acids (Hellstrom, 2004; Trapp & McFarlane, 1995)

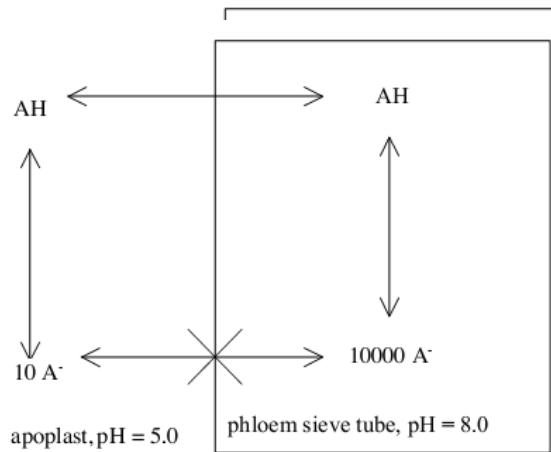


Figure 5.6 The accumulation of weak acids between xylem and phloem by ion trapping effect (Hellstrom, 2004)

The RCF, TSCF and SCF of some non-ionized and ionized chemicals had been collected from literatures which show in Table 5.1. However, these values are subject to be different depend on measured methods (hyponic culture or pressure chamber), length of exposure, initial concentration and plant species.

Table 5.1 The literature values of RCF and TSCF of some non-ionized and ionized chemicals

Chemicals	pH	Log K _{ow}	RCF (ml/g)	TSCF (ml/g)	References
Non-ionized chemicals					
Toluene	-	2.73	-	0.64	Dettenmaier et al.,2009
Benzene	-	2.13	-	0.59	Dettenmaier et al.,2009
Aldoxycarb	-	-0.57	0.65	0.18	Briggs et al. 1982
3-Phenoxybenzaldehyde 0-Methylcarbamoyloximes	-	3.12	8.62	0.29	Briggs et al. 1982
Ionized chemicals					
4-mesyl POA phenoxyaceticacid	4	0.06	2.62	0.12	Briggs et al. 1987
Atrazine	5-6.5	1.53	1.85	0.75	Shone et al. 1974
2,4 Dichloro-phenoxyaceticacid	4	2.81	88.4	3.12	Shone et al. 1974
2,4 Dichloro-phenoxyaceticacid	6.5	2.81	8.07	0.142	Shone et al. 1974

5.3 Materials and methods

The plant uptake capacity of AAs is determined by root uptake through nutrient solution in hydroponic culture system and sand culture system by cucumber plants. The experiment was started from incubation the cucumber seeds in germination box until plants were big enough before transfer to AAs spiked nutrient solution in hydroponic culture or sand applied with *Aristolochia Clematitis* seed in sand culture. After period of time, plants were harvest and analyzed the AAs in plant tissues included leaves, stems and roots by HPLC-FLD with pre-column derivatization reaction. The detail of experiment was described below.

5.3.1 Calibration curve

To prepare the plant matrix solution, 0.5 g fresh wt. of cucumber plant parts (leaves, stems, and roots) were macerated with pestle and mortar and extracted in 20 ml of 70% methanol. Solutions were left overnight, then sonicated in ultrasonic bath for 15 min. After that the mixtures were shaken in mechanical shaker at 180 rpm for 1 hr, and then centrifuged at 7,500 rpm for 30 min to separate the plant tissues, the supernatants were collected as leaves, stems and roots matrix solution.

The calibration solutions were prepared by spiking AAs in various amounts to plant matrix solution. Due to low concentration of AAs was expected in plant tissues, the HPLC-FLD with pre-column derivatization had been used to analyze AAs in the extract solution. To analyze, 1 ml of calibration solution were transferred to 1.5 ml Eppendorf tube, added 10 mg of Zinc powder and 50 μ l of concentrated acetic acid with periodic mixing with vortex mixer for 15 min. This procedure will derivatize Aristolochic acid I and II to Aristolactam I and II (ALs) as shown in Figure 5.7. Then the solutions were centrifuged at 13,000 rpm for 5 min and the supernatants were collected to analyze by HPLC-FLD (Chan et al., 2007). The Pelkin Elmer HPLC system equipped with Supelco Discovery C-18 column 25 cm x 4.6 mm, and 5 μ m particle diameter was used to analyze ALs. The fluorescence detector (FLD) was used at excitation and emission wavelength 393 and 455 nm, respectively. The mobile phase was the mixing solution between acetonitrile and 0.1% phosphoric acid water at the gradient of 40% to 80% of acetonitrile in 10 min and held for 3 min before recondition to starting condition. The flow rate was 1 ml/min. The calibration curve obtained from leaves, stems and roots solution were compared. The accuracy, precision, reproducibility, detection limit and recovery also had been determined.

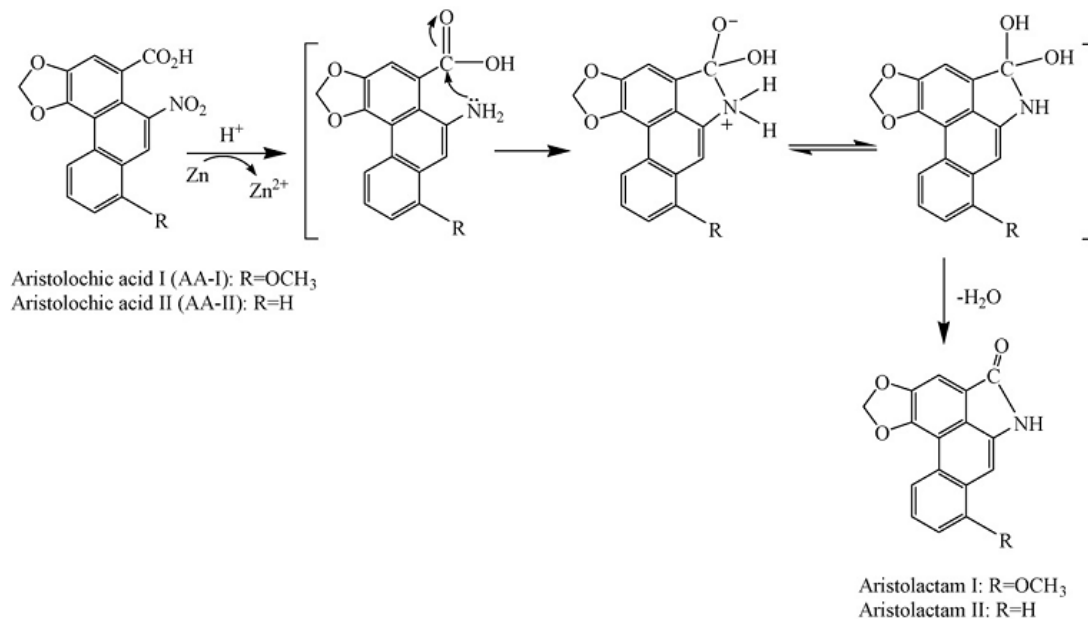


Figure 5.7 The derivatization of Aristolochic acids to Aristolactam by using zinc powder in acid solution (Chan et al., 2007)

5.3.2 Analytical method validation

To verify the above analytical method for determination of Aristolochic acids in plant matrix solution, the method validation included accuracy, precision, linearity and detection limit were determined.

5.3.2.1 Accuracy and precision

The accuracy of the HPLC-FLD method was tested by spiking stock solution of AA I and II to leave, stem or root matrix solution at three concentration (0.0225 , 0.09 and 0.225 $\mu\text{g/ml}$ for AA I and 0.0275 , 0.11 and 0.275 $\mu\text{g/ml}$ for AAII), derivatization to Aristolactam I and II and measured for 6 time in each concentration (n=6) . The percent recovery was calculated from Eq.5.8 and reported as accuracy.

$$\%recovery = \frac{\text{concentration from spiked solution} - \text{concentration of blank solution}}{\text{concentration of standard solution}} \times 100 \quad (5.8)$$

The precision of the method was checked by analyzing the above standard solution for 6 time in one day (intraday, n=6) and twice a day for 3 consecutive days (interday, n=6). The percent relative standard deviation (%RSD) of peak area of each concentration were calculated and reported as precision at each concentration

5.3.2.2 Linearity

The linearity of method was check by prepared six standard solution of Aristolactum I and II which derivatized from Aristolochic I and II 0.0225 -0.225 and 0.0275-0.275 ug/ml, respectively. Each concentration was analyzed for three times. The average peak areas were plotted with concentration. The linear regression equation and correlation coefficient (r^2) were obtained from the graph.

5.3.2.3 Limit of detection(LOD) and limit of quantification (LOQ)

The limit of detection and quantification were measured by analyzing the lowest standard concentration of AL I and II for 7 times and calculated the standard deviation (SD). The LOD calculated from 3 times of standard deviation (3 times of signal to noise ratio) and LOQ calculated from 10 of times of standard deviation (10 time of signal to noise ratio).

5.3.3 Nutrient solution preparation

The Knop's solution were used as nutrient solution in experiment which prepared by dissolved $\text{Ca}(\text{NO}_3)_2$ 1 g, KH_2PO_4 0.25 g, KCl 0.125 g, MgSO_4 0.25 g and trace of FeSO_4 in 1 liter of deionized water (The Gale Group, 2010) . The pH of Knop's solution was adjusted to 5.9 by adding aliquot of 1M NaOH before use.

5.3.4 Hydroponic culture experiment

The cucumber seeds were germinated on towel paper saturated with 0.05 mM CaSO₄ in germination box as shown in Figure 5.8. Seven day later, after seedling had developed the cotyledons and about 5 cm root length, all seedling were transferred to grow hydroponically in 25 ml glass bottle (2 plant per bottle) which filled with 20 ml of half strength of Knop's nutrient solution under 10/14 day/night cycle in well ventilated area . The light was supplied by 60 Watt full wavelength lamp. After 14 day of pre-culture, plants in each bottle were transferred to new nutrient solution containing the AA I and II at 1.4 and 3 µg/ml, respectively. The 5 ml of fresh half strength Knop's solution was added to each tube in every 2 days to avoid nutrient deficiency. The amounts of AAs in initial solution were measured to calculate the mass balance. The bottles were wrapped up with aluminum foil to protect from light and prevent the development of algae in nutrient solution. The hydroponic culture experimental set up are shown in Figure 5.9. Duplicate tubes were applied at each treatment. One control bottle was grown with the nutrient solution without spiked AAs. pH of solution was measured before and after treatment. After 20 days of exposure to AAs, the all plants were harvested and separated into different parts e.g. roots, stems and leaves and weighed as fresh weight as shown in Figure 5.10 . Roots were additional washed by soaking in 2.5 mM CaSO₄ for overnight to remove adsorbs AAs on the surface, rinsed with deionized water and blotted dry with Kim wipe paper before weighing. The washed solutions were kept to analyze the AAs desorbed from root surface. AAs remaining in nutrient solution was measured by taking 1ml of nutrient solution and centrifuged with Eppendorf tube at 13,000 rpm for 5 min to remove plant particles and analyzed by HPLC-DAD similar to soil sorption/octanol-water coefficient experiment.

The analyzed concentrations in plant parts and in nutrient solution were calculated as Root concentration factor (RCF) and stem concentration factor (SCF) as shown in Eq 5.1 and 5.2. The concentration in leaves, stems or roots was based on fresh weight basis. The reported concentration did not correct with recovery efficiency. Degradation of AAs in plants was assumed as negligible and concentration left in nutrient solutions was used as concentration in external solution.

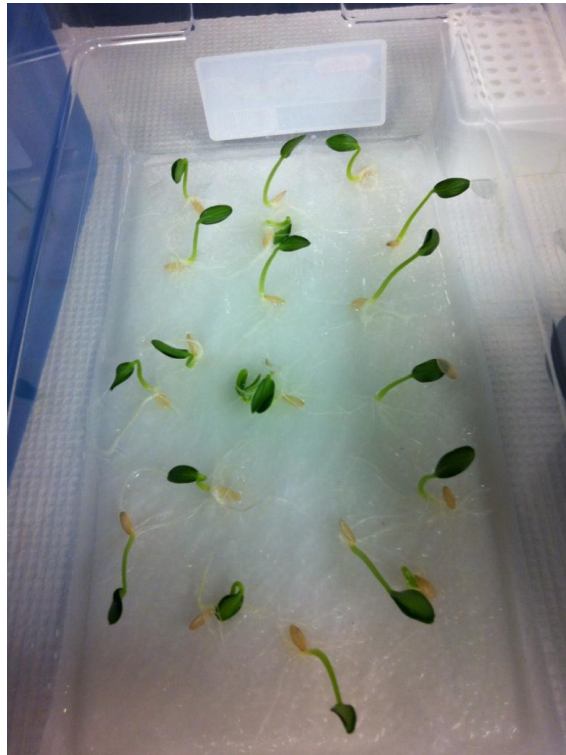


Figure 5.8 Cucumber seedlings germinated on wetted towel in box



Figure 5.9 AAs uptake by hydroponic culture experimental setup



Figure 5.10 Plant parts separation after harvesting

5.3.4.1 Extraction method and recovery test

The combined plants parts were macerated with pestle and mortar as shown in Figure 5.11 and dissolved with 5 ml of 70% methanol. These mixture solutions were let stand overnight. To extract AAs out from the plant tissues, the solutions were sonicated in ultra-sonic bath for 15 min as shown in Figure 5.12 and then shaken in mechanical shaker for 1 hr at 180 rpm. After that, the solutions were centrifuged at 7,500 rpm for 20 min to separate the plant tissue and supernatants were collect to analysis by HPLC-FLD as described above as shown in Figure 5.13. This extraction method was selected because of widely using in extraction the AAs from *Aristolochia* species plants (Sun, Wu, & Jia, 2001; J. B. Yuan et al., 2008; Zhang et al., 2006)



Figure 5.11 Plant parts maceration by pestle and mortar



Figure 5.12 Plant extracted by sonication in ultrasonic bath



Figure 5.13 Supernatant separation from plant tissue after centrifuge

The recovery of this extraction method was determined by spiking the aliquot of standard stock AAs solution at three different concentration to 0.5 g fresh weight of leaves, stems and roots which already homogenized by pestle and mortar . The spiked samples were left for 24 hr to allow spiking solution penetrated to plant tissues. After that the samples were extracted by same method as described above. % of recovery of each plant parts and spiked concentration were calculated.

5.3.4.2 Degradation of Aristolochic acids in nutrient solution

The degradation of Aristolochic acids in Knop's solution were tested to ensure that AAs were not degraded during uptake experiment. The several bottles of Knop's solution containing AAs were prepared in the same manner as uptake experiment. The 1 ml of solution was taken from bottles in day 4, 8, 12, 16, and 20 and analyzed AAs concentration remaining in solution by HPLC-DAD. pH also measured before and after experiment.

5.3.5 Sand culture experiment

5.3.5.1 Sand preparation

F-65 Ottawa Silica sand (SiO₂ 99.77%, Laguna Clay Co.) was used as a media to determine AAs uptake because it has low ability to adsorb the AAs and inert for chemical reactions. Before apply to experiment, sand was washed with deionized water for 2 times and dried in the fume hood. Then the dried sand was sterilized by autoclaving (10 min heat and 10 min dried cycle) to inhibit microbial activity. The ground *Aristolochia Clematits* seeds were added to the sand as a source of AAs. The AAs leaching from seeds and available concentration in sand were determined as described below.

5.3.5.2 The uptake experiment

The cucumber seedlings were germinated on towel paper saturated with 0.05 mM CaSO_4 in germination box same as in hydroponic experiment. After 7-10 days when the seedlings were long enough, they were transferred to grow in nutrient solution for 2 weeks. When true leaves came out, the seedlings were transferred to 4 oz. straight-side glass jar contained 40 g of treated sand and 0.02 g of ground *Aristolochia Clematitis* seeds. The 5 ml half strength Knop's nutrient solution was irrigated the cucumber plants in every two day to replace water evaporator and prevent nutrient deficiency. Three pots were prepared for AAs treatment plants and one control pot was included where no ground *Aristolochia Clematitis* seeds was applied. The plant uptake by sand culture experiment is shown in Figure 5.14



Figure 5.14 Plant uptake by sand culture experimental setup

Plants were harvest after 20 days of growing in sand. They were cut into different parts, weighed and rinsed with deionized water before extraction. The extraction and analysis procedure were similar to hydroponic culture experiments.

To determine available concentration of AAs to root, after plants were harvested, sand was irrigated with 5 ml of half strength Knop's solution, equilibrated for 1 hr and 0.5 ml of clear solution on top were collected and put into eppendorf tube for centrifuge to remove sand particle. The supernatants were collected to analyze AAs with HPLC-DAD. These concentrations were used as concentration in external media to calculate plant bioconcentration factors (RCF and SCF).

5.3.5.3 Determination of AAs degradation in sand

AAs degradation in sand was tested by batch incubation technique (Jenks et al., 1998). The 40 g of washed and sterilized Ottawa sand was mixed with 0.02 g of ground *Aristolochia clematitis* seeds and put into 4 oz. straight-side glass jar. These AAs mixed sand were cover with aluminum foil with small holes on the top for air flow. The jars were incubated for 20 days with measuring AAs concentration in sand in every two days. To determine the concentration of AAs in sand, 5 ml of half strength Knop's nutrient solution was applied to the jar and equilibrated for 1 hr before 0.5 ml of clear solution on top was taken to eppendorf tube for centrifuge to remove sand particle. The supernatant was analyzed for AAs by HPLC-DAD. The samples were prepared in duplicate.

5.4 Result and discussion

5.4.1 Analytical method validation

5.4.1.1 The calibration curve in plant matrix solution

The ALs standards solution of various plant matrices (leaves, stems, roots) were prepared and injected to HPLD-FLD system. The chromatograms of each plant matrix were shown in Figure 5.15. The retention time of AL I and II was 13.7 and 11.5 min, respectively. The figures indicate that plant extract compounds e.g. chlorophyll had no interference to ALs HPLC signals.

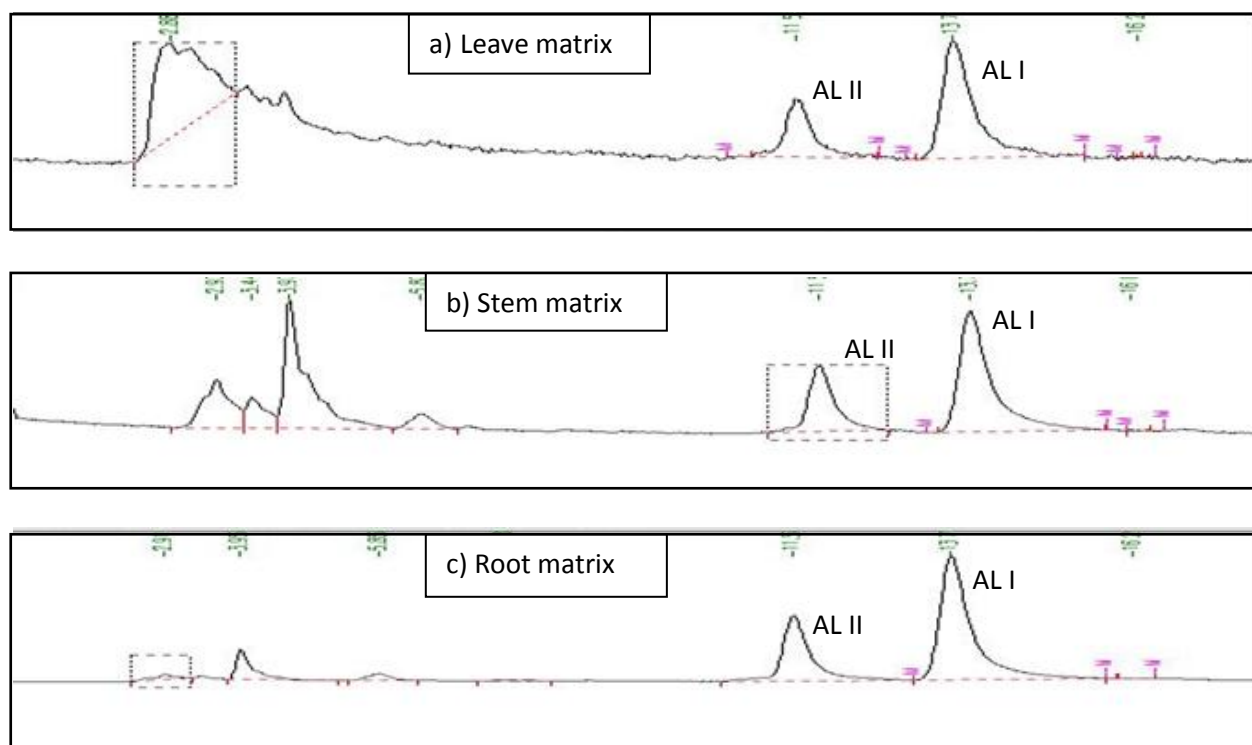


Figure 5.15 HPLC-FLD chromatogram of derivative Aristolactum I and II in leaves (a), stem (b) and root (c) matrices solution spiked with AA I and II

The peak areas of six standard solutions were measured for three times and the average peak areas were plotted with concentration as calibration curve as shown in Figure 5.16. The figures show that leaves, stem, root extract matrices did not have any enhancement or suppression effect on the ALs signal of HPLC. The calibration was linear over the range of concentration 0.0225 -0.225 for AA I and 0.0275-0.275 ug/ml for AA II, respectively.

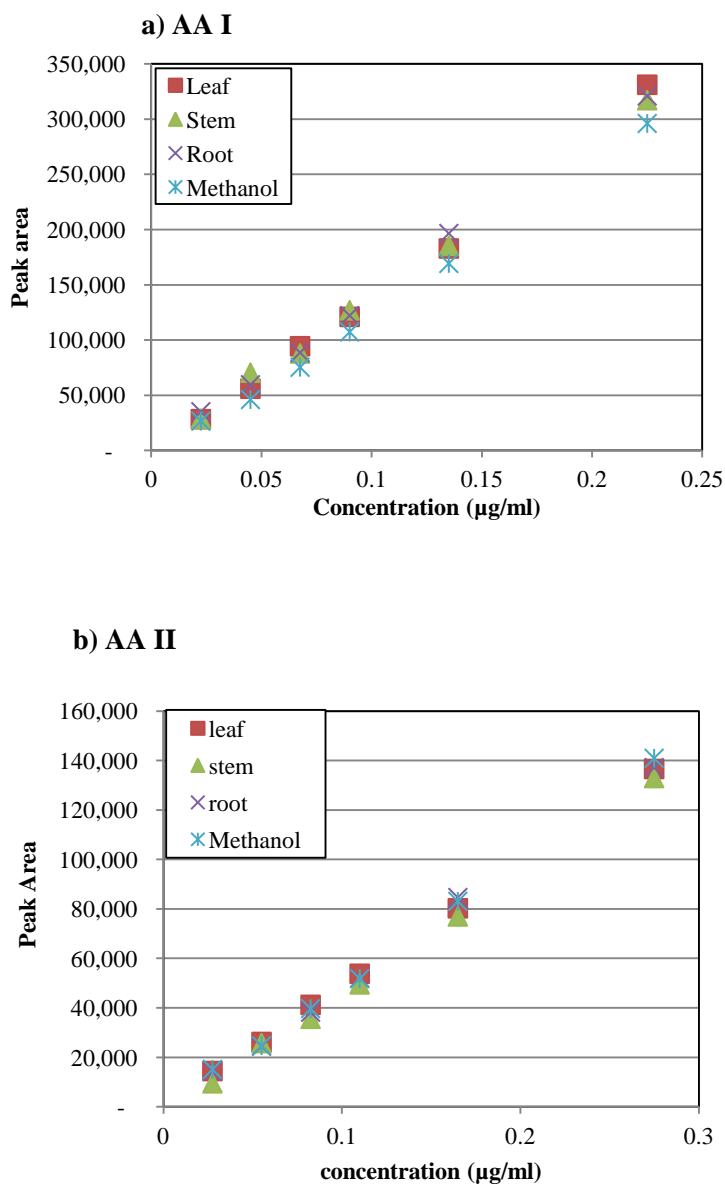


Figure 5.16 The calibration curve of AL I (a) and AL II (b) in leaf, stem, root matrix and methanol

5.4.1.2 Accuracy, precision and limit of detection

The accuracy of HPLC-FLD method was determined at low, medium and high concentration in leaves matrix solution and reported as % recovery while the precision reported as % relative standard deviation (%RSD). These data shows in Table 5.2. The results show that % recovery of AL I and II are over than 100% and % RSD less than 4%. The intraday and inter-day precisions were not much different. However, accuracy and precision at low concentration were less than at high concentration solution. These data indicated the HPLC-FLD with pre-column derivatization had good performance to analyzed AAs in plant matrices.

Table 5.2 % recovery (accuracy) and % RSD (intra-day and inter-day precision) of analysis ALs in leave matrix

Chemical	Concentration ($\mu\text{g/ml}$)	%Recovery (mean, n=6)	%RSD (intra-day, n=6)^a	%RSD (inter-day, n=6)^b
AL I	0.0225	114.77	3.22	3.78
	0.09	98.64	1.24	1.82
	0.225	104.56	0.51	1.17
AL II	0.0275	122.64	8.08	6.77
	0.11	100.16	1.35	1.77
	0.275	101.91	0.62	0.75

^a The samples were analyzed 6 times in 1 day.

^b The samples were analyzed 6 times over 3 three consecutive days

The limit of detection (LOD) and limit of quantification (LOQ) of ALs were determined from the 3 and 10 times of standard deviation of peak area at lowest calibration concentration. The results show the LOD of AA I and II were 0.002 and 0.0045 $\mu\text{g/ml}$ and LOQ of AA I and II 0.007 and 0.015 $\mu\text{g/ml}$. The sensitivity of AA II showed slightly less than AA I. The obtained

LOD and LOQ were higher than the reported from Chan et al., 2007 one order of magnitude which were 0.00039 $\mu\text{g/ml}$ for AA I and 0.00052 $\mu\text{g/ml}$ for AA II.

5.4.2 Recovery of plant extraction method

The recovery of plant extraction method was determined by spiking AAs standard solution to the leave and stem tissues at three different concentration. The extraction solutions were analyzed for ALs peaks and compared to the peaks obtained from standard solution at same concentration. The results show that the average %recovery of AA I and II were 89.24% and 70.38% for leaves and 91.02 and 79.92 for stems, as shown in Figure 5.17. The figures show that %recovery of AA I was more than AA II and % recovery from stems was more than leaves. This finding may indicated the sorption of AAs in leaves may be stronger than in stem. The % recovery from root tissue was not determined because the volume of root tissues was too small to adsorb the solution. The high % recovery indicated the good performance of extraction method.

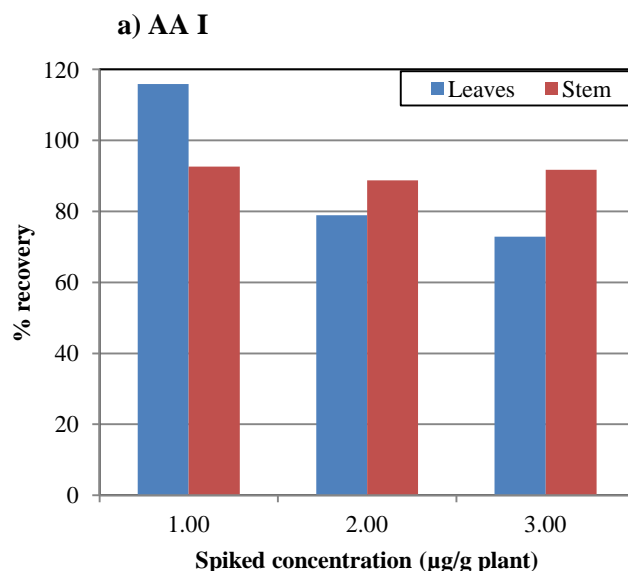
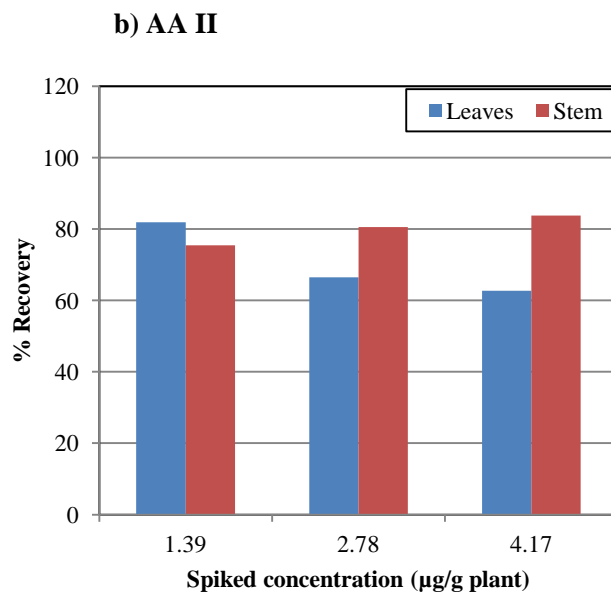


Figure 5.17 The % Recovery from spiked AA I (a) and II (b) standard solution to leaves and stem matrices

Figure 5.17 (cont'd)



5.4.3 Hydroponic culture experiment

5.4.3.1 The stability of AAs in Knop's nutrient solution

The AAs degradation in Knop's nutrient solution was tested. From Figure 5.18 , it shows that AAs were stable in a solution for whole experimental period (20 days). This indicated that AAs were not degraded by chemical processes in nutrient solution. However, this experiment did not account for the degradation by microorganisms which may happen when grow the plant.

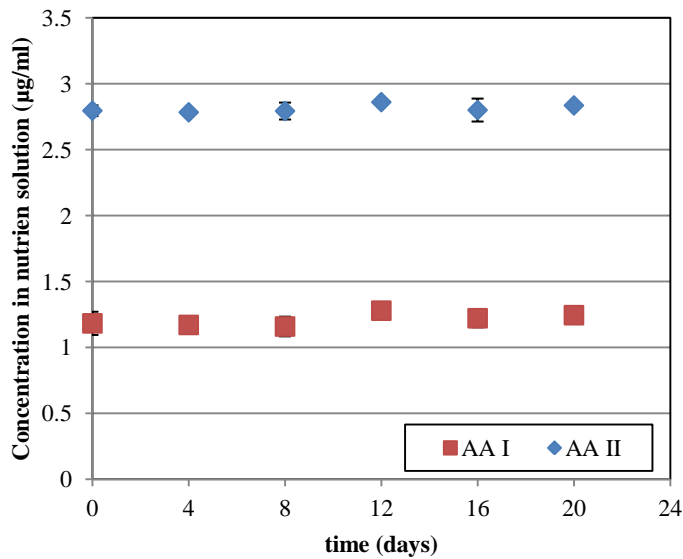


Figure 5.18 The stability of AAs in Knop’s solution as a function of time

5.4.3.2 Kinetic uptake experiment

The plant uptake kinetic had been tested by growing the cucumber plants in nutrient solution applied AAs and harvested in every 4 days interval. The AAs remaining in solution and concentration in shoot (stems and leaves) had been determined and showed in Figure 5.19 and 5.20, respectively. The AAs remaining in nutrient solution found to decrease in first 4-8 day and then slightly decrease until the end of exposure period (20 days). The presence of AAs in solution at end of periods indicated AAs were not completely degraded by microorganisms, so the absence of AAs from solution should reflect to amount of AAs that taken up by plant. However, the concentration found in shoot did not show the relationship with the exposure time. The uptake ability is expected to depend on individual plant and it is difficult to predict plant uptake equilibrium (Briggs et al., 1983).

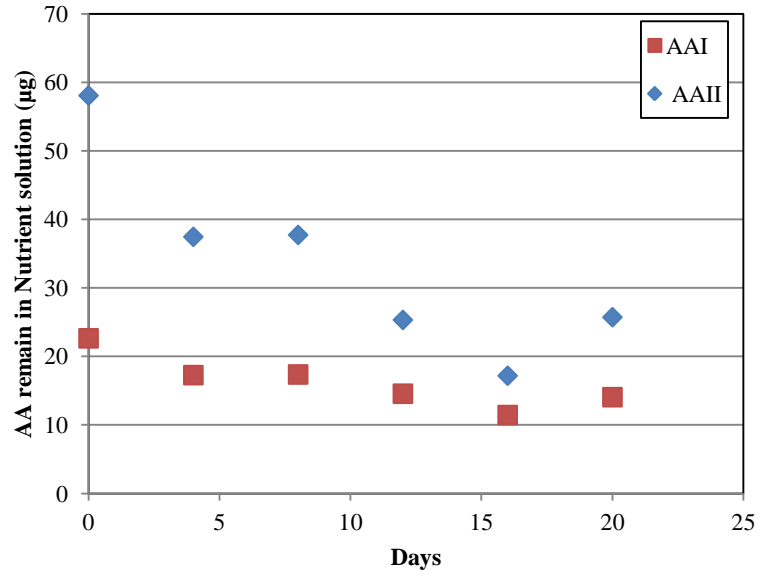


Figure 5.19 The AA I and II remaining in solution as a function of exposure time

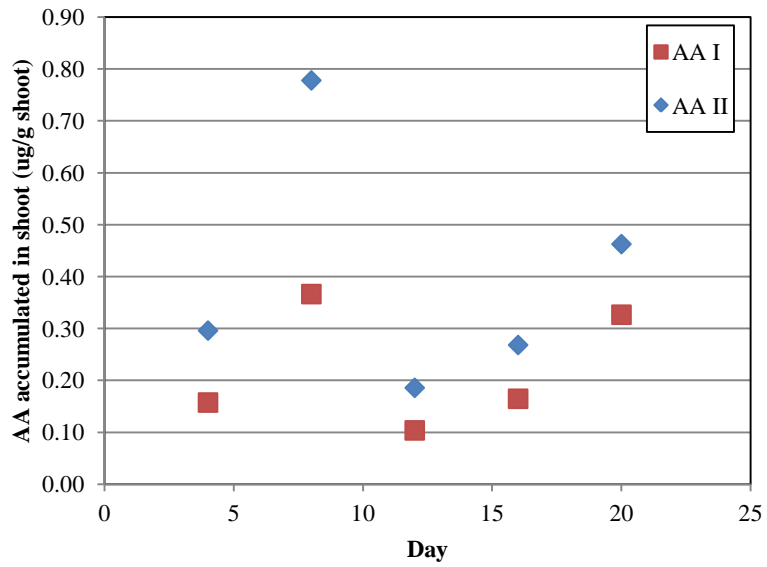


Figure 5.20 The AA I and II concentration in shoot as a function of exposure time

5.4.3.3 AAs accumulation in plant part

The AAs concentration in different parts of cucumber plants are shown in Figure 5.21. The concentration in nutrient solution and root wash solution were also determined. From the mass balance calculation, the average AA I and II in remaining nutrient solution 61 and 59 %, in root wash solution 6 and 3%, in stem tissues 1.8 and 1.4 %, in root tissues 6 and 3%, and mass loss 24 and 32% ,respectively. Very small AAs amount were detected in leaves. The loss portion was expected to be occurred in sample handling during experiment (Zhu, Han, Xiao, & Jin, 2008). The plant metabolism and non-extractable of AAs in plant tissues may also account for this loss (Redshaw, Wootton, & Rowland, 2008).

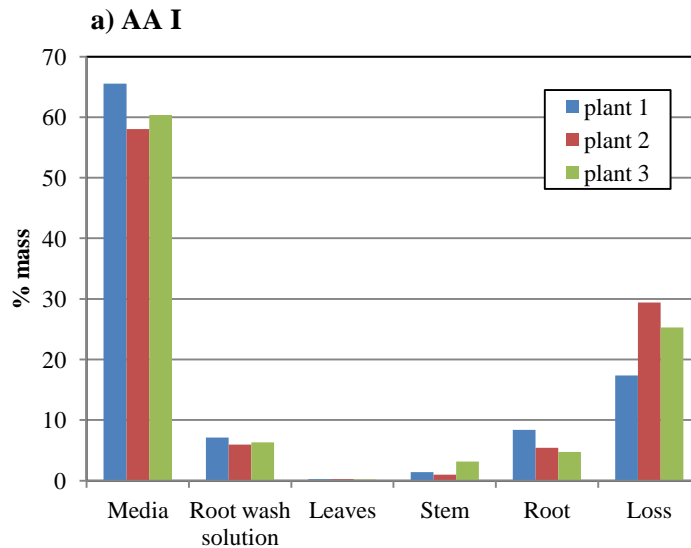


Figure 5.21 The percentage of AA I (a) and AA II (b) in different parts in cucumber plant parts and residual in media

Figure 5.21 (cont'd)

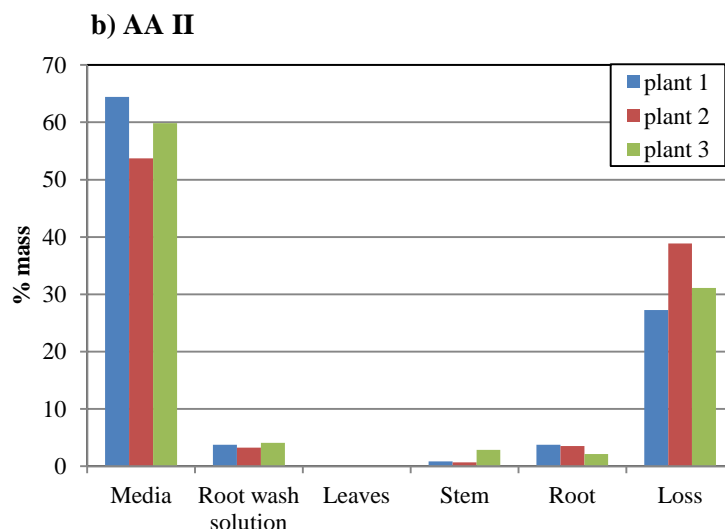
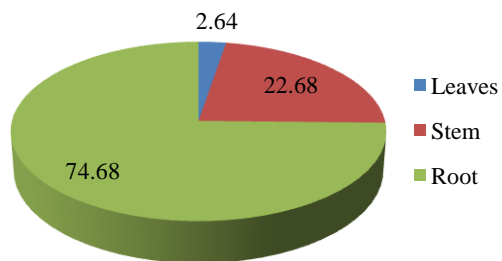


Figure 5.22 shows % distribution of AA I and II that accumulated in different cucumber parts. It shows that about 70% of AAs was accumulated in the roots, 22-30% in stem and 0-2% in leaves. This indicated AAs tended to accumulate in the roots more than the stems and leaves. The low translocation to the shoot was expected from the difficulty to cross the lipid membrane of high polarity anion AAs. The very low concentration in leaves also indicated AAs were not mainly translocated by water in transpiration process to the leave (Shenker et al., 2011; Ucisik, Trapp, & Kusk, 2007). This may be caused by the partitioning of AAs in lipid components in the stem or trapped in the pholem by ion trapping mechanism (Hellstrom, 2004).

a) AA I



b) AA II

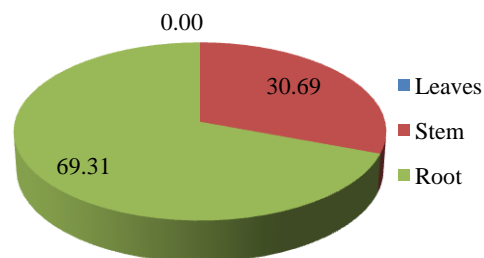


Figure 5.22 AA I (a) and AA II (b) distribution in cucumber plant parts in hydroponic culture

Figure 5.23 (a) shows concentration of AA I and II found in root and stem tissues and Figure 5.23 (b) shows the calculated root concentration factor (RCF) and stem concentration factor (SCF) of AA I and II. The RCF of AA I and II were 8.48 and 4.37 and the SCF of AA I and II were 0.78 and 0.61, respectively. The obtained RCF values were large when compare to other common organic compounds indicated that AA I and II can be effectively taken by root. RCF and SCF of AA I are more than AA II indicated AA I can be taken up by plants more than AA II which caused by more hydrophobicity of AA I.

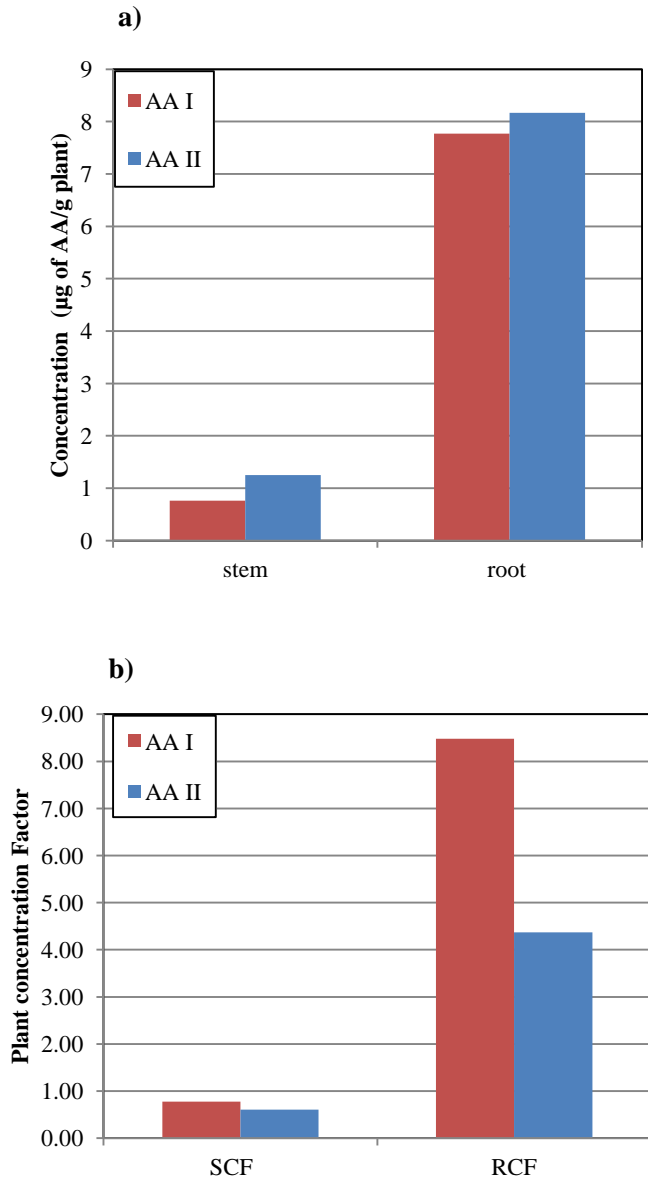


Figure 5.23 AAs concentration found in stem and root tissues (a) and stem and leaf concentration factor (b) (SCF and RCF) of cucumber plant uptake AAs from spiked nutrient solution

5.4.4 Sand culture experiment

5.4.4.1 The AAs available in treating sand

The leaching AAs concentration in the sand from *A. Clematitis* seeds was tested as a function of incubation time to determine whether AAs degradation had been occurred. The result is shown in Figure 5.24 where AA I concentration was decrease when time proceeded whereas AA II concentration was quite constant. The reduce concentration of AAs may response by the degradation by microorganisms which may be contaminated from the air, even though sand was sterilized (Y. Z. Gao & Zhu, 2004). The irreversible adsorption in the sand may be the cause too. However, this figure can confirm that there were AAs available in the sand for a whole experiment period (20 days).

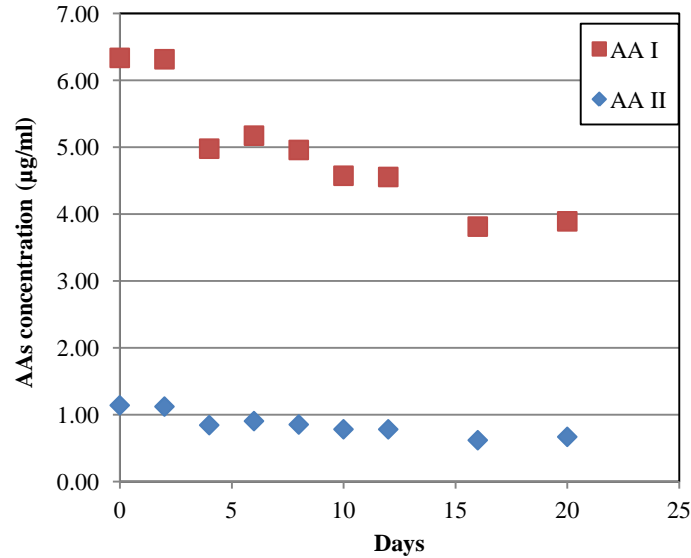


Figure 5.24 AA I and II concentration available in sand as a function of incubation time

5.4.4.2 AAs accumulation in plant parts

The AAs concentration distribution in the plants which exposed to treated sand are shown in Figure 5.25. However, the distribution pattern was not similar to hydroponic culture where the accumulation in the stems was increase or even larger than concentration in the roots in case of AA I. This evidence can be explained that plants were grown better in sand culture because their roots were fixed. As a result, the transpiration of the plants in sand culture was better in hydroponic culture. AA I was quite effective for translocation from root to shoot. No AA I and II found in leaves. The AAs concentration found in plant tissues are shown in Figure 5.26 (a). The concentration of AA I in plants was higher than AA II because *A. Clematitis* seeds contained AA I ten times more than AA II. From Figure 5.26 (b), the RCF of AA I and II were 6.28 and 4.39 and SCF of AA I and II were 2.54 and 2.72, respectively. The higher than 1 of these numbers indicated the concentration in plants was relative higher than concentration in sand. When compare to hydroponic culture, the SCF from sand culture was increased whereas the RCF was decreased. These indicated AAs have more translocated and accumulated when growing in sand culture than hydroponic culture.

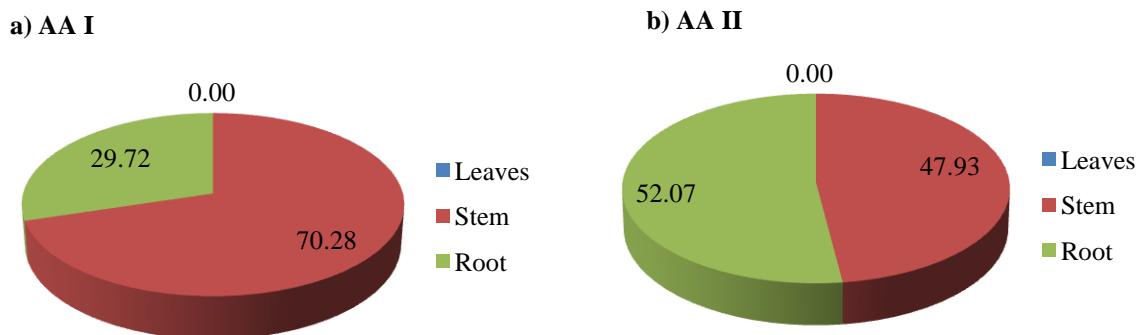


Figure 5.25 AA I (a) and AA II (b) distribution in cucumber plant parts in sand culture

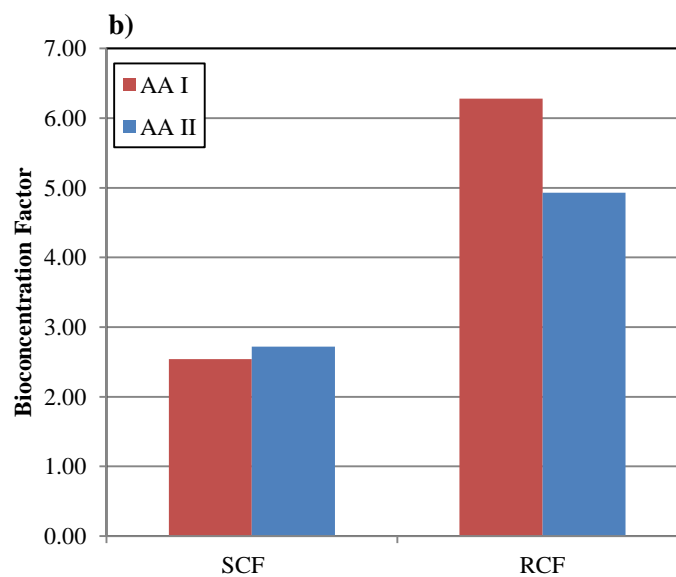
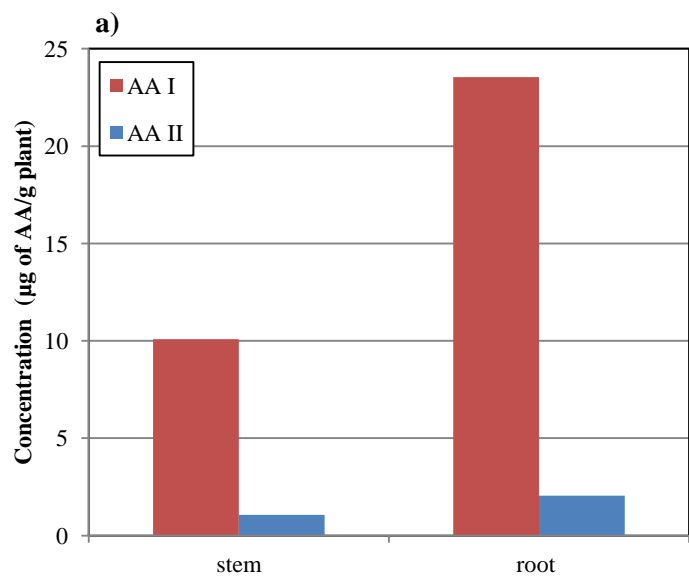


Figure 5.26 AAs concentration found in stem and root tissues (a) and stem and leaf concentration factor (b) (SCF and RCF) of cucumber plants grown in *Aristolochia Clematitis* seed treating sand

5.5 Conclusion

The kinetic test showed that AAs can be uptake after 4 days but the plant uptake equilibrium was difficult to determine because it depends on uptake ability of individual plant. Most of taken up AAs was found in root and the less far was translocated to the shoot which expected from the low root membrane permeability of anion AAs. RCF from both hydroponic and sand culture were much higher than 1 indicated AAs has highly potential to accumulate in the root. The translocation of AAs was better in sand culture when plants growed better. The finding contamination of AAs in the plants that growed in AAs contained media suggested the hypothesis of food chain contamination is possible.

REFERENCES

REFERENCES

- Aslund, M. L. W., Rutter, A., Reimer, K. J., & Zeeb, B. A. (2008). The effects of repeated planting, planting density, and specific transfer pathways on PCB uptake by *Cucurbita pepo* grown in field conditions. *Science of the Total Environment*, 405(1-3), 14-25. doi: 10.1016/j.scitotenv.2008.07.066
- Briggs, G. G., Bromilow, R. H., & Evans, A. A. (1982). RELATIONSHIPS BETWEEN LIPOPHILICITY AND ROOT UPTAKE AND TRANSLOCATION OF NON-IONIZED CHEMICALS BY BARLEY. *Pesticide Science*, 13(5), 495-504. doi: 10.1002/ps.2780130506
- Briggs, G. G., Bromilow, R. H., Evans, A. A., & Williams, M. (1983). RELATIONSHIPS BETWEEN LIPOPHILICITY AND THE DISTRIBUTION OF NON-IONIZED CHEMICALS IN BARLEY SHOOTS FOLLOWING UPTAKE BY THE ROOTS. *Pesticide Science*, 14(5), 492-500. doi: 10.1002/ps.2780140506
- Briggs, G. G., Rigitano, R. L. O., & Bromilow, R. H. (1987). PHYSICO-CHEMICAL FACTORS AFFECTING UPTAKE BY ROOTS AND TRANSLOCATION TO SHOOTS OF WEAK ACIDS IN BARLEY. *Pesticide Science*, 19(2), 101-112. doi: 10.1002/ps.2780190203
- Chan, W., Lee, K.-C., Liu, N., & Cai, Z. (2007). A sensitivity enhanced high-performance liquid chromatography fluorescence method for the detection of nephrotoxic and carcinogenic aristolochic acid in herbal medicines. *Journal of Chromatography A*, 1164(1-2). doi: 10.1016/j.chroma.2007.06.055
- Chiou, C. T., Sheng, G. Y., & Manes, M. (2001). A partition-limited model for the plant uptake of organic contaminants from soil and water. *Environmental Science & Technology*, 35(7), 1437-1444. doi: 10.1021/es0017561
- Cui, L. W., Feng, X. B., Lin, C. J., Wang, X. M., Meng, B., Wang, X., & Wang, H. (2014). ACCUMULATION AND TRANSLOCATION OF (198)HG IN FOUR CROP SPECIES. *Environmental Toxicology and Chemistry*, 33(2), 334-340. doi: 10.1002/etc.2443
- de Carvalho, R. F., Bromilow, R. H., & Greenwood, R. (2007a). Uptake and translocation of non-ionised pesticides in the emergent aquatic plant parrot feather *Myriophyllum aquaticum*. *Pest Management Science*, 63(8), 798-802. doi: 10.1002/ps.1394
- de Carvalho, R. F., Bromilow, R. H., & Greenwood, R. (2007b). Uptake of pesticides from water by curly waterweed *Lagarosiphon major* and lesser duckweed *Lemna minor*. *Pest Management Science*, 63(8), 789-797. doi: 10.1002/ps.1389

- Dettenmaier, E. (2008). *Measuring and modeling of plant root uptake of organic chemicals*. Utah State University.
- Diffen. Phloem vs Xylem. from http://www.diffen.com/difference/Phloem_vs_Xylem
- Gao, Y. Z., & Zhu, L. Z. (2004). Plant uptake, accumulation and translocation of phenanthrene and pyrene in soils. *Chemosphere*, 55(9), 1169-1178. doi: 10.1016/j.chemosphere.2004.01.037
- Hashimoto, Y. (2005). Dieldrin residue in the soil and cucumber from agricultural field in Tokyo. *Journal of Pesticide Science*, 30(4), 397-402. doi: 10.1584/jpestics.30.397
- Hellstrom, A. (2004). Uptake of organic pollutants in plants. <http://info1.ma.slu.se/IMA/Publikationer/internserie/2004-01.pdf>
- Hulster, A., Muller, J. F., & Marschner, H. (1994). SOIL-PLANT TRANSFER OF POLYCHLORINATED DIBENZO-P-DIOXINS AND DIBENZOFURANS TO VEGETABLES OF THE CUCUMBER FAMILY (CUCURBITACEAE). *Environmental Science & Technology*, 28(6), 1110-1115.
- Inoue, J., Chamberlain, K., & Bromilow, R. H. (1998). Physicochemical factors affecting the uptake by roots and translocation to shoots of amine bases in barley. *Pesticide Science*, 54(1), 8-21. doi: 10.1002/(sici)1096-9063(199809)54:1<8::aid-ps793>3.0.co;2-e
- Jenks, B. M., Roeth, F. W., Martin, A. R., & McCallister, D. L. (1998). Influence of surface and subsurface soil properties on atrazine sorption and degradation. *Weed Science*, 46(1), 132-138.
- Kipopoulou, A. M., Manoli, E., & Samara, C. (1999). Bioconcentration of polycyclic aromatic hydrocarbons in vegetables grown in an industrial area. *Environmental Pollution*, 106(3), 369-380. doi: 10.1016/s0269-7491(99)00107-4
- Lin, D. H., Zhu, L. Z., He, W., & Tu, Y. T. (2006). Tea plant uptake and translocation of polycyclic aromatic hydrocarbons from water and around air. *Journal of Agricultural and Food Chemistry*, 54(10), 3658-3662. doi: 10.1021/jf052909c
- McCrary, J. K., McFarlane, C., & Lindstrom, F. T. (1987). THE TRANSPORT AND AFFINITY OF SUBSTITUTED BENZENES IN SOYBEAN STEMS. *Journal of Experimental Botany*, 38(196), 1875-1890. doi: 10.1093/jxb/38.11.1875
- Oconnor, G. A., Kiehl, D., Eiceman, G. A., & Ryan, J. A. (1990). PLANT UPTAKE OF SLUDGE-BORNE PCBS. *Journal of Environmental Quality*, 19(1), 113-118.
- Orita, N. (2012). *Root uptake of organic contaminants into plants: species differences*. Utah State University.

- Polder, M. D., Hulzebos, E. M., & Jager, D. T. (1995). VALIDATION OF MODELS ON UPTAKE OF ORGANIC-CHEMICALS BY PLANT-ROOTS. *Environmental Toxicology and Chemistry*, 14(9), 1615-1623. doi: 10.1897/1552-8618(1995)14[1615:vomouo]2.0.co;2
- Raveton, M., Ravanel, P., Serre, A. M., Nurit, F., & Tissut, M. (1997). Kinetics of uptake and metabolism of atrazine in model plant systems. *Pesticide Science*, 49(2), 157-163. doi: 10.1002/(sici)1096-9063(199702)49:2<157::aid-ps517>3.0.co;2-m
- Redshaw, C. H., Wootton, V. G., & Rowland, S. J. (2008). Uptake of the pharmaceutical Fluoxetine Hydrochloride from growth medium by Brassicaceae. *Phytochemistry*, 69(13), 2510-2516. doi: 10.1016/j.phytochem.2008.06.018
- Sandermann, H., Scheel, D., & Vandertrenck, T. (1984). USE OF PLANT-CELL CULTURES TO STUDY THE METABOLISM OF ENVIRONMENTAL CHEMICALS. *Ecotoxicology and Environmental Safety*, 8(2), 167-182. doi: 10.1016/0147-6513(84)90059-9
- Shenker, M., Harush, D., Ben-Ari, J., & Chefetz, B. (2011). Uptake of carbamazepine by cucumber plants - A case study related to irrigation with reclaimed wastewater. *Chemosphere*, 82(6), 905-910. doi: 10.1016/j.chemosphere.2010.10.052
- Steudle, E., & Peterson, C. A. (1998). How does water get through roots? *Journal of Experimental Botany*, 49(322), 775-788. doi: 10.1093/jexbot/49.322.775
- Su, Y. H., Liu, T., & Liang, Y. C. (2010). Transport via xylem of trichloroethylene in wheat, corn, and tomato seedlings. *Journal of Hazardous Materials*, 182(1-3), 472-476. doi: 10.1016/j.jhazmat.2010.06.055
- Su, Y. H., Zhu, Y. G., & Du, X. (2005). Co-uptake of atrazine and mercury by rice seedlings from water. *Pesticide Biochemistry and Physiology*, 82(3), 226-232. doi: 10.1016/j.pestbp.2005.03.002
- Su, Y. H., Zhu, Y. G., & Liang, Y. C. (2009). Interactions of mixed organic contaminants in uptake by rice seedlings. *Chemosphere*, 74(7), 890-895. doi: 10.1016/j.chemosphere.2008.10.057
- Sun, Q., Wu, Y., & Jia, L. (2001). Quantitative Determination of Aristolochic Acid in Asarum heterotropoides Fr. Schmidt var. mandshuricum(Maxim.) Kitag. *Asian Journal of Traditional Medicines*.
- The Gale Group, I. (2010). Nutrient solution. from <http://encyclopedia2.thefreedictionary.com/Nutrient+Solution>

- Trapp, S. (2000). Modelling uptake into roots and subsequent translocation of neutral and ionisable organic compounds. *Pest Management Science*, 56(9), 767-778. doi: 10.1002/1526-4998(200009)56:9<767::aid-ps198>3.3.co;2-h
- Trapp, S. (2004). Plant uptake and transport models for neutral and ionic chemicals. *Environmental Science and Pollution Research*, 11(1), 33-39. doi: 10.1065/espr2003.08.169
- Trapp, S., & McFarlane, J. C. (1995). *Plant contamination-Modeling and simulation of organic chemical processes*. USA: Lewis.
- Ucisik, A. S., Trapp, S., & Kusk, K. O. (2007). Uptake, accumulation, phytotoxicity, and removal of 2,4-dichlorophenol in willow trees. *Environmental Toxicology and Chemistry*, 26(6), 1165-1171. doi: 10.1897/06-353r1.1
- Yuan, J. B., Liu, Q., Zhu, W. F., Ding, L., Tang, F., & Yao, S. Z. (2008). Simultaneous analysis of six aristolochic acids and five aristolactams in herbal plants and their preparations by high-performance liquid chromatography-diode array detection-fluorescence detection. *Journal of Chromatography A*, 1182(1), 85-92. doi: 10.1016/j.chroma.2007.12.076
- Zhang, C. Y., Wang, X., Shang, M. Y., Yu, J., Xu, Y. Q., Li, Z. G., . . . Namba, T. (2006). Simultaneous determination of five aristolochic acids and two aristolactams in *Aristolochia* plants by high-performance liquid chromatography. *Biomedical Chromatography*, 20(4), 309-318. doi: 10.1002/bmc.565
- Zhu, H., Han, J., Xiao, J. Q., & Jin, Y. (2008). Uptake, translocation, and accumulation of manufactured iron oxide nanoparticles by pumpkin plants. *Journal of Environmental Monitoring*, 10(6), 713-717. doi: 10.1039/b805998e

Chapter 6

Root exudates of *Aristolochia* plants and leaching and decomposition of *Aristolochia Clematitis* seeds

6.1 Introduction

Plant can release chemicals to soil by 2 major pathways, the root exudates from live plants and the leachates from decomposition of dead plants tissues. These plants and their parts can serve as source of chemicals into the soil and also other environment compartment. These released chemicals can impact to ecosystem around the living areas. Some chemicals are toxic to food crops and induce the problems such as crop rotation failure, crop selection in mix cropping, the growth reduction of vegetables or fruits which affect to agricultural economy or even toxic to human when chemicals incorporate to the food chain (U. K. Sahoo, Vanlalhratpuia, Upadhyaya, & Roy, 2011; Yu & Matsui, 1994) .

Root exudates define as substances that release from plant root to surrounding media. It consists of various compounds e.g. sugar, amino acid, and organic acids. They have both benefit or can be toxic to other plants. They found to enhance the nutrient mineral acquisition which required for plant growth (Dakora & Phillips, 2002). In the other hand, they can inhibit the growth or even kill the other plants (Rietveld, Schlesinger, & Kessler, 1983). This effect called “allelopathy” (Hasanuzzaman; Yu & Matsui, 1994).

Other than root exudates, the potential sources of chemicals into the soil can be from leaching and decomposition of dead plant parts e.g. roots, stems, leaves, and seeds. When the

plant litter falls to the ground, they will be decomposed and release the chemical. Rain can wash the chemicals from plant biomass and carries to the soil. These chemicals can be accumulated in the soil if the degradation is low. Rietveld et al., 1983 reported the phytotoxic chemical “juglone” from black walnut tree that can harm the nearby trees to declined and died within a few years. The contribution of large amount of leachate from walnut biomass and the limited soil microorganism metabolism can build up the juglone to toxic level.

Aristolochia clematitis is a weed plant that had the cycle in crop field in BEN area for long time. The previous studies showed that the BEN field were heavily invaded by living of *A. Clematitis* plant and soil had accumulation of dead plant tissue, so the releasing of AAs from *A. Clematitis* plant and dead plant tissues to soil would be expected (Hranjec et al., 2005; Pavlovic et al., 2013). There is evidence that the growth of corn fields in Romania which were largely invaded by *Aristolochia Clematitis* was suppressed or even damaged. This indicated the interaction between *Aristolochia Clematitis* plant that released chemicals to the soil and the corn plants that uptake these chemicals (Pavlovic et al., 2013).

. To our best knowledge, there are no reports that study about the potential sources of AAs such as root exudates or leaching/biodegradation from *Aristolochia* plants. Therefore, this study was aimed to investigate the role of root exudates from *Aristolochia* species plant and the leaching and biodegradation of *A. Clematitis* seeds as potential sources of AAs that release and accumulate in the soil.

6.2 Literature reviews

6.2.1 Plant root exudates

Organic compounds can release from plant roots to rhizosphere which we known as root exudates. Although plants in different species give their own exudates, these compounds quite similar but may be different in quantity. The identified compounds in exudates have wide range of chemicas which consist of carbohydrates, amino acids, organic acids, sugars, vitamins and enzymes which are listed in Table 6.1.

Table 6.1 The organic compounds identified in root exudates (modified from Yoshitomi, 2001)

Organic acids	Sugars	Vitamins	Enzymes
Acetic	Arabinose	p-Amino-benzoate	Amylase
Butyric	Deoxyribose	Biotin	Invertase
Citric	Galactose	Choline	Protease
Fumaric	Glucose	Inositol	
Glycolic	Maltose	Nicotinic acid	
Lactic	Ribose	Pantothenate	
Malic	Sucrose		
Oxalic	Xylose		

The quality and quantity of root exudation are affected by many factors such as age of the plant, the presence of microorganisms and environmental stress e.g. soil moisture and nutrient stress. The presence of microorganism can increase exudation of some plants significantly whereas may have no effect to other plant. These results suggested the dependent on plant species(Biondini, Klein, & Redente, 1988). The microbial metabolite may contain plant growth regulator such as gibberellins, auxins, cytokinins and also phytotoxins such as phenolic acid and hydrogen cyanide. Moreover, the presence of microbe will utilize the organic carbon compound

exude at root surface which increase driving concentration gradient for passive diffusion (Yoshitomi, 2001). The soil moisture also have significant effect to amount of exudates where the release amount of carbon increase for soil which have water stress (Martin, 1977) . The nutrient stress can affect the composition of root exudates where plant will modify the exudates to enhance the uptake of scarce nutrients.

Root exudates can be released to the soil by either the passively concentration gradient between root cells and soil solution or actively response to some activation such as metal toxicity, nutrient stress and microbial activity. Even though it has only small amount, exudates has significant role in soil nutrient availability because of their chelating properties and stimulation of microbial activity (Phillips, Erlitz, Bier, & Bernhardt, 2008). Root exudates will occur in narrow zone of soil around root which has closely interaction with microorganism. These may have positive and negative effect to the plant. For example the exudates will promote the plant growth by chemicals released from bacteria . The intensity of bacteria in rhizosphere also enhance degradation of pollutants e.g. PAHs in soil (Aprill & Sims, 1990; Reilley, Banks, & Schwab, 1996). The negative effect may include the soil borne pathogen or parasites infection to plants because of colonization around the root.

The root exudates of some plants can damage to other neighboring plants, this plant to plant interaction is called “allelopathy”. The chemicals in exudates that have capability in inhibition seed germination and plan growth called “allelochemical” (Yamane, Nishimura, & Mizutani, 1992). The examples of allelochemicals included phenolic acids, terpinoids, flavinoids, polyacetylene and fatty acids which presence in root exudates and also various plant parts. These chemicals can inhibit the photosynthetic and oxygen evaluation process which is essential process for plant growth. They also can modify microbial community dynamic in

rhizosphere (Buehler, 2010). The example weed which has allelopathy effect to the crop is Quack grass. It is important weed that highly reduce yield of corn fields by interfere nitrogen and potassium uptake by maize. The allelochemical “ethylene” which produce by microbial activity in soil was found at rhizomes of Quack grass and response for interruption of mineral uptake (Hasanuzzaman; Inderjit, 1996). A well known allelochemical from the walnut tree “juglone”, 5-hydroxy-1,4-naphthoquinone, found to have high accumulation of in the root zone and decreasing with increasing distance from the trees(von Kiparski, Lee, & Gillespie, 2007).

6.2.2 Root exudates collect method

In general, the exudates collection methods will comply with these constraint (a) it must capture exudates before microbial assimilation (b) the medium should not affect the root physiology or adsorp the root exudates and (c) the exudates can be distinguish from other soluble organic compounds in the medium(Phillips et al., 2008). A large number of methods had been developed to collect exudates but most of them are complex and also required a lot of laboratory processes (Matsumoto, Okada, & Takahashi, 1979; Prikryl & Vancura, 1980; Wadhwa & Narula, 2012) . Generally, there are two methods to study chemical composition and concentration of root exudates: in *situ* direct measuring from the soil and culture-based system which is more often used because exudates can be more trapped and separated from the medium. The culture-based system is also divided into two different types: static and dynamic trap solutions. Both types are mainly similar that the roots are submerged in the medium where exudates will be collected for a period of time. The primary difference is the removing and re-adding the medium solution in dynamic type to maintain diffusion gradient between root cells and medium solution and minimizing the re-uptake of exudates e.g. sugars and amino acids back to roots (Phillips et al., 2008).

The solution culture give advantage in simplicity of sample collection and maintenance. However, it does not have solid matrix to hold the plant which may affect to root morphology and exudation rate. The small glass bead and acid-washed sand are commonly use but they also has some limitation due to the sorption of exudates compounds. Another point to consider is the sterility of culture media. The sterile culture system can ensure that the exudates will not be utilized by microorganisms in the media. However, the microbial may stimulate the exudation, so the sterile culture may reduce rate of exudation and affect to composition of exudates (Phillips et al., 2008)

6.2.3 Plant litter leaching and decomposition

When plant died and fall down to the soil, the organic substances in the plant can be released to the soil by decomposition process. The decomposition is the combining of physical, chemical and biological processes altering the chemicals on organic substrate in the plant. The plant litters contained several groups of organic compounds which vary with the parts such as leaves, stems, roots and bark but generally consist of water soluble compounds and hard degraded compounds e.g. cellulose and lignin. The major group of soluble compounds include sugar, phenolic acids and some nutrients. The sugars e.g. mono and oligosaccharide are from metabolism of plants. The phenolic compounds found as defensive agent from insects or precursor of lignin.

In early stage of decomposition, these soluble compound are readily released from plant by leaching or dissolution with water and may sequestrated by organic matter and clay in the soil. The degradation process of soluble organic substance e.g. simple sugar glucose and fructose is quite rapid and quickly finish with in few month due to easy of run out with water and

microbial utilization (J. S. Singh & Gupta, 1977). The leachate of some plants contain allelochemicals e.g. phenolics, flavonoids and terpenoids which inhibit growth of surrounding plants (U. Sahoo, Jeecelee, Vanlalhratpuia, Upadhyaya, & Lalremruati, 2010; H. Singh, Batish, & Kohli). After the soluble was leached out and degraded, the carbohydrate e.g. starch and unshield cellulose which is accessible will be next degraded. Finally, the lignin and cellulose will be the last stage of degradation, the degradation is difficult and rate are much more slowly (Kuiters & Sarink, 1986) . Only some bacteria and fungi have the enzyme which can digest the chemical bonds in lignin and cellulose.

The decomposition of soluble or non-soluble e.g. cellulose and lignin in plant substrate can be aerobic and anaerobic. In aerobic condition, the decomposition will give CO₂ and release from the soil. In anaerobic condition, such as waterlogged in soil , the organic acids e.g. acetic acid will be produce instead of CO₂. The long chain of fiber cellulose will be degraded to soluble short chain of glucose units. Lignin will be degraded until formation the stable humus where rate of decomposition is zero. Some microorganism have ability to completely mineralize lignin to CO₂ and H₂O (Berg & Mcclaugherty, 2014). Rate of decomposition can measure by mass loss or CO₂ release which will be effect by litter composition, soil oxic condition and climate (Bragazza, Buttler, Siegenthaler, & Mitchell, 2009)

6.2.4 Cellulose degradation in activated sludge medium

Cellulose and lignin are the carbon substrate that hard to degrade by general microorganism due to their insoluble and special enzyme needed. They can be degraded by cellulolytic fungi found in soil or natural water and cellulolytic bacteria which can be found in both aerobic and anaerobic culture media such as in wastewater treatment plant. Normally,

activated sludge is mainly used for breakdown the soluble organic material. However, there are some studies show that activated sludge is efficient to degrade these fibers as well (Edberg & Hofsten, 1975).

Verachtert et al. show that the degradation of cellulose of filter paper and cotton wool in activated sludge tank can achieve to 80% and 60% w/w with 4-5 weeks incubation time (Verachtert, Ramasamy, Meyers, & Bevers, 1982). This shows that the cellulolysis degradation is active in activated sludge. The most detected cellulolytic microorganism is gram-negative bacteria such as *Sporocytophaga myxococcoides* which is most efficient aerobically cellulose degrading bacteria (Edberg & Hofsten, 1975). The cellulolytic bacteria found to grow in close contact or adhere with their substrates which result in long contact time. The direct contact between bacteria and fiber is necessary for efficient degradation. This study showed the ratio between cellulose to lignin was change from 1.2 in primary sludge to 0.4 in activated sludge which indicated the lignin utilization is slower (Edberg & Hofsten, 1975; Verachtert et al., 1982).

6.2.5 Cellulose degradation in anaerobic environment

Cellulose degradation also was determined in anaerobic condition. The experiment showed that 60% of cellulose can be degraded by bacteria in aerobic treatment whereas the left 50-60% was degraded during anaerobic digestion (Verachtert et al., 1982). The rate of degradation was found to similar to the digesting with activated sludge in aerobic condition which required several days for degradation of cellulose to be occurred. The temperature had the effect to rate of degradation. For example, the 50% loss of cellulose was obtained in 25 days when incubated at 30°C but it will take 40-45 days if temperature was 17°C. The anaerobic

cellulolytic bacteria can be found in soil, sediment or waste water sludge. The most effective anaerobic cellulolytic bacter is *Clostridium* (Edberg & Hofsten, 1975).

The anaerobic digestion is complex biodegradation process that involve the series of reactions including hydrolysis, fermentation and methanogenesis to convert organic compounds to methane and carbon dioxide (Siegert & Banks, 2005). Unlike aerobic decomposition, anaerobic decomposition required diverse microorganisms because they have to perform various fermentation and respiration processes which use various electron acceptors e.g. CO_2 , NO_3^- , SO_4^{2-} instead of O_2 . The key processes are similar in soil, sediment or anaerobic digester where cellulolytic bacteria produce the enzyme to depolymerize cellulose to glucose and some sugars. These sugars will be fermented by cellulolytic bacteria and yield as CO_2 , H_2 , and organic acids such as acetate, propionate, butyrate and alcohols. These CO_2 , H_2 and organic acids will not be released to environment but instead immediately consumed by methanogenic bacteria to change to CH_4 (Leschine, 1995).

6.3 Material and method

6.3.1 Root exudates from hydroponic culture

The *Aristolochia* plant species: *Aristolochia littoralis*, *Aristolochia tribota* and *Aristolochia Macrophylla* were plant to collect the root exudates. *Aristolochia* plants were removed from pots, cleaned the roots with deionized water and transfered to glass jar filled with aerated 50%strength Knop's solution for hydroponic cultivation. These plants were grown under the light in 14/10 hr day/night cycle. To collect root exudates, the *Aristolochia* plants were thoroughly rinse with deionized water and move to beaker which filled 200 ml of 50% strength Knop's solution as shown in Figure 6.1. The exudates were expected to release and mixed with

nutrient solution. At day of taking sample, 15 ml nutrient solution were collected, centrifuge at 7,500 rpm for 20 min to remove the root debris and then 10 ml of supernatants were taken to increase concentration by condensation method where the supernatant were dried with evaporation unit under air stream as shown in Figure 6.2. The residual in the tube was re-dissolved with 0.5 ml 70% methanol (20 fold concentrate). The re-dissolved samples were centrifuge in eppendorf tube at 12,000rpm for 3 min to remove precipitated salt before analyze with HPLC-DAD. The samples were taken in every 2 day for consecutive 12 day cultivation. The 15 ml of fresh nutrient solution was refilled to balance the taken volume sample.



Figure 6.1 The experimental setup to collect root exudates in hydroponic culture



Figure 6.2 The condensation of collected root exudates by evaporation unit

6.3.2 Root exudates from sands culture

After collect root exudates from hydroponic culture, *Aristolochia* plant: *Aristolochia littoralis*, *Aristolochia tribota* and *Aristolochia Macrophylla* were transfered to beaker which contain 150 g pre-treatment sand. The experimental setup for sand culture showed in Figure 6.3. To prepare pre-treatment sand, F-65 Ottawa Silica sand was washed with deionized water for 2 times and dried in the fume hood. Then the dried sand were autoclaved (10 min heat and 10 min dried cycle) to inhibit microbial activity. The 50% knop nutrient solution was used to irrigate in everyday to keep water level cover the sand surface. After 10 day of acclimation, the root exudates was started to collect. To collect the root exudates, 30ml of 50% Knop solution was added to the beaker and equilibrated for 1 hr to dissolve out all soluble compound from root and sand, then 15ml of leachate wascollected from top solution. These solutions were centrifuged to remove sand and any particulate and10 ml of supernatants was collected to increase concentration by condensation method and analyzed for AAs same as hydroponic cultivation. These root exudates was collected in every 2 day.



Figure 6.3 The experimental setup to collect root exudates in sand culture

6.3.3 Leaching from decomposition of *Aristolochia Clematitis* seeds

6.3.3.1 The decomposition in aerobic condition by activated sludge and soil

The AAs leaching from decomposition of *Aristolochia Clematitis* seeds was conducted by batch experiment. Ottawa sand was used as solid media. Activated sludge and soils were used as sources of microorganisms. The sterile and non-sterile samples by autoclaving were used to determine the effect of biodegradation. Five bottles were prepared which consisted of bottle A contained 30 g of Ottawa sand and 30 ml pure water, bottle B and C contained 30 g of Ottawa sand, 25 ml pure water and 5ml of activated sludge, bottle D and E contained 30 g of Ottawa sand, 25 ml pure water, and 1 gram of garden soil. The bottle A, B and D were sterilized by autoclaving 10 min cycle to inhibit microorganism activity. The bottle C and E were not autoclaved where the biodegradation by microorganism in activated sludge and soil expect to be occurred. The bottles were prepared in duplicated. Before incubation, 0.02 g of ground A.

Clematitis seeds was added to each bottle and then covered with sponge plug to prevent microbial contaminated from the air while the O₂ can still pass. The prepared bottles are shown in Figure 6.4. The bottles were incubated by shaking in orbital shaker at 180 rpm under room temperature and keep out from the light. To collect the sample, 1 ml of solution were withdrawn from bottles and put into eppendorf tube to centrifuge at 12,000rpm for 3min, then the supernatants were collect to analyze AAs with HPLC-DAD. The samples were taken at interval time of 5 hr, 1 day, 2day, 4day, and every 2 days until 20 days.



Figure 6.4 The prepared bottles for decomposition of *A. Clematitis* seeds in aerobic condition

6.3.3.2 The decomposition in anaerobic condition by activated sludge and soil

To determine the decomposition of *A.Clematitis* seeds in anaerobic condition, five set of bottles were prepared similar to aerobic decomposition but the bottles were purged with the N₂ gas before leaving in glove box under N₂ atmosphere for 5 day to ensure the solution in anaerobic condition as shown in Figure 6.5. Activated sludge and soil were also used as sources of anaerobic microorganisms and were put in glove box for 5 days too. To collect the sample, the needle syringe was used to draw the solution from rubber septum cap for the time interval similar to aerobic experiment.



Figure 6.5 The set of bottles prepared in glove box under N₂ atmosphere

6.4 Results and discussion

6.4.1 Root exudates of *Aristolochia* plant from hydroponic and sand culture

The analysis for AA I and II in root exudates collected from hydroponic and sand culture were shown in Table 6.2. The table shows that no AA I and II were found in all *Aristolochia* plant species (*Aristolochia littoralis*, *Aristolochia tribota* and *Aristolochia Macrophylla*) root exudates for the whole experiment period (12 days). This indicated that root exudates of *Aristolochia* plants is not the main pathway that released AAs to the soil. However, because our culture system was not sterile, the microorganisms in the *Aristolochia* species plant root may contain from the original soil and degrade AAs during exudates collection periods.

Table 6.2 The AAs analysis in root exudates from three Aristolochia plants over 12 day periods

Days	Aristolochia Littoralis				Aristolochia Tribota				Aristolochia Macrophylla			
	AA I		AA II		AA I		AA II		AA I		AA II	
	Hydroponic culture	Sand culture	Hydroponic culture	Sand culture	Hydroponic culture	Sand culture	Hydroponic culture	Sand culture	Hydroponic culture	Sand culture	Hydroponic culture	Sand culture
2	NF	NF	NF	NF	NF	NF	NF	NF	NF	NF	NF	NF
4	NF	NF	NF	NF	NF	NF	NF	NF	NF	NF	NF	NF
6	NF	NF	NF	NF	NF	NF	NF	NF	NF	NF	NF	NF
8	NF	NF	NF	NF	NF	NF	NF	NF	NF	NF	NF	NF
10	NF	NF	NF	NF	NF	NF	NF	NF	NF	NF	NF	NF
12	NF	NF	NF	NF	NF	NF	NF	NF	NF	NF	NF	NF

NF is not found

6.4.2 Leaching from the decomposition of *Aristolochia Clematitis* seeds

6.4.2.1 The decomposition in aerobic condition by activated sludge and soil

The AAs concentration released during the *Aristolochia Clematitis* seeds decomposition with/without sources of microorganisms as function of incubation time are shown in Figure 6.6. The figures show that AA I and II start to release from all bottles in the first few days after apply the *A. Clematitis* seeds. For bottle A, B and D where solutions were autoclaved to inhibit microbial activity, the AAs continued to release until they reach the maximum concentration after 12 day. The concentration of AA I which leached from *A. Clematitis* seed was more than AA II about 10 times which according to the previous report about AAs content in *Aristolochia* herbal plants (Chan et al., 2007).

Not similar to bottle A, B and D, bottle C and E where solutions were not sterilized showed the degradation of AA I and II after 8 days and were completely consumed in 12 days for activated sludge bottle and 18 day for soil bottle. This indicated the aerobic microorganism in activated sludge and soil can degrade AA I and II but microorganisms in activated sludge may degrade AAs faster than soil. Figure 6.7 (c) showed the microbe in activated sludge grown by adhering on *A. Clematitis* seeds which is typical for cellulolytic bacteria. This evidence cannot be seen in bottle B where the microbe had been killed as shown in Figure 6.7(b). The chromatogram of AA I and II in leachate from bottle A analyzed by HPLC-DAD is shown in Figure 6.8.

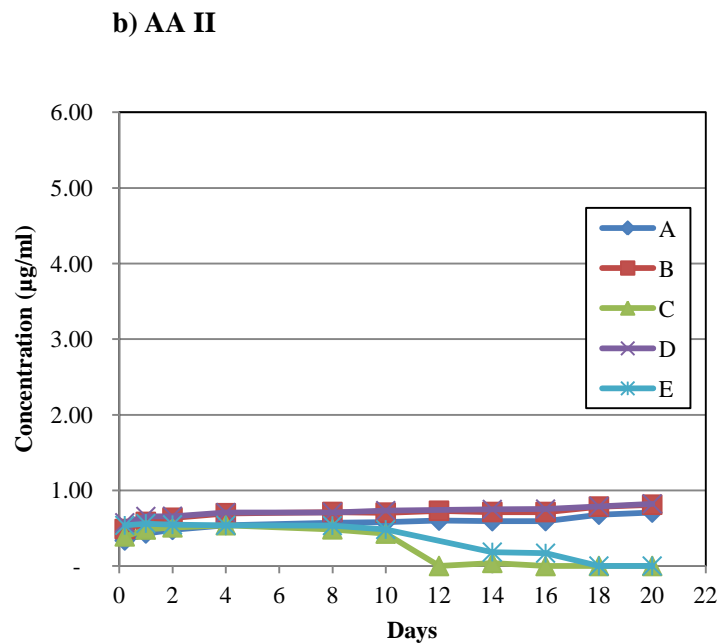
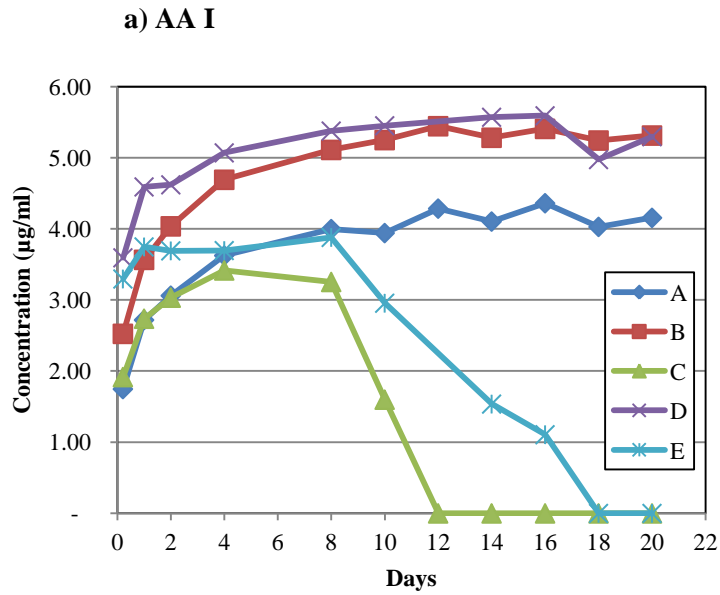


Figure 6.6 AA I (a) and II (b) leaching from the decomposition of *A. Clematis* seeds in aerobic condition from bottle set A, B, C, D and E as a function of time : A=no microorganism + sterile, B=activated sludge + sterile, C=activated sludge + non sterile, D =soil + sterile, E=soil + non sterile

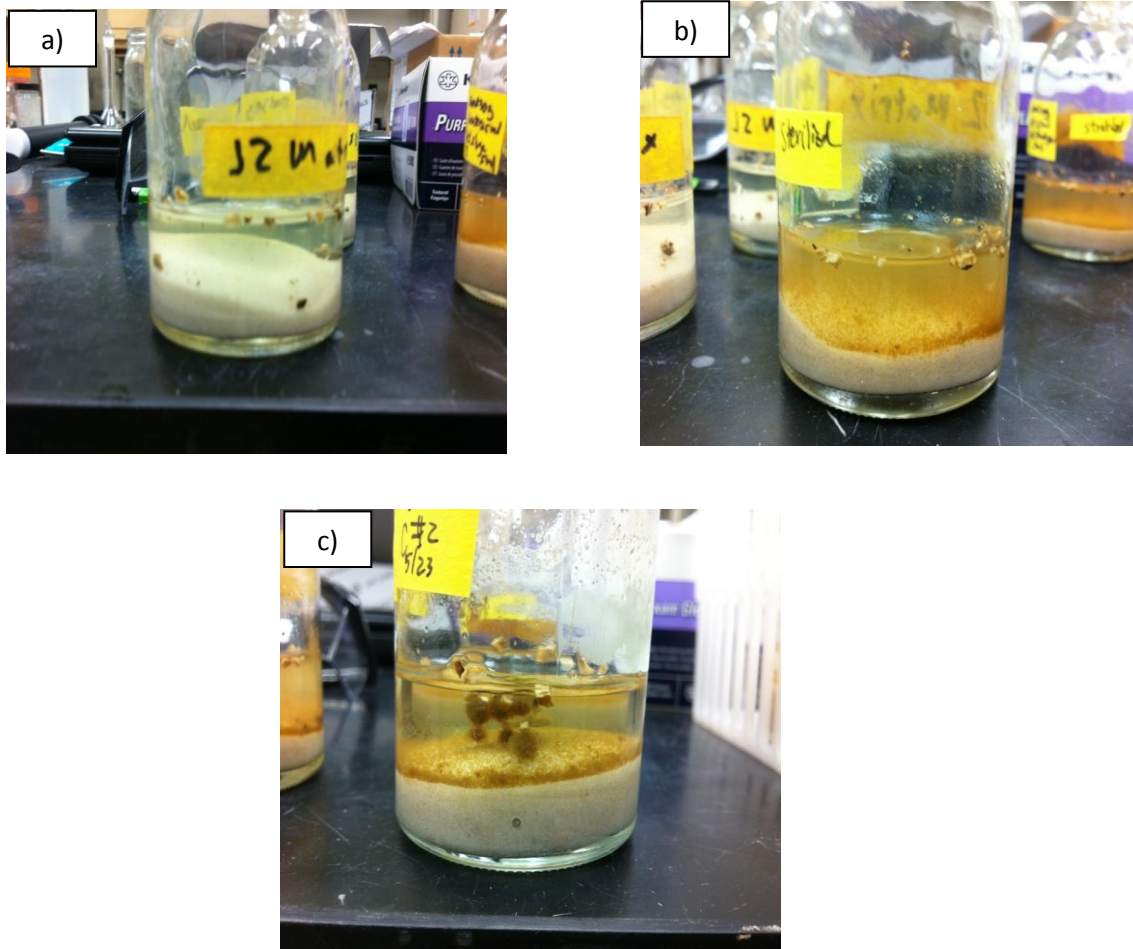


Figure 6.7 The growing of microorganism from activated sludge in bottle A (a) , bottle B (b) and bottle C (c) in aerobic decomposition experiments

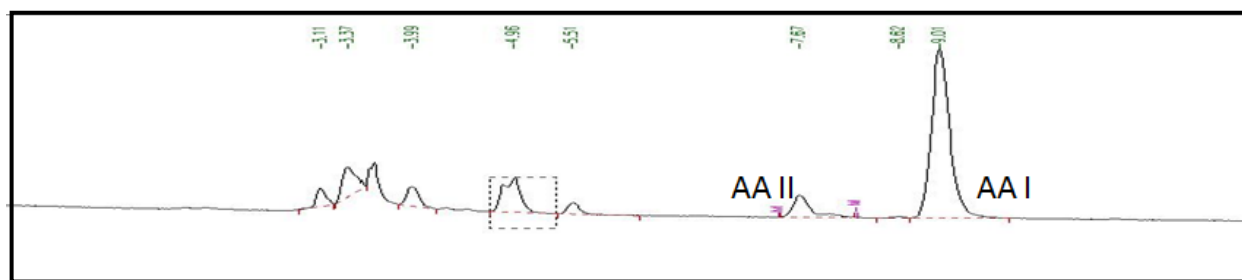


Figure 6.8 The chromatogram of AA I and II leaching from *A. Clematitis* (bottle set A) analyzed by HPLC-DAD

6.4.2.2 The decomposition in anaerobic condition by activated sludge and soil

The AAs leaching during decomposition under anaerobic and sterile and non-sterile condition are shown in Figure 6.9. Likewise the aerobic decomposition, the bottles which were autoclaved to kill microorganism (bottle A, B and D) show continually release AAs to solution. However, for the bottles which were not autoclave (bottle C and E), the AAs concentration found to decrease with time until they deplete in 5 days which may be faster than aerobic decomposition. The decreasing AAs concentration in bottles that contain soil was expected from the adsorption of AAs into the soil. These results indicated that AAs can be easily degraded even in anaerobic condition too.

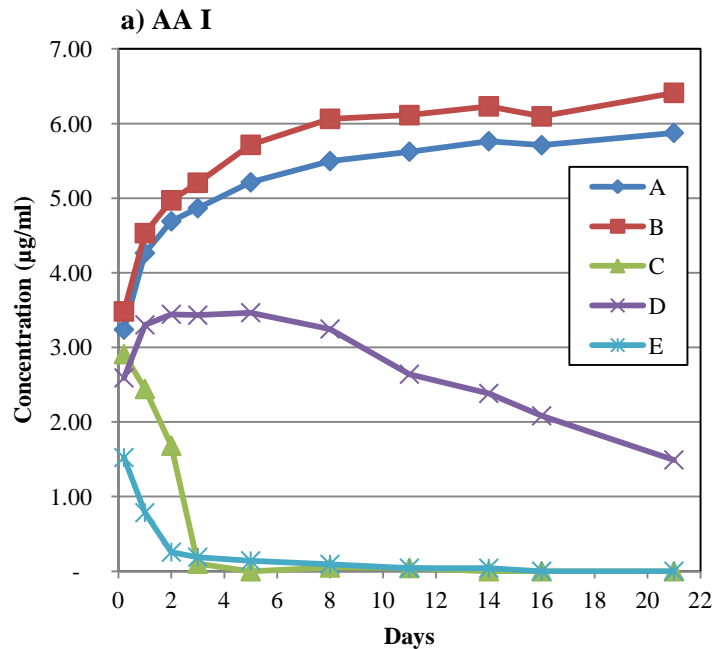
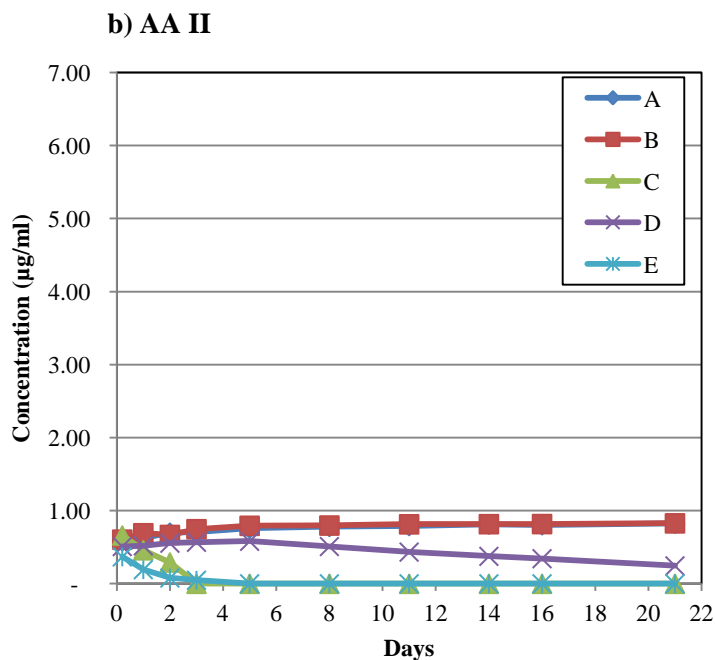


Figure 6.9 AA I (a) and II (b) leaching from the decomposition of *A. Clematis* seeds in anaerobic condition from bottle set A, B, C, D and E as a function of time : A=no microorganism + sterile, B=activated sludge + sterile, C=activated sludge + non sterile, D =soil + sterile, E=soil + non sterile

Figure 6.9 (cont'd)



6.5 Conclusion

The root exudates collecting from different *Aristolochia* plants by both hydroponic and sand culture did not contain AAs which indicates root exudates is not the main pathway that released AAs to soil. Instead, high concentration of AAs was found in leachates from the decomposition of *A. Clematitidis* seeds and this should be the main releasing pathway of AAs to soil if seeds suspend in water. However, the released AAs were found to be degraded by both aerobic and anaerobic microorganisms which may suggest that AAs are not persistent chemicals in environment.

REFERENCES

REFERENCES

- Aprill, W., & Sims, R. C. (1990). EVALUATION OF THE USE OF PRAIRIE GRASSES FOR STIMULATING POLYCYCLIC AROMATIC HYDROCARBON TREATMENT IN SOIL. *Chemosphere*, 20(1-2), 253-265. doi: 10.1016/0045-6535(90)90100-8
- Berg, B., & Mcclaugherty, C. (2014). *Plant Litter: Decomposition, Humus Formation, Carbon Sequestration* (3rd ed.): Springer.
- Biondini, M., Klein, D. A., & Redente, E. F. (1988). CARBON AND NITROGEN LOSSES THROUGH ROOT EXUDATION BY AGROPYRON-CRISTATUM, AGROPYRON-SMITHII AND BOUTELOUA-GRACILIS. *Soil Biology & Biochemistry*, 20(4), 477-482. doi: 10.1016/0038-0717(88)90061-2
- Bragazza, L., Buttler, A., Siegenthaler, A., & Mitchell, E. A. D. (2009). Plant Litter Decomposition and Nutrient Release in Peatlands. *Carbon Cycling in Northern Peatlands*, 184, 99-110. doi: 10.1029/2008gm000815
- Buehler, C. P. (2010). *Soil modification and potential allelopathy: an investigation into how the invasive CASUARINA EQUISETIFOLIA L. (Australian pine) modify their environment.* (Master of Science in Geosciences), Mississippi State University.
- Chan, W., Lee, K.-C., Liu, N., & Cai, Z. (2007). A sensitivity enhanced high-performance liquid chromatography fluorescence method for the detection of nephrotoxic and carcinogenic aristolochic acid in herbal medicines. *Journal of Chromatography A*, 1164(1-2). doi: 10.1016/j.chroma.2007.06.055
- Dakora, F. D., & Phillips, D. A. (2002). Root exudates as mediators of mineral acquisition in low-nutrient environments. *Plant and Soil*, 245(1), 35-47. doi: 10.1023/a:1020809400075
- Edberg, N., & Hofsten, B. V. (1975). CELLULOSE DEGRADATION IN WASTEWATER TREATMENT. *Journal Water Pollution Control Federation*, 47(5), 1012-1020.
- Hasanuzzaman, M. Allelopathy.
<http://hasanuzzaman.weebly.com/uploads/9/3/4/0/934025/allelopathy.pdf>
- Hranjec, T., Kovac, A., Kos, J., Mao, W. Y., Chen, J. J., Grollman, A. P., & Jelakovic, B. (2005). Endemic nephropathy: the case for chronic poisoning by Aristolochia. *Croatian Medical Journal*, 46(1), 116-125.
- Inderjit. (1996). Plant phenolics in allelopathy. *Botanical Review*, 62(2), 186-202. doi: 10.1007/bf02857921
- Kuiters, A. T., & Sarink, H. M. (1986). LEACHING OF PHENOLIC-COMPOUNDS FROM LEAF AND NEEDLE LITTER OF SEVERAL DECIDUOUS AND CONIFEROUS

- TREES. *Soil Biology & Biochemistry*, 18(5), 475-480. doi: 10.1016/0038-0717(86)90003-9
- Leschine, S. B. (1995). CELLULOSE DEGRADATION IN ANAEROBIC ENVIRONMENTS. *Annual Review of Microbiology*, 49, 399-426. doi: 10.1146/annurev.mi.49.100195.002151
- Martin, J. K. (1977). EFFECT OF SOIL-MOISTURE ON RELEASE OF ORGANIC-CARBON FROM WHEAT ROOTS. *Soil Biology & Biochemistry*, 9(4), 303-304. doi: 10.1016/0038-0717(77)90039-6
- Matsumoto, H., Okada, K., & Takahashi, E. (1979). EXCRETION PRODUCTS OF MAIZE ROOTS FROM SEEDLING TO SEED DEVELOPMENT STAGE. *Plant and Soil*, 53(1-2), 17-26. doi: 10.1007/bf02181875
- Pavlovic, N. M., Maksimovic, V., Maksimovic, J. D., Orem, W. H., Tatu, C. A., Lerch, H. E., . . . Paunescu, V. (2013). Possible health impacts of naturally occurring uptake of aristolochic acids by maize and cucumber roots: links to the etiology of endemic (Balkan) nephropathy. *Environmental Geochemistry and Health*, 35(2), 215-226. doi: 10.1007/s10653-012-9477-8
- Phillips, R. P., ERLITZ, Y., Bier, R., & Bernhardt, E. S. (2008). New approach for capturing soluble root exudates in forest soils. *Functional Ecology*, 22(6), 990-999. doi: 10.1111/j.1365-2435.2008.01495.x
- Prikryl, Z., & Vancura, V. (1980). ROOT EXUDATES OF PLANTS .6. WHEAT ROOT EXUDATION AS DEPENDENT ON GROWTH, CONCENTRATION GRADIENT OF EXUDATES AND THE PRESENCE OF BACTERIA. *Plant and Soil*, 57(1), 69-83. doi: 10.1007/bf02139643
- Reilley, K. A., Banks, M. K., & Schwab, A. P. (1996). Dissipation of polycyclic aromatic hydrocarbons in the rhizosphere. *Journal of Environmental Quality*, 25(2), 212-219.
- Rietveld, W. J., Schlesinger, R. C., & Kessler, K. J. (1983). ALLELOPATHIC EFFECTS OF BLACK WALNUT ON EUROPEAN BLACK ALDER COPLANTED AS A NURSE SPECIES. *Journal of Chemical Ecology*, 9(8), 1119-1133. doi: 10.1007/bf00982216
- Sahoo, U., Jeecelee, L., Vanlalhriatpuia, K., Upadhyaya, K., & Lalremruati, J. (2010). Allelopathic Effects of Leaf Leachate of *Mangifera indica* L. on Initial Growth Parameters of Few Homegarden Food Crops. *World Journal of Agricultural Sciences*, 6(5), 579-588.
- Sahoo, U. K., Vanlalhriatpuia, K., Upadhyaya, K., & Roy, S. (2011). Effects of leaf extracts of common home garden trees on food crops. *Allelopathy Journal*, 28(1), 123-134.

- Siegert, I., & Banks, C. (2005). The effect of volatile fatty acid additions on the anaerobic digestion of cellulose and glucose in batch reactors. *Process Biochemistry*, 40(11), 3412-3418. doi: 10.1016/j.procbio.2005.01.025
- Singh, H., Batish, D., & Kohli, R. Allelopathic effect of *Leucaena leucocephala* on *Zea Mays*. *Journal of Tropical Forest Science*, 11(4), 801-808.
- Singh, J. S., & Gupta, S. R. (1977). PLANT DECOMPOSITION AND SOIL RESPIRATION IN TERRESTRIAL ECOSYSTEMS. *Botanical Review*, 43(4), 499-528.
- Verachtert, H., Ramasamy, K., Meyers, M., & Bevers, J. (1982). INVESTIGATIONS ON CELLULOSE BIODEGRADATION IN ACTIVATED-SLUDGE PLANTS. *Journal of Applied Bacteriology*, 52(2), 185-190. doi: 10.1111/j.1365-2672.1982.tb04839.x
- von Kiparski, G. R., Lee, L. S., & Gillespie, A. R. (2007). Occurrence and fate of the phytotoxin juglone in alley soils under black walnut trees. *Journal of Environmental Quality*, 36(3), 709-717. doi: 10.2134/jeq2006.0231
- Wadhwa, K., & Narula, N. (2012). A novel technique to collect root exudates from mustard (*Brassica juncea*). *Journal of Basic Microbiology*, 52(5), 613-615. doi: 10.1002/jobm.201100407
- Yamane, A., Nishimura, H., & Mizutani, J. (1992). ALLELOPATHY OF YELLOW FIELD CRESS (*RORIPPA-SYLVESTRIS*) - IDENTIFICATION AND CHARACTERIZATION OF PHYTOTOXIC CONSTITUENTS. *Journal of Chemical Ecology*, 18(5), 683-691. doi: 10.1007/bf00994606
- Yoshitomi, K. J. (2001). *Influence of root exudates on soil microbial population*. University of Cincinnati.
- Yu, J. Q., & Matsui, Y. (1994). PHYTOTOXIC SUBSTANCES IN ROOT EXUDATES OF CUCUMBER (*CUCUMIS-SATIVUS* L). *Journal of Chemical Ecology*, 20(1), 21-31. doi: 10.1007/bf02065988

SECTION II

Biogeochemical Modeling of Fate and Transport of Copper from Mining Waste in Torch Lake Sediment

Chapter 7

Introduction

7.1 The problem of concern and Torch Lake history

Lake contaminated with heavy metal from mining waste is one of major environmental problems which deteriorate water resource. It raises the metal concentration in sediment, overlying water and also in aquatic organism to exceed safe level for consumption and decreasing number of fish population as well (Adams, Atchison, & Vetter, 1980; Moore & Sutherland, 1981). Torch Lake, located in Houghton County, MI, had been impacted by copper mining for a hundred years between 1867-1968. Two hundred million tons of copper waste had been deposited on shoreline and the basin which was estimated as 20% of lake volume. These wastes were also discharged to Lake Superior by Kewenaw waterway which connect with Torch Lake and portage Lake (Lopez & Lee, 1977). Moreover, after ceasing of mining activities, there was a large spill of cupric ammonium carbonate in October, 1971 and June, 1972 which increased copper concentration in Torch lake water from 40 $\mu\text{g/ml}$ at the surface to 100 $\mu\text{g/ml}$ at the bottom. The Cu-bearing ore that lay in bottom sediment and shoreline act as a copper reservoir continual providing to lake water. Those reported dissolved Cu concentrations in Torch

Lake were exceeded the criteria of US EPA 30 µg/l and quite persist throughout annual cycle. The copper criteria range of lethal dose and teratogenicity to egg of sensitive species fishes and amphibians is 5-10 µg/L. The recommend a maximum allowable value for copper concentration for aquatic life is 12-43 µg/L (USGS, 1997). Even toxic level concentration, substantial fish population were reported in Torch Lake which may result from the sorption of copper onto iron and manganese hydrous oxides resulting in non-toxic form (Lopez & Lee, 1977).

Because of significant copper concentration above background level, high incidence of undetermined cause fish tumor and degradation of benthos in bottom sediment. In 1986, Torch Lake was added to US EPA National Priorities List and declared as Area of Concern and Superfunds site for 3 reason: Fish Tumor and Other Deformities, Restrictions on Fish and Wildlife Consumption, and Degradation of Benthos (MDEQ, 2007). US EPA attempted to delist Torch Lake from area of concern by started remediation on 1998. The stamp sand and slags deposits were stabilized through covering by the clean soil and vegetative to reduce metal erosion by wind and water from shoreline into the lake. However, for the sediment , US EPA determine that the contamination had no unacceptable threat to human health and select “no action” or natural attenuation as remediation step except long term monitoring and reviewing in every five years (MDEQ, 2007).

7.2 Torch Lake study site

Torch Lake is natural deep lake located on eastern side of Keweenaw Peninsula, Houghton County. It has the surface area around 20.5 km². The average depth is 15 m and the maximum depth is 37 m. It has 9.3 km long and 2.2 km wide at the widest point, near the middle of lake. It contains two distinct basins, north and south. Torch lake water flows to the Portage

Lake which located on the south and continually flows to Lake Superior on the west and Keweenaw Bay on the east via Keweenaw waterway as shown in Figure 7.1. Torch Lake is oligotrophic (low nutrient content and low algal production) which has the water residence time about 1 year. The watershed was mostly covered by hard woods and limited farming activities (Cusack & Mihelcic, 1999; J.D. Fett, 2003; Jeong, Urban, & Green, 1999; Lopez & Lee, 1977).

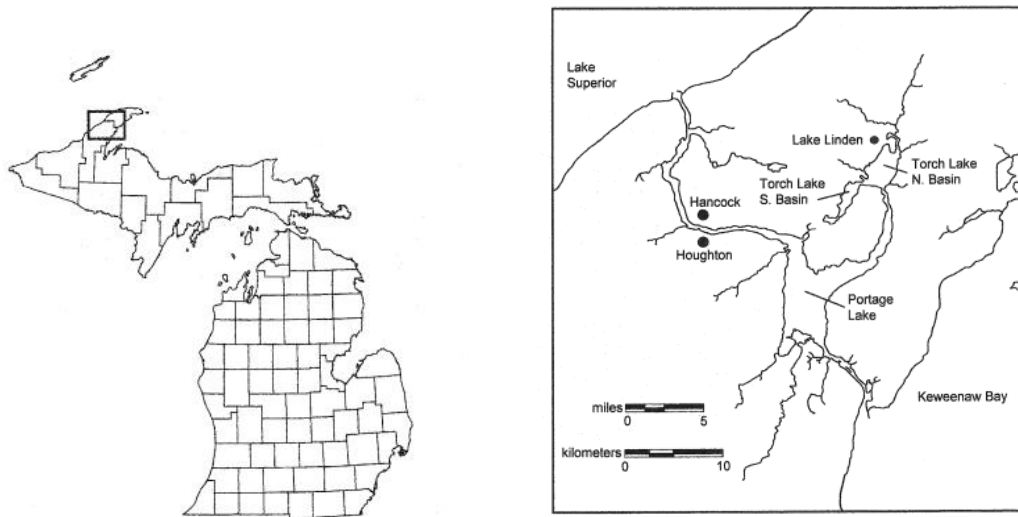


Figure 7.1 Map showing location of Torch Lake, Keweenaw Peninsula, Michigan (Fett, 2003)

7.3 The copper state in Torch Lake sediment

Although the remediation of shoreline had been greatly improved the water quality and clarity of lake and some sites were delisted from Superfund, many studies indicated that total copper concentration in recent deposited sediment had increased and has higher concentration than mine tailing itself (J.D. Fett, 2003; McDonald, Urban, Barkach, & McCauley, 2010).

These evidence showed Torch Lake sediment cannot be remediated by natural processes and raise the question how copper concentration in post sediment increased.

The Torch lake sediment divide into 2 clearly separation section, the mine tailing sediment which has grayish-purple color and post mining sediment which has black color as shown in Figure 7.2. The mine tailing sediment mainly consists of clay-sized stamp sand particles containing solid copper concentration more than 1,000 mg/L (Cusack & Mihelcic, 1999). It is extremely fine grain and loose with porosities about 80%. This sediment has 8 m height which reflected the high sedimentation rate in that mining period (14-28 mm/yr). This mine tailing was overlaid by 3 – 7 cm natural sediment after stop mining operation which had much lower sediment accumulation rate 5 – 9 mm/yr. It can refer as cap layer which is typical lake bottom sediments. This porosity of the cap layer is greater than 90% (Konstantinidis et al., 2003). The sedimentation flux rate which measured by sediment trap and the sediment accumulation which calculated by radioisotope dating indicated the re-suspension of surface sediment was not significant. The organic matter in post-mining layer was high about 10-18% whereas organic matter in mine tailing was lower about 1.9-2.7%. The solid copper concentration in sediment showed clearly the different between mine tailing and post-mining sediment as shown in Figure 7.3. The post-mining sediment was 1,800 – 2,800 mg/kg whereas underlying mine tailing was half lower 800 – 1,300 mg/kg (J.D. Fett, 2003; McDonald et al., 2010). The mean copper concentration of particles in overlay water was 790 – 1,090 mg/kg which was nearly to shoreline tailing deposit. These data showed that settling particle contained less copper than post-mine tailing sediment which means the sedimentation of erosion shoreline particle is not the only process that control copper concentration in sediment but it also has other sources that supply the copper to surface sediment. Moreover, the stamp sand on the shoreline had been covered by soil and vegetation which would greatly reduced copper particle input to the

lake. Not only the copper, some metals e.g. Zn, and Pb had similar pattern in the sediment (Konstantinidis et al., 2003).

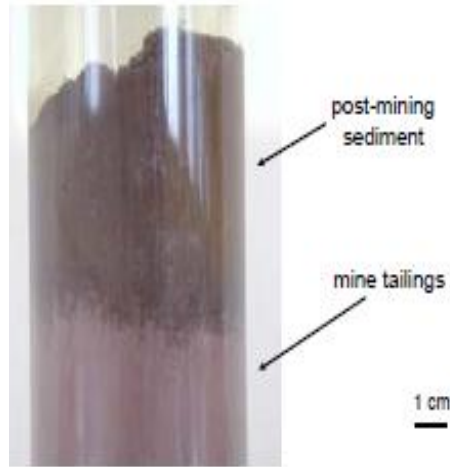


Figure 7.2 Torch Lake sediment core (McDonald & Urban)

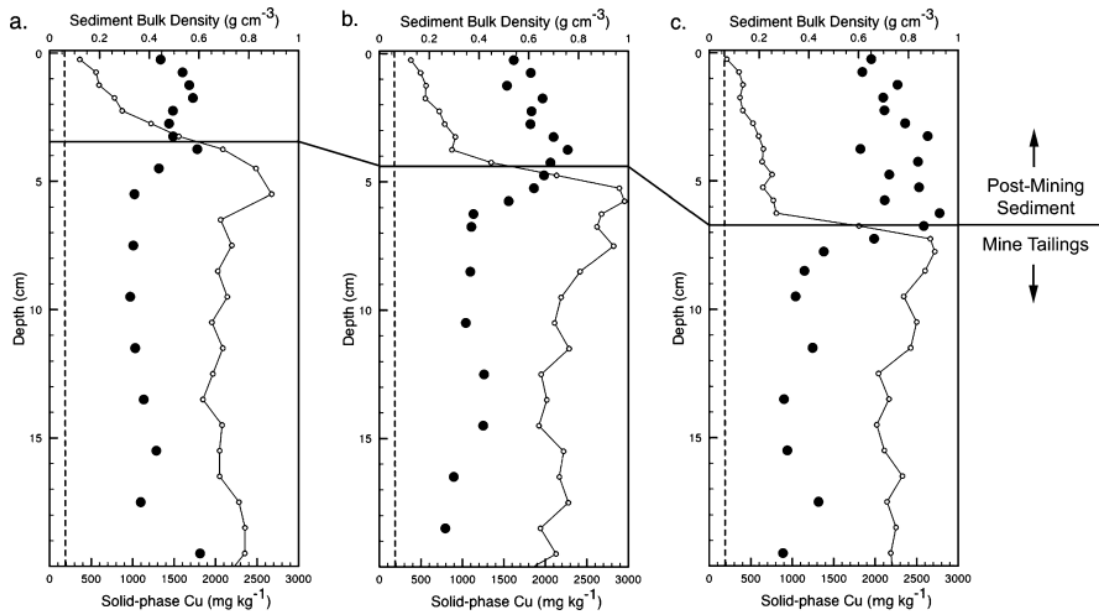


Figure 7.3 Bulk density (open circles) and solid phase copper concentration (solid circles) profiles of Torch lake sediment at different water depth (a) 10 m (b) 13 m and (c) 20 m (modified from C. P. McDonald et al., 2010)

7.4 State of recovery

The Gratiot Lake located on eastern side of Keweenaw peninsula was used as reference lakes to study of the recovery state of Torch Lake as shown in Figure 7.4. It has the same bedrock geology, surficial geology and had no impact from mining activities. The plot of Cu/Zn ratio of Torch lake sediment showed that they are largely over than ratio from Gratiot Lake but close to ratio of stamp sand which indicate the continual input from shore line stamp sand. However, the plot of other ions such as the ratio of Co/Zn showed the new sediment from local watershed entering to the Torch Lake. This indicate the state of recovery of Torch lake except the copper (J.D. Fett, 2003).

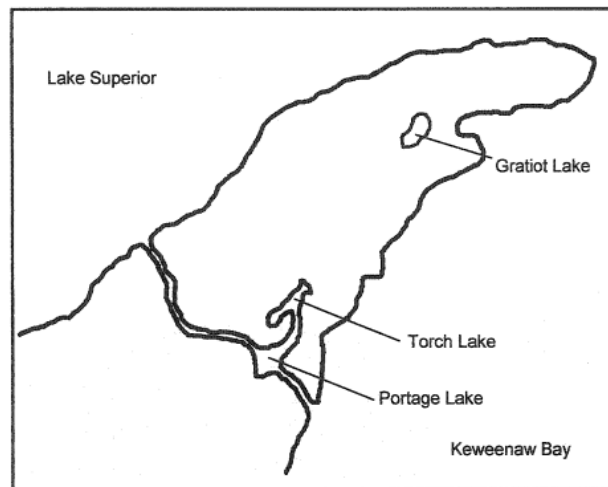


Figure 7.4 The location of Gratiot Lake, Torch Lake and Portage Lake (Fett, 2003)

7.5 The redox state

The redox condition in Torch lake sediment can be presented by the concentration profile of redox sensitive elements such as Fe and Mn as shown in Figure 7.5. This figure shows that the oxidizing condition had occur at surface sediment due to peak concentration of Fe and Mn. In deeper sediment, their concentration decrease and remain constant where indicate reducing condition. However, the copper profile differed from Fe and Mn, it was relatively uneffect by changing in redox condition where concentration of copper should be higher in reducing condition at deep sediment (Joel D Fett, 2003).

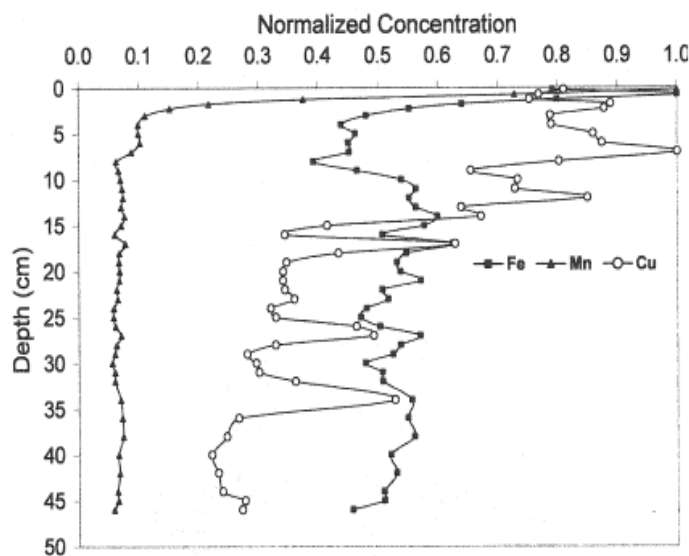


Figure 7.5 Normalized concentration of Fe, Mn and Cu in Torch Lake sediment (Fett, 2003)

7.6 The evidence of microbial copper sequestration

From the long history of dumping high concentration copper waste, Torch lake sediment is extremely environment for development and evolution of microbial communities. However, the study of structure of community can identify at least 20 phlotypes in there. These isolated

strains are classified in only two genera, *Ralstonia* and *Arthrobacter* bacteria, that can aerobically grow in high level of Cu (>800 ppm) and resistance to other metals, e.g. Zn, Cd and Ni as well (Konstantinidis et al., 2003). The *Ralsotia* species can turn the colonies to green hue when plating with CuSO₄ which indicated that the cells can sequester copper. This sequestration can be seen by scanning electron microscopy (SEM) images as shown in Figure 7.6. Cells grown in presence of copper will have extracellular material appeared on outer envelope whereas the smooth surface had been observed for cells grown in absence of copper (Konstantinidis et al., 2003). These blebs were expected to contain copper excreted from the cells. These evidences indicated that microbial sequestration could be responsible of high copper concentration in Torch lake surface sediment.

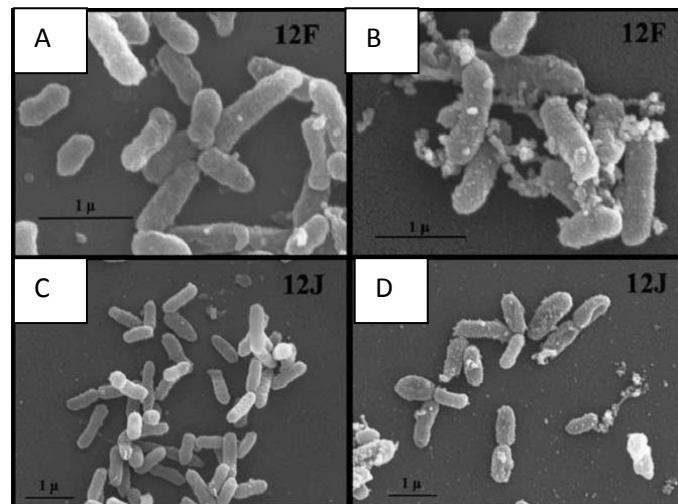


Figure 7.6 Scanning electron microscopy of *Ralstonia* isolated from Torch lake grown on copper free agar (A) and (C); grown on copper-supplemented agar (B) and (D) (modified from Konstantinidis et al., 2003)

From thin section of transmission electron microscopy (TEM) images (Figure 7.7), intracellular vesicle was observed in non copper contained media cells (Figure 7.7 C) whereas the greater thickness of outer membrane was observed in copper contained media cells (Figure 7.7 D). Figure 7.7 F shows the accumulation of copper at outer envelope. However, the specific location of bound copper was not clear between in outer membrane, periplasm or inner membrane (F. Yang et al., 2010).

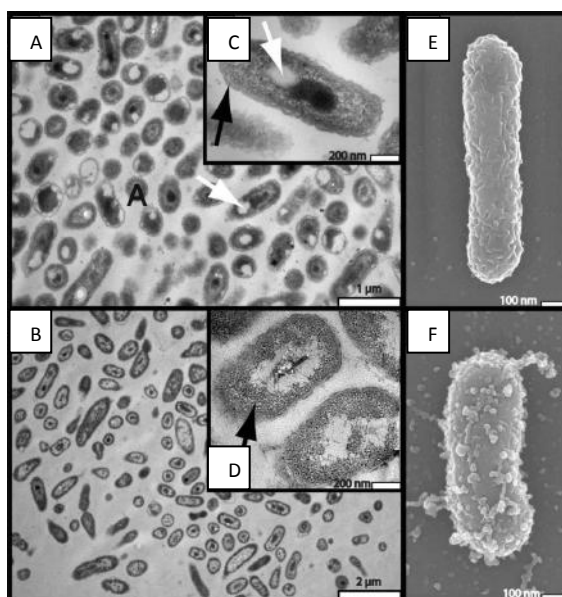


Figure 7.7 TEM and SEM of *R. pickettii* strain 12 J grown in absence copper (TEM: A, C ; SEM: E) and presence copper (TEM: B, D ; SEM: F) (modified from Yang et al., 2010)

The binding isotherm studies between viable and heat-killed cells of *Ralstonia* showed that both cells can bind to copper but the viable cells can bind 5-6 times more than heat-killed cells which indicated the copper sequestration was more effective by viable cells (F. Yang et al., 2010). Linear isotherm was described for binding of heat-kill cells whereas the sorption isotherm of viable cells cannot be described by linear, Freundlich or Langmuir model. The study of X-ray absorption spectroscopy showed the valance state of bound copper was Cu(II) and associated

with oxygen, nitrogen and carbon ligands. This indicated that the bound copper was not a precipitated (hydr)oxide minerals but associated with organic material instead (F. Yang et al., 2010). The genome sequencing analysis data showed the cell chromosome were enriched with metal resistance and transporter genes e.g. copper binding protein, mercury resistance operon, iron permease, cop ABCD operon (copper resistance), Czc(cadmium, zinc, cobalt) operon, metal translocating P-type ATPases and heavy metal signal/sensor proteins. This founding of the efflux systems showed cells had effort to transport copper out of their body and those genes revealed the rapid adaption to environment by gene duplication and horizontal transfer. This indicated *Ralstonia* has highly adaptive capacity to modify their genome to correspond the high concentration of copper and may be the dominant role of their evolution (F. Yang et al., 2010). The capability of *Ralstonia* copper sequestration may response for the persisting of high copper concentration in Torch Lake surface sediment.

7.7 Torch Lake Sediment composition and mineralogy

The analysis of copper in stamp sand deposited along the lakeshores and wetland in Torch Lake area represented the mine tailing in bottom sediment and in post-mining surface sediment showed the different type of minerals. The X-ray diffraction analysis of mining waste showed that Cuprite (Cu_2O), Tenorite (CuO), Malachite($\text{Cu}_2\text{CO}_3(\text{OH})_2$), Chalcopyrite(CuFeS_2) presented as copper minerals and Calcite (CaCO_3), Quartz(SiO_4), Hematite (Fe_2O_3), Orthoclase(KAlSi_3O_8) and Sanidine ($(\text{K,Na})(\text{Si,Al})_4\text{O}_8$) presented as the other major minerals. The sequential extraction techniques (SET) showed the carbonates and oxides were main fraction of copper (45-60%) in mining waste whereas the copper carbonates and copper-organic matter were main fractions (61%) in post mining sediment. The changing forms of copper minerals was expected from weathering processes. Some studies proposed that the copper associated with

iron/manganese oxides in mine tailing was reduced and released to solution and it was bound to organic matter on the post mining surface sediment (Jeong, 2003; Jeong et al., 1999).

7.8 Hypothesis and Approach

From the evidence of raising and persisting of copper in top sediment, I hypothesize that the copper solid phase in top sediment contributed from the dissolution of copper in mining tailing by microbial mediation or TEAP (Terminal Electron Acceptor process) to porewater which diffused upward and was sequestered by organic matter and bacteria on post surface sediment as shown in Figure 7.8.

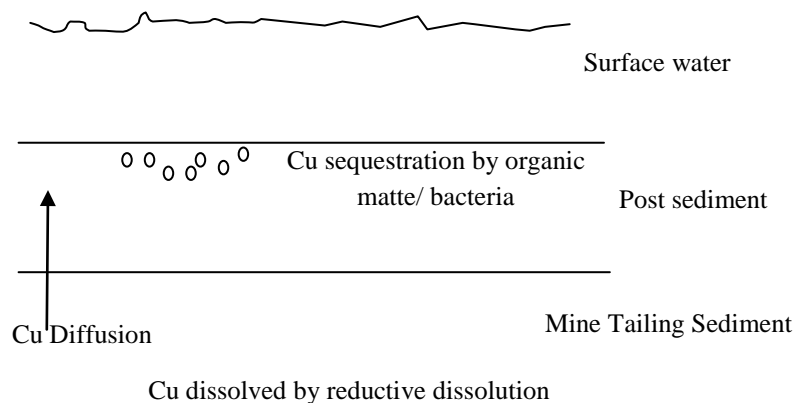


Figure 7.8 Model of copper upward diffusion from mine tailing sediment and sequestration by organic matter and bacteria at the surface sediment.

To understand the mobility of copper in Torch lake sediment and decide whether natural attenuation can remediate, the biogeochemical modeling was selected as tool to quantify the process that control the fate and transport of copper in the Torch Lake sediment. Because metal behavior in sediment is a result from combining between physical, chemical and biological processes such as adsorption, dissolution/precipitation of minerals, redox reaction, microbial

mediated reaction and advection/diffusion, this study combined these processes into the geochemical modeling through mathematical equation. However, the accuracy of the models are highly depend on estimating model parameter obtained from experimental data or literature sources (Steefel & Van Cappellen, 1998).

Phreeqc (Parkhurst & Appelo, 2013) is one of widely used geochemical modeling programs that contains equilibrium thermodynamic database of several minerals. It has capabilities to calculate the solubility and speciation of substances. It also has the feature of kinetic control reaction, surface complexation and ion exchange. In addition, Phreeqc also can handle transport simulation by advection or diffusion in porous media. So, in this study, Phreeqc was used to perform a variety of calculation to conduct the copper reactive transport process in Torch Lake sediment. The results from the models were used to describe the existing copper profile in sediment to understanding the cause of persistent and also the implication for the future remediation.

REFERENCES

REFERENCES

- Adams, T. G., Atchison, G. J., & Vetter, R. J. (1980). THE IMPACT OF AN INDUSTRIALLY CONTAMINATED LAKE ON HEAVY-METAL LEVELS IN ITS EFFLUENT STREAM. *Hydrobiologia*, 69(1-2), 187-193. doi: 10.1007/bf00016549
- Cusack, C. C., & Mihelcic, J. R. (1999). Sediment toxicity from copper in the Torch Lake (MI) Great Lakes Area of Concern. *Journal of Great Lakes Research*, 25(4), 735-743.
- Fett, J. D. (2003). *Assessing Recovery of Anthropogenically Disturbed Lakes Using Reference Systems and Multi-elemental Techniques*. (M.S.), Michigan State University.
- Jeong, J. (2003). Solid-phase speciation of copper in mine wastes. *Bulletin of the Korean Chemical Society*, 24(2), 209-218.
- Jeong, J., Urban, N. R., & Green, S. (1999). Release of copper from mine tailings on the Keweenaw Peninsula. *Journal of Great Lakes Research*, 25(4), 721-734.
- Konstantinidis, K. T., Isaacs, N., Fett, J., Simpson, S., Long, D. T., & Marsh, T. L. (2003). Microbial diversity and resistance to copper in metal-contaminated lake sediment. *Microbial Ecology*, 45(2), 191-202. doi: 10.1007/s00248-002-1035-y
- Lopez, J. M., & Lee, G. F. (1977). ENVIRONMENTAL CHEMISTRY OF COPPER IN TORCH LAKE, MICHIGAN. *Water Air and Soil Pollution*, 8(4), 373-385.
- McDonald, & Urban. Modeling Copper Transport in the sediments of Torch Lake, Houghton County, MI. from [http://www.mtcws.mtu.edu/pdf/CWSPoster_1stPlace_McDonald_Cory.pdf](http://www.mtcws.mtu.edu/pdf/CWSPPoster_1stPlace_McDonald_Cory.pdf)
- McDonald, C. P., Urban, N. R., Barkach, J. H., & McCauley, D. (2010). Copper profiles in the sediments of a mining-impacted lake. *Journal of Soils and Sediments*, 10(3), 343-348. doi: 10.1007/s11368-009-0171-0
- MDEQ. (2007). The Michigan Department of Environmental Quality Biennial Remedial Action Plan Update For Torch Lake Area of Concern. from http://www.epa.gov/glnpo/aoc/trchlke/2007_TorchLkUpdate.pdf
- Moore, J. W., & Sutherland, D. J. (1981). DISTRIBUTION OF HEAVY-METALS AND RADIONUCLIDES IN SEDIMENTS, WATER, AND FISH IN AN AREA OF GREAT BEAR LAKE CONTAMINATED WITH MINE WASTES. *Archives of Environmental Contamination and Toxicology*, 10(3), 329-338.
- Parkhurst, D. L., & Appelo, C. A. J. (2013). *Description of Input and Examples for PHREEQC Version 3—A Computer Program for Speciation, Batch-Reaction, One-Dimensional*

Transport, and Inverse Geochemical Calculations. U.S. Geological Survey, Denver, Colorado.

Steeffel, C. I., & Van Cappellen, P. (1998). Reactive transport modeling of natural systems - Preface. *Journal of Hydrology*, 209(1-4), 1-7.

USGS. (1997). Copper Hazard to Fish, Wildlife and Invertebrates: A Synoptic review. from <http://www.dtic.mil/cgi-bin/GetTRDoc?AD=ADA347472>

Yang, F., Pecina, D. A., Kelly, S. D., Kim, S. H., Kemner, K. M., Long, D. T., & Marsh, T. L. (2010). Biosequestration via cooperative binding of copper by *Ralstonia pickettii*. *Environmental Technology*, 31(8-9), 1045-1060. doi: 10.1080/09593330.2010.487290

Chapter 8

Literature reviews

8.1 Copper speciation, control mechanism and transport in natural water

Copper in aquatic environment can present in three phases: the aqueous phase (free ion and soluble complex substances), solid phase (mineral, adsorbed on particulate/colloid) and biological phase (adsorbed to microorganism). However, most of copper present in natural water are in the solid form. Dissolved coppers can present in both free ion state or form the complexes with anions e.g. sulfide, chloride and bicarbonate, phosphate and cyanide which highly reduced copper toxicity to aquatic organism (Flemming & Trevors, 1989). Some anions such as silicate, sulfate and nitrate are considered as non-complex species. The valence state can be I, II, and III but Cu(II) is most common of soluble species in normal oxidation state. Cu(I) is most presented in insoluble phase and Cu(III) are unstable in aqueous media (Nriagu, 1979).

There are three main mechanisms that control copper speciation and forms in natural water: complexation, precipitation and adsorption which also control mobility and bioavailability in environment.

8.1.1 Complexation

The relative stabilities of Cu(I) and Cu(II) are depended on the complex formation constant and type of ligand presence in water. The Cu(I) is most stable with forming the complexes with some ligands and become as insoluble compounds such as CuI, CuCl, CuBr, Cu₂O Cu₂S . Copper (II) is strong complexing agent. Most of Cu(II) salts are soluble and these

Cu(II) are readily to form complex with other ligands presented in water. The major complexes are hydroxyl species (CuOH^+ , Cu(OH)_2^0 , $\text{Cu}_2(\text{OH})_2^{2+}$) and carbonate species (CuCO_3^0 , $\text{Cu}(\text{CO}_3)_2^{2-}$) which depend on pH and hardness of solution. The increasing water hardness will highly reduce free Cu(II) (Stiff, 1971). The other important complex species of Cu(II) are sulfide (HS^-), phosphate (PO_4^{3-}), chloride (Cl^-) and ammonia (NH_3). However, the halide and cyanide are more stable with Cu(I) more than Cu(II).

In natural water, Cu(II) can form strong complexes with many organic ligands, typically composed of oxygen, nitrogen and sulfur donor atom. The stability constant of organic complexes are higher than inorganic complexes in many order of magnitude. The common organic copper complexes found in natural water included cyanide, amino acids, polypeptides and humic substances. The high degree of organic complexation were reported to cover 75-99% of dissolved copper in river water (Stiff, 1971). Some of stability constants of inorganic and organic Cu complexes of Cu(I) and Cu(II) show in Table 8.1. These stability constants are used to calculate copper speciation in natural water.

The examples of copper-organic complex were shown in Figure 8.1. The complexation of carbonate and hydroxide are the major forms of copper speciation in fresh water. The monocarbonate complex (CuCO_3^0) is major form at neutral pH indicating the strong binding between Cu(II) and carbonate ion. When pH increase, the hydroxide complex (Cu(OH)_2^0) will be dominated and prevented copper from precipitation. However, when presence of organic ligand such as nitrilotriacetic acid (NTA), it can form extremely stable complex with copper and dominant over carbonate and hydroxide complex at low and neutral pH. The complexation is important process that regulate copper concentration in water which affect to precipitation and/or adsorption process.

Table 8.1 Stability constant of complex formation of copper (Nriagu, 1979; Stiff, 1971)

Complexes	Log of stability constants
$\text{Cu}^{2+} + \text{OH}^- = \text{CuOH}^+$	6.1
$2\text{Cu}^{2+} + 2\text{OH}^- = \text{Cu}_2(\text{OH})_2^{2+}$	17.7
$\text{Cu}^{2+} + \text{CO}_3^{2-} = \text{CuCO}_3^0$	6.73
$\text{Cu}^{2+} + \text{Cl}^- = \text{CuCl}^+$	0.5
$\text{Cu}^{2+} + \text{F}^- = \text{CuF}^+$	1.23
$\text{Cu}^{2+} + \text{SO}_4^{2-} = \text{CuSO}_4^0$	2.3
$\text{Cu}^{2+} + 3\text{HS}^- = \text{Cu}(\text{HS})_3^-$	26.5
$\text{Cu}^{2+} + \text{H}^+ + \text{PO}_4^{3-} = \text{Cu}(\text{HPO}_4)^0$	16.6
$\text{Cu}^{2+} + \text{NH}_3 = \text{Cu}(\text{NH}_3)^{2+}$	5.8
$\text{Cu}^{2+} + \text{Glycine} = \text{Cu}(\text{Glycine})$	8.1
$\text{Cu}^{2+} + \text{Nitrilotriacetic acid (NTA)} = \text{CuNTA}$	12.7
$\text{Cu}^{2+} + 4\text{Citric acid} = \text{Cu}(\text{Citric acid})_4$	13.2
$\text{Cu}^{2+} + \text{Fluvic acid} = \text{Cu}(\text{Fluvic acid})$	8.69(pH 5)
$\text{Cu}^+ + 2\text{Cl}^- = \text{CuCl}_2^-$	5.5
$\text{Cu}^+ + 3\text{Cl}^- = \text{CuCl}_3^{2-}$	5.7
$\text{Cu}^+ + \text{NH}_3 = \text{Cu}(\text{NH}_3)^+$	5.5
$\text{Cu}^+ + 2\text{NH}_3 = \text{Cu}(\text{NH}_3)_2^+$	10.3

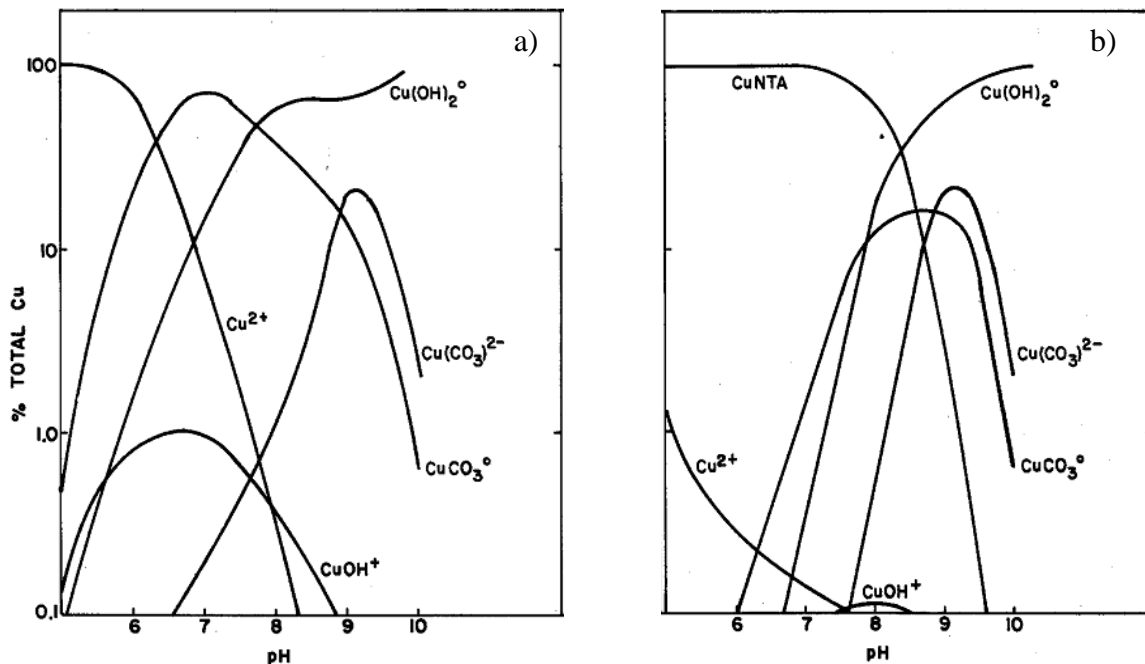


Figure 8.1 Calculated copper speciation in fresh water when absence (a) and presence (b) of organic chelation NTA (modified from Elder & Horne, 1978)

8.1.2 Precipitation/dissolution

Next mechanism that control copper in natural water is precipitation which greatly reduced the soluble copper. Copper can react with inorganic ligands as a complexes which have very low solubility and precipitate as solid forms. In surficial natural water pH (6.5 -8), the major form of precipitates included Cupric hydroxide (Cu(OH)_2), Tenorite (CuO), Malachite ($\text{Cu}_2(\text{OH})_2(\text{CO}_3)$) and Azurite ($\text{Cu}_3(\text{OH})_2(\text{CO}_3)_2$) (Sylva, 1976). Some solubility constants of copper minerals are shown in Table 8.2 Figure 8.2 also shows the stability of copper solid forms as a function of pH and pCO_2 . At the common level of pCO_2 in soil and sediment ($1 < \text{pCO}_2 < 3.5$), Malachite ($\text{Cu}_2(\text{OH})_2(\text{CO}_3)$) is the stable phase (Nriagu, 1979).

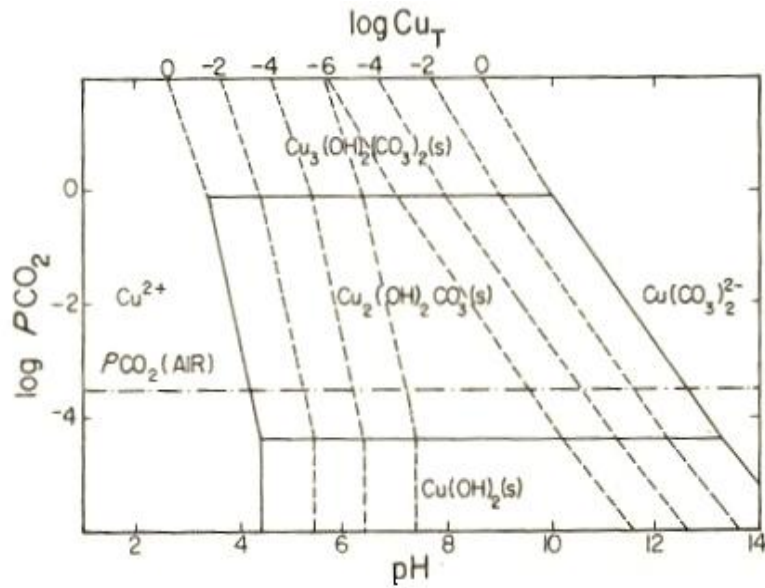


Figure 8.2 The stability diagram for ternary system Cu(II)-H₂O-CO₂(g) (Nriagu, 1979)

Table 8.2 Solubility of copper minerals (Elder & Horne, 1978; Nriagu, 1979; Parkhurst & Appelo, 2013)

Mineral	Log of solubility constant
Cu ₂ O (Cuprite)	-23.6
CuO(Tenorite)	-20.4
CuCO ₃	-9.6
Cu(OH) ₂	-18.6
Cu ₂ (OH) ₂ CO ₃ (Malachite)	-34.0
Cu ₃ (OH) ₂ (CO ₃) ₂ (Azurite)	-45.8
CuS (Covellite)	-35.89
Cu ₂ S (Chalcocite)	-48.1
CuFeS ₂ (Chalcopyrite)	-35.27

In lake, the dissolved copper concentration is high in upper part due to controlled by precipitation of carbonate minerals. However, concentration will decrease with the depth until lowest at bottom because of precipitation of insoluble copper sulfide under anoxic condition. In high alkalinity lake, most Ca and Mg carbonate minerals are formed at the sediment. However, with presence of Cu, Cu can compete Ca and Mg and form to carbonate minerals instead (Sanchez & Lee, 1973). The sulfide comes from generation of H₂S of decomposition of organic matter by sulfate reducing bacteria at bottom sediment. Bounding sulfide is mainly immobilization process for copper in lake sediment (Jackson, 1978; Sanchez & Lee, 1978). Even sulfide precipitation has high tendency to control copper in water but in the presence of organic matter, the high stability constant and kinetic rate of complexation of organic ligand can compete sulfide precipitation and remobilized the copper into the water (Elder & Horne, 1978; Jackson, 1978).

8.1.3 Adsorption

Copper, similar to other heavy metal, has high potential to adsorb on particulate matter in the natural water which include inorganic minerals as well as organic matter both living and non-living microorganism and falling into sediment (Chen et al., 2005; Ramamoorthy & Rust, 1978; Savvaidis, Hughes, & Poole, 2003). Adsorption is important process that controlling the solubility and mobility of copper in environment because it can remove or release the copper in the water depending on competition from other cations for surface sites or other ligands presented in solution. The sediment is one compartment that has high capacity to adsorb the copper. There are 4 main particulates in natural water which have high sorption capacity to copper including iron/manganese oxides, clays, organic matter and microorganisms.

8.1.3.1 Sorption to metal hydrous oxides

Metal hydrous oxides e.g. $\text{Fe}_2\text{O}_3 \cdot n\text{H}_2\text{O}$, $\text{MnO}_2 \cdot n\text{H}_2\text{O}$, $\text{Al}_2\text{O}_3 \cdot n\text{H}_2\text{O}$ and SiO_2 have high affinity to copper because they have hydroxyl reactive charged sites and high surface area. The binding mechanism can be covalent bond or electrostatic force. The sorption on hydrous metal oxides will depend on pH where the sorption increase when pH increase. This is a result from the increasing of negatively charged on surface sites or cation exchange capacity. However, at highly pH, copper will precipitate as CuO and coat on the colloid particles (Babich & Stotzky, 1980; Subramaniam, Yiacomou, & Tsouris, 2001). These hydrous metal oxides have selective affinity, for example, Mn oxides show highest specificity to Cu whereas Fe oxides have lowest specificity to Cu (Flemming & Trevors, 1989). Not only adsorption, copper also can be removed from water by coprecipitation with Fe/Mn hydrous oxides.

8.1.3.2 Sorption to clays

Clays also have high sorption capacity to copper. Clays are hydrous alumino-silicate minerals where their surfaces contain negative charges and charge-compensate cations e.g. H^+ , K^+ , Na^+ , Ca^{2+} , Mg^{2+} which can exchange to other cations in environment expressed as cation exchange capacity or CEC (Babich & Stotzky, 1980). Copper can be adsorbed on clay by ion exchange with the cations on surface or chemical binding. The degree of adsorption follow the order of increasing CEC of clays e.g. Kaolinite < Illite < Montmorillonite (Riemer & Toth, 1970). The adsorption on clays is varied with solution pH. The sorption increases when pH increase from 3 to 7 as shown in Figure 8.3 because of adsorption of OH^- groups on the surface which acted as a bridge to metal ions. However, at higher pH value, the sorption will be decrease where metals are precipitated as hydroxide minerals (Babich & Stotzky, 1980; Payne &

Pickering, 1975). Although clays are significantly sorbent to remove copper, competitive from other cations such as Ca^{2+} and Mg^{2+} will lower copper binding to clay (Gupta & Harrison, 1981).

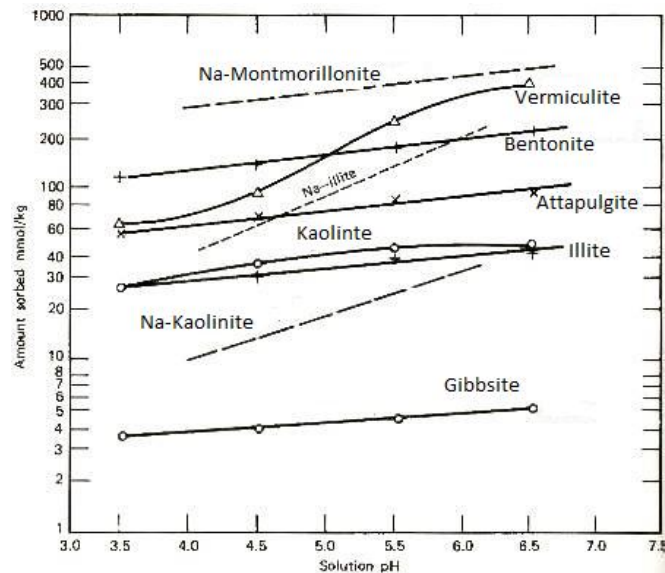


Figure 8.3 Sorption of copper by clay minerals as a function of pH (modified from Nriagu, 1979)

8.1.3.3 Sorption to organic matter

Copper found to highly partitioning to organic material. Cu(II) is highest sorption to organic matter among naturally occurring bivalent cations. It was believed that organic matter in soil or sediment regulates the mobility of copper in environment (Elliott, Liberati, & Huang, 1986; Perez-Novo et al., 2008; Ratasuk, Parkpian, Jugsujinda, & DeLaune, 2003). Organic matters in natural water are the stable dead-cell products of microorganism, plants or animals and compose of humic acid, fluvic acid and humin. Heavy metals are adsorbed to organic matter by three main mechanisms: by coordination bonding or chelation, by covalent bonding to some functional groups e.g. carboxyl (COOH), carbonyl group (CO), sulfhydryl group (SH) in humic or fluvic acids, and by cation exchange to humic acids and soluble fluvic acids which are major

binding sites of copper in natural water. However, the adsorption of copper by organic matter is lower under basic condition where organic soluble complexes are formed and minerals precipitation occur (Elliott et al., 1986).

8.1.3.4 Sorption to microorganism

Copper also can be adsorbed or sequestered from natural water by live or dead microorganisms. It will bind at the cell wall by extracellular polymers and then transport into the cells which depend on their metabolism. This sorption process is quite rapid and concentration and pH dependent (Cotter & Trevors, 1988; Trevors & Cotter, 1990). The metal binding were reported to occur at peptidoglycan and lipopolysaccharide of outer cells (Ferris & Beveridge, 1986; Hoyle & Beveridge, 1984). Some studies showed no difference of copper uptake between living and killed cell (Cotter & Trevors, 1988; Savvaidis et al., 2003). However, for high copper resistant bacteria, the binding capacity of living cells showed much higher than non-living cells whereas desorption efficiency from living cells were also lower than non-living cells. This suggested copper binding is enhanced by intracellular accumulation (Chen et al., 2005). Even the uptake of copper by microorganisms is rapid process, the portion of this pathway may be very small when compare to total copper dissolved in aquatic system because microbes require copper in very low orders of magnitude (Elder & Horne, 1978).

8.2 Factors control copper mobility in sediment

As discuss above, mobility of copper in environment depends on three main processes e.g. complexation, precipitation and adsorption. However, these processes are influenced by environmental factors such as pH and redox state which are described below.

8.2.1 pH

pH is most important factor that controls mobility of copper because it determine the complex forms, precipitated minerals, and amount of adsorption sites. The stability of inorganic and organic copper complexes are depend on pH where the stability constant increase when pH increase (Sunda & Hanson, 1979). At pH below than 6, copper will quite mobile but the mobility will be less when pH increase because of increasing of adsorption by clays and organic matters (Elliott et al., 1986)

8.2.2 Redox state

Redox condition has influence to mobility and dissolved concentration of copper by changing their forms. Oxidation – reduction potential is measured and reported as pE which indicates the availability of electron in that condition. The positive pE means oxidative environment and negative pE means reductive environment (Babich & Stotzky, 1980). Changing in pE and pH can change valence state of copper and their stable forms as shown in Figure 8.4. This figure shows stability diagram of solid copper in aqueous solution which contain dissolved sulfur 0.1M and CO₂ at atmospheric condition ($p\text{CO}_2 = 10^{-3.5}$). At pH lower than 6, the copper is more soluble in form Cu²⁺ in oxidizing environment. However, under reductive (anaerobic) condition where microbial change sulfate (SO₄²⁻) to sulfide (HS⁻), the dissolved copper will be immobilized by sulfide precipitation as Cuprous sulfide(Cu₂S) and Cupric sulfide (CuS) and stable in environment . When pE increase until oxidizing condition , elemental copper will be the stable phase (Hermann & Neumannmahlkau, 1985; Nriagu, 1979). At this partial pressure of CO₂, Malachite (Cu₂(OH)₂CO₃) is more stable form than Tenorite (CuO). However, this figure had been created from specific components in the system which may be limited in applying to the field.

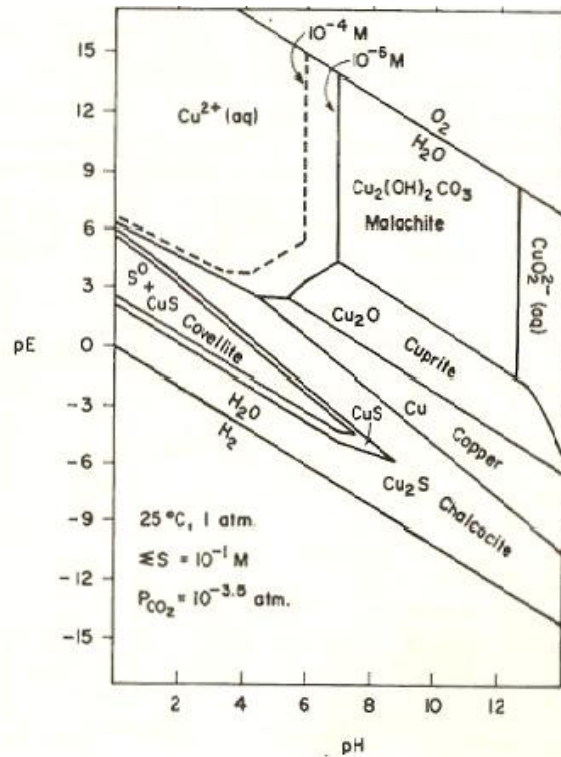


Figure 8.4 The stability relation between copper compound in system of $\text{Cu} + \text{H}_2\text{O} + \text{O}_2 + \text{S} + \text{CO}_2$ ($P_{\text{CO}_2} = 10^{-3.5}$ atm), total dissolved sulfur species 10^{-1} M at 25°C and 1 atm (Nriagu, 1979)

Figure 8.5 shows the speciation of copper at reducing condition, at low pE the major copper species is Cu(II) bisulfide ($\text{Cu}(\text{HS})_3^-$) but when pE increase, the solubility of copper will increase by formation of the complex of cuprous ion (Cu(I)) with chloride and ammine.

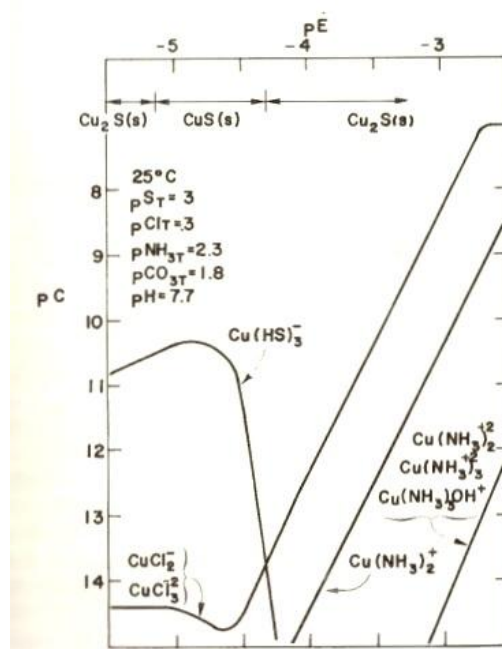


Figure 8.5 The equilibrium aqueous concentration of copper species as a function of pE (Nriagu, 1979)

8.3 Microbial mediated reaction

Microorganisms are well known to alter the chemistry in sediment by controlling the redox potential. They oxidize the organic compounds in the sediment with the favorable sequence of terminal electron acceptor or “TEAP”. These electron acceptors include oxygen, nitrate, manganese oxide, iron oxide, sulfate and carbon dioxide. The sequence will vary vertically with depth as shown in Figure 8.6.

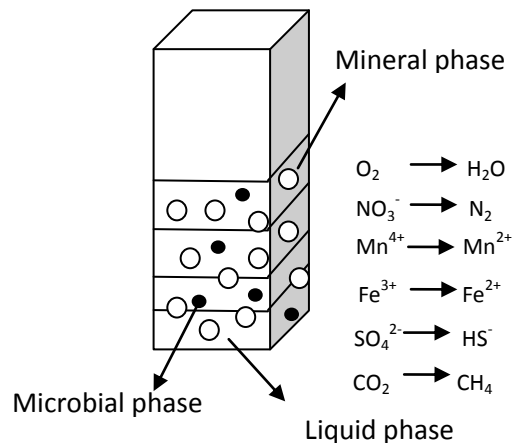


Figure 8.6 Biodegradation with sequential terminal electron acceptors

The microorganism will utilize the organic compounds in aerobic condition on the top surface sediment where oxygen available. The anaerobic condition will apply in deeper sediment when O_2 was completely consumed and NO_3^- , Mn^{4+} , Fe^{3+} , SO_4^{2-} will be used as alternative electron acceptor, respectively. After all electron acceptor deplete, the methanogenesis will be applied by using CO_2 as electron acceptor and produce the methane gas. The reaction of utilization organic compounds by sequential of terminal electron acceptor are shown in Table 8.3. Acetate is used as example of dissolved organic compound which assume to be unlimited (Sengor, Spycher, Ginn, Sani, & Peyton, 2007).

After organic matter had been degraded and the reduced compounds produced, these reduced compounds e.g. NH_4^+ , Mn^{2+} , Fe^{2+} , H_2S or HS^- and CH_4 will diffuse upward to the oxic zone and will be oxidized by oxygen as secondary oxidation reactions which show in Table 8.4. The oxidation of Mn^{2+} is driven by bacterial process whereas oxidation of Fe^{2+} and HS^- occur by abiotic and propotional to concentration (S. S. Park & Jaffe, 1996).

Table 8.3 The biodegradation reaction of sequential terminal electron acceptor

Description	Reaction
1. Aerobic respiration	$\text{CH}_3\text{COO}^- + 2\text{O}_2 \longrightarrow 2\text{CO}_3^{2-} + 3\text{H}^+$
2. Denitrification	$\text{CH}_3\text{COO}^- + 1.6\text{NO}_3^- \longrightarrow 2\text{CO}_3^{2-} + 0.8\text{N}_2 + 1.4\text{H}^+ + 0.8\text{H}_2\text{O}$
3. Mn oxide reduction	$\text{CH}_3\text{COO}^- + 4\text{MnO}_2 + 5\text{H}^+ \longrightarrow 2\text{CO}_3^{2-} + 4\text{Mn}^{2+} + 4\text{H}_2\text{O}$
4. Iron oxide reduction	$\text{CH}_3\text{COO}^- + 8\text{FeOOH} + 13\text{H}^+ \longrightarrow 8\text{Fe}^{2+} + 2\text{CO}_3^{2-} + 12\text{H}_2\text{O}$
5. Sulfate reduction	$\text{CH}_3\text{COO}^- + \text{SO}_4^{2-} \longrightarrow 2\text{CO}_3^{2-} + \text{HS}^- + 2\text{H}^+$
6. Methanogenesis	$\text{CH}_3\text{COO}^- + \text{H}^+ \longrightarrow \text{CH}_4 + \text{CO}_2$

Table 8.4 Secondary redox reactions

Description	Reaction
1. Oxidation of ammonia	$\text{NH}_4^+ + 2\text{O}_2 \longrightarrow \text{NO}_3^- + \text{H}_2\text{O} + 2\text{H}^+$
2. Oxidation of Mn^{2+}	$2\text{Mn}^{2+} + \text{O}_2 + 2\text{H}_2\text{O} \longrightarrow 2\text{MnO}_2 + 4\text{H}^+$
3. Oxidation of Fe^{2+}	$4\text{Fe}^{2+} + \text{O}_2 + 6\text{H}_2\text{O} \longrightarrow 4\text{FeOOH} + 8\text{H}^+$
4. Oxidation of HS^-	$\text{HS}^- + 2\text{O}_2 \longrightarrow \text{SO}_4^{2-} + \text{H}^+$
5. Oxidation of methane	$\text{CH}_4 + 2\text{O}_2 \longrightarrow \text{CO}_2 + 2\text{H}_2\text{O}$

8.4 Releasing of heavy metal by reductive dissolution of iron oxides

One of important results from microbial mediation reaction is reductive dissolution of iron (III) oxyhydroxide. Reducing condition from TEAP with depth causes iron oxyhydroxide to be dissolved after O_2 , NO_3^- and MnO_2 has been consumed. Even there is low dissolved organic carbon, this iron (III) reduction still occur due to thermodynamically favored. Due to Iron oxyhydroxide are mostly adsorbed or co-precipitated with copper, so the reduction of these minerals will release copper to the porewater as shown in Eq. 8.1 (Charlatchka & Cambier, 2000;

Ribet, Ptacek, Blowes, & Jambor, 1995; Sengor et al., 2007). This process also drives the pH and Fe^{2+} to increase.



The produced ferrous ion (Fe^{2+}) can be sink by competing to precipitate as siderite (FeCO_3) as shown in Eq. 8.2 or iron(II)sulfide in Eq. 8.3 (Sengor 2007). Some of ferrous ion (Fe^{2+}) can diffuse upward to aerobic zone where they will be oxidized and precipitated as goethite (FeOOH).



The reductive dissolution of iron oxides also was reported as mechanism that can release other heavy metals such as Zn, Pb and As from the mine tailing sediment in reducing condition which behave as a source to supply heavy metals to overlaying water (Gallon, Tessier, Gobeil, & La Torre, 2004; McGeehan & Naylor, 1994).

REFERENCES

REFERENCES

- Babich, H., & Stotzky, G. (1980). ENVIRONMENTAL-FACTORS THAT INFLUENCE THE TOXICITY OF HEAVY-METAL AND GASEOUS POLLUTANTS TO MICROORGANISMS. *Crc Critical Reviews in Microbiology*, 8(2). doi: 10.3109/10408418009081123
- Borrok, D. M., & Fein, J. B. (2005). The impact of ionic strength on the adsorption of protons, Pb, Cd, and Sr onto the surfaces of Gram negative bacteria: testing non-electro static, diffuse, and triple-layer models. *Journal of Colloid and Interface Science*, 286(1), 110-126. doi: 10.1016/j.jcis.2005.01.015
- Charlatchka, R., & Cambier, P. (2000). Influence of reducing conditions on solubility of trace metals in contaminated soils. *Water Air and Soil Pollution*, 118(1-2), 143-167. doi: 10.1023/a:1005195920876
- Chen, X. C., Wang, Y. P., Lin, Q., Shi, J. Y., Wu, W. X., & Chen, Y. X. (2005). Biosorption of copper(II) and zinc(II) from aqueous solution by *Pseudomonas putida* CZ1. [Article]. *Colloids and Surfaces B-Biointerfaces*, 46(2), 101-107. doi: 10.1016/j.colsurfb.2005.10.003
- Cotter, C., & Trevors, J. T. (1988). COPPER ADSORPTION BY ESCHERICHIA-COLI. *Systematic and Applied Microbiology*, 10(3), 313-317.
- Elder, J. F., & Horne, A. J. (1978). COPPER CYCLES AND CUSO₄ ALGICIDAL CAPACITY IN 2 CALIFORNIA LAKES. *Environmental Management*, 2(1), 17-30. doi: 10.1007/bf01866443
- Elliott, H. A., Liberati, M. R., & Huang, C. P. (1986). COMPETITIVE ADSORPTION OF HEAVY-METALS BY SOILS. [Article]. *Journal of Environmental Quality*, 15(3), 214-219.
- Fein, J. B., Daughney, C. J., Yee, N., & Davis, T. A. (1997). A chemical equilibrium model for metal adsorption onto bacterial surfaces. *Geochimica Et Cosmochimica Acta*, 61(16), 3319-3328. doi: 10.1016/s0016-7037(97)00166-x
- Ferris, F. G., & Beveridge, T. J. (1986). SITE SPECIFICITY OF METALLIC ION BINDING IN ESCHERICHIA-COLI K-12 LIPOPOLYSACCHARIDE. [Article]. *Canadian Journal of Microbiology*, 32(1), 52-55.
- Flemming, C. A., & Trevors, J. T. (1989). COPPER TOXICITY AND CHEMISTRY IN THE ENVIRONMENT - A REVIEW. *Water Air and Soil Pollution*, 44(1-2), 143-158. doi: 10.1007/bf00228784

- Fowle, D. A., & Fein, J. B. (1999). Competitive adsorption of metal cations onto two gram positive bacteria: Testing the chemical equilibrium model. *Geochimica Et Cosmochimica Acta*, 63(19-20), 3059-3067. doi: 10.1016/s0016-7037(99)00233-1
- Gallon, C., Tessier, A., Gobeil, C., & La Torre, M. (2004). Modeling diagenesis of lead in sediments of a Canadian Shield lake. *Geochimica Et Cosmochimica Acta*, 68(17), 3531-3545. doi: 10.1016/j.gca.2004.02.013
- Gupta, G. C., & Harrison, F. L. (1981). EFFECT OF CATIONS ON COPPER ADSORPTION BY KAOLIN. [Article]. *Water Air and Soil Pollution*, 15(3), 323-327.
- Hermann, R., & Neumannmahlkau, P. (1985). THE MOBILITY OF ZINC, CADMIUM, COPPER, LEAD, IRON AND ARSENIC IN GROUND-WATER AS A FUNCTION OF REDOX POTENTIAL AND PH. [Article]. *Science of the Total Environment*, 43(1-2), 1-12. doi: 10.1016/0048-9697(85)90027-0
- Hoyle, B. D., & Beveridge, T. J. (1984). METAL-BINDING BY THE PEPTIDOGLYCAN SACCULUS OF ESCHERICHIA-COLI K-12. *Canadian Journal of Microbiology*, 30(2), 204-211.
- Jackson, T. A. (1978). BIOGEOCHEMISTRY OF HEAVY-METALS IN POLLUTED LAKES AND STREAMS AT FLIN FLON, CANADA, AND A PROPOSED METHOD FOR LIMITING HEAVY-METAL POLLUTION OF NATURAL-WATERS. *Environmental Geology*, 2(3), 173-189.
- Lofts, S., & Tipping, E. (2000). Solid-solution metal partitioning in the Humber rivers: application of WHAM and SCAMP. *Science of the Total Environment*, 251, 381-399. doi: 10.1016/s0048-9697(00)00418-6
- McGeehan, S. L., & Naylor, D. V. (1994). SORPTION AND REDOX TRANSFORMATION OF ARSENITE AND ARSENATE IN 2 FLOODED SOILS. *Soil Science Society of America Journal*, 58(2), 337-342.
- Nriagu, J. O. (1979). *Copper in the environment*. New York: John Wiley & Sons, Inc.
- Park, S. S., & Jaffe, P. R. (1996). Development of a sediment redox potential model for the assessment of postdepositional metal mobility. *Ecological Modelling*, 91(1-3), 169-181. doi: 10.1016/0304-3800(95)00188-3
- Parkhurst, D. L., & Appelo, C. A. J. (2013). *Description of Input and Examples for PHREEQC Version 3—A Computer Program for Speciation, Batch-Reaction, One-Dimensional Transport, and Inverse Geochemical Calculations*. U.S. Geological Survey, Denver, Colorado.

- Payne, K., & Pickering, W. F. (1975). INFLUENCE OF CLAY-SOLUTE INTERACTIONS ON AQUEOUS COPPER-ION LEVELS. *Water Air and Soil Pollution*, 5(1), 63-69. doi: 10.1007/bf00431580
- Perez-Novo, C., Pateiro-Moure, M., Osorio, E., Novoa-Munoz, J. C., Lopez-Periago, E., & Arias-Estevez, M. (2008). Influence of organic matter removal on competitive and noncompetitive adsorption of copper and zinc in acid soils. *Journal of Colloid and Interface Science*, 322(1). doi: 10.1016/j.jcis.2008.03.002
- Ramamoorthy, S., & Rust, B. R. (1978). HEAVY-METAL EXCHANGE PROCESSES IN SEDIMENT - WATER-SYSTEMS. *Environmental Geology*, 2(3).
- Ratasuk, P., Parkpian, P., Jugsujinda, A., & DeLaune, R. D. (2003). Factors governing adsorption and distribution of copper in Samut Prakarn coastal sediment, Thailand. [Article]. *Journal of Environmental Science and Health Part a-Toxic/Hazardous Substances & Environmental Engineering*, 38(9), 1793-1810. doi: 10.1081/ese-120022879
- Ribet, I., Ptacek, C. J., Blowes, D. W., & Jambor, J. L. (1995). THE POTENTIAL FOR METAL RELEASE BY REDUCTIVE DISSOLUTION OF WEATHERED MINE TAILINGS. *Journal of Contaminant Hydrology*, 17(3), 239-273. doi: 10.1016/0169-7722(94)00010-f
- Riemer, D. N., & Toth, S. J. (1970). ADSORPTION OF COPPER BY CLAY MINERALS, HUMIC ACID AND BOTTOM MUDS. [Article]. *Journal American Water Works Association*, 62(3), 195-&.
- Sanchez, I., & Lee, G. F. (1973). SORPTION OF COPPER ON LAKE MONONA SEDIMENTS - EFFECT OF NTA ON COPPER RELEASE FROM SEDIMENTS. *Water Research*, 7(4), 587-593. doi: 10.1016/0043-1354(73)90058-4
- Sanchez, I., & Lee, G. F. (1978). ENVIRONMENTAL CHEMISTRY OF COPPER IN LAKE MONONA, WISCONSIN. *Water Research*, 12(10), 899-903. doi: 10.1016/0043-1354(78)90043-x
- Savvaiddis, I., Hughes, M. N., & Poole, R. K. (2003). Copper biosorption by *Pseudomonas cepacia* and other strains. *World Journal of Microbiology & Biotechnology*, 19(2), 117-121. doi: 10.1023/a:1023284723636
- Sengor, S. S., Spycher, N. F., Ginn, T. R., Sani, R. K., & Peyton, B. (2007). Biogeochemical reactive-diffusive transport of heavy metals in Lake Coeur d'Alene sediments. *Applied Geochemistry*, 22(12), 2569-2594. doi: 10.1016/j.apgeochem.2007.06.011
- Stiff, M. J. (1971). CHEMICAL STATES OF COPPER IN POLLUTED FRESH WATER AND A SCHEME OF ANALYSIS TO DIFFERENTIATE THEM. *Water Research*, 5(8), 585-&. doi: 10.1016/0043-1354(71)90114-x

- Subramaniam, K., Yiacoumi, S., & Tsouris, C. (2001). Copper uptake by inorganic particles - equilibrium, kinetics, and particle interactions: experimental. *Colloids and Surfaces a-Physicochemical and Engineering Aspects*, 177(2-3), 133-146.
- Sunda, W. G., & Hanson, P. J. (1979). *Chemical Speciation of Copper in River Water*. Paper presented at the Chemical Modeling in Aqueous Systems: Speciation, Sorption, Solubility, and Kinetics.
- Sylva, R. N. (1976). ENVIRONMENTAL CHEMISTRY OF COPPER(II) IN AQUATIC SYSTEMS. *Water Research*, 10(9), 789-792. doi: 10.1016/0043-1354(76)90097-x
- Trevors, J. T., & Cotter, C. M. (1990). COPPER TOXICITY AND UPTAKE IN MICROORGANISMS. *Journal of Industrial Microbiology*, 6(2). doi: 10.1007/bf01576426

Chapter 9

Materials and methods

The Phreeqc biogeochemical modelings (Parkhurst and Appelo, 1999) which developed by US Geological Survey were employed in this study to simulate the reactive transport of copper in Torch Lake sediment, combining between geochemical and biological processes. The models were coupled by set of inorganic reactions which were complexation, precipitation/dissolution, adsorption, ion exchange, biological processes which were the oxidation of organic matter by bacteria controlled by sequential terminal electron acceptors or TEAP and diffusion transport processes. The models were divided into individual process which was more practical to examine the contribution from each process. The individual model included speciation and saturation indices of surface and porewater model, adsorption of copper to hydrous ferric oxides, clays, organic matters and bacteria surfaces model, the microbial mediation reaction or TEAP model, the reductive dissolution of iron oxyhydroxide model and the diffusion transport model. Finally, these models were combined together as full model which can show us the concentration profiles of dissolved coppers, copper solid phases and other chemicals species along the sediment. The approach and all parameters in each model were shown below.

9.1 Copper speciation and saturation indices modeling

Because the measured chemical composition of Torch Lake surface water and porewater in literatures did not provide the actual distribution of dissolve species, so the concentrations of various speciation species were calculated. The saturation indices (SI) were also calculated by

the model to determine the presence minerals that controlled dissolved concentration of metals in sediment.

9.1.1 Surface water and top sediment porewater modeling

The data of surface water and top sediment porewater of Torch Lake applied in the model were collected from literatures. Some of data was referred from the U.S. Geological Survey report of assessment ground water and surface water interaction of three lakes (North, Teal, and Taylor) on the Grand Portage Reservation in northeastern Minnesota (Jones, 2006). These lakes were used as reference lakes due to located in Lake Superior area, completed surface water and porewater data and no impact from mining wastes. All these values have been listed in Table 9.1. The thermodynamic constants for all calculations were based on *minteq* database in Phreeqc. Because of no mention type of organic compounds in these waters, the Nitritriacetic acid (NTA) were used as dissolved organic carbon in the model. The Phreeqc code of surface water and top sediment pore water modeling are shown in Appendix A.1 and A.2, respectively.

9.1.2 Mine tailing porewater modeling

Since mine tailing porewater composition was not reported in any studies, the simulation of composition of mine tailing pore water is necessary. We simulated by equilibrating fresh water with mining waste minerals which included Cuprite (Cu_2O), Chalcopyrite (CuFeS_2) and Chalcocite (Cu_2S). These minerals were added to water as a source of dissolved copper. The other minerals were Calcite (CaCO_3), Quartz (SiO_2), Hematite (Fe_2O_3), Orthoclase (KAlSi_3O_8) and Sanidine ($(\text{K,Na})(\text{Si,Al})_4\text{O}_8$). These minerals were reported as minerals found in stamp sand deposited along Torch Lake shoreline. The Phreeqc code of mine tailing porewater modeling is shown in Appendix A.3.

Table 9.1 Modeling input of surface water and top sediment pore water

Parameter	Surface water	Top sediment porewater	unit
pH	7.8 ^a , 8.1 ^b	6.6 ^b , 8.2 ^c	-
temperature	2.2-19.4 ^e	18 ^d	°c
Alkalinity	38 ^a , 11.2 ^b	78 ^d	mg/l as CaCO ₃
O ₂	6.3 ^d	0.3 ^d	mg/l
Cu	0.081 ^a , 0.003 ^b	2.5 ^b , 0.59-0.81 ^c	mg/l
Fe	0.062 ^a	1.58 ^d	mg/l
Zn	0.008 ^a	-	
Mn	0.020 ^a	0.049 ^d	mg/l
DOC	5.2 ^a	29 ^a , 39.7 ^c	mg/l
Na	0.96 ^d	1.15 ^d	mg/l
K	0.09 ^d	0.4 ^d	mg/L
Ca	13.6 ^d	23 ^d	mg/L
Mg	2.7 ^d	2.66 ^d	mg/L
Cl ⁻	0.12 ^d	0.35 ^d	mg/L
SO ₄ ²⁻	0.6 ^d	0.2 ^d	mg/L
NO ₃ ⁻	0.26 ^d	0.26 ^d	mg/L

a from Lopez & Lee 1977, b from Jeong et al., 1999, c from Cusack & Mihelcic, 1999, d from Jones, 2006, e from Jeong, 2002

9.2 Adsorption modeling

This study simulated the copper surface complexation to multi-surfaces e.g. iron oxides surfaces, organic matters, clays and bacteria by diffuse double layer model implemented in Phreeqc.

9.2.1 Adsorption to Hydrous Ferric Oxide (HFO) modeling

Hydrous Ferric Oxide (HFO) was considered to be major sorbing mineral in Torch lake sediment. The adsorption model of heavy metals e.g Cu, Pb, Zn on HFO were already implemented in Phreeqc by using surface keyword data block. In Phreeqc, two proton binding sites were considered in HFO, weak sites and strong sites. The numbers of “low affinity” or weak sites were typically much larger than “high affinity” or strong sites. To model, the acidity constant and surface complexation constants of HFO were needed. For the Cu^{2+} and Cu^+ , the adsorption reaction onto HFO and their complexation constants are shown in Table 9.2 (Parkhurst & Appelo, 2013; Sengor et al., 2007). The surface characteristics of HFO are shown Table 9.3 (DZomback and Morel, 1990).

Table 9.2 Acidity constant of HFO and Equilibrium constants (Log K) of copper surface complexation on HFO

Reaction	Log K (25°C)
Acidity constant	
$\text{Hfo_sOH} + \text{H}^+ = \text{Hfo_sOH}^{2+}$	7.29
$\text{Hfo_sOH} = \text{Hfo_sO}^- + \text{H}^+$	-8.93
$\text{Hfo_wOH} + \text{H}^+ = \text{Hfo_wOH}^{2+}$	7.29
$\text{Hfo_wOH} = \text{Hfo_wO}^- + \text{H}^+$	-8.93
Cu surface complexation constant	
$\text{Hfo_sOH} + \text{Cu}^{+2} = \text{Hfo_sOCu}^+ + \text{H}^+$	2.89
$\text{Hfo_wOH} + \text{Cu}^{+2} = \text{Hfo_wOCu}^+ + \text{H}^+$	0.6
$\text{Hfo_sOH} + \text{Cu}^+ = \text{Hfo_sOCu} + \text{H}^+$	-2.21
$\text{Hfo_wOH} + \text{Cu}^+ = \text{Hfo_wOCu} + \text{H}^+$	-5.44

Hfo_sOH means strong sites, Hfo_wOH means weak sites

Table 9.3 The surface characterization parameters of HFO used in the model

Parameter	Value
Strong surface site density	0.005mol/mol Fe
Weak surface site density	0.2 mol/mol Fe
Specific surface area	600 m ² /g or 5.33x10 ⁴ m ² /mole

The model parameters for HFO were calculated by assuming the sediment contain 2% of total iron or 3.4 mol/kg and 10% of iron was Hydrous ferric oxide (HFO), so the total HFO is $3.4 \times 0.1 = 0.34$ mol HFO/kg sediment (Sengor et al., 2007). The strong surface site density was $0.005 \times 0.34 = 0.0017$ mole site/kg and the weak site density was $0.2 \times 0.34 = 0.068$ mole site/kg. Mass of hydrous ferric oxide was calculated by $89 \text{ g HFO/mol Fe} \times 0.34 \text{ mol Fe/kg} = 30.26 \text{ g HFO/L}$. The Phreeqc code for HFO sorption modeling is shown in Appendix B.1

9.2.2 Adsorption to organic matter modeling

The model of the binding of copper ions to humic substances had been described by Tipping and Hurley (Tipping, 1998; Tipping & Hurley, 1992). The model describes the interaction between proton binding of humic and fluvic acids with metal. The rigid sphere is assumed as a picture of humic acids which contained ion binding sites on the surface. It was assumed that there are two major metal binding sites which include 4 groups of carboxylic acid or type A and 4 groups of phenolic acid or type B on the humic acids surface. These eight proton dissociated groups can individually interact with metal as monodentate binding sites or they can be pairing between the binding sites and form twelve bidentate sites. Because surface complexation of metal to humic acid database does not include in Phreeqc model, the reactions and their constants need to define to the Phreeqc. The proton dissociation constants and surface

complexation of Cu^{2+} binding to humic acids were brought from WHAM program and showed in Table 9.4.

Table 9.4 Proton dissociation constants and surface complexation constants of copper binding to humic acid in Tipping and Hurley's database, WHAM (Windermere Humic Acid Model of Tipping and Hurley) modeling

Reaction	Log K
Proton dissociation constants of monodentate binding sites	
Type A	
$\text{H}_{\text{aH}} = \text{H}_{\text{a}^-} + \text{H}^+$	-1.59
$\text{H}_{\text{bH}} = \text{H}_{\text{b}^-} + \text{H}^+$	-2.70
$\text{H}_{\text{cH}} = \text{H}_{\text{c}^-} + \text{H}^+$	-3.82
$\text{H}_{\text{dH}} = \text{H}_{\text{d}^-} + \text{H}^+$	-4.93
Type B	
$\text{H}_{\text{eH}} = \text{H}_{\text{e}^-} + \text{H}^+$	-6.88
$\text{H}_{\text{fH}} = \text{H}_{\text{f}^-} + \text{H}^+$	-8.72
$\text{H}_{\text{gH}} = \text{H}_{\text{g}^-} + \text{H}^+$	-10.56
$\text{H}_{\text{hH}} = \text{H}_{\text{h}^-} + \text{H}^+$	-12.40
Proton dissociation constants of bidentate binding sites	
$\text{H}_{\text{abH}_2} = \text{H}_{\text{abH}^-} + \text{H}^+$	-1.59
$\text{H}_{\text{abH}^-} = \text{H}_{\text{ab}^{2-}} + \text{H}^+$	-2.70
$\text{H}_{\text{adH}_2} = \text{H}_{\text{adH}^-} + \text{H}^+$	-1.59
$\text{H}_{\text{adH}^-} = \text{H}_{\text{ad}^{2-}} + \text{H}^+$	-4.93
$\text{H}_{\text{afH}_2} = \text{H}_{\text{afH}^-} + \text{H}^+$	-1.59
$\text{H}_{\text{afH}^-} = \text{H}_{\text{af}^{2-}} + \text{H}^+$	-8.72

Table 9.4 (cont'd)

Reaction	Log K
$H_{ah}H_2 = H_{ah}H^- + H^+$	-1.59
$H_{ah}H^- = H_{ah}^{-2} + H^+$	-12.40
$H_{bc}H_2 = H_{bc}H^- + H^+$	-2.70
$H_{bc}H^- = H_{bc}^{-2} + H^+$	-3.82
$H_{be}H_2 = H_{be}H^- + H^+$	-2.70
$H_{be}H^- = H_{be}^{-2} + H^+$	-6.88
$H_{bg}H_2 = H_{bg}H^- + H^+$	-2.70
$H_{bg}H^- = H_{bg}^{-2} + H^+$	-10.56
$H_{cd}H_2 = H_{cd}H^- + H^+$	-3.82
$H_{cd}H^- = H_{cd}^{-2} + H^+$	-4.93
$H_{cf}H_2 = H_{cf}H^- + H^+$	-3.82
$H_{cf}H^- = H_{cf}^{-2} + H^+$	-8.72
$H_{ch}H_2 = H_{ch}H^- + H^+$	-3.82
$H_{ch}H^- = H_{ch}^{-2} + H^+$	-12.40
$H_{de}H_2 = H_{de}H^- + H^+$	-4.93
$H_{de}H^- = H_{de}^{-2} + H^+$	-6.88
$H_{dg}H_2 = H_{dg}H^- + H^+$	-4.93
$H_{dg}H^- = H_{dg}^{-2} + H^+$	-10.56
Complexation constants of Cu binding to monodentate site	
$H_aH + Cu^{+2} = H_aCu^+ + H^+$	-0.63
$H_bH + Cu^{+2} = H_bCu^+ + H^+$	-0.63
$H_cH + Cu^{+2} = H_cCu^+ + H^+$	-0.63

Table 9.4 (cont'd)

Reaction	Log K
$H_{dH} + Cu^{+2} = H_{dCu} + H^+$	-0.63
$H_{eH} + Cu^{+2} = H_{eCu} + H^+$	-3.75
$H_{fH} + Cu^{+2} = H_{fCu} + H^+$	-3.75
$H_{gH} + Cu^{+2} = H_{gCu} + H^+$	-3.75
$H_{hH} + Cu^{+2} = H_{hCu} + H^+$	-3.75
Complexation constants of Cu binding to bidentate sites	
$H_{abH_2} + Cu^{+2} = H_{abCu} + 2H^+$	-1.26
$H_{adH_2} + Cu^{+2} = H_{adCu} + 2H^+$	-1.26
$H_{afH_2} + Cu^{+2} = H_{afCu} + 2H^+$	-4.38
$H_{ahH_2} + Cu^{+2} = H_{ahCu} + 2H^+$	-4.38
$H_{bcH_2} + Cu^{+2} = H_{bcCu} + 2H^+$	-1.26
$H_{beH_2} + Cu^{+2} = H_{beCu} + 2H^+$	-4.38
$H_{bgH_2} + Cu^{+2} = H_{bgCu} + 2H^+$	-4.38
$H_{cdH_2} + Cu^{+2} = H_{cdCu} + 2H^+$	-1.26
$H_{cfH_2} + Cu^{+2} = H_{cfCu} + 2H^+$	-4.38
$H_{chH_2} + Cu^{+2} = H_{chCu} + 2H^+$	-4.38
$H_{deH_2} + Cu^{+2} = H_{deCu} + 2H^+$	-4.38
$H_{dgH_2} + Cu^{+2} = H_{dgCu} + 2H^+$	-4.38

The model parameters for Cu-humic acid surface complexation were calculated by assuming there was organic matter 237 g in 1 kg of sediment. Assuming charge on each binding site is -2.84×10^{-3} eq/g OM. So, charge on type A monodentate sites is $-2.84 \times 10^{-3} / 4 \times 237 = 1.68 \times 10^{-1}$ eq/kg sediment and half off for type B, $0.5 \times 1.68 \times 10^{-1} = 0.84 \times 10^{-1}$ eq/kg sediment. The

charge on each 12 bidentate sites is $-2.84 \times 10^{-3} / 12 \times 237 = 5.61 \times 10^{-2}$ eq/kg sediment. The specific surface area of organic matter was 46,514 m²/g (Parkhurst & Appelo, 2013). The Phreeqc code for adsorption on organic matter modeling is shown in Appendix B.2.

9.2.3 Adsorption/ion exchange on clay modeling

The adsorption of copper on clay was modeled by ion exchange process. The ion exchange model of heavy metals on clay was already implemented in Phreeqc by using exchange keyword data block. The reaction of copper ion exchange on clay and their constant are shown in Table 9.5 (Parkhurst & Appelo, 2013).

Table 9.5 Copper ion exchange reaction and its constant

Reaction	Log K
$\text{Cu}^{2+} + 2\text{X}^- = \text{CuX}_2$	0.6

The model parameters for ion exchange on clay were calculated by assuming that sediment contained clays 30%. The cation exchange capacity (CEC) of clays was assumed as 50 meq/100g. For 1 kg sediment which contained 300 g of clay, the CEC will be $3 \times 50 \times 10^{-3} = 150 \times 10^{-3}$ eq/kg. The Phreeqc code for adsorption/ion exchange of Cu on clay modeling is shown in Appendix B.3.

9.2.4 Adsorption to bacteria surface modeling

To model the metal adsorption on bacteria surface, the sorption sites on bacterial surface need to be defined. The reactive sites on bacteria can divide into three sites according acid-base properties of anionic functional group: carboxyl (COOH) group as acid sites, phosphate group (PO₄³⁻) as neutral sites and hydroxyl (OH) and amine (NH) groups as basic sites. These sites will

dissociate upon the pH. The deprotonated sites can interact with metal ions to form surface complex.

Some bacterial had been studied the properties in sorption to the heavy metals such as *B. Subtilis* which was used in this model. Since sorption of metal to bacteria surface database does not include in Phreeqc model, so the reaction and their deprotonation and stability constants need to define to Phreeqc. The deprotonation constant (pK_a) and stability constants of copper with each surface functional groups of *B. Subtilis* are shown in Table 9.6.

Table 9.6 Deprotonation and stability constants of the copper and anionic functional groups on *B. Subtilis* cell surface (Daughney, Fein, & Yee, 1998; Fein, Daughney, Yee, & Davis, 1997)

Reaction	
Deprotonation	pKa
$(R-COO)H^0 = (R-COO)^- + H^+$	4.8
$(R-PO)H^0 = (R-PO)^- + H^+$	6.9
$(R-O)H^0 = (R-O)^- + H^+$	9.4
Surface complexation	Log K
$Cu^{2+} + (R-COO)^- = (R-COO)(Cu)^+$	4.4
$Cu^{2+} + (R-PO)^- = (R-PO)(Cu)^+$	6.0
$Cu^{2+} + (R-O)^- = (R-O)(Cu)^+$	-

The concentrations of each functional group per unit weight of bacteria *B. Subtilis* are shown in Table 9.7

Table 9.7 The concentration of each functional groups per unit weight of bacteria *B. Subtilis* (Fein et al., 1997)

Functional group	Concentration
Carboxyl sites	$1.2 \pm 0.2 \times 10^{-4}$ moles /g of bacteria
Phosphate sites	$4.4 \pm 0.3 \times 10^{-5}$ moles /g of bacteria
Hydroxyl sites	$6.2 \pm 0.4 \times 10^{-5}$ moles /g of bacteria

The model parameters were calculated by assuming 1 kg sediment contained 10 g of bacteria. So, the concentration of carboxyl sites is $10 \times 1.2 \times 10^{-4} = 1.2 \times 10^{-3}$ mole/kg sediment and concentration of phosphate sites is $10 \times 4.4 \times 10^{-5} = 4.4 \times 10^{-4}$ mole/kg. The surface area of *B. Subtilis* is $140 \text{ m}^2/\text{g}$. The Phreeqc code for adsorption of copper on bacteria surface is shown in Appendix B.4.

9.2.5 Contribution of all sorbent modeling

To see the contribution from all sorbent, the sorption model of copper to hydrous ferric oxides (HFO), organic matters, clays and bacteria surfaces were put together. Source of Cu^{2+} in solution were assumed from the dissolved CuCl_2 . The Cu^{2+} will form the surface complexation to these sorbents depending on the stability constant. The Phreeqc code that determine the contribution of adsorption of Cu on all sorbents is shown in Appendix B.5

9.3 Oxidation of dissolve organic compounds by microorganism or TEAP modeling

The biodegradation of organic matter in sediment can be described by sequential terminal electron acceptor process or TEAP. To model, we assume that the multiple microbial populations e.g. aerobes, nitrate reducers, iron reducers, sulfate reduces and methanogenesis bacteria are available in the sediment and acetate will be used as unlimited carbon source in the

model. Acetate was used as carbon and energy source because it is the common end product of many fermentation processes in the sediment. For simplicity, no net growth and no transport of bacterial population were assumed. The reduction reactions of sequential electron acceptor (TEAP) were shown again in Table 9.8. The terminal electron acceptors were used in the order of O_2 , NO_3^- , MnO_2 , $Fe(OH)_3$, SO_4^{2-} and acetate itself. To describe the kinetic rates of biodegradation of acetate with terminal electron acceptors, the Monod-type equation was used as shown in Table 9.9 where V_m was maximum reaction rate constant, K_s was half saturation constant. Due to acetate was assumed to have in excess amount, so there was no acetate concentration term in kinetic rate equation. In this study, the inhibiting constant (K_i^{in}) was implemented in the kinetic rates to impede the lower redox acceptors when higher electron acceptors were still available (Sengor et al., 2007). The parameter values of each Monod kinetic reaction (V_m , K_s and K_i^{in}) were taken from literatures and shown in Table 9.10. Finally, rate of methanogenesis where bacteria used acetate as electron acceptor was modeled by applying only methanogenesis rate constant (k^{CH_4}) and the inhibiting term. The Phreeqc code of microbial mediated reaction or TEAP is shown in Appendix C.1.

Table 9.8 The biodegradation reaction of sequential terminal electron acceptor

Description	Reaction
1. Aerobic respiration	$CH_3COO^- + 2O_2 \longrightarrow 2CO_3^{2-} + 3H^+$
2. Denitrification	$CH_3COO^- + 1.6NO_3^- \longrightarrow 2CO_3^{2-} + 0.8N_2 + 1.4H^+ + 0.8H_2O$
3. Manganese oxide reduction	$CH_3COO^- + 4MnO_2 + 5H^+ \longrightarrow 2CO_3^{2-} + 4Mn^{2+} + 4H_2O$
4. Iron oxide reduction	$CH_3COO^- + 2Fe(OH)_3 + H^+ \longrightarrow 2Fe^{2+} + 2CO_3^{2-} + 2H_2O$
5. Sulfate reduction	$CH_3COO^- + SO_4^{2-} \longrightarrow 2CO_3^{2-} + HS^- + 2H^+$
6. Methanogenesis	$CH_3COO^- + H^+ \longrightarrow CH_4 + CO_2$

Table 9.9 The kinetic rate law of sequential biodegradation reaction

Description	Rate law
1. Aerobic respiration	$R_{O_2} = V_m^{O_2} \frac{[O_2]}{[O_2] + K_s^{O_2}}$
2. Denitrification	$R_{NO_3} = V_m^{NO_3} \frac{[NO_3^-]}{[NO_3^-] + K_s^{NO_3}} * \frac{K_{O_2}^{in}}{K_{O_2}^{in} + [O_2]}$
3. Manganese oxide reduction	$R_{Mn} = V_m^{Mn} \frac{[MnO_2]}{[MnO_2] + K_s^{Mn}} * \frac{K_{O_2}^{in}}{K_{O_2}^{in} + [O_2]} * \frac{K_{NO_3}^{in}}{K_{NO_3}^{in} + [NO_3^-]}$
4. Iron oxide reduction	$R_{Fe} = V_m^{Fe} \frac{[Fe(OH)_3]}{[Fe(OH)_3] + K_s^{Fe}} * \frac{K_{O_2}^{in}}{K_{O_2}^{in} + [O_2]} * \frac{K_{NO_3}^{in}}{K_{NO_3}^{in} + [NO_3^-]} * \frac{K_{Mn}^{in}}{K_{Mn}^{in} + [MnO_2]}$
5. Sulfate reduction	$R_{SO_4^{2-}} = V_m^{SO_4} \frac{[SO_4^{2-}]}{[SO_4^{2-}] + K_s^{SO_4}} * \frac{K_{O_2}^{in}}{K_{O_2}^{in} + [O_2]} * \frac{K_{NO_3}^{in}}{K_{NO_3}^{in} + [NO_3^-]} * \frac{K_{Mn}^{in}}{K_{Mn}^{in} + [MnO_2]} * \frac{K_{Fe}^{in}}{K_{Fe}^{in} + [Fe(OH)_3]}$
6. Methanogenesis	$R_{CH_4} = k^{CH_4} * \frac{K_{O_2}^{in}}{K_{O_2}^{in} + [O_2]} * \frac{K_{NO_3}^{in}}{K_{NO_3}^{in} + [NO_3^-]} * \frac{K_{Mn}^{in}}{K_{Mn}^{in} + [MnO_2]} * \frac{K_{Fe}^{in}}{K_{Fe}^{in} + [Fe(OH)_3]} * \frac{K_{SO_4}^{in}}{K_{SO_4}^{in} + [SO_4^{2-}]}$

V_m^i is maximum substrate utilization rate constant, K_s^i is half saturation constant, K_i^{in} is inhibition constant. k^{CH_4} is rate of methanogenesis

Table 9.10 Kinetic Parameter constants of microbial mediation reaction using in the model

Parameter	Value	Unit	References
$V_m^{O_2}$	5×10^{-9}	/sec	a
$V_m^{NO_3}$	2×10^{-10}	/sec	a
V_m^{Mn}	3.17×10^{-10}	/sec	b
V_m^{Fe}	1.58×10^{-10}	/sec	b
$V_m^{SO_4}$	3.17×10^{-9}	/sec	b
k^{CH_4}	3.17×10^{-10}	/sec	b
$K_s^{O_2}$	2.41×10^{-5}	M	a
$K_s^{NO_3^-}$	1.13×10^{-4}	M	a
K_s^{Mn}	2×10^{-4}	M	b

Table 9.10 (cont'd)

Parameter	Value	Unit	References
K_s^{Fe}	2×10^{-4}	M	b
$K_s^{SO_4^{2-}}$	1×10^{-3}	M	a
$K_{O_2}^{in}$	1.61×10^{-8}	M	a
$K_{NO_3}^{in}$	1×10^{-7}	M	a
K_{Mn}^{in}	9×10^{-7}	M	c
K_{Fe}^{in}	9×10^{-5}	M	c
$K_{SO_4}^{in}$	1.5×10^{-5}	M	c

a from Sengor et al., 2007; b from Park & Jaffe, 1996; c from Smith & Jaffe, 1998

9.4 Reductive dissolution of iron oxides modeling

To simulate the reductive dissolution, the reduction of Ferrihydrite ($Fe(OH)_3$) was used. The Ferrihydrite was used as hydrous ferric oxides (HFO) sorption sites. The dissolved coppers were set to adsorb on Ferrihydrite. When Ferrihydrite was reduced by TEAP process, the adsorbed copper will be released to sediment porewater according to Eq.8.1. The sorption parameters of hydrous ferric oxides were mention in Table 9.3. The reducing condition were developed by TEAP process where O_2 , NO_3 , Pyrolusite (MnO_2) and then Ferrihydrite were consumed according to reaction inTable 9.8. The kinetic and rate of TEAP precess were refered to Table 9.9 and 9.10. The Tenorite (CuO) was used as representative of copper wastes and was added to model to supply dissolved copper to soution. The Phreeqc code of reductive dissolution modeling is shown in Appendix D.1.

9.5 Diffusion transport modeling

The transport model was set up as 1-D column which had 40 cm in depth and divided into 2 sections, 10 cm of post mining sediment and 30 cm of mine tailing as shown in Figure 9.1. The top sediment (10cm) was separated into 20 cell and 0.5 cm in each cell. The lower mine tailing sediment (30 cm) was separated into 30 cell and 1 cm length of each cell. The grid refinement on the upper section was set to catch up the quick change of concentration at water-sediment interface. The top sediment had high water content (60-70%) and mostly contained fine particles or silt whereas mine tailing had lower water content and larger particle size mixing between gravel and coarse sand (Jeong, 2003). The transport properties e.g. bulk density, porosity, diffusion coefficient, %organic matter of both sediments were shown in Table 9.11. The surface water was used as top boundary and initial pore water composition. The mine tailing pore water which was in reducing condition was used as bottom boundary. Because of low concentration of copper in simulated mine tailing porewater, the high concentration of copper at 10 ppm in mine tailing porewater was assumed to ensure that copper were diffuse upward. These surface water and porewater were allowed to diffuse through the column for a period of time. The only diffusion process was applied in the model because advection process was not expected to occur in sediment. The bioirrigation and bioturbation by benthic fauna were not included to the model. The diffusion coefficients of all dissolved species were assumed to be equal. The time step which is the diffusion period in one cell was 10,880 second or 3 hours (Sengor et al., 2007).

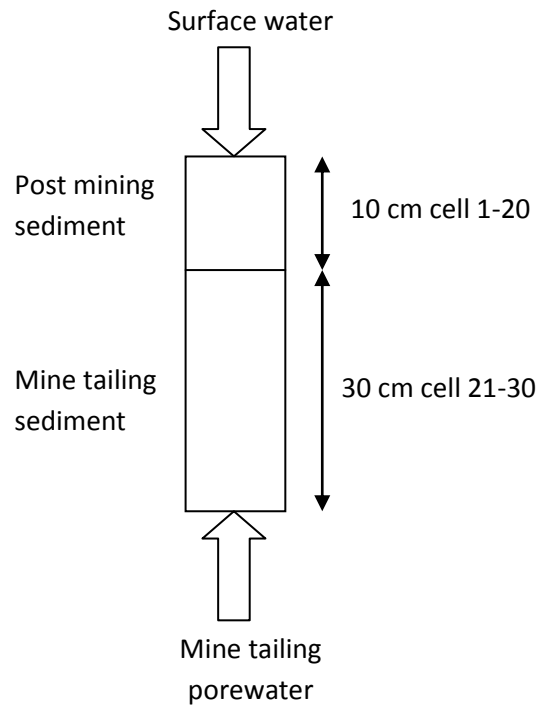


Figure 9.1 The 1-D column for diffusion process modeling between surface water and mine tailing porewater.

Table 9.11 Some physical transport properties of Torch Lake sediment in transport modeling

Parameters	Post mining sediment	Mine tailing	Unit
Diffusion coefficient	4.21e-6 ^a	4.21e-6 ^a	cm ² /sec
Porosity	0.9 ^b	0.8 ^b	-
Bulk density	0.1-0.3 ^a	0.6-0.9 ^a	g/cm ³
% organic matter	10-18 ^a	1.9-2.7 ^a	-

a McDonald et al., 2010, b from Konstantinidis et al., 2003

9.6 Diffusion transport with reductive dissolution of iron oxides and TEAP modeling

This model was cooperated the reductive dissolution and TEAP process to the diffusion process. The TEAP process was included secondary oxidation which shown in Table 9.12 where the reduced products e.g. NH_4^+ , Mn^{2+} , Fe^{2+} , HS^- and CH_4 can diffuse upward and react with oxygen at the surface sediment. The oxidation of CH_4 were modeled by Monod type kinetics whereas the oxidation of Mn^{2+} , Fe^{2+} and HS^- were modeled by second order rate reaction. Their kinetic rate laws and parameters were shown in Table 9.13 and 9.14.

Table 9.12 Secondary redox reactions

Description	Reaction
Oxidation of ammonia	$\text{NH}_4^+ + 2\text{O}_2 \longrightarrow \text{NO}_3^- + \text{H}_2\text{O} + 2\text{H}^+$
Oxidation of Mn^{2+}	$2\text{Mn}^{2+} + \text{O}_2 + 2\text{H}_2\text{O} \longrightarrow 2\text{MnO}_2 + 4\text{H}^+$
Oxidation of Fe^{2+}	$4\text{Fe}^{2+} + \text{O}_2 + 6\text{H}_2\text{O} \longrightarrow 4\text{FeOOH} + 8\text{H}^+$
Oxidation of HS^-	$\text{HS}^- + 2\text{O}_2 \longrightarrow \text{SO}_4^{2-} + \text{H}^+$
Oxidation of methane	$\text{CH}_4 + 2\text{O}_2 \longrightarrow \text{CO}_2 + 2\text{H}_2\text{O}$

Table 9.13 The kinetic rate law of secondary oxidation reaction

Description	Rate law
Oxidation of ammonia	$R = V_m \frac{[\text{O}_2]}{[\text{O}_2] + K_s} [\text{NH}_4^+]$
Oxidation of Methane	$R = V_m \frac{[\text{O}_2]}{[\text{O}_2] + K_s} [\text{CH}_4]$
Oxidation of Mn^{2+}	$R = k_{mc}[\text{O}_2][\text{Mn}^{2+}]$
Oxidation of Fe^{2+}	$R = k_{mc}[\text{O}_2][\text{Fe}^{2+}]$
Oxidation of HS^-	$R = k_{mc}[\text{O}_2][\text{HS}^-]$

Table 9.14 Kinetic parameter constant of secondary oxidation reaction

Parameter	Value	unit	Reference
V_m	9.51e-7	/sec	a
K_s	1e-5	M	a
k_{mc}	3.17e-7	/sec	a

a from Park & Jaffe, 1996

TEAP was applied into the whole column but the reductive dissolution of Ferrihydrite was applied in bottom sediment. The redox species and dissolved copper concentration profiles were created to determine the effect of reductive dissolution and TEAP. The Phreeqc code of diffusion transport with reductive dissolution and TEAP modeling is shown in Appendix E.1.

9.7 Full combined processes modeling

Finally, the full model that incorporated the adsorption process of various sorbents such as hydrous ferric oxide, organic matter, clay and bacteria surface and precipitation /dissolution of oxides, carbonates and sulfides of copper minerals into reductive dissolution, TEAP and diffusion transport model had been created and tested. This concept can be drawn as diagram as shown in Figure 9.2. We assume the adsorption of copper on organic matter, bacteria occurred only in top sediment whereas sorption of copper on Ferrihydrite and clays occurred in bottom sediment. The precipitation of copper minerals e.g. Chalcocite, Chalcopyrite, Covellite, CupricFerrite, CuprousFerrite, Malachite, Cuprite and Tenorite and other minerals e.g. Ferrihydrite, Goethite, Pyrite, Pyrolusite were allowed in the whole column. The Phreeqc code of full model is shown in Appendix F.1.

The concentration profiles included pH, pE, redox species, dissolved copper and copper solid phases were created from the model. These profiles were used to determine the key role processes that control copper fate and transport in Torch Lake sediment.

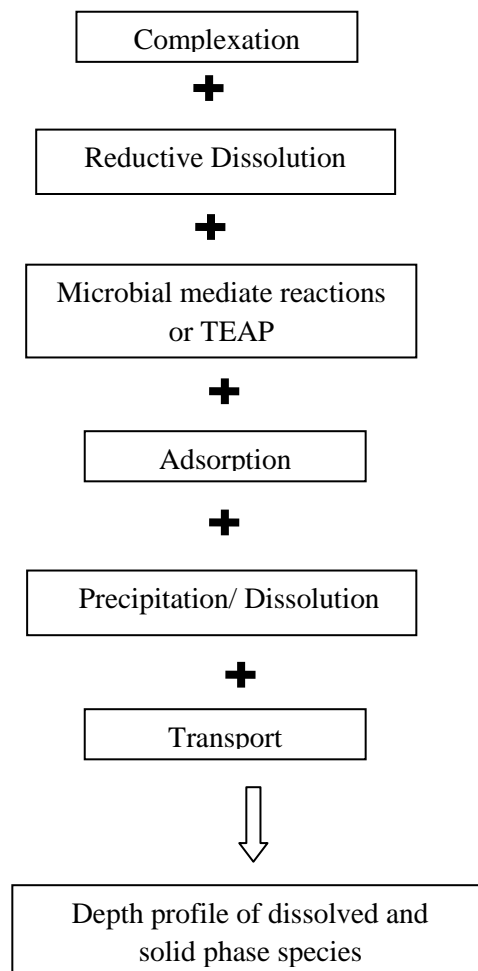


Figure 9.2 The diagram of all processes combined as full model

APPENDICES

Appendix A.1

Copper speciation in Torch lake surface water modeling

```
Title Surface_water Torch Lake sediment with Acetate
SOLUTION 0
units mg/L
temp 10
pH 7.8
redox O(0)/O(-2)
Alkalinity 38 mg/l as Ca0.5(CO3)0.5
O(0) 6.3
Cu 0.081
Fe 0.062
Zn 0.008
Mn 0.02
Nta 5.2
Na 0.96
K 0.09
Ca 13.6
Mg 2.7
Cl 0.12
S(6) 0.6
N(+5) 0.26
End
```

Appendix A.2

Copper speciation in top sediment pore water modeling

```
TITLE Pore_water Torch Lake sediment
SOLUTION 1
units mg/L
redox O(-2)/O(0)
pH 6.6
Alkalinity 78 as Ca0.5(CO3)0.5
O(0) 0.3
Cu 2.5
Fe 1.58
Mn 0.049
Acetate 29
Na 1.15
K 0.4
Ca 23
Mg 2.66
Cl 0.35
S(+6) 0.2
N(5) 0.26
End
```

Appendix A.3

Chemical composition in mine tailing pore water modeling

```
Title Stamp sand Pore_water Torch Lake
SOLUTION 1
EQUILIBRIUM_PHASES 1
  cuprite          0    10
  chalcopyrite    0    10
  chalcocite      0    10
  calcite         0    10
  quartz          0    10
  hematite        0    10
  K-feldspar      0    10
  Sanidine(H)    0    10
END
```

Appendix B.1

Adsorption to Hydrus Ferric Oxide (HFO) modeling

```
TITLE Torch Lake surface water sorption to HFO
SOLUTION 1
units mg/L
pH      7
redox   pe
units   mg/l
density 1
Alkalinity 38    mg/l as Ca0.5(CO3)0.5
O(0)    6.3
Cu      0.081
Fe      0.062
Zn      0.008
Mn      0.02
Nta     5.2
Na      0.96
K       0.09
Ca      13.6
Mg      2.7
Cl      0.12
S(6)    0.6
N(+5)   0.26

SURFACE 1
Hfo_s 0.0017 600. 30.26
Hfo_w 0.068
-equilibrate 1
end

USER_GRAPH 1
-headings pH Cu1_solute Cu2_solute Cu2_weaksites Cu2_strongsites Cu1_Weaksite
Cu1_strongsite Cu(Nta)-
-chart_title "Total Cu"
-axis_titles pH "Moles per kilogram water"
-axis_scale x_axis 4.0 10.0 1 0.25
-axis_scale y_axis 1e-13 1e-4 1 1 log
-initial_solutions false
-start
10 GRAPH_X -LA("H+")
20 GRAPH_Y tot("Cu(1)"),tot("Cu(2)"), MOL("Hfo_wOCu+"), MOL("Hfo_sOCu+"),
mol("Hfo_wOCu"), mol("Hfo_sOCu"), mol("Cu(Nta)-")
-end
END

use solution 1
use surface 1
equilibrium_phases 1
  Fix_H+ -2.01 HCl 2
  -force_equality
end
```

```
use solution 1
use surface 1
equilibrium_phases 1
  Fix_H+ -2.50 HCl 2
  -force_equality
end
...
use solution 1
use surface 1
equilibrium_phases 1
  Fix_H+ -12.0 NaOH 2
  -force_equality
end
```

Appendix B.2

Adsorption to organic matter modeling

```
Title Torch Lake surface water adsorption to organic matter
SOLUTION 1
units mg/L
  pH      7
  redox   pe
Alkalinity 38 mg/l as Ca0.5(CO3)0.5
O(0) 6.3
Cu 0.081
Fe 0.062
Zn 0.008
Mn 0.02
Nta 5.2
Na 0.96
K 0.09
Ca 13.6
Mg 2.7
Cl 0.12
S(6) 0.6
N(+5) 0.26

surface 1
H_a 1.68e-1 46.5e3 237
H_b 1.68e-1; H_c 1.68e-1; H_d 1.68e-1

H_e 0.84e-01; H_f 0.84e-01; H_g 0.84e-01; H_h 0.84e-01

H_ab 5.61e-02; H_ad 5.61e-02; H_af 5.61e-02; H_ah 5.61e-02
H_bc 5.61e-02; H_be 5.61e-02; H_bg 5.61e-02; H_cd 5.61e-02
H_cf 5.61e-02; H_ch 5.61e-02; H_de 5.61e-02; H_dg 5.61e-02
-Donnan
-equilibrate 1
end

USER_GRAPH 1
-headings pH Cu1_solute Cu2_solute Cu_OM
-chart_title "Total Cu"
-axis_titles pH "Moles per kilogram water"
-axis_scale x_axis 4.0 10.0 1 0.25
-axis_scale y_axis 1e-13 1e-4 1 1 log
-initial_solutions false
-start
10 H_Cu = SURF("Cu", "H") + EDL("Cu", "H")
20 GRAPH_X -LA("H+")
30 GRAPH_Y tot("Cu(1)"),tot("Cu(2)"), H_Cu
-end
END

use solution 1
use surface 1
equilibrium_phases 1
```

```
    Fix_H+ -2.01 HCl 5
    -force_equality
end
....

use solution 1
use surface 1
equilibrium_phases 1
    Fix_H+ -10.0 NaOH 1
    -force_equality
end
```

Appendix B.3

Adsorption/ion exchange on clay modeling

```
TITLE Torch lake surface water adsorption on clay
SOLUTION 1
units mg/L
pH 7
redox pe
Alkalinity 38      mg/l as Ca0.5(CO3)0.5
O(0) 6.3
Cu 0.081
Fe 0.062
Zn 0.008
Mn 0.02
Nta 5.2
Na 0.96
K 0.09
Ca 13.6
Mg 2.7
Cl 0.12
S(6) 0.6
N(+5) 0.26
EXCHANGE 1
-equilibrate 1
      X 150e-3
USER_GRAPH 1
-headings pH Cu1_solute Cu2_solute CuX2
-chart_title "Total Cu"
-axis_titles pH "Moles per kilogram water"
-axis_scale x_axis 4.0 10.0 1 0.25
-axis_scale y_axis 1e-13 1e-4 1 1 log
-initial_solutions false
-start
10 GRAPH_X -LA("H+")
20 GRAPH_Y tot("Cu(1)"),tot("Cu(2)"), mol("CuX2")
-end
END
use solution 1
use exchange 1
equilibrium_phases 1
  Fix_H+ -2.01 HCl 2
  -force_equality
end
use solution 1
use exchange 1
equilibrium_phases 1
  Fix_H+ -12.0 NaOH 2
  -force_equality
End
```

Appendix B.4

Adsorption to Bacteria surface modeling

```
TITLE Torch lake surface water adsorption to bacteria surface
SOLUTION 1
units mg/L
pH 7
redox pe
Alkalinity 38      mg/l as Ca0.5(CO3)0.5
O(0) 6.3
Cu 0.081
Fe 0.062
Zn 0.008
Mn 0.02
Nta 5.2
Na 0.96
K 0.09
Ca 13.6
Mg 2.7
Cl 0.12
S(6) 0.6
N(+5) 0.26

surface 1      # assume 140 m2/g bacteria ,10g of bacteria/L sediment
R_a 1.2e-3 140 10
R_b 4.4e-4
-equilibrate 1
end

USER_GRAPH 1
-headings pH Cu1_solute Cu2_solute R_Cu
-chart_title "Total Cu"
-axis_titles pH "Moles per kilogram water"
-axis_scale x_axis 4.0 10.0 1 0.25
-axis_scale y_axis 1e-13 1e-4 1 1 log
-initial_solutions false
-start
10 R_Cu = mol("R_aCu+") + mol("R_bCu+")
20 GRAPH_X -LA("H+")
30 GRAPH_Y tot("Cu(1)"),tot("Cu(2)"), R_Cu
-end
END

use solution 1
use surface 1
equilibrium_phases 1
  Fix_H+ -2.01 HCl 2
  -force_equality
End
....

use solution 1
use surface 1
```

```
equilibrium_phases 1
  Fix_H+ -12.0 NaOH 1
  -force_equality
end
```

Appendix B.5

Contribution of all sorbent modeling

Title Torch lake surface water sorption of all sorbent

SOLUTION 1

units mg/L

pH 7

redox pe

Alkalinity 38 mg/l as Ca0.5(CO3)0.5

O(0) 6.3

Cu 0.081

Fe 0.062

Zn 0.008

Mn 0.02

Nta 5.2

Na 0.96

K 0.09

Ca 13.6

Mg 2.7

Cl 0.12

S(6) 0.6

N(+5) 0.26

surface 1

sorption to Hydrous ferric oxide

Hfo_s 0.0017 600. 30.26

Hfo_w 0.068

sorption to organic matter

H_a 1.68e-1 46.5e3 237

H_b 1.68e-1; H_c 1.68e-1; H_d 1.68e-1

H_e 0.84e-01; H_f 0.84e-01; H_g 0.84e-01; H_h 0.84e-01

H_ab 5.61e-02; H_ad 5.61e-02; H_af 5.61e-02; H_ah 5.61e-02

H_bc 5.61e-02; H_be 5.61e-02; H_bg 5.61e-02; H_cd 5.61e-02

H_cf 5.61e-02; H_ch 5.61e-02; H_de 5.61e-02; H_dg 5.61e-02

-Donnan

sorption to clay

EXCHANGE 1

X 150e-3

-equilibrate 1

sorption to bacteria surface

R_a 1.2e-3 140 10

R_b 4.4e-4

-equilibrate 1

REACTION 1

CuCl2 1

2e-3 in 20

INCREMENTAL_REACTIONS true

USER_GRAPH 1

-headings Cu_dissolve Cu_OM CuX2 Cu_HFO Bact_Cu Total Cu1 Cu2 Cu(Nta)-

```

-axis_titles "Dissolve Cu in ug/kg" "Sorb Cu in ug/Kg sed"
-initial_solutions false
-start
10 H_Cu =
(mol("H_aCu+") + mol("H_bCu+") + mol("H_cCu+") + mol("H_dCu+") + mol("H_eCu+") + mol("H
_fCu+")
+ mol("H_gCu+") + mol("H_hCu+") + mol("H_abCu") + mol("H_adCu") + mol("H_afCu") + mol("H
_ahCu") + mol("H_bcCu") + mol("H_beCu") + mol("H_bgCu") + mol("H_cdCu") + mol("H_cfCu")
+ mol("H_chCu") + mol("H_deCu") + mol("H_dgCu")) # this is Cu ads on OM
20 CuX2 = mol("CuX2")
30 Hfo_Cu = (mol("Hfo_wOCu+") + mol("Hfo_sOCu+") + mol("Hfo_wOCu") +
mol("Hfo_sOCu"))
40 Bact_Cu = (mol("R_aCu+") + mol("R_bCu+"))
50 total = H_Cu + CuX2 + Hfo_Cu + Bact_Cu
60 x = TOT("Cu(2)") * 63.54e6
70 GRAPH_X x
80 GRAPH_Y H_Cu, CuX2, Hfo_Cu, Bact_Cu, total
-end
END

```

Appendix C.1

Oxidation of dissolved organic compounds by microorganism or TEAP modeling

```
Title TEAP modeling
SOLUTION 1
units mol/kgw
pH      8.3
pe      -7.9
Acetate  0.1
Al       1.639e-05
C(4)    2.616e-03
Ca       2.616e-03
  Cu(1)  1.502e-04
  Cu(2)  4.215e-12
  Fe(2)  2.262e-05
  Fe(3)  1.078e-15
  H(0)   2.435e-04
K        1.639e-05
O(0)    0.01
N(5)    0.0001
  S(-2)  1.764e-04
  S(6)   4.678e-33
Si       9.229e-05

equilibrium_phases 1
Ferrihydrite 0 0.00001
Pyrolusite 0 0.001

Rates
  Oxygen
  -start
10 VmO2 = 5e-9 # unit is per second
20 KsO2= 2.41e-5 # unit is per second
30 fO1 = mol("O2")/(mol("O2")+ KsO2)
40 rate = -VmO2*fO1
50 moles= rate*TIME
200 save moles
  -end

.....
  Sulfate
10 VmSO4 =3e-9
20 KsSO4= 1e-3
30 KinO2= 1.61e-8
40 KinNO3 = 1e-7
50 KinMn = 9e-7
60 KinFe= 9e-5
70 fS1 = mol("SO4-2")/(mol("SO4-2")+ KsSO4)
80 fS2= KinO2/(KinO2+mol("O2"))
90 fS3= KinNO3/(KinNO3+mol("NO3-"))
100 fS4= KinMn/(KinMn+equi("Pyrolusite"))
```

```

110 fS5= KinFe/(KinFe+equi("Ferrihydrite"))
120 rate = -VmSO4*fS1*fS2*fS3*fS4*fS5
130 moles= rate*TIME
200 save moles
-end
Methanogenesis
10 kCH4 = 3.17e-10
20 KinO2= 1.61e-8
30 KinNO3 = 1e-7
40 KinMn = 9e-7
50 KinFe= 9e-5
60 KinSO4= 1.5e-5
70 fMe1= KinO2/(KinO2+mol("O2"))
80 fMe2= KinNO3/(KinNO3+mol("NO3-"))
90 fMe3= KinMn/(KinMn+equi("Pyrolusite"))
100 fMe4= KinFe/(KinFe+equi("Ferrihydrite"))
110 fMe5= KinSO4/(KinSO4+mol("SO4-2"))
120 rate = -kCH4*fM1*fM2*fM3*fM4*fMe5
130 moles= rate*TIME
200 save moles
-end
Kinetics 1
Oxygen
-formula Acetate- 1 CO3-2 -2 H+ -3 O2 2

Nitrate
-formula Acetate- 1 NO3- 1.6 CO3-2 -2 N2 -0.8 H+ -1.4 H2O -0.8

Manganese
-formula Acetate- 1 Pyrolusite 4 H+ 5 CO3-2 -2 Mn+2 -4 H2O -4

Iron
-formula Acetate- 1 Goethite 8 H+ 13 CO3-2 -2 Fe+2 -8 H2O -12

sulfate
-formula Acetate- 1 SO4-2 1 CO3-2 -2 HS- -1 H+ -2

Methanogenesis
-formula Acetate- 1 H+ 1 CH4 -1 CO2 -1

-steps 10e6 in 100 steps #86400 sec is 1 day ,2.59e6 is 30 day
INCREMENTAL_REACTIONS true
user_graph
-headings time pe pH acetate O2 NO3 N2 Fe3+ Fe2+ SO4 HS- CH4 Cu2 Cu1
Zn Ca Fe(OH)3 MnO2 Mn2+
-axis_titles "time(days)" " " "conc. (molal)"
-initial_solutions true
-start
10 graph_x total_time/3600/24
20 graph_y -la("e-"), -la("H+"), mol("Acetate-"), mol("O2"), mol("NO3-"),
mol("N2"), mol("Fe+3"), mol("Fe+2"), mol("SO4-2"), mol("HS-"),
mol("CH4"), mol("Cu+2"), mol("Cu+"), mol("Zn+2"), mol("Ca+2"),
equi("Ferrihydrite"), equi("Pyrolusite"), mol("Mn+2")

-end

End

```

Appendix D.1

Reductive dissolution modeling

```
Title Reduction dissolution modeling
SOLUTION 1
units mol/kgw
pH 8.3
pe -7.9
Acetate          0.1
Al               1.639e-05
C(4)            2.616e-03
Ca              2.616e-03
Cu(1)           1.502e-04
Cu(2)           4.215e-12
Fe(2)           2.262e-05
Fe(3)           1.078e-15
H(0)            2.435e-04
K               1.639e-05
O(0)            0.001
N(5)            0.0001
S(-2)           1.764e-04
S(6)            4.678e-33
Si              9.229e-05

equilibrium_phases 1
Pyrolusite 0 0.0001
Ferrihydrite 0 0.0001
end
surface 1
Hfo_s  Ferrihydrite      0.005  53400
Hfo_w  Ferrihydrite      0.2
-equil 1
end

USER_GRAPH
-headings time pe pH  acetate O2  NO3 N2 Fe3+  Fe2+  SO4  HS-  CH4  Cu2 Cu1
Zn Ca Fe(OH)3 MnO2 Mn2+ Hfo_Cu Tenorite
-axis_titles "step", "(molal)",
-initial_solutions false
-start
10 graph_x  step_no
20 Hfo_Cu = (mol("Hfo_wOCu+") + mol("Hfo_sOCu+"))
30 graph_y  -la("e-"), -la("H+"), mol("Acetate-"), mol("O2"), mol("NO3-"),
mol("N2"), tot("Fe(3)"), tot("Fe(2)"), tot("S(6)"), tot("S(-2)"),
mol("CH4"), tot("Cu(2)"), tot("Cu(1)"), mol("Zn(2)"), mol("Ca+2"),
equi("Ferrihydrite"), equi("Pyrolusite"), mol("Mn+2"), Hfo_Cu,
equi("tenorite")
-end
end
use surface 1
use solution 1
equilibrium_phases 2
Pyrolusite 0 0.0001
```

```
Ferrihydrite 3 0.0001
tenorite 0 0.001
save solution 2
```

Rates

```
  Oxygen
  -start
10 VmO2 = 5e-9 # unit is per second
20 KsO2= 2.41e-5 # unit is per second
30 fO1 = mol("O2")/(mol("O2")+ KsO2)
40 rate = -VmO2*fO1
50 moles= rate*TIME
200 save moles
  -end
```

```
  Nitrate
10 VmNO3 = 2e-10
20 KsNO3= 1.13e-4
30 KinO2 =1.61e-8
40 fN1 = mol("NO3-")/(mol("NO3-")+ KsNO3)
50 fN2 = KinO2/(KinO2+mol("O2"))
60 rate = -VmNO3*fN1*fN2
70 moles= rate*TIME
200 save moles
  -end
```

```
  Manganese
10 VmMn =3.17e-10
20 KsMn =2e-4
30 KinO2=1.61e-8
40 KinNO3= 1e-7
50 fMn1= equi("Pyrolusite")/(equi("Pyrolusite")+KsMn)
60 fMn2= KinO2/(KinO2+mol("O2"))
70 fMn3= KinNO3/(KinNO3+mol("NO3-"))
80 rate = -VmMn*fMn1*fMn2*fMn3
90 moles= rate*TIME
200 save moles
  -end
```

```
  Iron
10 VmFe = 1.58e-10
20 KsFe= 2e-4
30 KinO2= 1.61e-8
40 KinNO3 = 1e-7
50 KinMn = 9e-7
60 fI1 = equi("Ferrihydrite")/(equi("Ferrihydrite")+ KsFe)
70 fI2= KinO2/(KinO2+mol("O2"))
80 fI3= KinNO3/(KinNO3+mol("NO3-"))
90 fI4= KinMn/(KinMn+equi("Pyrolusite"))
100 rate = -VmFe*fI1*fI2*fI3*fI4
110 moles= rate*TIME
200 save moles
  -end
```

```
  Sulfate
10 VmSO4 =3e-9
20 KsSO4= 1e-3
30 KinO2= 1.61e-8
```

```

40 KinNO3 = 1e-7
50 KinMn = 9e-7
60 KinFe= 9e-5
70 fS1 = mol("SO4-2")/(mol("SO4-2")+ KsSO4)
80 fS2= KinO2/(KinO2+mol("O2"))
90 fS3= KinNO3/(KinNO3+mol("NO3-"))
100 fS4= KinMn/(KinMn+equi("Pyrolusite"))
110 fS5= KinFe/(KinFe+equi("Ferrihydrite"))
120 rate = -VmSO4*fS1*fS2*fS3*fS4*fS5
130 moles= rate*TIME
200 save moles
-end
Methanogenesis
10 kCH4 = 3.17e-10
20 KinO2= 1.61e-8
30 KinNO3 = 1e-7
40 KinMn = 9e-7
50 KinFe= 9e-5
60 KinSO4= 1.5e-5
70 fMe1= KinO2/(KinO2+mol("O2"))
80 fMe2= KinNO3/(KinNO3+mol("NO3-"))
90 fMe3= KinMn/(KinMn+equi("Pyrolusite"))
100 fMe4= KinFe/(KinFe+equi("Ferrihydrite"))
110 fMe5= KinSO4/(KinSO4+mol("SO4-2"))
120 rate = -kCH4*fM1*fM2*fM3*fM4*fMe5
130 moles= rate*TIME
200 save moles
-end
Kinetics 2
Oxygen
-formula Acetate- 1 CO3-2 -2 H+ -3 O2 2

Nitrate
-formula Acetate- 1 NO3- 1.6 CO3-2 -2 N2 -0.8 H+ -1.4 H2O -0.8

Manganese
-formula Acetate- 1 Pyrolusite 4 H+ 5 CO3-2 -2 Mn+2 -4 H2O -4

Iron
-formula Acetate- 1 Ferrihydrite 2 H+ 1 CO3-2 -2 Fe+2 -2 H2O -2

sulfate
-formula Acetate- 1 SO4-2 1 CO3-2 -2 HS- -1 H+ -2

Methanogenesis
-formula Acetate- 1 H+ 1 CH4 -1 CO2 -1

-steps 3e6 in 100 steps #86400 sec is 1 day ,2.59e6 is 30 day
INCREMENTAL_REACTIONS true
End

```

Appendix E.1

Diffusion transport with reductive dissolution and TEAP modeling

Title Diffusion transport with reduction dissolution and TEAP modeling

SOLUTION 0

temp	10
pH	7.8
pe	4
redox	O(-2)/O(0)
units	mg/l
density	1
Acetate	40
C(4)	46.56
Ca	13.6
Cl	0.12
Cu	0.081
Fe	0.062
K	0.09
Mg	2.7
Mn	0.02
N(5)	0.26
Na	0.96
Nta	5.2
O(0)	6.3
S(6)	0.6
Zn	0.008
-water	1 # kg

SOLUTION 1-50

temp	25
pH	7
pe	4
redox	pe
units	mg/l
density	1
Acetate	40
C(4)	46.56
Ca	13.6
Cl	0.12
Cu	0.081
Fe	0.062
K	0.09
Mg	2.7
Mn	0.02
N(5)	0.26
Na	0.96
Nta	5.2
O(0)	6.3
S(6)	0.6
Zn	0.008
-water	1 # kg

SOLUTION 51

temp 25
pH 9.702
pe -7.908
redox pe
units mol/kgw
density 1
Al 1.125e-005
C(4) 0.0001468
Ca 0.0001468
Cu 10 mg/kgw
Fe(2) 1.9e-010
Fe(3) 1.31e-014
H(0) 3.647e-007
K 1.125e-005
O(0) 0
S(-2) 2.443e-007
S(6) 4.378e-018
Si 0.0001592
-water 1 # kg

equilibrium_phases 1-20

Pyrolusite 0 0
Goethite 0 0

equilibrium_phases 21-50

Pyrolusite 0 0.0001
Ferrihydrite 3 0.0001
tenorite 0 0.001

SURFACE 21-50

Hfo_s Ferrihydrite equilibrium_phase 0.005 53400
Hfo_w Ferrihydrite equilibrium_phase 0.2

Rates

Oxygen
-start
10 VmO2 = 5e-9 # unit is per second
20 KsO2= 2.41e-5 # unit is per second
30 fO1 = mol("O2")/(mol("O2")+ KsO2)
40 rate = -VmO2*fO1
50 moles= rate*TIME
200 save moles
-end

.....

Methanogenesis

10 kCH4 = 3.17e-10
20 KinO2= 1.61e-8
30 KinNO3 = 1e-7
40 KinMn = 9e-7
50 KinFe= 9e-5
60 KinSO4= 1.5e-5
70 fMe1= KinO2/(KinO2+mol("O2"))
80 fMe2= KinNO3/(KinNO3+mol("NO3-"))

```

90 fMe3= KinMn/(KinMn+equi("Pyrolusite"))
100 fMe4= KinFe/(KinFe+equi("Ferrihydrite"))
110 fMe5= KinSO4/(KinSO4+mol("SO4-2"))
120 rate = -kCH4*fm1*fm2*fm3*fm4*fMe5
130 moles= rate*TIME
200 save moles
-end
  Oxidation_CH4
  -start
10 VmCH4 = 9.5e-7
20 ks = 1e-5
30 fme =mol("O2")/(mol("O2") + ks)
40 rate= VmCH4*fme*mol("CH4")
50 moles= rate*TIME
200 save moles
-end
  Oxidation_Mn
  -start
10 kmc = 3.17e-7
20 rate= kmc*mol("O2")*mol("Mn+2")
30 moles= rate*TIME
200 save moles
-end
  Oxidation_Fe
  -start
10 kmc = 3.17e-7
20 rate= kmc*mol("O2")*mol("Fe+2")
30 moles= rate*TIME
200 save moles
-end
  Oxidation_HS
  -start
10 kmc = 3.17e-7
20 rate= kmc*mol("O2")*mol("HS-")
30 moles= rate*TIME
200 save moles
-end

KINETICS 1-50
Oxygen
  -formula  Acetate- 1 CO3-2 -2 H+ -3 O2 2
Nitrate
  -formula  Acetate- 1 NO3- 1.6 CO3-2 -2 N2 -0.8 H+ -1.4 H2O -0.8
Manganese
  -formula  Acetate- 1 Pyrolusite 4 H+ 5 CO3-2 -2 Mn+2 -4 H2O -4
Iron
  -formula  Acetate- 1 Ferrihydrite 2 H+ 1 CO3-2 -2 Fe+2 -2 H2O -2
sulfate
  -formula  Acetate- 1 SO4-2 1 CO3-2 -2 HS- -1 H+ -2
Methanogenesis
  -formula  Acetate- 1 H+ 1 CH4 -1 CO2 -1

Oxidation_CH4
  -formula  CH4 1 O2 2 CO2 -1 H2O -2
Oxidation_Mn
  -formula  Mn+2 2 O2 1 H2O 2 Pyrolusite -2 H+ -4

```

```

Oxidation_Fe
-formula Fe+2 4 O2 1 H2O 6 Goethite -4 H+ -8
Oxidation_HS
-formula HS- 1 O2 2 SO4-2 -1 H+ -1
-steps 1
-step_divide 1
-runge_kutta 3
-bad_step_max 500

SELECTED_OUTPUT
-file basecaselyearDiffRedDisSTEAP.sel
-reset true
-distance true
-ph true
-pe true
-totals S(6) S(-2) C(-4) Cu(2) Cu(1)
-molalities Acetate- O2 NO3- N2
Fe+3 Fe+2 Cu+2 Cu+
Mn+2 Cu(Nta)- Cu(S4)2-3
-equilibrium_phases Goethite Pyrolusite Ferrihydrite Siderite
Chalcocite Sphalerite Covellite CupricFerrite
CuprousFerrite Chalcopyrite Cuprite Tenorite
Malachite Azurite Cu(OH)2

USER_PUNCH
-headings Sorption_OM Sorption_clay Sorption_HFO Sorption_Bact total_sorption
total_Cu_Solid
-start
10 H_Cu =
mol("H_aCu+") + mol("H_bCu+") + mol("H_cCu+") + mol("H_dCu+") + mol("H_eCu+") + mol("H_
fCu+")
+ mol("H_gCu+") + mol("H_hCu+") + mol("H_abCu") + mol("H_adCu") + mol("H_afCu") + mol("H
_ahCu") + mol("H_bcCu") + mol("H_beCu") + mol("H_bgCu") + mol("H_cdCu") + mol("H_cfCu")
+ mol("H_chCu") + mol("H_deCu") + mol("H_dgCu")
20 punch H_Cu
30 punch mol("CuX2")
40 Hfo_Cu = mol("Hfo_wOCu") + mol("Hfo_sOCu") + mol("Hfo_wOCu") +
mol("Hfo_sOCu")
50 punch Hfo_Cu
60 R_Cu = mol("R_aCu+") + mol("R_bCu+")
70 punch R_Cu
80 total_sorption = H_Cu + CuX2 + Hfo_Cu + R_Cu
90 punch total_sorption
100 total_Cu_Solid =
total_sorption + equi("Chalcocite") + equi("Chalcopyrite") + equi("CuprousFerrite")
+ equi("CupricFerrite") + equi("Tenorite")
110 punch total_Cu_Solid
-end

TRANSPORT
-cells 50
-shifts 2880
-time_step 10800 1 # seconds
-flow_direction diffusion_only
-boundary_conditions flux flux
-lengths 20*0.005 30*0.01
-dispersivities 50*0.002

```

```
-correct_disp      true
-diffusion_coefficient 4.21e-010
-thermal_diffusion 2 4.21e-010
-punch_frequency 2880
-multi_d           true 4.21e-010 0.9 0 1
```

end

Appendix F.1

Full combined processes modeling

Title Full combined processes modeling

SOLUTION 0

temp	10
pH	7.8
pe	4
redox	O(-2)/O(0)
units	mg/l
density	1
Acetate	40
C(4)	46.56
Ca	13.6
Cl	0.12
Cu	0.081
Fe	0.062
K	0.09
Mg	2.7
Mn	0.02
N(5)	0.26
Na	0.96
Nta	5.2
O(0)	6.3
S(6)	0.6
Zn	0.008
-water	1 # kg

SOLUTION 1-50

temp	25
pH	7
pe	4
redox	pe
units	mg/l
density	1
Acetate	40
C(4)	46.56
Ca	13.6
Cl	0.12
Na	0.96
Nta	5.2
O(0)	6.3
S(6)	0.6
Zn	0.008
-water	1 # kg

SOLUTION 51

temp	25
pH	9.702
pe	-7.908
redox	pe
units	mol/kgw
density	1

```

Al      1.125e-005
C(4)   0.0001468
Ca      0.0001468
Cu      10 mg/kgw #about 1.57e-4M
O(0)   0
S(-2)  2.443e-007
S(6)   4.378e-018
Si      0.0001592
-water  1 # kg

```

EQUILIBRIUM_PHASES 1-20

```

Pyrolusite 0 0
Ferrihydrite 0 0
Goethite 0 0
Chalcocite 0 0
Cuprite 0 0
CuprousFerrite 0 0
Malachite 0 0
Pyrite 0 0

```

equilibrium_phases 21-50

```

Pyrolusite 0 0.0001
Ferrihydrite 3 0.0001
tenorite 0 0.001
#Goethite 0 0
Chalcocite 0 0
CuprousFerrite 0 0
Malachite 0 0
Pyrite 0 0

```

```

surface 1-20 # run sorption only on top sediment
# Sediment 1kg has 237 g OC, distributed over the sites:
# Example: SS = 46514 m2/g for I = 0.003 mol/l
# charge on 4 nHA sites: -2.84e-3/ 4 * 237 = 1.68e-1 (eq)
H_a 1.68e-1 46.5e3 237
H_b 1.68e-1; H_c 1.68e-1; H_d 1.68e-1

```

```

# charge on 4 nHB sites: 0.5 * charge on nHA sites
H_e 0.84e-01; H_f 0.84e-01; H_g 0.84e-01; H_h 0.84e-01

```

```

# charge on 12 diprotic sites: -2.84e-3/12 * 237
H_ab 5.61e-02; H_ad 5.61e-02; H_af 5.61e-02; H_ah 5.61e-02
H_bc 5.61e-02; H_be 5.61e-02; H_bg 5.61e-02; H_cd 5.61e-02
H_cf 5.61e-02; H_ch 5.61e-02; H_de 5.61e-02; H_dg 5.61e-02
-Donnan

```

```

#Hfo_s Ferrihydrite equilibrium_phase 0.005 53400
#Hfo_w Ferrihydrite equilibrium_phase 0.2

```

```

R_a 1.2e-3 140 10
R_b 4.4e-4
-equilibrate 1

```

SURFACE 21-50

```

Hfo_s Ferrihydrite equilibrium_phase 0.005 53400
Hfo_w Ferrihydrite equilibrium_phase 0.2

```

EXCHANGE 21-50 # run exchange entire sediment

```

X 150e-3
-equilibrate 1

Rates
  Oxygen
  -start
10 VmO2 = 5e-9 # unit is per second
20 KsO2= 2.41e-5 # unit is per second
30 fO1 = mol("O2")/(mol("O2")+ KsO2)
40 rate = -VmO2*fO1
50 moles= rate*TIME
200 save moles
  -end

  Nitrate
10 VmNO3 = 2e-10
20 KsNO3= 1.13e-4
30 KinO2 =1.61e-8
40 fN1 = mol("NO3-")/(mol("NO3-")+ KsNO3)
50 fN2 = KinO2/(KinO2+mol("O2"))
60 rate = -VmNO3*fN1*fN2
70 moles= rate*TIME
200 save moles
  -end

  Manganese
10 VmMn =3.17e-10
20 KsMn =2e-4
30 KinO2=1.61e-8
40 KinNO3= 1e-7
50 fMn1= equi("Pyrolusite")/(equi("Pyrolusite")+KsMn)
60 fMn2= KinO2/(KinO2+mol("O2"))
70 fMn3= KinNO3/(KinNO3+mol("NO3-"))
80 rate = -VmMn*fMn1*fMn2*fMn3
90 moles= rate*TIME
200 save moles
  -end

  Iron
10 VmFe = 1.58e-10
20 KsFe= 2e-4
30 KinO2= 1.61e-8
40 KinNO3 = 1e-7
50 KinMn = 9e-7
60 fI1 = equi("Ferrihydrite")/(equi("Ferrihydrite")+ KsFe)
70 fI2= KinO2/(KinO2+mol("O2"))
80 fI3= KinNO3/(KinNO3+mol("NO3-"))
90 fI4= KinMn/(KinMn+equi("Pyrolusite"))
100 rate = -VmFe*fI1*fI2*fI3*fI4
110 moles= rate*TIME
200 save moles
  -end

  Oxidation_CH4
  -start
10 VmCH4 = 9.5e-7
20 ks = 1e-5
30 fme =mol("O2")/(mol("O2") + ks)
40 rate= VmCH4*fme*mol("CH4")
50 moles= rate*TIME
200 save moles

```

```

-end
  Oxidation_Mn
  -start
10 kmc = 3.17e-7
20 rate= kmc*mol("O2")*mol("Mn+2")
30 moles= rate*TIME
200 save moles
-end
  Oxidation_Fe
  -start
10 kmc = 3.17e-7
20 rate= kmc*mol("O2")*mol("Fe+2")
30 moles= rate*TIME
200 save moles
-end
  Oxidation_HS
  -start
10 kmc = 3.17e-7
20 rate= kmc*mol("O2")*mol("HS-")
30 moles= rate*TIME
200 save moles
-end

KINETICS 1-50
Oxygen
  -formula  Acetate- 1 CO3-2 -2 H+ -3 O2 2
Nitrate
  -formula  Acetate- 1 NO3- 1.6 CO3-2 -2 N2 -0.8 H+ -1.4 H2O -0.8
Manganese
  -formula  Acetate- 1 Pyrolusite 4 H+ 5 CO3-2 -2 Mn+2 -4 H2O -4
Iron
  -formula  Acetate- 1 Ferrihydrite 2 H+ 1 CO3-2 -2 Fe+2 -2 H2O -2
sulfate
  -formula  Acetate- 1 SO4-2 1 CO3-2 -2 HS- -1 H+ -2
Methanogenesis
  -formula  Acetate- 1 H+ 1 CH4 -1 CO2 -1
Oxidation_CH4
  -formula  CH4 1 O2 2 CO2 -1 H2O -2
Oxidation_Mn
  -formula  Mn+2 2 O2 1 H2O 2 Pyrolusite -2 H+ -4
Oxidation_Fe
  -formula  Fe+2 4 O2 1 H2O 6 Goethite -4 H+ -8
Oxidation_HS
  -formula  HS- 1 O2 2 SO4-2 -1 H+ -1

-steps      1
-step_divide 1
-runge_kutta 3
-bad_step_max 500

SELECTED_OUTPUT
  -file      basecase10dayDiffRedDissTEAPSorppreci.sel
  -reset     true
  -distance  true
  -ph        true
  -pe        true
  -totals    S(6) S(-2) C(-4) Cu(2) Cu(1)

```

```

-molalities          Acetate- O2 NO3- N2
                    Fe+3 Fe+2 Cu+2 Cu+
                    Mn+2 Cu(Nta)- Cu(S4)2-3
-equilibrium_phases  Goethite Pyrolusite Ferrihydrite Siderite
                    Chalcocite Sphalerite Covellite CupricFerrite
                    CuprousFerrite Chalcopyrite Cuprite Tenorite
                    Malachite Azurite Cu(OH)2

```

USER_PUNCH

```

-headings Sorption_OM Sorption_clay Sorption_HFO Sorption_Bact total_sorption
total_Cu_Solid
-start
10 H_Cu =
mol("H_aCu+") + mol("H_bCu+") + mol("H_cCu+") + mol("H_dCu+") + mol("H_eCu+") + mol("H_
fCu+")
+ mol("H_gCu+") + mol("H_hCu+") + mol("H_abCu") + mol("H_adCu") + mol("H_afCu") + mol("H
_ahCu") + mol("H_bcCu") + mol("H_beCu") + mol("H_bgCu") + mol("H_cdCu") + mol("H_cfCu")
+ mol("H_chCu") + mol("H_deCu") + mol("H_dgCu")
20 punch H_Cu
30 punch mol("CuX2")
40 Hfo_Cu = mol("Hfo_wOCu+") + mol("Hfo_sOCu+") + mol("Hfo_wOCu") +
mol("Hfo_sOCu")
50 punch Hfo_Cu
60 R_Cu = mol("R_aCu+") + mol("R_bCu+")
70 punch R_Cu
80 total_sorption = H_Cu + CuX2 + Hfo_Cu + R_Cu
90 punch total_sorption
100 total_Cu_Solid =
total_sorption + equi("Chalcocite") + equi("Chalcopyrite") + equi("CuprousFerrite")
+ equi("CupricFerrite") + equi("Tenorite")
110 punch total_Cu_Solid
-end

```

TRANSPORT

```

-cells              50
-shifts            50
-time_step         10800 1 # seconds
-flow_direction    diffusion_only
-boundary_conditions flux flux
-lengths          20*0.005 30*0.01
-dispersivities   50*0.002
-correct_disp      true
-diffusion_coefficient 4.21e-010
-thermal_diffusion 2 4.21e-010
-punch_frequency   50
-multi_d           true 4.21e-010 0.9 0 1

```

end

REFERENCES

REFERENCES

- Appelo, C. A. J. Appelo and Postma: Geochemistry, Groundwater and Pollution. from <http://www.hydrochemistry.eu/a&p/index.html>
- Daughney, C. J., Fein, J. B., & Yee, N. (1998). A comparison of the thermodynamics of metal adsorption onto two common bacteria. *Chemical Geology*, 144(3-4), 161-176. doi: 10.1016/s0009-2541(97)00124-1
- Fein, J. B., Daughney, C. J., Yee, N., & Davis, T. A. (1997). A chemical equilibrium model for metal adsorption onto bacterial surfaces. *Geochimica Et Cosmochimica Acta*, 61(16), 3319-3328. doi: 10.1016/s0016-7037(97)00166-x
- Jeong, J. (2003). Solid-phase speciation of copper in mine wastes. *Bulletin of the Korean Chemical Society*, 24(2), 209-218.
- Jones, P. M. (2006). Ground-Water/Surface-Water Interaction in Nearshore Areas of Three Lakes on the Grand Portage Reservation, Northeastern Minnesota, 2003–04. Virginia: U.S. Geological Survey.
- Parkhurst, D. L., & Appelo, C. A. J. (2013). *Description of Input and Examples for PHREEQC Version 3—A Computer Program for Speciation, Batch-Reaction, One-Dimensional Transport, and Inverse Geochemical Calculations*. U.S. Geological Survey, Denver, Colorado.
- Sengor, S. S., Spycher, N. F., Ginn, T. R., Sani, R. K., & Peyton, B. (2007). Biogeochemical reactive-diffusive transport of heavy metals in Lake Coeur d'Alene sediments. *Applied Geochemistry*, 22(12), 2569-2594. doi: 10.1016/j.apgeochem.2007.06.011
- Tipping, E. (1998). Humic ion-binding model VI: An improved description of the interactions of protons and metal ions with humic substances. *Aquatic Geochemistry*, 4(1), 3-48. doi: 10.1023/a:1009627214459
- Tipping, E., & Hurley, M. A. (1992). A UNIFYING MODEL OF CATION BINDING BY HUMIC SUBSTANCES. *Geochimica Et Cosmochimica Acta*, 56(10), 3627-3641. doi: 10.1016/0016-7037(92)90158-f

Chapter 10

Result and discussion

The Phreeqc biogeochemical models had been created to simulate the mobility of copper in Torch Lake sediment. The individual model including speciation and saturation indices of surface and porewater model, adsorption of copper to hydrous ferric oxides, organic matter, clay and bacteria model, the TEAP model, the reductive dissolution model and the diffusion transport model were created and tested. Finally, these models were combined together as a full model where the concentration profiles of the dissolved redox species, the dissolved coppers and copper solid phases were plotted and used to verify the hypothesis. The results of each model were described below.

10.1 Copper speciation and saturation indices modeling

10.1.1 Surface water and top sediment porewater modeling

This model calculated the speciation of copper and saturation indices of copper mineral in Torch lake surface water and top sediment porewater, to determine the major dissolved copper species and minerals in the lake. The data input was pH, temperature, oxidation-reduction potential (pE) and chemical composition.

The results were shown in Table 10.1, for surface water, Cu(II) was the main oxidation state with nearly 100% and solution was in oxidizing condition with pE 14. The major species of Cu(II) was $\text{Cu}(\text{Nta})^-$ 99.14% which indicated most of copper in surface water was complexed with dissolved organic carbon. For the top sediment porewater, the main oxidation state was Cu(II) as well indicated this pore water was still in oxidizing condition. The main Cu(II) species

was $\text{Cu}(\text{Nta})^-$ 99.87%. This was caused by the high stability constant between Cu^{2+} and Nta (see Table 2.1). This data was agree with prior studies which indicated more than 90% of Torch Lake surface water and top sediment porewater were complexed with DOC (Jeong et al., 1999).

Table 10.1 Oxidation state and speciation of copper in surface water and top sediment porewater

Surface water					Top sediment Porewater				
Oxidation state	Molality	Percent	Speciation	Percent	Oxidation state	Molality	Percent	Speciation	Percent
Cu(I)	1.25e-23	0%	Cu ⁺	99.6%	Cu(I)	4.87e-22	0%	Cu ⁺¹	98.89%
			CuCl	0.39%				CuCl	1.11%
Cu(II)	1.28e-6	100%	$\text{Cu}(\text{Nta})^-$	99.14%	Cu(II)	3.94e-5	100%	CuNta-	99.87%
			$\text{CuOH}(\text{Nta})^{-2}$	0.87%				$\text{CuOH}(\text{Nta})^{-2}$	0.12%

The saturation index was calculated from Phreeqc to determine what minerals equilibrate in the water. The simulation shows that all copper oxides and carbonate minerals were undersaturation for both surface water and top sediment porewater but it shows the supersaturation of copper iron oxide (CupricFerrite) as shown in Table 10.2. This result may be explained that all copper still formed complex with DOC and there was high concentration of iron oxides in these water. This indicated dissolve organic carbon can compete to form dissolved complex with copper more than to precipitates as oxides or carbonates mineral. This results were consistent with prior reports where the copper complex with organic matter were the major pool of copper in top sediment (Jeong et al., 1999).

Table 10.2 Saturation index of copper minerals in surface water and top sediment porewater

Mineral	Formula	Surface water	Top sediment porewater
Cuprite	Cu ₂ O	-29.99	-28.08
Tenorite	CuO	-4.3	-4.83
Malachite	Cu ₂ (OH) ₂ CO ₃	-7.52	-8.86
Azurite	Cu ₃ (OH) ₂ (CO ₃) ₂	-14.99	-14.25
Copper carbonate	CuCO ₃	-5.98	-5.48
Cupric hydroxide	Cu(OH) ₂	-5.26	-5.86
Cupric Ferrite	CuFe ₂ O ₄	6.21	4.48
Cuprous Ferrite	CuFeO ₂	-1.25	-1.99

10.1.2 Mine tailing porewater modeling

To determine mine tailing porewater, the model was simulated by saturated the fresh water with 10 mol of Cuprite (Cu₂O), Chalcocite(Cu₂S) and Chalcopyrite(CuFeS₂) for copper minerals and Calcite (CaCO₃), Quartz(SiO₄), Hematite (Fe₂O₃), Orthoclase(KAlSi₃O₈) and Sanidine ((K,Na)(Si,Al)₄O₈) for other minerals. Some properties and composition of this porewater from model are shown in Table 10.3. The table shows that mine tailing porewater had pH 8.71, pE -8.76 and Cu(I) was major oxidation state which reflected the reducing condition. The major form of Cu(I) was sulfide complex Cu(S₄)₂⁻³ and major form of Cu(II) complex was hydroxide complex Cu(OH)₂. This solution will be used as bottom boundary in diffusion model.

Table 10.3 Some properties and copper composition from mine tailing porewater modeling

Parameter	Value	
pH	8.71	
pE	-8.76	
	Molality	%
Cu⁺	1.81E-04	
- Cu(S ₄) ₂ ⁻³	1.24E-04	68.40
- Cu ⁺	3.42E-05	18.91
Cu²⁺	5.98E-13	
- Cu(OH) ₂	5.91E-13	98.95
- CuCO ₃	5.43E-15	0.91
- CuOH ⁺	5.77E-16	0.10

10.2 Adsorption Modeling

10.2.1 Adsorption to Hydrous Ferric Oxide (HFO) modeling

The sorption model of HFO was tested by varying the pH. From Figure 10.1, the adsorption of Cu⁺ and Cu²⁺ on HFO increased when the pH increased. This trend was consistent with literature (Babich & Stotzky, 1980). The adsorption at high pH highly reduced the dissolved copper remaining in solution. The copper bound to the strong sites more than weak sites and the Cu²⁺ can be adsorbed more than Cu⁺. This was due to the larger surface complexation constant of Cu²⁺.

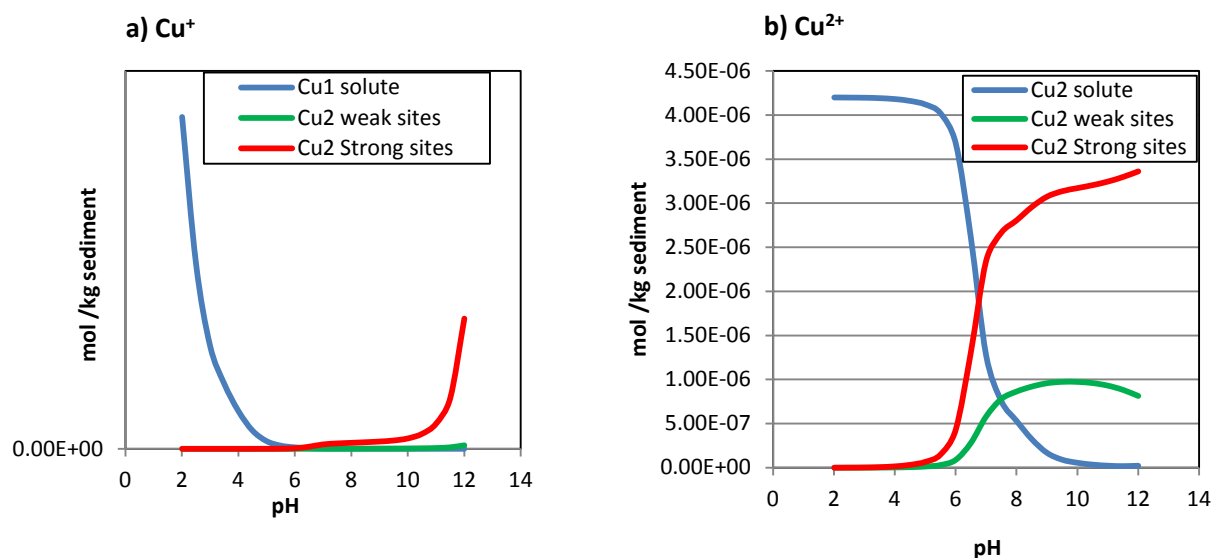


Figure 10.1 The simulation result of adsorption of Cu^+ (a) and Cu^{2+} (b) on strong and weak surface sites of hydrous ferric oxide as a function of pH

10.2.2 Adsorption to organic matter modeling

The adsorption model of copper to organic matter was tested by varying the pH. The Figure 10.2 shows the adsorption to organic matter (OM) decrease when pH increase. This was according to the literatures which indicated the stable of copper complex with dissolve organic carbon and hydroxide increase with the pH (Elliott et al., 1986; Payne & Pickering, 1975).

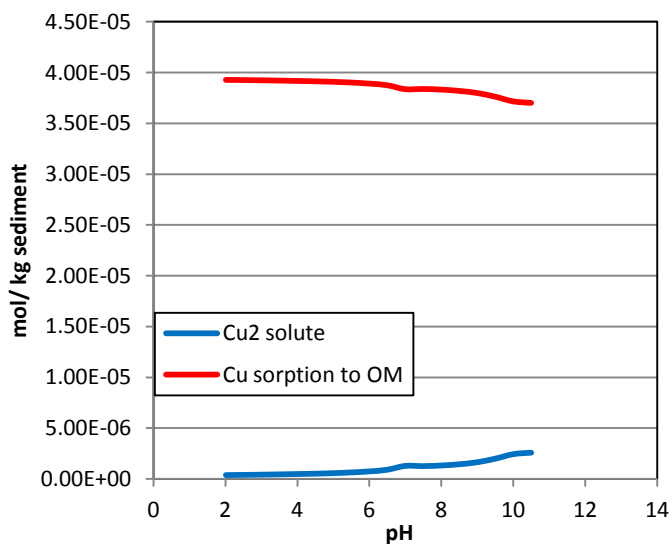


Figure 10.2 The simulation result of adsorption of Cu^{2+} on organic matter as a function of pH

10.2.3 Adsorption/ion exchange on clay modeling

Similar to the adsorption on organic matter, Figure 10.3 shows the sorption of copper to clays which decreased when pH increased. This may be a result from the increasing of stability of copper hydroxides and dissolved organic carbon complex at high pH

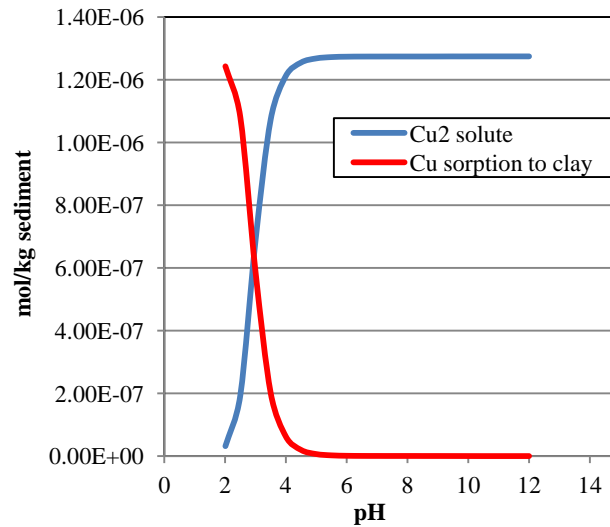


Figure 10.3 The simulation result of adsorption/ion exchange of Cu²⁺ on clay

10.2.4 Adsorption to bacteria surface modeling

The adsorption model of copper to bacteria was tested by varying the pH. The Figure 10.4 shows the sorption slightly increased when pH increased from 2 to 10, which according to the literature that adsorption of metal on bacterial surface will increase with increasing pH (Fowle & Fein, 1999). At low pH, the organic functional groups at the cell wall are fully protonated and there are no sorption sites available. However, at higher pH, the functional groups are deprotonated which increase the available sorption sites for the cation. The adsorption turned to decrease after pH 10 which caused by the stronger complex of copper with dissolved organic carbon and hydroxides.

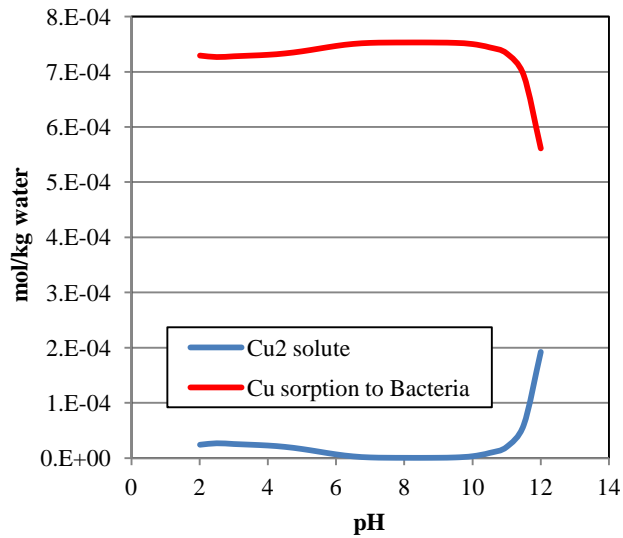


Figure 10.4 The simulation result of adsorption of Cu^{2+} onto bacteria surface

10.2.5 Contribution from various sorbents

The sorption of copper to all sorption sites model was tested by varying initial concentration of dissolved copper. Figure 10.5 shows the copper in solution mainly bound to bacteria surface at low concentration but when concentration increase, the copper would mainly bound to organic matter. Adsorption of copper to bacteria at low concentration was larger than organic matter because bacteria had surface complexation constants more than organic matter. However, because the bacteria had limit sorption sites, so when copper concentration increased, it could not adsorb on bacteria surface anymore and organic matter became main sorption sites. The sorption of copper on hydrous ferric oxide and clays may be negligible.

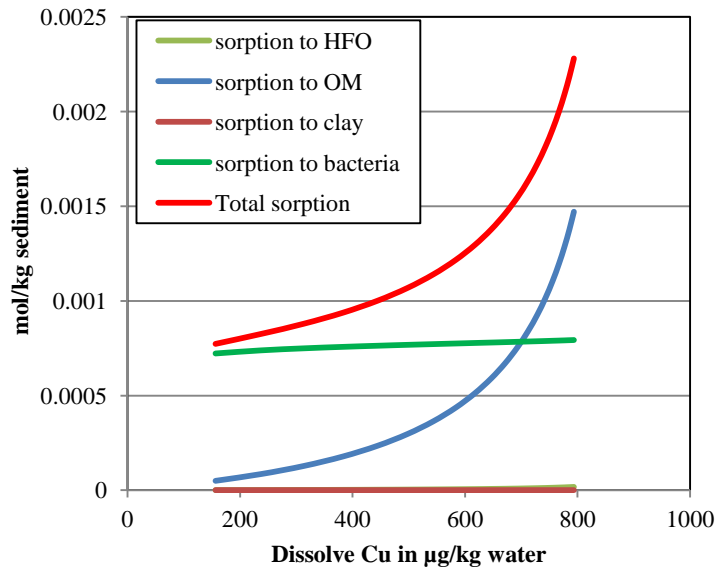


Figure 10.5 The simulation result of the distribution of copper adsorption on hydrous ferric oxide (HFO), organic matter, clay, bacteria surface and total sorption of all sites at different dissolved copper concentration

10.3 Oxidation of dissolve organic compounds by microorganism or TEAP modeling

The simulation results of TEAP model were shown in Figure 10.6 where the dissolved organic matter (in this case was acetate) was degraded by responsible microorganisms with sequential electron acceptors. The figure shows that, first the oxygen was consumed until it depleted and then nitrate will be used. The MnO_2 was used as next electron acceptor and Mn^{2+} was released to solution. In the same manner, the $\text{Fe}(\text{OH})_3$ was used after MnO_2 had been depleted and Fe^{2+} were produced. Sulfate was next electron acceptor, and the sulfide had been produced. After the sulfate depleted, the methanogenesis had occurred as last step which used acetate itself as electron acceptor and the product methane gas was released. The pE stepwise decrease when O_2 , NO_3 and MnO_2 were consumed but it will decrease rapidly to reducing zone (negative pE) when $\text{Fe}(\text{OH})_3$ was consumed. After that the pE was not change so much until

methanogenesis. These results indicate the created model follows the sequence of TEAP process but the time consuming in each step depended on kinetic rate parameters.

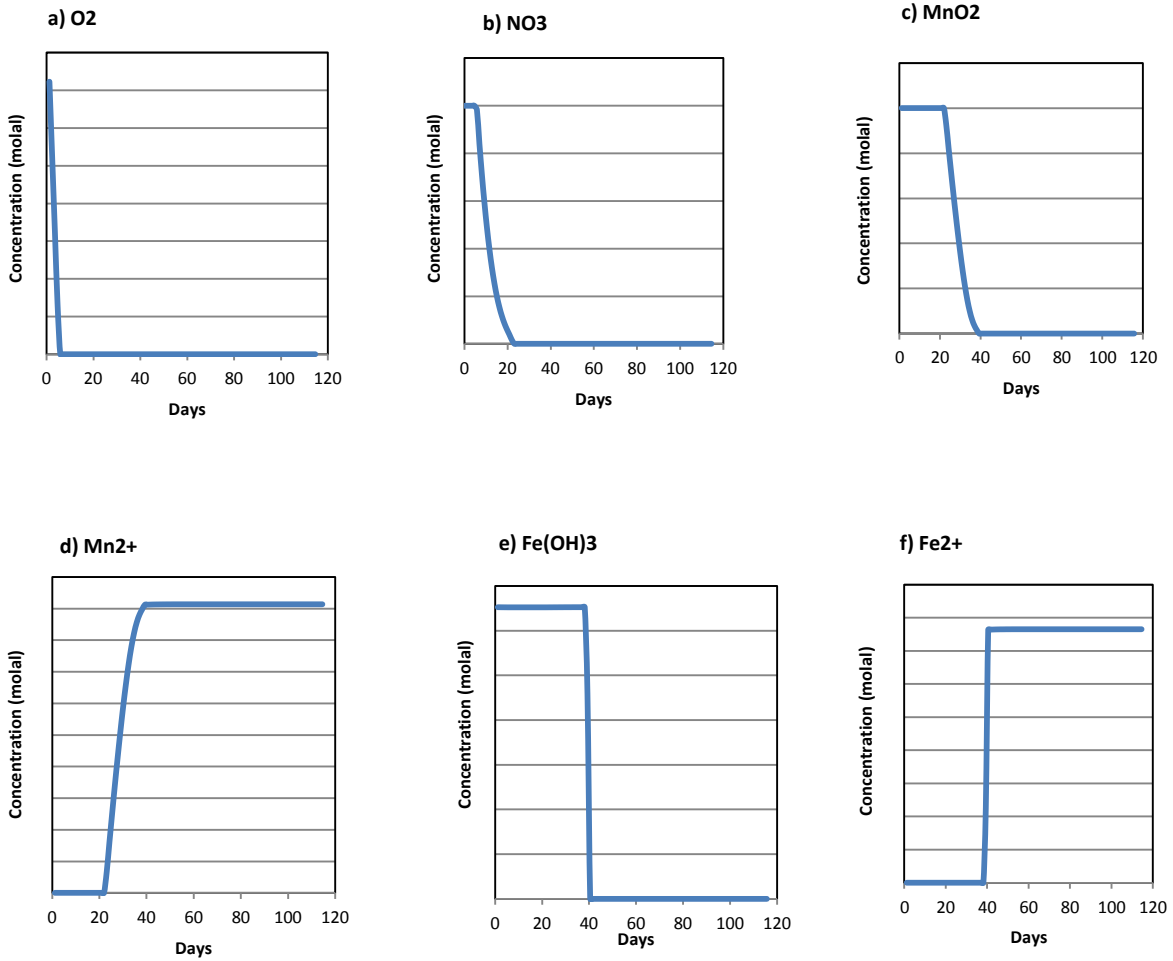
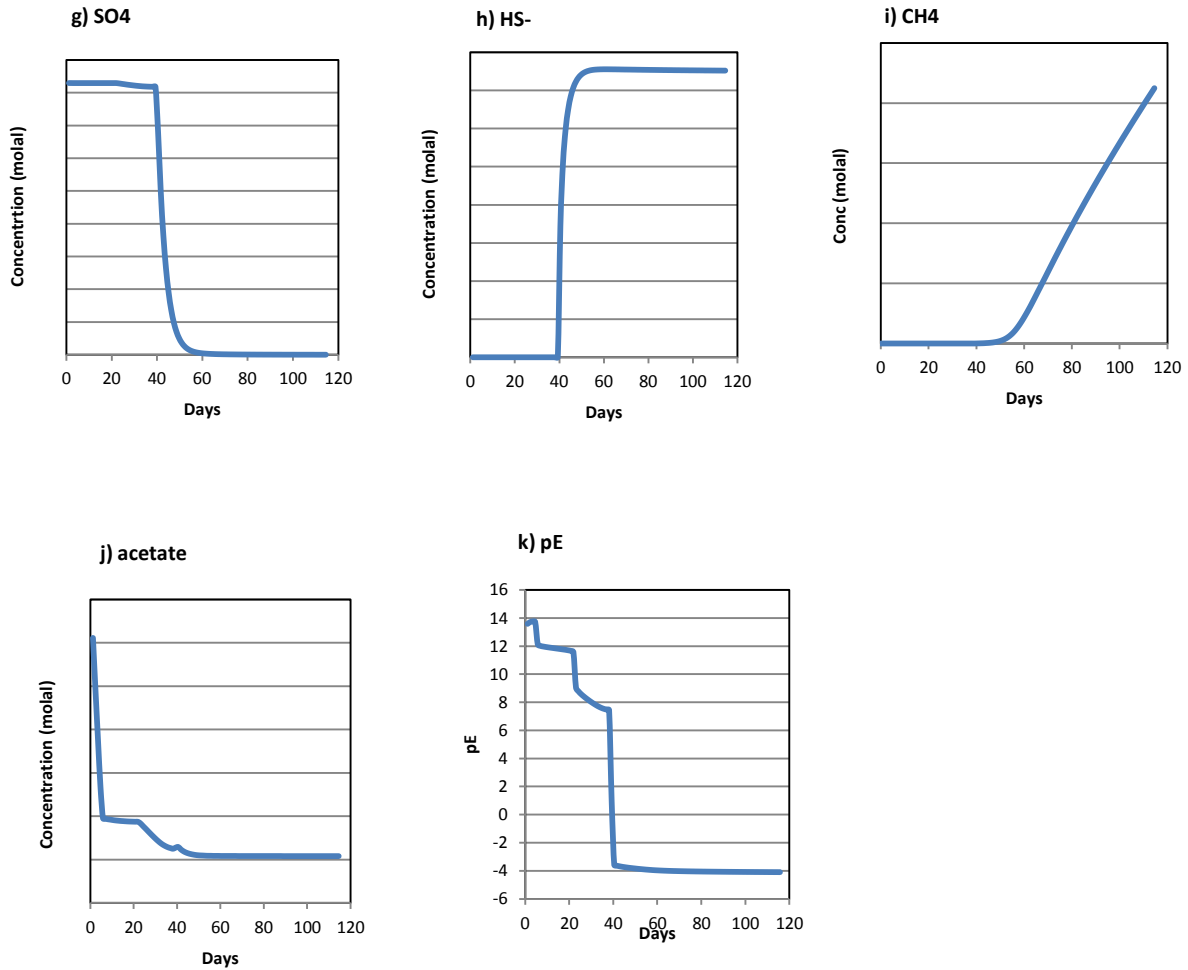


Figure 10.6 Concentration of redox species as a function of time result from the sequential biodegradation or TEAP modeling

Figure 10.6 (cont'd)



10.4 Reductive dissolution modeling

The reductive dissolution of iron oxides was added to TEAP model where the Ferrihydrite was used as iron oxide electron acceptor in TEAP series. Ferrihydrite was used as sorption sites for copper in the solution and Tenorite was used as source of copper mineral in the solution. The results of this process were shown in Figure 10.7. In the first step, O₂, NO₃, and MnO₂ were reduced and then Ferrihydrite (Fe(OH)₃) (Figure 10.7 a–d). Obviously, the dissolved

Fe^{2+} and $\text{Cu}(1)$ had increased which expected from dissolution of Ferrihydrite as shown in Figure 10.7 e and f. The Figure 10.7 g shows Tenorite had been dissolved to supply the dissolved copper to maintain the equilibrium of copper in the solution. The Figure 10.7 h shows copper that adsorbed on Ferrihydrite was released to solution. The pE was largely decreased during Ferrihydrite reduction and the pH large increased because of H^+ consumption in Ferrihydrite reduction as shown in Eq. 8.1 (Figure 10.7 i and j).

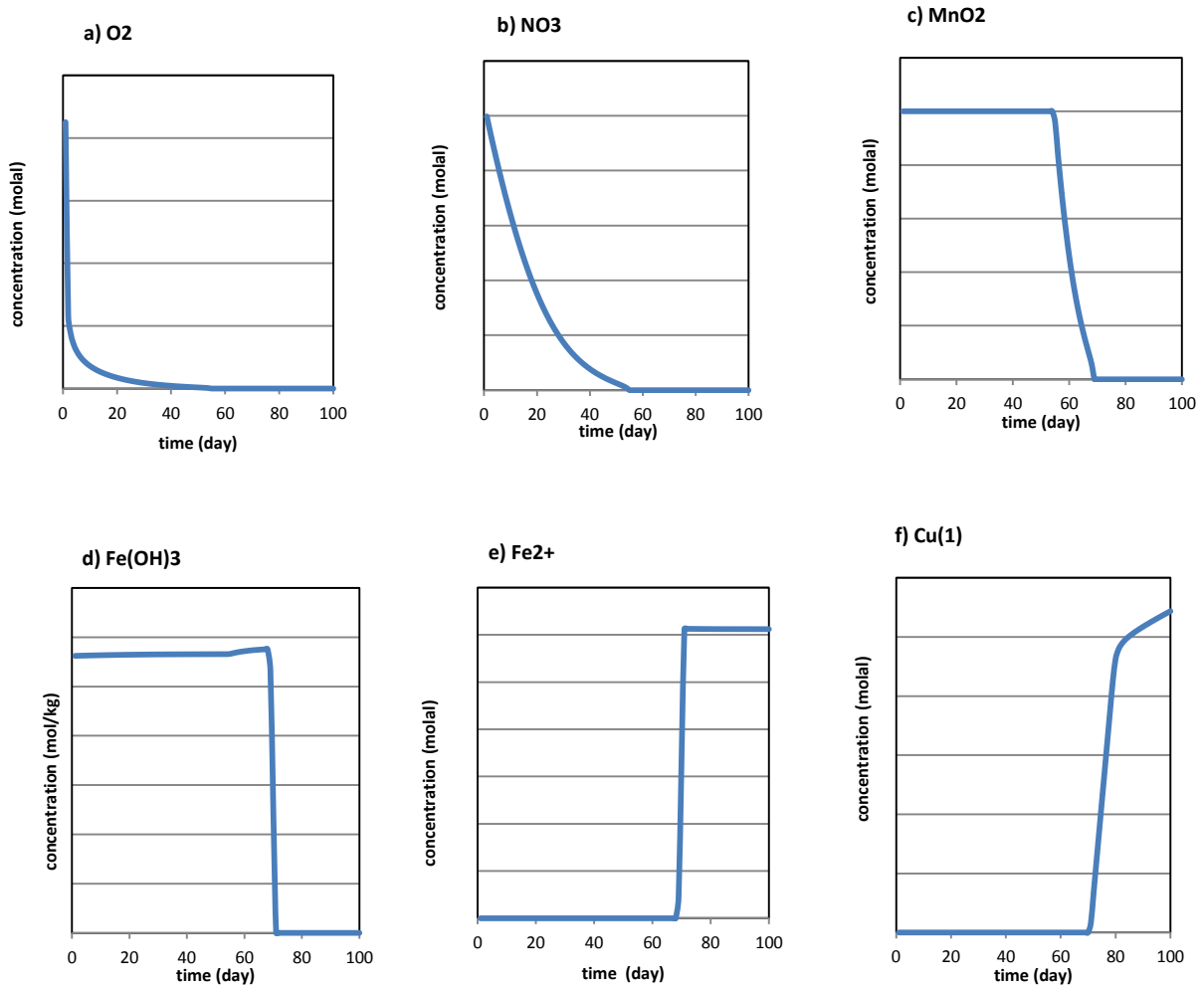
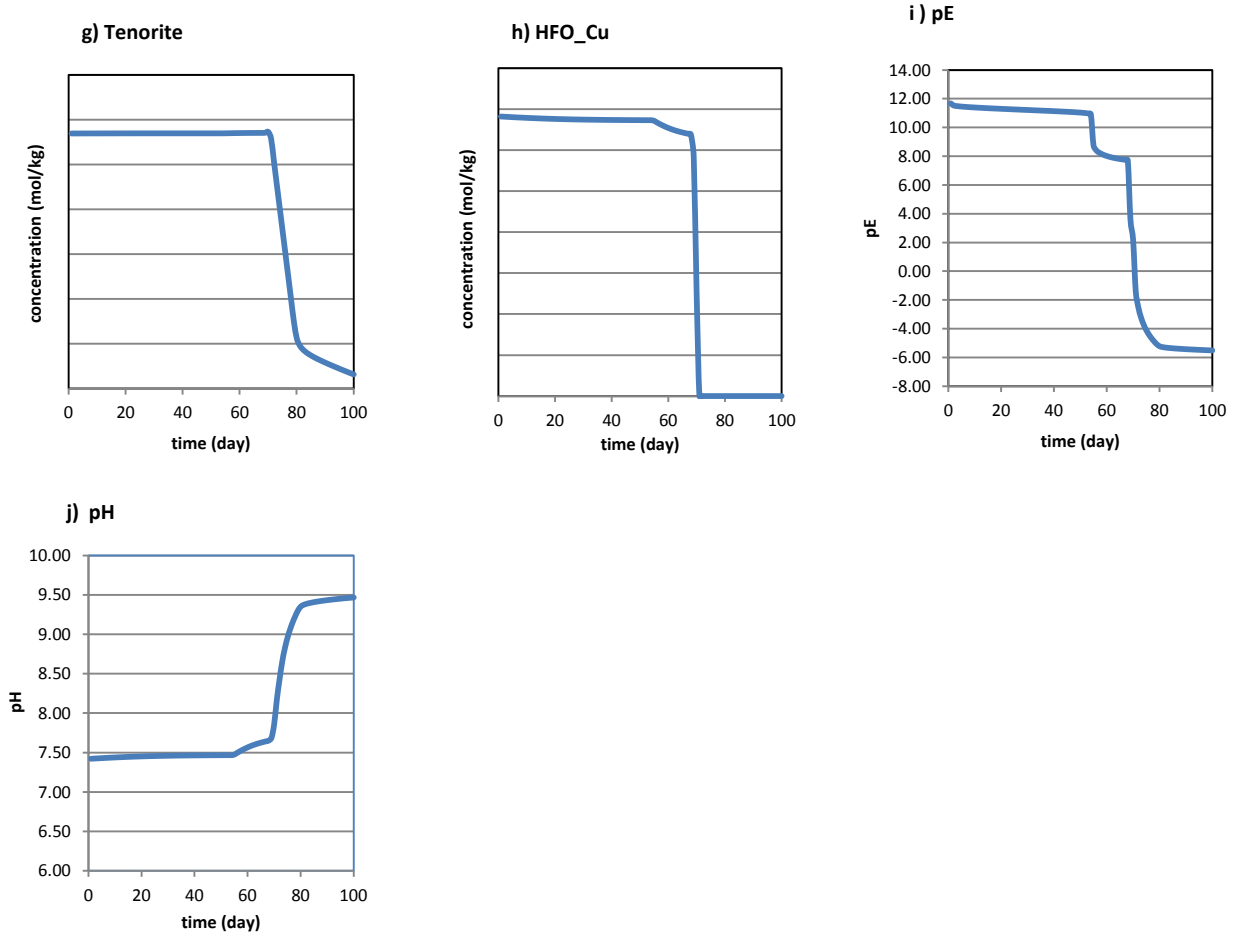


Figure 10.7 Concentration of some redox species, dissolved copper, Tenorite, pE and pH as a function of time in reductive dissolution modeling

Figure 10.7 (cont'd)



10.5 Diffusion transport with reductive dissolution and TEAP modeling

The 1-D column was used to represent the diffusion model where the surface water was used as top boundary solution and initial porewater, and mine tailing porewater was used as bottom boundary solution. The TEAP and reductive dissolution process were applied to the diffusion model and the results show in Figure 10.8. Figure 10.8 a shows that the redox condition of whole sediment was turn to reducing condition after 1 month of diffusion period, where the pE largely decreased from about 11 to -6. The pH of porewater in column found to increase with

time as shown in Figure 10.8 b which expected from the reductive dissolution of Ferrihydrite. The O_2 was quickly depleted at the interface and then NO_3 was consumed (Figure 10.8 c and d). For next electron acceptor, the MnO_2 and $Fe(OH)_3$, was consumed and depleted after 1 month (Figure 10.8 e and f). Fe^{2+} found to release after the Ferrihydrite was dissolved but the concentration was decreased with time due to the diffusion (Figure 10.8 g). The SO_4^{2-} started to be consumed after 3 month and in the same time HS^- found to build up in the sediment (Figure 10.8 h and i) Finally, the methanogenesis had occurred and CH_4 was found in sediment after 1 year (Figure 10.8 j). The dissolved $Cu(2)$ which was equilibrium concentration of Teneorite were constant in bottom sediment (Figure 10.8 k). The $Cu(1)$ concentration found to increase and diffuse upward to top sediment as shown in Figure 10.8 l This expected from the dissolution of Tenorite in reducing condition as shown in Figure 10.8 m.

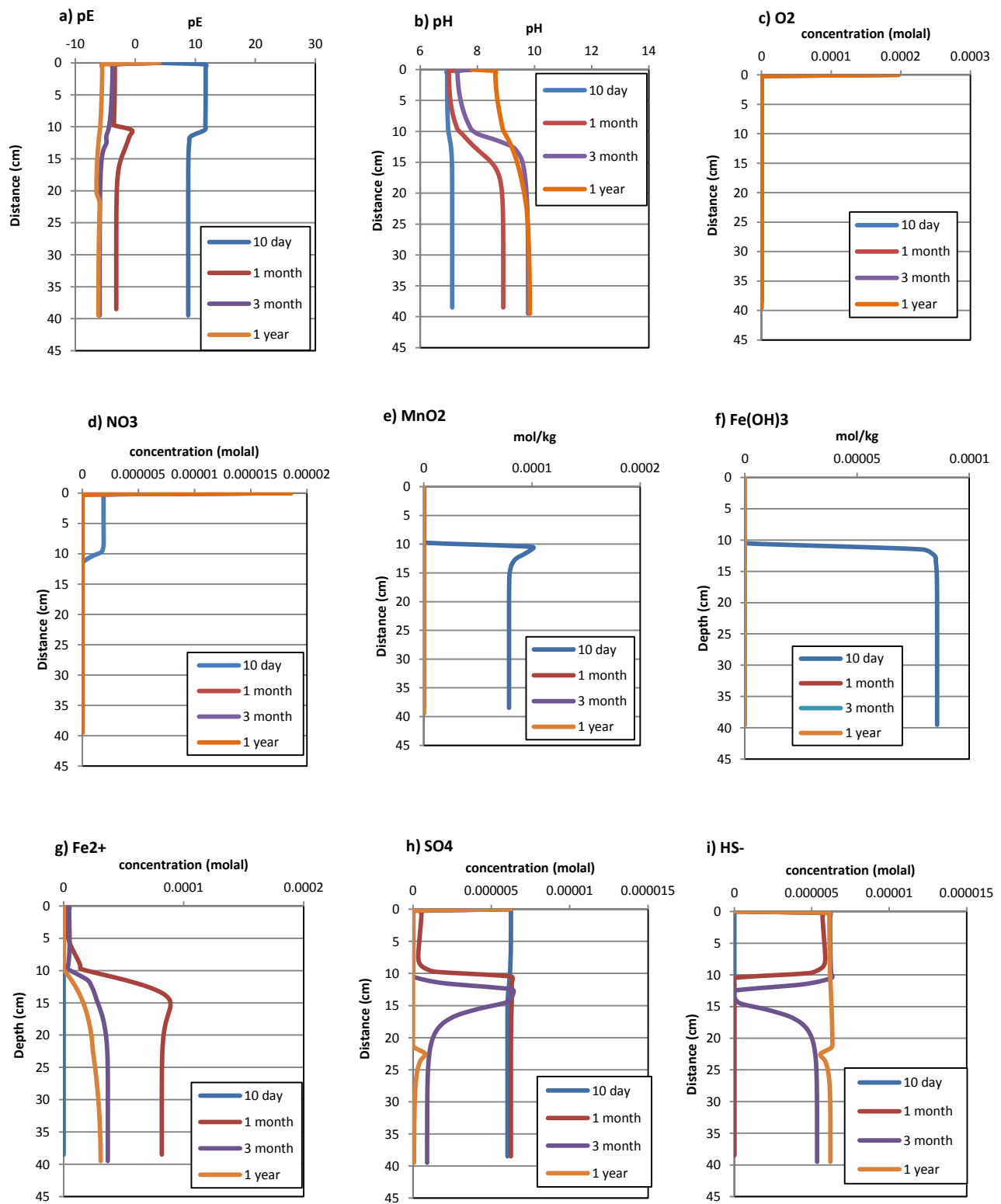
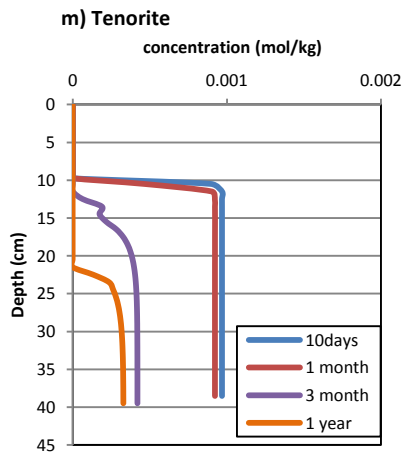
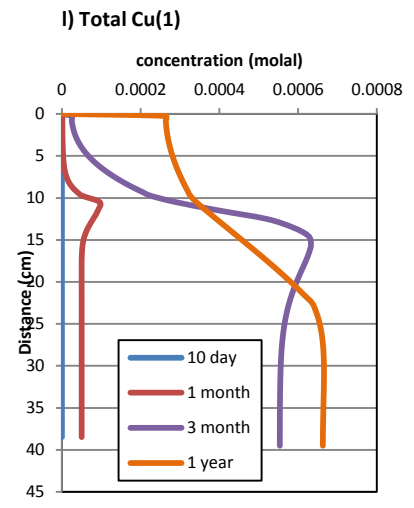
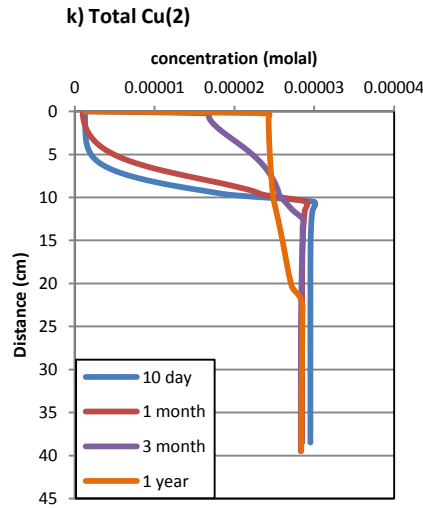
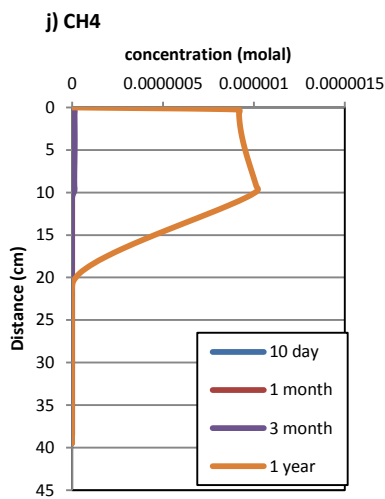


Figure 10.8 The simulation results of pE, pH, some redox species, dissolved copper and Tenorite concentration profile from diffusion transport with reductive dissolution and TEAP modeling

Figure 10.8 (cont'd)



10.6 Full combined processes modeling

This model implied the precipitation and adsorption processes to the reductive dissolution, TEAP and diffusion transport model. The concentration profiles of dissolved redox species, the dissolved copper phase, and copper solid phases were presented. The result of this model indicated the contribution from precipitation and adsorption process to fate and transport of copper in sediment.

10.6.1 The dissolved redox species and dissolved copper concentration

The pE profile in Figure 10.9 a. shows that, in the early period of diffusion, the sediment was in oxidizing condition of whole sediment. Then, pE in bottom sediment was decrease and turn to reducing condition when time increase whereas pE the top sediment was still constant in oxidizing condition. This was expected that the adsorption process which applied in the top of sediment can slow the TEAP process. However, after 2 year of diffusion, the whole sediment was turned to the reducing condition. The pH of pore water found to stable at 6-7 and seem to be constant with time (Figure 10.9 b). This was due to the Cuprousferrite precipitation which was release H^+ to neutral the OH^- released from reductive dissolution of Ferrihydrite. Unlike to the diffusion transport with only reductive dissolution and TEAP modeling, the O_2 and NO_3^- had not been quickly depleted at the interface but they were slowly consumed until deplete after 1 year (Figure 10.9 c and d). This suggests that adsorption process keep top sediment in oxidizing condition. MnO_2 and $FeOOH$ found to precipitate and build up at the top sediment. However, they were dissolved after 1 year when pE in top sediment start to decrease (Figure 10.9 e and f). The SO_4^{2-} become the next favorable electron acceptor which was started to be consumed after 3 month in bottom sediment and 2 year in top sediment. However, the produced HS^- was found in very low concentration which expected from precipitation of copper sulfide minerals (Figure 10.9 g and h). The methane gas was found in top sediment after 2 year diffusion when SO_4^{2-} was depleted. Figure 10.9 j and k shows the dissolved $Cu(2)$ and $Cu(1)$ in the column. The low concentration of $Cu(2)$ in top sediment was controlled by the adsorption of bacteria whereas the $Cu(2)$ in bottom sediment show the equilibrium concentration with Tenorite which was reduced and until deplete when Tenorite was completely consumed. The dissolved $Cu(1)$ was precipitated

as Cuprousferrite and Chalcocite, so no Cu(1) was left in the column. This process reduced the driving force of dissolved copper to diffuse out to surface water.

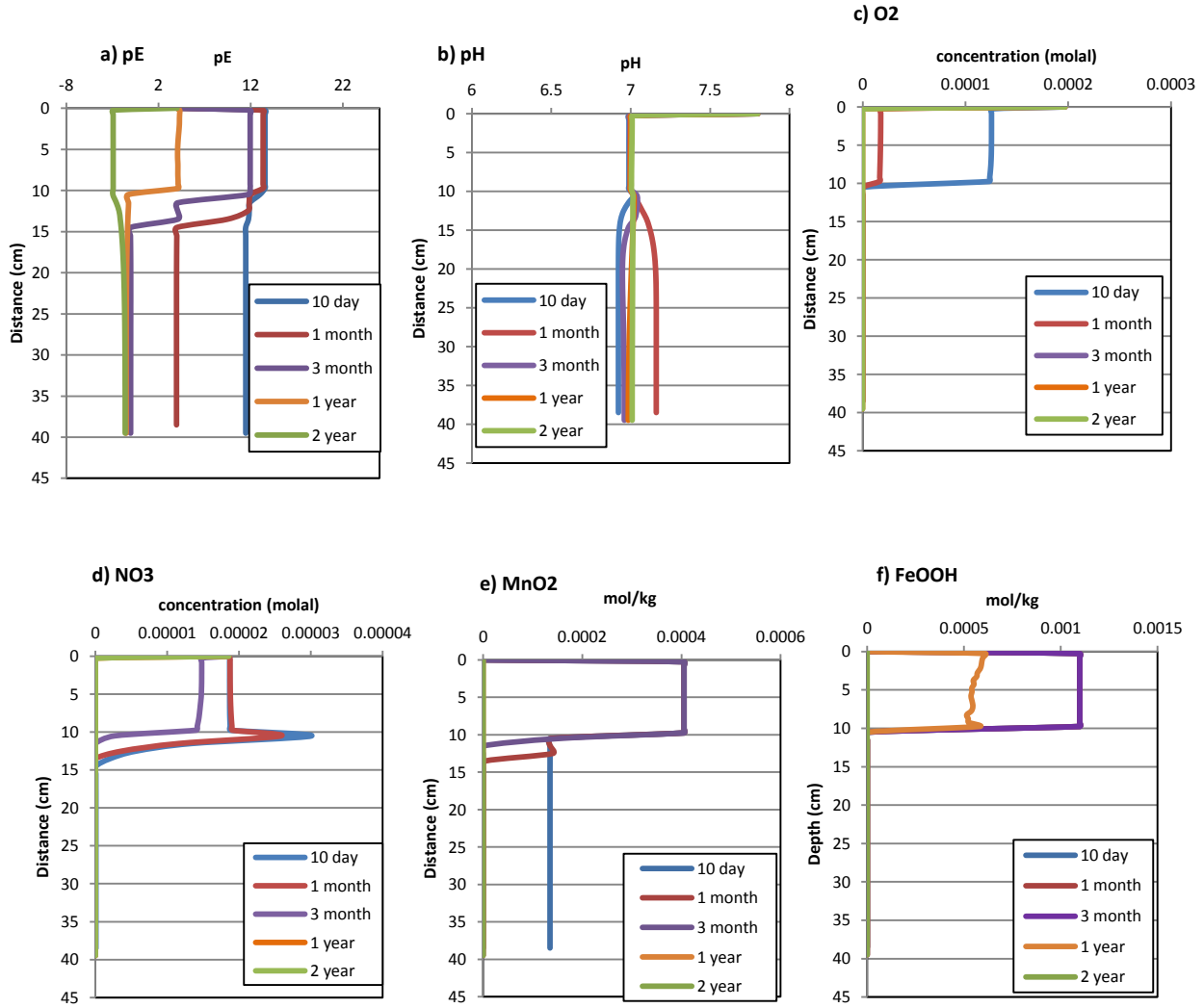
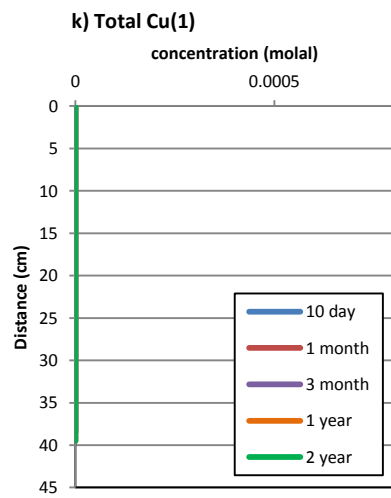
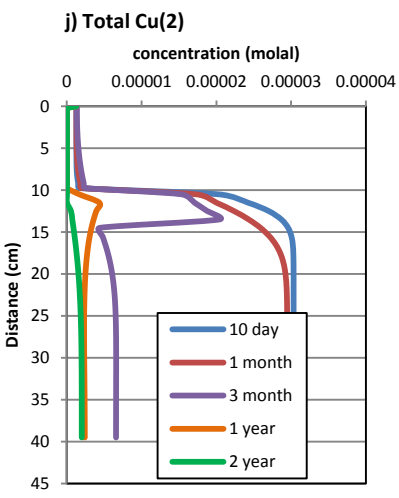
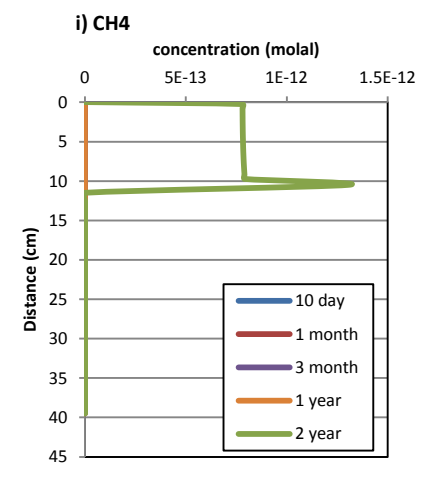
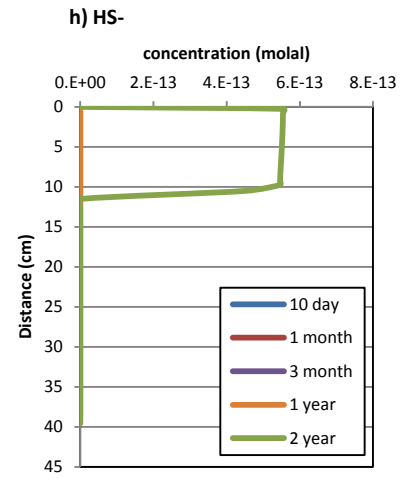
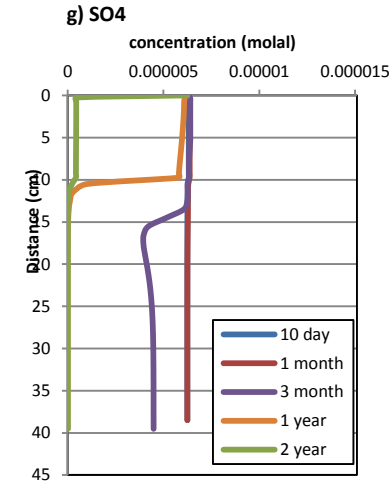


Figure 10.9 The simulation results of dissolved redox species concentration as a function of depth and time in the full combined processes modeling

Figure 10.9 (cont'd)



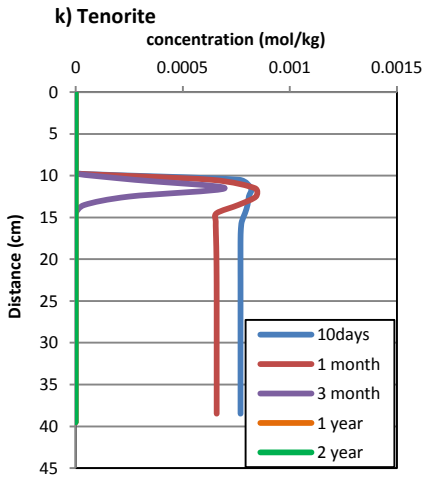
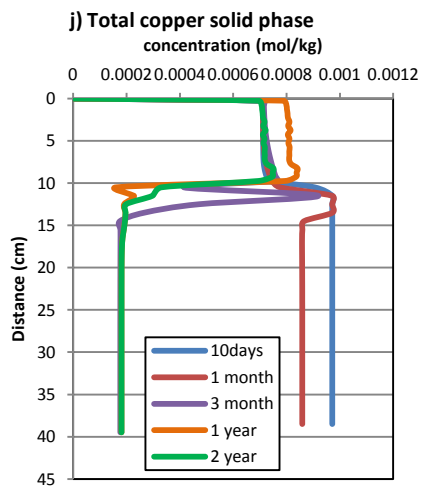
10.6.2 Copper solid phase concentration

When applied adsorption and precipitation to the model, the copper sorption solid phase and the precipitated copper minerals were calculated and showed in Figure 10.10 a - e. Due to most of dissolved Cu(1) and Cu(2) at bottom sediment was precipitated out, so the copper solid phase that found in top sediment expected to diffuse downward from surface water. Figure 10.10 a – d show the copper sorption phases of bacteria, organic matter, hydrous ferric oxide and clay, respectively. Mostly of copper adsorbed on the bacteria in the top sediment, and much less adsorbed by organic matter, hydrous ferric oxide (HFO). However, after pE decreased at 1 year diffusion, the sorption phase on the bacteria found to decrease until depleted after 2 year. This expected from the changing form of copper solid phase when sediment turn to reducing condition. The sorption on clay was dominant over other sorption phases in bottom sediment. However, it found to decrease until depletion when time increased too as shown in Figure 10.10 d. Figure 10.10 e show total sorption phase, where after 2 year, no copper sorption phases left in the column. Figure 10.10 f – j show the copper mineral phases that precipitate in the sediment. Chalcocite (Cu_2S) was precipitated after 3 month in bottom sediment and after 2 year in top sediment by the reaction between Cu^+ and HS^- according to Eq. 10.1 where sediment turn to reducing condition and HS^- was produced in sediment (Figure 10.10 f). The Cuprousferrite became the dominant mineral that precipitate in the bottom sediment which occurred from reaction between Cu^+ and Fe^{+3} according to Eq. 10.2. After 1 year diffusion, CuprousFerrite was found to precipitate and became main copper solid phase in top sediment which expected from the dissolution of Goethite (FeOOH) and copper-bacteria sorption phase and formed as CuprousFerrite which was more stable at reducing condition (Figure 10.10 h). Chalcopyrite (CuFeS_2) was not found in whole sediment (Figure 10.10 g). The Tenorite found to dissolve due

to reductive dissolution process and depleted after 3 month (Figure 10.10 j). Figure 10.10 k represents the total copper solid phase in the column which combined between the copper adsorbed on all sorption sites and all copper minerals that precipitated. The concentration of total copper solid phase in top sediment found to increase over time due to the precipitation of Chalcocite and Cuprous Ferrite even it had the dissolution of copper-bacteria sorption phase. In the mean time, the total copper solid phase in bottom sediment were decrease from dissolving of copper mineral, in this case Tenorite. This evidence may be an example that explains why there was high concentration of copper solid phase in top sediment. These results show the importance of the reductive dissolution of iron oxides process, adsorption by bacteria process and precipitation of copper iron oxides and sulfides in controlling fate and transport of copper in sediment.



Figure 10.10 (cont'd)



REFERENCES

REFERENCES

- Babich, H., & Stotzky, G. (1980). ENVIRONMENTAL-FACTORS THAT INFLUENCE THE TOXICITY OF HEAVY-METAL AND GASEOUS POLLUTANTS TO MICROORGANISMS. *Crc Critical Reviews in Microbiology*, 8(2). doi: 10.3109/10408418009081123
- Elliott, H. A., Liberati, M. R., & Huang, C. P. (1986). COMPETITIVE ADSORPTION OF HEAVY-METALS BY SOILS. *Journal of Environmental Quality*, 15(3), 214-219.
- Fowle, D. A., & Fein, J. B. (1999). Competitive adsorption of metal cations onto two gram positive bacteria: Testing the chemical equilibrium model. *Geochimica Et Cosmochimica Acta*, 63(19-20), 3059-3067. doi: 10.1016/s0016-7037(99)00233-1
- Jeong, J., Urban, N. R., & Green, S. (1999). Release of copper from mine tailings on the Keweenaw Peninsula. *Journal of Great Lakes Research*, 25(4), 721-734.
- Payne, K., & Pickering, W. F. (1975). INFLUENCE OF CLAY-SOLUTE INTERACTIONS ON AQUEOUS COPPER-ION LEVELS. *Water Air and Soil Pollution*, 5(1), 63-69. doi: 10.1007/bf00431580

Chapter 11

Conclusion

This study had investigated the fate and transport of copper in Torch Lake sediment which had a unique pattern of persisting high concentration of solid copper in post sediment and never be remediated by natural processes. From applying the variety of biogeochemical processes to to diffusion process in Phreeqc modeling, we found that the reductive dissolution of iron oxides mediated by TEAP process can release copper from the minerals in sediment. However, these dissolved coppers were removed by precipitation of iron oxides of copper in bottom sediment. The bacteria in top sediment can adsorb large amount of copper but it expects from downward diffuse of overlay water. However, when time increase, the reducing condition was developed in top sediment and the copper-bacteria sorption phase was dissolved and transformed to iron oxides or sulfides of copper minerals instead which were more stable. This series of processes is an example that may explain the high concentration of copper solid phase in top sediment. The results indicate that the redox condition was the main parameter that controlled the fate and transport of copper in sediment.

However, the results of this model still have some limitation. For example, because of a long time calculation of the program, the diffusion of 2 yr was applied and that may be too short to understand the evolution of copper evidence that developed in Torch Lake for more than fifty years. Moreover, the model was assumed that all microorganisms that responded in TEAP reactions were presented in sediment and all reactions had been occurred which may be not true in real situation.

This study shows the complexity of biogeochemical processes occurred in the Lake sediment that affect to the fate and transport of heavy metals. This modeling approach may be useful to apply to other environment problems which show how to couple the physical, chemical and biological processes with transport processes to computer modeling.